# Regulation of the respiratory metabolism of apple during (dynamic) controlled atmosphere storage

JELENA BOECKX

Supervisors:

Prof. B. Nicolai
Prof. A. Geeraerd
Dr. M. Hertog

Members of the examination committee:

Prof. M. De Proft
Prof. J. Robben
Prof. A. Saquet (Federal Institute of Science and Education Farroupilha)
Prof. J. Van Impe

Chairman:

Prof. T. Niewold

Dissertation presented in partial fulfilment of the requirements for the degree of Doctor of Bioscience Engineering (PhD).

August 2018

Doctoraatsproefschrift nr. 1517 aan de faculteit Bio-ingenieurswetenschappen van de KU Leuven

© 2018 KU Leuven, Science, Engineering & Technology
Uitgegeven in eigen beheer, Jelena Boeckx, Predikherenstaat 3, 3000 Leuven

Alle rechten voorbehouden. Niets uit deze uitgave mag worden vermenigvuldigd en/of openbaar gemaakt worden door middel van druk, fotokopie, microfilm, elektronisch of op welke andere wijze ook zonder voorafgaandelijke schriftelijke toestemming van de uitgever.

All rights reserved. No part of the publication may be reproduced in any form by print, photoprint, microfilm, electronic or any other means without written permission from the publisher.

# Dankwoord

Deze doctoraatsthesis is de kers op de taart van een hobbelig, maar vooral heel leerrijk en uitdagend parcours. De voorbije jaren heb ik ontelbare appels geschild, proeven opgezet, stalen geanalyseerd, protocols geoptimaliseerd, nachten doorgebracht in het labo, congressen bijgewoond,… Maar gelukkig maak je een doctoraat nooit alleen en kreeg ik de hulp van heel wat mensen.

In de eerste plaats wil ik mijn promotoren, Bart, Annemie en Maarten bedanken voor het vertrouwen en steun die ze mij gegeven hebben tijdens mijn onderzoek. Maarten, als mijn dagelijkse begeleider wil ik jou extra hard bedanken. Je hebt me geleerd hoe ik degelijk wetenschappelijk onderzoek moet doen, hoe ik altijd kritisch mijn data moet interpreteren, dat het de moeite loont om dingen volledig te begrijpen, hoe ik een goed artikel moet schrijven, dat ik niet moet opgeven, maar moet blijven doorgaan. Bedankt om mij deze dingen bij te brengen en altijd klaar te staan om me op te vangen en opnieuw te motiveren als het even wat minder ging. Ook de andere leden van mijn examencommissie wil ik graag bedanken om mijn doctoraatsthesis zo zorgvuldig na te lezen en me de nodige opmerkingen en suggesties te geven, die dit werk zeker hebben verbeterd. Zonder geld is onderzoek helaas niet mogelijk, dus ik zou ook graag het IWT bedanken om in mijn project te geloven en me financiering te geven voor vier jaar.

Graag wil ik ook alle (ex)collega's bedanken voor de leuke sfeer, de gezellige babbels tijdens de pauze, de etentjes in de Via Via, de after-work drinks in de baarr,… zonder

enige twijfel zijn velen ondertussen goede vrienden geworden! Niet alleen kon ik op jullie rekenen voor een aangename tijd samen, maar ook op professioneel vlak wil ik graag een aantal mensen extra bedanken. Matthi, merci om steeds mijn (niet altijd even slimme) vragen te beantwoorden en me te helpen het bos door de bomen te zien bij het analyseren van de RNA sequencing data. Bert, Matti en Niels, merci dat ik doorheen de jaren steeds op jullie kon rekenen om kleine en grote problemen op te lossen. Elfie, een dikke merci om mijn stalen met zoveel zorg en nauwkeurigheid te meten. En tenslotte wil ik graag ook alle collega's bedanken die me hebben geholpen tijdens mijn nacht-experimenten, zonder jullie was dit nooit mogelijk geweest!

Ook buiten het werk kon ik op heel wat steun rekenen en ik prijs me dan ook heel gelukkig met zo'n geweldige familie en vriendengroep. Moeke en Vake, ik wil jullie graag heel hard bedanken om er altijd voor mij te zijn en me de kansen te bieden om mijn dromen na te jagen. Vincent, ook jij heel hard bedankt om me te steunen en altijd voor me op te komen. Koekje, jammer genoeg kan je dit moment niet meer samen met mij meemaken, maar ik ben er zeker van dat je samen met Peter heel trots zou geweest zijn. Tenslotte wil ik heel graag "de nichtjes", "Biomiekes" en "Amigas" bedanken. Jullie hebben me door dik en dun gesteund en zorgden voor de gewenste afleiding tijdens mijn doctoraat.

Bedankt!
Jelena Boeckx

# Abstract

After harvest, apple (*Malus* x *domestica* Borkh.) fruit remains metabolically active and continues to ripen. The main goal of postharvest storage is to slow down this metabolic activity and its associated fruit ripening. Therefore, large volumes of apple fruit are routinely stored under controlled atmosphere (CA) conditions (low temperature, low oxygen and high carbon dioxide partial pressures) with recent developments moving towards dynamic CA (DCA) storage. During DCA storage, the oxygen partial pressure in the cool store is reduced towards the anaerobic compensation point until the physiological response of the fruit indicates that its metabolism has switched from aerobic respiration to fermentation. In this way, fruit ripening can be delayed more effectively than under regular CA storage. However, altering the normal atmospheric conditions is not without any risk at the fruit physiology level: it may induce low-oxygen stress. To be able to further improve the development of the DCA storage technology, it is important to fully understand the impact of low-oxygen stress on the physiology of apple fruit.

Nowadays, little is known about the precise mode of action of low-oxygen concentrations on the metabolic processes and their regulation in apple fruit. Therefore, the main objective of this dissertation was to unravel the metabolic changes of the central carbon metabolism and its regulation introduced by low-oxygen stress in 'Jonagold' apple fruit. Due to oxygen consumption and slow diffusion present in the apple fruit, the oxygen concentration declines towards the centre of the fruit. In order to avoid oxygen gradients experiments were all

conducted on thin slices of the apple cortex tissue. To diminish the influence of wound ethylene on the metabolism, the apple slices were flushed with humidified air before the start of the experiments.

If the oxygen concentration in the fruit tissue is too low, fermentation will be induced, which can lead to alcoholic off-flavours and internal storage disorders. However, as of today, little information is available on the *in vivo* regulatory mechanism of the fermentative metabolism under low-oxygen stress. Based on *in vitro* experiments, it was proposed that fermentation could be regulated via a molecular and a metabolic control system, but experimental conditions *in vitro* are not necessarily a correct representation of the situation *in vivo*. Therefore, the first focus of this study was to get a better insight into the regulation of the fermentative metabolism *in vivo* under different oxygen concentrations and temperature levels, and this immediately after harvest as well as after storage. A combination of experimental techniques and a kinetic modelling approach was used to study the regulation of the fermentative metabolism.

To correctly measure the *in vitro* activity of the fermentation enzymes, pyruvate decarboxylase (PDC) and alcohol dehydrogenase (ADH), enzyme assays were optimized to increase the signal to noise ratio. Furthermore, an elaborated kinetic model based method was developed to accurately estimate the *in vitro* specific enzyme activity of PDC and ADH from spectrophotometric assay data. The models are based on Michaelis-Menten and first-order kinetics, which describe the reaction mechanism catalysed by the enzymes. In contrast to the linear regression approach, the models can be used to estimate the enzyme activity regardless of whether linearity is achieved since they take into account the complete progress curve. The advantage of using a kinetic modelling approach is that the maximum activity of the enzyme can be estimated through extrapolation, even if saturating substrate conditions are not fully realized.

The regulation of the fermentative metabolism appeared to be highly depending on the conditions applied. Temperature changed the overall metabolic reaction rate, which appeared to have a large influence on the induction and regulation of the fermentative metabolism. At 1 °C, the metabolic rate was low and fermentation was only slightly induced and largely metabolically controlled. However, at 18 °C, the overall metabolic rate was faster and a ten-fold increase in ethanol levels was observed. In this case, the ethanol pathway was regulated by a combination of molecular and metabolic control systems. Also, the model indicated that under anoxic conditions at harvest the *in vivo* regulation was located at the fast induction of PDC activity, whether after six months of storage an extra regulation on ADH activity seemed to be present. Furthermore, a different regulation of the ethanol pathway was observed between hypoxic and anoxic conditions. Even though fermentation was clearly induced under all experimental conditions applied, the flux through the fermentative metabolism started to decrease again after prolonged low-oxygen stress.

To investigate whether 'Jonagold' apple fruit reduces the negative effects of fermentation by shuttling pyruvate into alternative pathways, a detailed pathway analysis, based on RNA-sequencing data, was performed to study the transcriptional regulation of the central carbon metabolism during low-oxygen stress in more detail. This revealed that apple fruit, exposed to 0.5 kPa $O_2$, diminishes the energy crisis by upregulating the glycolytic flux and the PPi-dependent reactions, saves carbon atoms by shuttling pyruvate into the alanine metabolism and limits cytosolic acidification by activating the alanine metabolism and the GABA shunt. Furthermore, evidence was provided supporting the presence of an oxygen sensing mechanism in 'Jonagold' apple fruit, indicating that besides the substrate inhibition of the electron transport chain by limiting oxygen levels, an active regulatory mechanism of the central carbon metabolism is present.

Future research is necessary to characterize the influence of different (dynamically changing) low-oxygen partial pressures on the central carbon metabolism of multiple cultivars and to better understand the operation of the oxygen sensors in apple fruit. Furthermore, a system biology model should be developed, implementing data of all the organizational levels, to help us better understand the influence of low-oxygen stress on the physiology of apple fruit.

# Samenvatting

Bijna de helft van de appelproductie (*Malus* x *domestica* Borkh.) wereldwijd is bestemd voor langdurige bewaring. Na de oogst blijven appelen metabolisch actief en rijpen ze verder. Tijdens de bewaring is het belangrijk om de metabolische activiteit en daarmee het rijpingsproces van de vruchten te vertragen. Daarom worden grote hoeveelheden appelen opgeslagen onder condities met gecontroleerde atmosfeer (CA) (lage temperatuur en lage zuurstofpartieeldruk in combinatie met hoge koolstofdioxidepartieeldruk) met recente ontwikkelingen gaande in de richting van bewaring onder dynamisch CA (DCA). Bij DCA-bewaring wordt het zuurstofniveau in de bewaarruimte gradueel verlaagd richting het anaeroob compensatiepunt, tot het moment waarop een biorespons vanuit het fruit aangeeft dat het ademhalingsmetabolisme van de vruchten te laag wordt en leidt tot fermentatie, waarna het zuurstofniveau terug verhoogd wordt. Het wijzingen van de normale atmosferische condities is echter niet zonder risico voor de vruchtfysiologie: het kan namelijk lagezuurstofstress veroorzaken. Om de technologie van DCA-bewaring verder te verbeteren, is het van belang om de volledige impact van lagezuurstofstress op de vruchtfysiologie te begrijpen.

Momenteel is er weinig bekend over hoe de lage zuurstofconcentraties de metabole processen en hun regulatie in appelen juist beïnvloeden. Daarom is de hoofddoelstelling van dit proefschrift om de metabole veranderingen van het centrale koolstofmetabolisme die geïnduceerd worden door lagezuurstofstress en hun regulatie in Jonagold-appelen te ontrafelen. Door de aanwezigheid van

zuurstofgradiënten in de vrucht is de zuurstofconcentratie rond het klokhuis lager dan in het vruchtvlees net onder de schil. Om er voor te zorgen dat de zuurstofconcentraties in het vruchtweefsel overal hetzelfde zijn, werden alle experimenten uitgevoerd met dunne schijfjes appel, afkomstig van dezelfde regio in de vrucht zonder schil en klokhuis.

Als de zuurstofconcentraties in het vruchtweefsel te laag worden, zal fermentatie geïnduceerd worden, wat kan zorgen voor smaakveranderingen (bv. ethanol) en fysiologische afwijkingen in de vruchten. Momenteel is er echter weinig informatie beschikbaar over de *in vivo* regulatie van het fermentatiemetabolisme bij lagezuurstofstress. Op basis van *in vitro* experimenten werd gesuggereerd dat het fermentatiemetabolisme geregeld wordt via een moleculair en een metabolisch controlesysteem, maar experimentele omstandigheden *in vitro* zijn niet noodzakelijkerwijs een correcte weergave van de situatie *in vivo*. Daarom is de eerste focus van dit proefschrift om een beter inzicht te geven in de regulatie van het fermentatie-metabolisme *in vivo* bij verschillende zuurstofconcentraties en temperaturen zowel onmiddellijk na de oogst als na bewaring. Hiervoor werd gebruik gemaakt van een combinatie van experimentele technieken en kinetische modellen.

Om de *in vitro* activiteit van de fermentatie-enzymen, pyruvaatdecarboxylase (PDC) en alcoholdehydrogenase (ADH), correct te meten, werden meetprotocollen geoptimaliseerd om de signaal/ruis-verhouding te verhogen. Verder werd er een methode ontwikkeld, gebaseerd op een kinetisch model, om nauwkeurig de *in vitro* specifieke enzymactiviteit van PDC en ADH te schatten op basis van spectrofotometrische data. De modellen zijn gebaseerd of Michaelis-Menten en eerste-orde-kinetiek, die het reactiemechanisme van de enzymen beschrijven. In tegenstelling tot de lineaire regressiemethode, kunnen deze modellen worden gebruikt om de enzymactiviteit te bepalen, ongeacht of lineariteit werd bereikt, omdat ze de volledige voortgangscurve in rekening brengen. Het voordeel van het

gebruikte kinetisch model is dat de maximale activiteit van het enzym kan geschat worden door extrapolatie, zelfs als de substraatverzadiging niet volledig werd gerealiseerd.

De regulatie van het fermentatiemetabolisme bleek sterk afhankelijk van de toegepaste omstandigheden. Temperatuur veranderde de algemene metabole reactiesnelheid, die op zijn beurt een grote invloed bleek te hebben op de inductie en regulatie van het fermentatiemetabolisme. Verder gaf het model aan dat de *in vivo* regulatie van het fermentatiemetabolisme verschillend was onder anoxische en hypoxische omstandigheden, als ook dat er een extra regulatie aanwezig was na 6 maanden bewaring. Ondanks dat het fermentatiemetabolisme duidelijk geïnduceerd werd onder alle toegepaste experimentele omstandigheden, begon de flux door het fermentatiemetabolisme weer af te nemen na langdurige lage zuurstofstress.

Om verder te onderzoeken of Jonagold-appelen de negatieve effecten van fermentatie verminderen door pyruvaat naar alternatieve routes te transporteren, werd er een gedetailleerde pathway-analyse uitgevoerd, gebaseerd op RNA-sequencing data, om de transcriptionele regulatie van het centrale koolstofmetabolisme tijdens lage zuurstofstress in meer detail te bestuderen. Hieruit bleek dat Jonagold-appelen de energiecrisis verminderen door de flux door de glycolyse te verhogen en PPi-afhankelijke reacties te bevoordelen, door koolstofatomen te sparen door pyruvaat naar het alaninemetabolisme te transporteren en door de verzuring van het cytoplasma tegen te gaan door het alaninemetabolisme en de GABA-shunt te activeren. Tenslotte, werd in dit proefschrift bewijs geleverd voor de aanwezigheid van een zuurstofwaarnemingsmechanisme in Jonagold-appelen, hetgeen aangeeft dat naast de substraatremming van de elektronentransportketen door de lage beschikbaarheid van zuurstof, een actief regulatiemechanisme van het centrale koolstofmetabolisme aanwezig is.

# List of abbreviations

| | |
|---|---|
| 2KG | 2-Ketoglutarate |
| 2KGDH | 2-Ketoglutarate dehydrogenase |
| AAT | Alcohol acyl transferase |
| ACA | Acetaldehyde |
| ACBP1 | Acyl-coenzyme A-binding protein 1 |
| ACO | Aminocyclopropane-1-carboxylic acid oxidase |
| ACP | Anaerobic compensation point |
| ACS | Aminocyclopropane-1-carboxylic acid synthase |
| ADH | Alcohol dehydrogenase |
| AlaAT | Alanine aminotransferase |
| AOX | Alternative oxidase |
| AS | Asparagine synthetase |
| AspAT | Aspartate aminotransferase |
| ATE | Arginyltransferase |
| ATP | Adenosine triphosphate |
| BOM | Biological oxygen monitor |
| BSTFA | N,O- Bis(trimethylsilyl(TMS))trifluoroacetamide |
| CA | Controlled atmosphere |
| $CO_2$ | Carbon dioxide |
| COX | Cytochrome C oxidase |

| | |
|---|---|
| CytC | Cytochrome C |
| DCA | Dynamic controlled atmosphere |
| DCA-CF | Chlorophyll fluorescence based DCA |
| DCS | Dynamic control system |
| DTT | 1,4-dithiothreitol |
| ERFs | Ethylene response factors |
| EthAC | Ethyl acetate |
| EthOH | Ethanol |
| $FADH_2$ | Flavin adenine dinucleotide |
| FC | Fold change |
| Fe2KGO | Fe-dependent 2-ketoglutarate oxygenase |
| FT | Fermentation threshold |
| FUH | Fumarase |
| GABA | γ-aminobutyric acid |
| GABA-T | GABA transaminase |
| GAD | Glutamate decarboxylase |
| GCMS | Gas chromatography mass spectrometry |
| GDH | Glutamate dehydrogenase |
| GO | Gene ontology |
| GS | Glutamine synthase |
| Hb | Haemoglobins |
| HRA1 | Hypoxia response attenuator 1 |
| IMM | Inner mitochondrial membrane |
| LDH | Lactate dehydrogenase |
| LOL | Lower oxygen limit |
| MAP | Methione aminopeptidase |
| MDH | Malate dehydrogenase |
| MDHAR | Monodehydroascorbate reductase |
| MES | 2-(N-morpholino) ethane sulfonic acid |
| mETC | Mitochondrial electron transport chain |

| | |
|---|---|
| $MgCl_2$ | magnesium chloride |
| MPC | Mitochondrial pyruvate carrier |
| MSD | Mass selective detector |
| NADH | Reduced nicotinamide adenine dinucleotide |
| NADH-GOGAT | NADH-dependent glutamine oxoglutarate amino transferase |
| ND2 | Non-phosphorylating NAD(P)H dehydrogenases |
| NIST | National Institute of Standards and Technology |
| NO | Nitric oxide |
| NP-GAPDH | $NADP^+$-dependent glyceraldehyde-3-phosphate dehydrogenase |
| NR | Nitrate reductase |
| $O_2$ | Oxygen |
| PCOs | Plant cysteine oxidases |
| PDC | Pyruvate decarboxylase |
| PDH | Pyruvate dehydrogenase complex |
| PDHK | Pyruvate dehydrogenase kinase |
| PEP | Phosphoenolpyruvate |
| PEPC | Phosphoenolpyruvate carboxylase |
| PFK | Phosphofructokinase |
| PFP | Pyrophosphate:fructose-6-phosphate phosphotransferase |
| PK | Pyruvate kinase |
| PPDK | Pyruvate-orthophosphate dikinase |
| Ppi | Pyrophosphate |
| PPP | Pentose phosphate pathway |
| PRT | Proteolysis E3 ligase |
| PYR | Pyruvate |
| RNS | Reactive nitrogen species |
| ROS | Reactive oxygen species |
| RQ-DCA | Respiratory quotient |
| RQ-DCA | Respiratory quotient based DCA |
| SCS | Succinate CoA ligase |

| | |
|---|---|
| SSADH | Succinate-semialdehyde dehydrogenase |
| SUS | Sucrose Synthase |
| TCA cycle | Tricarboxylic acid cycle |
| TF | Transcription factor |
| TPM | Transcripts per kilobase million |
| Tpp | Thiamine pyrophosphate |
| UGPase | UDP-glucose pyrophosphorylase |
| ULO | Ultra low oxygen storage |
| UQ | Ubiquinone |

# Table of content

**Dankwoord** ..... i

**Abstract** ..... iii

**Samenvatting** ..... vii

**List of abbreviations** ..... xi

**Table of content** ..... xv

**Chapter 1 General introduction and objectives** ..... 1

1.1 Importance of apple fruit ..... 1

1.2 Storage to preserve the quality of apple fruit ..... 3

1.3 Low-oxygen stress in plants ..... 4

1.4 Objectives and outline of the dissertation ..... 6

**Chapter 2 State of the art** ..... 9

2.1 Post harvest storage of apple fruit ..... 10

2.1.1 Fruit ripening ..... 10

2.1.2 Factors controlling the respiration rate of the fruit ..... 11

2.1.3 Internal gas gradients are present in apple fruit ..... 16

2.1.4 Controlled atmosphere storage of apple ..... 17

2.1.5 Dynamic controlled atmosphere storage of apple ..... 18

2.2 Central carbon metabolism of apple fruit ..... 22

2.2.1 Central carbon metabolism under no oxygen stress conditions ..... 23

2.2.2 Regulation of central carbon metabolism under no oxygen stress conditions ..... 28

2.2.3 Regulation of central carbon metabolism under low-oxygen stress conditions ..... 32

2.2.3.1 Energy-saving metabolic adaptations upon low-oxygen stress ..... 32

2.2.3.2 Fermentative metabolism ..... 36

2.2.3.3 Alternative pathways induced by low-oxygen stress ..... 37

2.2.4 Low-oxygen sensing and signalling ..... 42

2.2.4.1 Direct oxygen sensing ..... 42

2.2.4.2 Low-oxygen-associated secondary signalling pathway ..... 46

2.3 Unravelling the molecular and metabolic response induced by low-oxygen stress in a systems biology era ..... 46

2.3.1 High-throughput technologies to study the regulation of the hypoxic response ..... 47

2.3.2 Systems biology approach to interconnect all organizational levels ..... 50

2.4 Conclusions ..... 51

**Chapter 3 Kinetic modelling: an integrated approach to analyse enzyme activity assays** ..... 53

3.1 Introduction ..... 54

3.2 Materials and Methods ..... 56

3.2.1 Plant material ..... 56

3.2.2 Chemicals ..... 56

3.2.3 Enzyme extraction ..... 56

3.2.4 Enzyme activity measurement ..... 57

3.2.5 Determination of the absorption coefficient of NADH ..... 58

3.2.6 Data analysis ..... 58

3.3 Results and Discussion ..... 59

3.3.1 Optimization of the enzymatic assays ..... 59

3.3.2 Kinetic model development ..... 63

3.3.3 Kinetic model for alcohol dehydrogenase ..... 63

3.3.4 Kinetic model for pyruvate decarboxylase ..... 65

3.3.5 Comparison between linear regression and kinetic modelling approach to estimate enzyme activity ..... 68

3.3.6 Insights given by the model ..... 70

3.4 Conclusion ..... 73

**Chapter 4 The fermentative metabolism in apple fruit exposed to low-oxygen stress reveals highly flexible regulation** ..... 75

4.1 Introduction ..... 76

4.2 Materials and methods ..... 78

4.2.1 Plant material ..... 78

4.2.2 Experimental design ..... 78

4.2.3 Chemicals ..... 80

4.2.4 Enzyme extraction ..... 80

4.2.5 Enzyme activity measurement ..... 80

4.2.6 Fermentation metabolites....81

4.2.7 Model development....81

4.2.8 Data analysis....84

4.3 Results....84

4.3.1 General model findings....84

4.3.2 The effect of low-oxygen stress on the induction of fermentation at low temperature....86

4.3.3 The effect of low-oxygen stress on the induction of fermentation at high temperature....88

4.3.4 Does storage influence the induction of fermentation under low oxygen conditions?....89

4.4 Discussion....92

4.4.1 General fermentation patterns confirmed....92

4.4.2 The overall metabolic reaction rate influences the regulation of the fermentative metabolism....93

4.4.2.1 Fermentative metabolism is only metabolically controlled at a slow overall metabolic rate....94

4.4.2.2 Combination of molecular and metabolic control regulates the fermentative metabolism at a high overall metabolic rate....97

4.4.3 Influence of storage on the regulation of the fermentative metabolism....98

4.4.3.1 In vivo enzyme activity of PDC does not need additional activation after storage....100

4.4.3.2 In vivo enzyme activity of ADH increases during anoxia after storage....100

4.4.4 Fermentative metabolism is differently induced under anoxic and hypoxic conditions after storage ..... 101

4.4.5 Why are the concentrations of the fermentation metabolites decreasing towards the end of the experimental period? ..... 102

4.5 Conclusions ..... 103

**Chapter 5 Unravelling the regulation of the central carbon metabolism during low-oxygen stress** ..... 105

5.1 Introduction ..... 106

5.2 Materials and methods ..... 108

5.2.1 Plant material ..... 108

5.2.2 Experimental design ..... 108

5.2.3 Primary metabolite analysis ..... 111

5.2.4 Metabolite quantification and $^{13}C$-label enrichment ..... 112

5.2.5 RNA extraction and precipitation ..... 112

5.2.6 Library construction, sequencing and data processing ..... 113

5.2.7 RNA-sequencing data analysis ..... 114

5.2.8 Enzyme extraction and activity measurement ..... 115

5.2.9 Fermentation metabolites ..... 115

5.2.10 Respiration measurement ..... 115

5.3. Results and Discussion ..... 116

5.3.1 Preliminary experiments determining the optimal pyruvate concentration and confirming its cellular uptake ..... 116

5.3.2 Induction of fermentation ..... 119

5.3.3 Metabolic profiling and flux analysis of the apple cortex under low oxygen-stress ..... 121

5.3.4 Transcript profiling of the apple cortex under low-oxygen stress ..... 121

5.3.4.1 General overview of transcriptomic changes induced by low-oxygen stress ..... 121

5.3.4.2 Metabolic adaptations to save energy are induced ..... 125

5.3.4.3 Glycolytic flux is increased ..... 133

5.3.4.4 Pyruvate is no longer shuttled directly into the TCA cycle ..... 135

5.3.4.5 Fermentative metabolism is induced ..... 138

5.3.4.6 Changes in amino acids metabolism ..... 141

5.3.4.7 Oxygen sensing mechanism ..... 148

5.4. Conclusion ..... 153

**Chapter 6 General conclusions and future perspectives** ..... 155

6.1 General conclusions ..... 155

6.2 Future perspectives ..... 158

**Bibliography** ..... 163

**Appendices** ..... 185

Appendix 1 – Chapter 3 ..... 185

ADH_model ..... 185

PDC_model ..... 187

Appendix 2 – Chapter 5 ..... 189

**Publications** ..... 191

Articles in internationally reviewed academic journals ..... 191

Papers at international scientific conferences and symposia published in full in proceedings .....191

# Chapter 1

# General introduction and objectives

## 1.1 Importance of apple fruit

Apple fruit (*Malus* x *Domestica* Brokh.) belongs to the Rosacea family and is one of the most common fresh fruits. Together with pear fruit, apples are the most consumed fruit in Europe and the second most consumed fruit in the USA (WAPA). Apple fruit contains many bioactive compounds, such as vitamins, organic acids, phenolics and anti-oxidants (Mditshwa *et al.*, 2018). In 2016, more than 133 million tons of apple fruit were produced worldwide. Europe was the second largest producer of apple fruit (19,4 %) in 2016, after Asia (65.8 %) and before North and South America (11 %; Fig. 1.1; FAOstat, 2016). With a production of 238 244 tons apple fruit in 2016, Belgium takes the 41$^{st}$ position in the list of apple producing countries worldwide. The top 10 producers of apple fruit worldwide is represented in Table 1.1 (FAOstat, 2016).

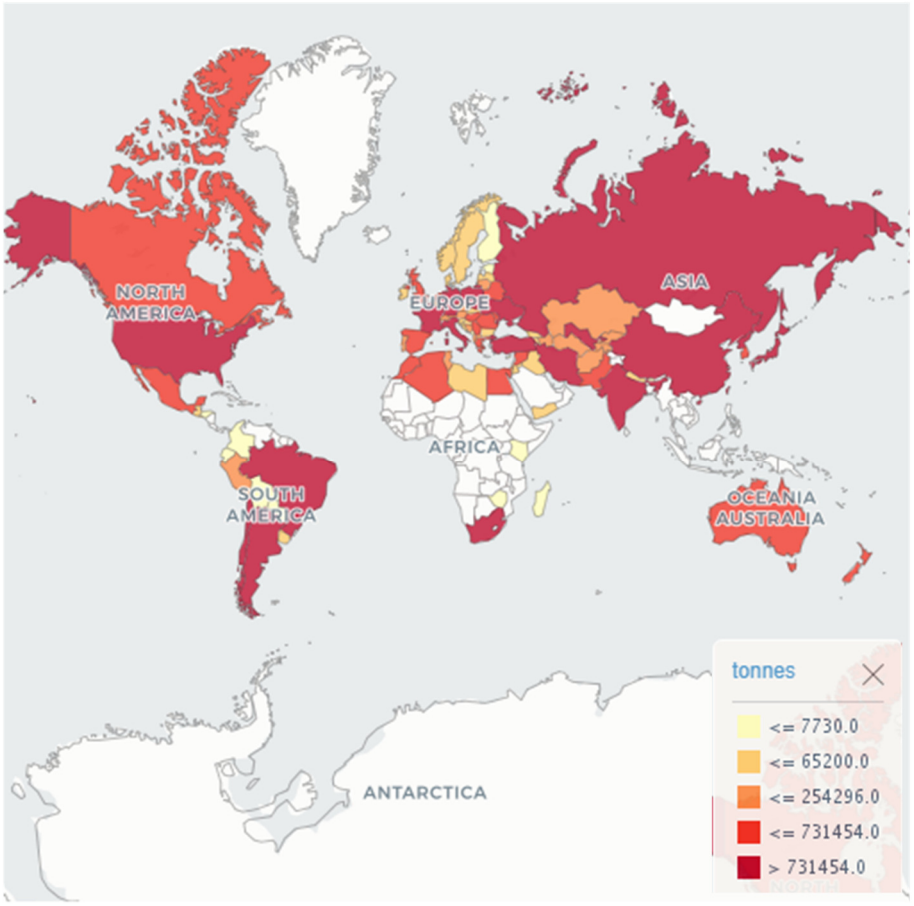


Figure 1.1: Production quantities of apple fruit per region in 2016 (FAOstat).

Most of the production of apple fruit in Belgium is localized in Flanders and is used for the domestic market. In Belgium, mainly 'Jonagold' apple fruit is grown, but over the last years also novel 'club varieties' appeared. However, the apple production in Belgium and Europe is under much pressure lately due to the import ban from Russia since August 2014 (deredactie,2014). The competition on the world market is high, hence, it becomes more and more important to focus on top quality apple fruit, so fruit growers can promote their high quality products not only in Belgium but also abroad on distant markets (VILT, 2018).

Table 1.1: Top 10 apple producing countries; the numbers are an average over the last 16 years (2000-2016).

| | Tons |
|---|---|
| China | 30 548 675 |
| USA | 4 424 506 |
| Iran | 2 645 284 |
| Turkey | 2 549 428 |
| Poland | 2 481 154 |
| Italy | 2 243 329 |
| India | 1 875 581 |
| France | 1 787 981 |
| Russia | 1 630 108 |
| Chile | 1 431 579 |

## 1.2 Storage to preserve the quality of apple fruit

As apple fruit are harvested only once a year in the Northern hemisphere, it is important to be able to provide consumers year round with high quality apple fruit. Apples are, therefore, traditionally stored under low temperature controlled atmosphere (CA) conditions (reduced oxygen and elevated carbon dioxide concentrations) to reduce ethylene biosynthesis and respiration rate. The optimal storage conditions are critical as fruit may develop storage disorders when stored under suboptimal conditions (Yahia, 2009). However, the exact optimum may vary with the season, cultivar, origin and picking date. Therefore, safe but likely suboptimal conditions are often maintained resulting in higher quality losses then strictly needed (Bessemans *et al.*, 2016; Wright *et al.*, 2011). Although the static approach of CA storage is able to preserve quality to a large extent, it does not always provide optimal post-storage shelf life results (Prange *et al.*, 2013).

To deal with market competition, quality losses and incidences of oxygen-related storage disorders need to be further minimized (Bessemans *et al.*, 2016). Therefore,

CA storage was further improved through the development of dynamic CA (DCA) storage. DCA storage is a more advanced storage technology, that changes the oxygen partial pressure over time to adapt to the changing fruit physiology. By monitoring the biological stress response of the stored fruit to low oxygen concentration and adapting and actively controlling the actual storage conditions, suboptimal oxygen concentrations can be avoided. DCA has been shown to delay ripening more effectively, deliver better post storage quality and better control certain storage disorders, i.e., superficial scald, as compared to normal CA storage (Bessemans *et al.*, 2016; Mditshwa *et al.*, 2018; Watkins, 2008).

## 1.3 Low-oxygen stress in plants

Even under normoxia, plants can experience low-oxygen stress due to steep oxygen gradients inside the tissue (Fig. 1.2). The supply of oxygen in plant tissues depends on passive transport, as they lack an active distribution system to transport oxygen. The oxygen consumption rate of the cells, the conductivity for gas transport in the tissue, the length of the transport pathway, the microscale geometrical features of the cell, such as shape and size, and the three-dimensional connectivity of cells and air spaces have all an influence on the internal oxygen concentrations (Ho *et al.*, 2011; van Dongen and Licausi, 2015). Low oxygen concentrations have been found in stem tissue (Fig. 1.2B; Van Dongen *et al*., 2003), the centre of developing seeds (Fig. 1.2A and E; Borisjuk and Rolletschek, 2009) and in bulky storage tissues such as potato tubers (Fig. 1.2F; Licausi et al., 2011a), large fruits (Fig. 1.2D; Ho *et al*., 2011) and roots (Fig. 1.2C; Armstrong *et al.*, 1994). If the oxygen availability in the environment decreases, the area of low oxygen concentration inside the tissue will expand (Ho *et al.*, 2011; van Dongen and Licausi, 2015).

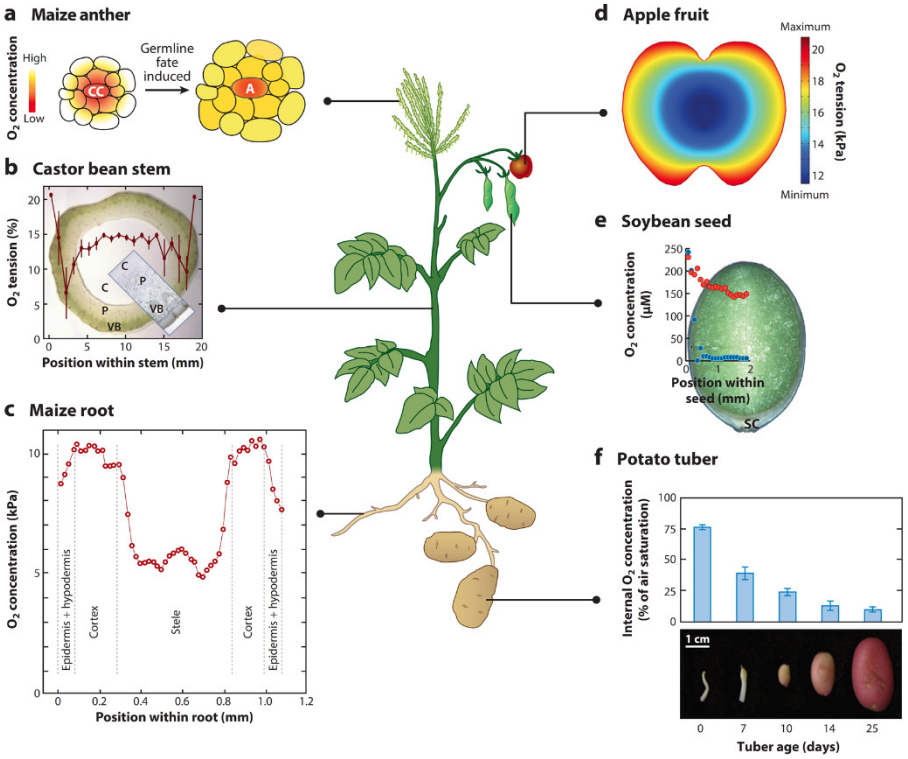


Figure 1.2: Oxygen gradients exist inside different types of plant tissue (van Dongen and Licausi, 2015; Used with permission).

Cells which experience low-oxygen stress, due to oxygen gradients in the plant tissue, undergo physiological changes to remain able to provide enough energy to survive. Oxygen then becomes limiting as a substrate for cytochrome c oxidase in the electron transport chain, and the ATP production via oxidative phosphorylation decreases. In order to meet the cellular demands of ATP to survive, plants can increase their glycolytic flux to enhance ATP production by substrate-level phosphorylation. To be able to maintain this high glycolytic flux, $NADP^+$ and $NAD^+$ have to be regenerated (António *et al.*, 2016; Bailey-Serres *et al.*, 2012; Geigenberger, 2003). Therefore, the increase in glycolytic flux is typically coupled to the fermentative metabolism (António *et al.*, 2016; Bailey-Serres *et al.*, 2012; Geigenberger, 2003; Gibbs and Greenway, 2003; Van Dongen and Licausi, 2015).

Besides the effect that DCA has on the main quality parameters, little is known about the precise effect of low oxygen concentrations on the metabolic processes and compositional changes of apple fruit. The lack of fundamental knowledge about the influence of low-oxygen stress on the central carbon metabolism in apple fruit, hampers the improvement of DCA storage.

## 1.4 Objectives and outline of the dissertation

To be able to further improve the development of the DCA storage technology to maximize fruit quality retention during storage, it is important to fully understand the impact of low-oxygen stress on the physiology of apple fruit. Therefore, the **main objective** of this dissertation is to investigate low-oxygen stress in 'Jonagold' apple by unravelling the regulation of the respiratory metabolism of apple during (dynamic) controlled atmosphere storage.

To achieve this main objective, the following research questions were formulated:

I. Under which conditions is the fermentative metabolism activated and how are these pathways regulated *in vivo*?
II. Besides fermentation, which other metabolic changes are introduced during low-oxygen stress and what is their impact on the survival of the fruit?
III. Is there a regulatory mechanism present which actively regulates the metabolic changes introduced by low-oxygen stress?

To be able to answer these research questions, the following research tasks were defined:

- To develop a kinetic modelling approach to analyse *in vitro* enzyme activity assays in order to study the enzyme activity of pyruvate decarboxylase and alcohol dehydrogenase.
- To study the regulation of the fermentative metabolism under different experimental conditions
- To characterize changes introduced by low-oxygen stress in the metabolome and fluxome of the central carbon metabolism in apple tissue discs fed with [U-$^{13}$C] pyruvate, using GC-MS metabolic profiling.
- To study the transcriptional regulation of the metabolic changes introduced by low-oxygen stress using RNA-sequencing.

The outline of this dissertation is represented in Fig. 1.3.

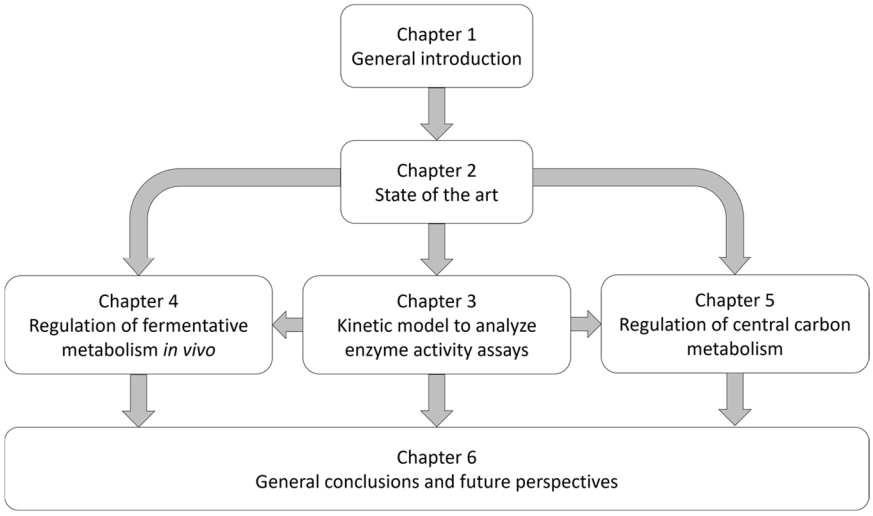


Figure 1.3: Schematic representation of the outline of this dissertation.

A literature review will be given in **Chapter 2**. In this chapter the state of the art on postharvest storage of apple fruit will be presented further focusing on the central carbon metabolism, both under normal oxygen conditions and under low-oxygen stress conditions. In addition, a short overview will be given of the mechanisms acting at different cellular organizational levels that regulate the metabolic response induced during postharvest storage.

In **Chapter 3** a novel method based on a kinetic modelling approach will be introduced to estimate the *in vitro* specific enzyme activity of pyruvate decarboxylase and alcohol dehydrogenase from spectrophotometric assay data. In contrast to the classical linear regression approach, these models can be used to estimate the enzyme activity regardless of whether linearity is achieved since they integrally take into account the complete progress curve.

In **Chapter 4** the *in vivo* regulation of the fermentative metabolism of 'Jonagold' apple fruit will be investigated by exposing apple tissue slices to different oxygen concentrations and temperatures at harvest and after storage. A combination of experimental techniques and a kinetic modelling approach will be used to translate the *in vitro* measured enzyme activity (analysed by the models developed in chapter 3) into *in vivo* activities and to provide new insights in the regulation of the fermentative metabolism.

In **Chapter 5**, the metabolic changes of the central carbon metabolism and its transcriptional regulation will be studied in more detail by a combination of metabolomics, fluxomics and transcriptomics analyses. Further evidence of the existence of an active regulatory mechanism of the central carbon metabolism by oxygen sensors will be provided.

In **Chapter 6**, general conclusions will be stated and possible future research perspectives will be addressed.

# Chapter 2

# State of the art

After harvest, apple fruit remains metabolically active and continues to ripen. The main goal of postharvest storage is to slow down the metabolic activity and with that the ripening process of the fruit, thus to provide consumers year round with high quality apple fruit. Generally, this is accomplished by storing apple fruit at low temperature in combination with low oxygen ($O_2$) and high carbon dioxide ($CO_2$) partial pressures. However, altering the normal atmospheric conditions is not without risk at the plant physiology level: it may induce low-oxygen stress. To further optimize the postharvest storage of apple fruit, it is important to better understand the physiological effects and their underlying regulation during postharvest storage.

This state-of-the-art chapter will start with setting the stage of postharvest storage of apple fruit. Then the focus will turn to the central carbon metabolism of the fruit, both under normal oxygen conditions and under low-oxygen stress conditions. In the next section, a short overview will be given of the different cellular organizational levels which regulate the metabolic response induced during postharvest storage and on the importance of studying their interconnection.

# 2.1 Post harvest storage of apple fruit

## 2.1.1 Fruit ripening

There are four defined physiological stages making up fruit development, namely fertilisation and cell division, growth, maturation and senescence (Biale, 1946; Wills and Golding, 2016). Fruit ripening is considered to cover the later stages of maturation until the beginning of senescence (Fig. 2.1): it is the process through which a fully grown, mature but inedible plant organ is transformed into an attractive edible fruit with an optimal blend of colour, aroma and texture. During this complex, highly coordinated and genetically programmed transformation process a sequence of changes occurs (Giovannoni, 2001). Fruit becomes softer by the enzymatic breakdown of cell walls. Volatile components for aroma and pigments for colour are being synthesized as well (Brummell, 2006; Dixon and Hewett, 1998; El-ramady *et al.*, 2015; Espino-Diaz *et al.*, 2016; Fellman *et al.*, 2003; Ganai *et al.*, 2015; Johnston *et al.*, 2002; Waldron *et al.*, 2003). Furthermore, starch hydrolysis takes place while sugars accumulate and organic acids disappear, contributing to fruit flavour (Nath *et al.*, 2014).

Ripening is closely related to the metabolic activity of the fruit, more specifically to respiration. The respiration rate differs depending on the developmental stage of the fruit. During the growth stage, before ripening starts, respiration rate decreases and reaches a minimum, which is called the pre-climacteric minimum. Fruit can be divided into two groups based on their subsequent respiratory behaviour during ripening: climacteric and non-climacteric fruit (Biale, 1946; Saltveit, 1999; Wills and Golding, 2016). For climacteric fruit like pear and apple, the ripening process is characterized by a rise in respiratory activity and ethylene production (Blackman and Parija, 1928; Krotkov, 1941; Lelievre *et al.*, 1997). This respiratory climacteric rise marks the end of a period of active synthesis and maintenance. After the respiratory

climacteric peak fruit senescence starts. For non-climacteric fruit, such as orange, lemon, pineapple, grapes and strawberry, there is no peak in respiration and ethylene production rates remain low (Fig. 2.1; Alexander and Grierson, 2002; Paul *et al.*, 2012; Wills and Golding, 2016). Tree-ripened apple fruit are known to have the best taste and aroma (Brückner and Wyllie, 2008; Song and Bangerth, 1996). However, to maximize their storage potential, apples are harvested one or two weeks before their climacteric rise. Subsequently, the fully grown but unripe fruit are stored under conditions retarding the metabolic activity of the fruit to delay subsequent fruit ripening and senescence.

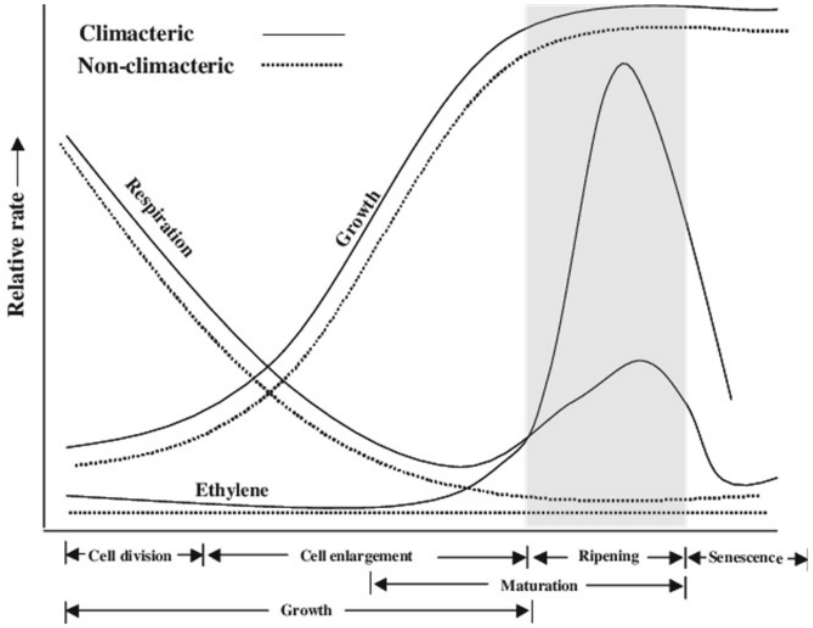


Figure 2.1: The relative respiration, growth and ethylene production rate during the different developmental stages of climacteric and non-climacteric fruit (Wills and Golding, 2016; used with permission).

## 2.1.2 Factors controlling the respiration rate of the fruit

The respiratory climacteric rise, and thus the increase in ethylene production, should be delayed as long as possible to successfully preserve the quality of fruit for an extended period (Brady, 1987; Paul and Pandey, 2014; Streif, 2010). Respiration rate

can be controlled by three environmental factors: temperature, oxygen and carbon dioxide concentration (Cameron *et al.*, 1994; Hertog *et al.*, 1998; Lammertyn *et al.*, 2001). Lammertyn *et al*. (2001) showed for pear that, of these factors, temperature is the most influential. The inhibitory effect of low temperature on the respiration rate is due to the decrease in catalytic activity of respiratory enzymes (Atkin *et al.*, 2005; Bron *et al.*, 2005; Falagán and Terry, 2018; Graham and Patterson, 1982; Lyons, 1973). Therefore, to minimize respiration, fruit is stored at the lowest possible temperature, with the obvious restriction that the fruit may not freeze or develop chilling injuries (Jackman *et al.*, 1989; Wang, 2010). Moreover, low temperature storage reduces the growth of fungi, bacteria and insects (Thompson, 2010; Yahia, 2006).

Not only temperature but also gas conditions have an influence on fruit respiration and ripening. As will be discussed in section 2.2.1, $O_2$ is used as a final electron acceptor in the electron transport chain. By lowering the $O_2$ concentration in the storage atmosphere, the respiration of many fruit and vegetables slows down (Biale, 1946; Ke *et al.*, 1991b; Teixeira and Durigan, 2010; Thompson, 1998; Yearsley *et al.*, 1996). The metabolic respiration chain consist of different pathways in which $CO_2$ is produced (TCA cycle) and $O_2$ is consumed (mitochondrial electron transport chain). As indicated in Fig. 2.2, the respiration rate, represented by the $O_2$ consumption rate (blue line) and the total $CO_2$ production rate (green line) until the fermentation threshold (FT), decreases as the $O_2$ concentration decreases. However, when the oxygen concentration is becoming close to anoxia, the fruit metabolism shifts from aerobic respiration to fermentation (see section 2.2.3 Geigenberger, 2003; Prange *et al*., 2005), resulting in flavour and storage disorders (Franck *et al.*, 2007; Kader *et al.*, 1989; Thompson, 2010). Due to this metabolic shift, the $CO_2$ produced by the glycolysis will increase again, as well as the $CO_2$ produced by fermentation (red line), leading to an increase in the total $CO_2$ production (green line). The oxygen concentration at which the total respiratory $CO_2$ production rate is minimal is called the anaerobic compensation point (ACP) (Boersig *et al.*, 1988; Prange *et al.*, 2005).

Low oxygen concentration does not only affect the respiration rate but also the production of ethylene, since oxygen is needed in the last step of ethylene production. Therefore, by reducing the oxygen partial pressure during storage, the postharvest ripening of the fruit will be slowed down.

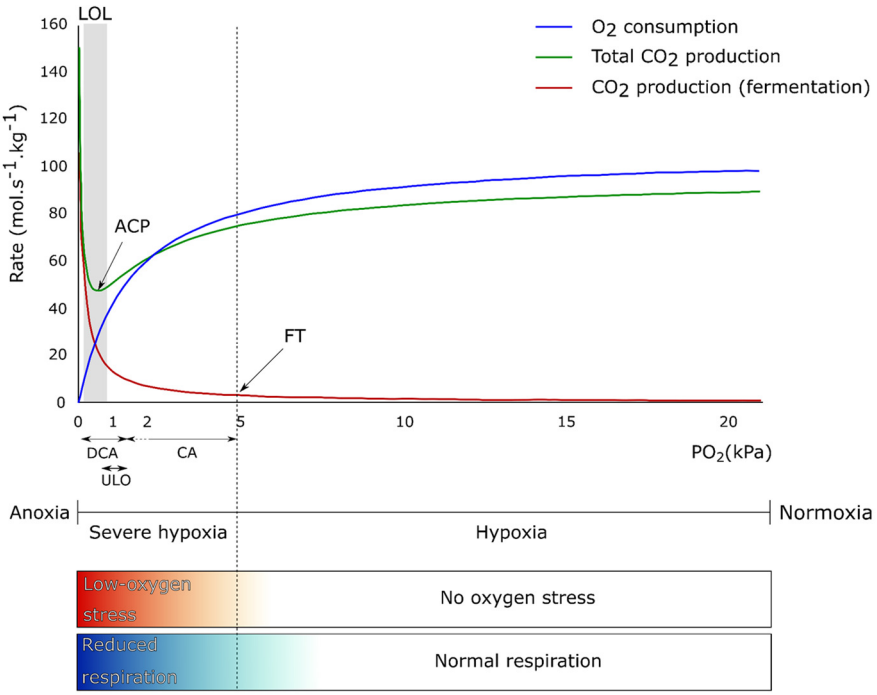


Figure 2.2: Theoretical effect of oxygen concentration on $O_2$ consumption (blue line), total $CO_2$ production (green line) and $CO_2$ production from fermentation (red line). The anaerobic compensation point (ACP), fermentation threshold (FT) and lower oxygen limit (LOL) are indicated, as well as the range of $PO_2$ applied in CA, ULO and DCA storage. The term "no oxygen stress" is used to define all oxygen levels where enough oxygen is available for the plant to have a normal respiratory metabolism, ranging from normoxia (typically 20.6 % oxygen and 0.03 % carbon dioxide at 101.325 kPa and 20 °C) and below (hypoxia). The term "low-oxygen stress" is used when oxygen levels are limited (severe hypoxia) or completely absent in the environment (anoxia) and plants need to reduce or adapt their respiratory metabolism.

Finally, also the $CO_2$ concentration can influence the respiration rate of the fruit. However, the role of $CO_2$ on the respiration metabolism is not completely understood. Increased $CO_2$ concentration has been shown to retard respiration rate

of broccoli, Belgian endives, mung bean sprouts, apples, melons, ripening tomatoes and bananas (Kubo and Inaba, 1989; Peppelenbos and Van 't Leven, 1996), whereas slight or no effect was found on the respiration rate of lemons, potatoes, sweet potatoes and cabbage and an increase in respiration was observed in lettuce, eggplants and cucumbers (Kubo and Inaba, 1989). The response of fruit and vegetables on elevated $CO_2$ concentration is determined by the sensitivity of the commodity, the $CO_2$ partial pressure in the storage room, the physiological state of the produce, and the temperature and duration of exposure (Kubo and Inaba, 1989; Mathooko, 1996). It was speculated that the different sensitivity of the various commodities may be due to differing internal concentrations of $CO_2$ which arises because of a different respiration rate and a different anatomical structure of the produce or due to specific enzymatic reactions (Mathooko, 1996; Monning, 1983). Several studies suggested that $CO_2$ could act as a controlling factor by inhibiting the activity of various enzymes of the respiratory metabolism (Ke *et al.*, 1995; Kerbel *et al.*, 1988; Knee, 1973; Monning, 1983; Shipway and Bramlage, 1973). Furthermore, it has been shown that high concentrations of carbon dioxide might inhibit growth of spoilage microorganisms (Conesa *et al.*, 2007) but may cause brown discoloration and softening of flesh tissue (Conesa *et al.*, 2007; Ke *et al.*, 1991a; Pedreschi *et al.*, 2008).

Commonly, the total inhibitory effect can be greater when a combination of these three environmental factors is applied (Kader *et al.*, 1989). Hertog *et al*., (1998) collected data on gas exchange at different temperatures and gas conditions for apple ('Golden Delicious'). They could observe a clear effect of $O_2$ concentration on the level of respiration and on the occurrence of fermentation, as can be seen in Fig. 2.3. Both the maximum observed respiration rate at high oxygen concentration and the maximum fermentation rate at 0 % $O_2$ depended on temperature. Furthermore, respiration and fermentation showed an increased level of inhibition with increasing $CO_2$ concentrations. However the overall effect of temperature was more pronounced than the effect of $CO_2$ (Hertog *et al.*, 1998).

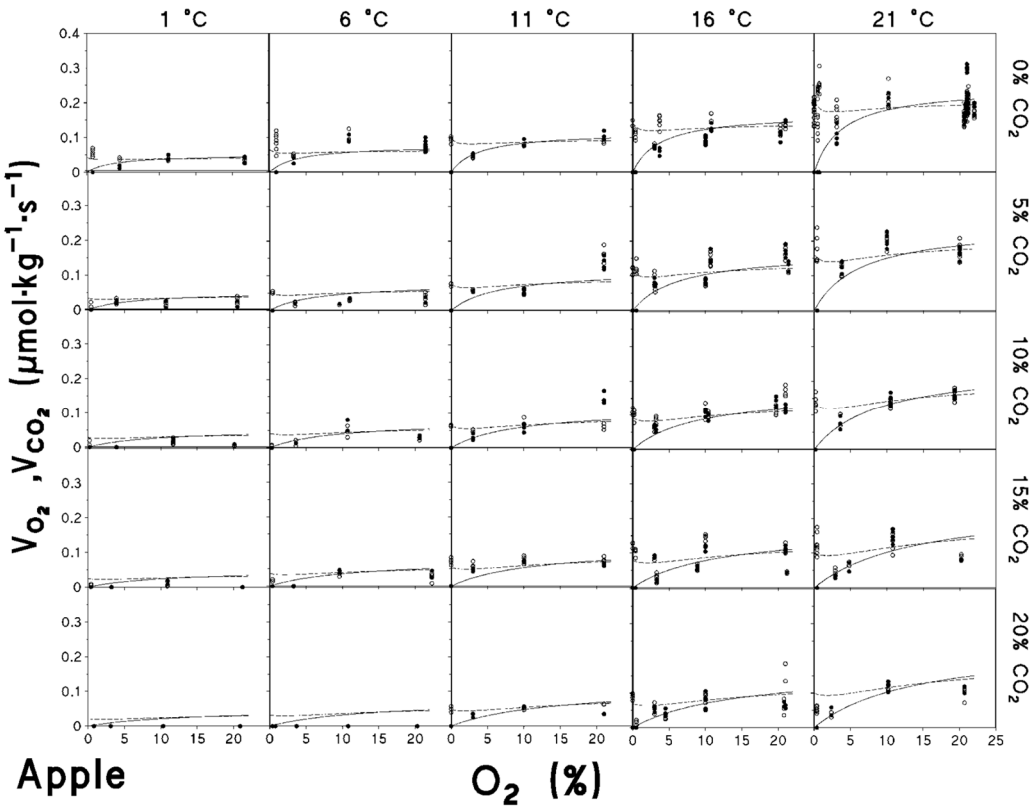


Figure 2.3: Gas exchange profiles of 'Golden Delicious' at different temperatures (columns of graphs) and different gas conditions ($O_2$; x-axes and $CO_2$; rows of graphs). $O_2$ consumption is indicated on the graphs with closed symbols and continuous lines, whereas CO2 productions is indicated with open symbols and dotted lines (Hertog *et al.*, 1998; used with permission).

### 2.1.3 Internal gas gradients are present in apple fruit

In bulky plant organs such as roots, tubers, stems, seeds and fruit, the gas exchange of $O_2$ and $CO_2$ with the environment might be insufficient, leading to gas gradients in the tissue (Drew, 1997; Geigenberger *et al.*, 2000; Ho *et al.*, 2013, 2011, 2010; Lammertyn *et al.*, 2003; Verboven *et al.*, 2008). Therefore, one needs to be careful by changing the external atmosphere around a bulky plant, as the core can become anoxic. The internal $O_2$ and $CO_2$ concentrations are determined by the local respiration rate of the fruit tissue and by the gas transport properties of the fruit for $O_2$ and $CO_2$ from the epidermis to parenchyma (Ho *et al.*, 2013). The skin of apple fruit is known to have a very dense tissue structure, making diffusion of gasses difficult (Schotsmans *et al.*, 2004). It has been shown that in the cortex tissue of fruits, an internal ventilation system is present which consists of intercellular pores interconnected by small capillary channels creating a gas transport system, which facilitates gas exchange throughout the tissue (Mendoza *et al.*, 2007; Verboven *et al.*, 2008).

Models have been developed to describe gas exchange of fruit with their environment (Ho *et al.*, 2013, 2011, 2010, 2008; Lammertyn *et al.*, 2003). Ho *et al.* (2011) developed a multiscale model to calculate gas exchange in the fruit using both the macroscopic gas concentration profiles and the microscale geometry of the tissue. They observed that it was important to take the microscale structure of the tissue into account in the model to be able to calculate the correct intracellular concentrations (Ho *et al.*, 2011). Furthermore, Ho *et al.* (2010) observed that different apple cultivars have a different microscale geometry of the tissue (different porosities, pore size distribution and interconnectivity), which highly influences the internal gas transport properties. The macroscale simulation showed that 'Braeburn' apple fruit have a higher risk to develop storage disorders at low oxygen storage as compared to 'Jonagold' and 'Kanzi' apple fruit due to the stronger diffusion barrier of the cortex tissue (Ho *et al.*, 2010).

## 2.1.4 Controlled atmosphere storage of apple

To extend the useful marketing period after harvest and to preserve the quality of apple fruit, they are commonly stored under controlled atmosphere (CA) conditions. During CA storage, the three most important environmental conditions (temperature, $O_2$ and $CO_2$) are controlled, as well as the duration of storage, and relative humidity (Dilley, 2010; Saltveit, 2003). The optimal storage conditions are critical as fruit may develop storage disorders when stored under suboptimal conditions such as a too low temperature, whereas a too high temperature is also suboptimal as it would increase ripening and thus decrease the potential storage life. Therefore, the storage conditions in commercial cool stores are set at safe and steady values that are maintained for the whole storage period. The optimal conditions vary depending on the cultivar, geographic location, harvest date, expected storage duration, and season (Dilley, 2010; Saltveit, 2003; Watkins and Nock, 2012). Apple fruit are stored at the lowest safe temperature to avoid freezing or chilling injury. The temperature at which chilling injuries appear is mostly cultivar dependent. Some apple cultivars such as 'McIntosh' are sensitive to low temperature and require storage at 3 – 4.5 °C (Lévesque *et al.*, 2006), while other cultivars like 'Jonagold' are chilling insensitive and can be safely stored at 0 – 1 °C (Saquet and Streif, 2008). The gas conditions are kept at the lowest safe oxygen partial pressure (2.0 – 5.0 kPa $O_2$; Fig 2.2) and the highest safe carbon dioxide partial pressure (2.0 – 5.0 kPa $CO_2$) with the actual values depending on the cultivar (Dilley, 2010; Yahia, 2009). However, it was observed that further lowering the $O_2$ partial pressure may result in an even better quality after storage. During "ultra-low oxygen (ULO)" storage, the oxygen partial pressure is further reduced to 0.8 – 1.2 kPa $O_2$ (Fig 2.2) in combination with 0.5 – 2.0 kPa $CO_2$ partial pressure (Yahia, 2009). Apples stored in ULO maintain higher flesh firmness (Zanella *et al.*, 2008) and less physiological disorders, such as superficial scald (Zanella, 2003), flesh breakdown and mealiness (Weber *et al.*, 2011). Both during regular CA and ULO storage, the static $O_2$ partial pressure needs to be set above the lower oxygen limit (LOL) – which is the lowest $O_2$

concentration at which the fruit can be stored without developing flavour and storage disorders (Wright *et al.*, 2011; Yahia, 2009; Yearsley *et al.*, 1997). Often, the ACP of the stored fruit is used as a target point for the LOL. However, depending on the cultivar, the preharvest conditions and the postharvest handling of the fruit, the LOL can be lower or slightly higher as compared to the ACP (indicated on Fig 2.2 by a grey zone; Yearsley *et al.*, 1996). Since the LOL may be slightly different every year, a safe but likely suboptimal oxygen concentration slightly above the ACP is often maintained resulting in higher quality losses (Bessemans *et al.*, 2016; Wright *et al.*, 2011).

Furthermore, the relative humidity in the storage room is kept high (more than 95 %), in order to avoid moisture loss, and thus weight loss, from the commodity (Dilley, 2010). Finally, fruit may be treated with ethylene biosynthesis inhibitors and signal transduction blockers to suppress the initiation or development of climacteric ripening and fruit senescence (Dilley, 2010; Zanella, 2003) or ethylene can be removed out of the storage room via ethylene scrubbers (Lau, 1990).

### 2.1.5 Dynamic controlled atmosphere storage of apple

The static approach of CA and ULO storage technologies preserves quality to a large extent, but does not always provide optimal post-storage shelf life results (Prange *et al.*, 2013). In order to meet the increasing demands of consumers and to deal with market competition, quality losses (decreasing firmness, discoloration) and incidences of oxygen related storage disorders, such as superficial scald, need to be minimized (Bessemans *et al.*, 2016). To fulfil these demands, CA storage was further improved through the development of dynamic CA (DCA) storage (Mditshwa *et al.*, 2018). During DCA storage, fruit are no longer stored at suboptimal oxygen concentrations, but the CA conditions change over time to adapt to the changing fruit physiology. By storing fruit at oxygen concentrations closer to, and preferably

at the LOL (Fig 2.2), ripening can be delayed more effectively than in regular CA or ULO storage (Bessemans *et al.*, 2016; Mditshwa *et al.*, 2018; Watkins, 2000).

Crucial to any DCA approach is the close monitoring of the fruit's metabolic response, timely indicating increased low-oxygen stress. There are several types of DCA storage technologies available, which monitor different parameters to detect low-oxygen stress in the fruit. The most noticeable technologies are chlorophyll fluorescence-based DCA (DCA-CF), ethanol-based DCA (Dynamic control system (DCS)) and respiratory quotient-based DCA (RQ-DCA) (Bessemans *et al.*, 2016; Gasser *et al.*, 2008; Maxwell and Johnson, 2000; Prange *et al.*, 2003; Schouten *et al.*, 1998; Veltman *et al.*, 2003). The DCA-CF system, HarvestWatch™, is currently the most implemented DCA system. According to their website, more than 1680 DCA-CF rooms were being used in 15 countries worldwide at the end of 2015. Chlorophyll fluorescence can be used to measure low-oxygen stress, as the fluorescence signal will increase if oxygen partial pressure becomes too low. The system uses a fluorescence-interactive response monitor to sense fluorescence changes in real time. However, the disadvantages of this system are on one hand the limited sample size since only a few HarvestWatch™ systems, each containing six fruit, are used in a commercial storage room, which are assumed to represent all fruit in the storage room, and on the other hand the fact that the adjustment of the CA gas composition requires human intervention and only happens in the first two weeks of storage, after which it is put at a safe and steady oxygen partial pressure (0.2 % above the LOL) (Bessemans *et al.*, 2016; Prange and Zanella, 2009; Watkins, 2000). The dynamic control system (DCS) uses a small box containing 20 kg of fruit, which is placed inside the storage facility. Ethanol concentrations measured in the headspace are being used as an indication of low-oxygen stress in the fruit (Veltman *et al.*, 2003). However, the ethanol concentration measured is an underestimation of the low-oxygen stress experienced by the fruit. Ethanol is highly soluble in water, causing most ethanol formed through fermentation to stay inside the fruit cells. Additionally, ethanol can be further metabolized by the fruit (Sander, 2015). Similar as in the DCA-

CF system, only a small amount of fruit is used to represent the bulk of the stored fruit. The third DCA technology is RQ-DCA, which measures the respiratory quotient (RQ) of the stored fruit to detect low-oxygen stress in the fruit (Bessemans *et al.*, 2016; Mditshwa *et al.*, 2018). The RQ is defined as the ratio of the carbon dioxide production rate to the oxygen consumption rate of the stored fruit and is a direct measurement of the respiratory and fermentative status of the fruit (Bessemans *et al.*, 2016; Yearsley *et al.*, 1996). Because leakage of the storage room can corrupt the RQ measurements, RQ was only measured off-line before (Gasser *et al.*, 2005). However, measuring the RQ continuously would be ideal, since the lower oxygen limit may change throughout the storage season. Recently, several commercial RQ-based systems have been introduced to the market, which avoid or compensate for leakage and measure the RQ semi-continuously. Most commercially available RQ-DCA systems (Safepod, ICA,UK (Schaefer and Bishop, 2014; CA 2746152 C); Box, Isolcell, IT (Brackmann, 2015; EP 2918179 B1)) use small containers which are placed inside a storage room to avoid leakage. However, similar to the DCA-CF and DCS systems this has the disadvantage that the gas composition in the cool room is regulated based on the bio-response of a small amount of fruit. Van Amerongen CA Technology developed a RQ-DCA system which measures the changes of the gas composition in an entire storage room. They circumvent the impact of leakage of the room on the RQ determination by creating a slight overpressure in the room (Veltman, 2013; EP 2816890 A1). The MeBioS Postharvest group (Bessemans *et al.*, 2017; EP 2017062040 Delele *et al.*, 2014; EP 2547213 B1) developed a RQ-DCA system which uses an accurate leakage model to predict pressure driven transport of gasses over the storage facility wall to correct the RQ for leakage. This RQ-DCA system is not yet commercial available but has been thoroughly tested in the lab (Bessemans *et al.*, 2016).

As compared to regular CA and ULO storage, the DCA systems have been shown to reduce respiration rate, as well as ethylene biosynthesis, and thus ripening, even more. Cukrov *et al*. (2016) found that under hypoxic conditions ethylene production

is negatively affected through a repressive effect on both aminocyclopropane-1-carboxylic acid synthase (ACS) and aminocyclopropane-1-carboxylic acid oxidase (ACO) transcript expression in an oxygen concentration dependent way. DCA has been shown to better maintain and control some commercial quality parameters. This technology reduced the incidence of superficial scald in susceptible cultivars such as 'Granny Smith' (Bessemans *et al.*, 2016). Furthermore, DCA proved to be effective in retaining firmness and acidity in specific varieties such as 'Holsteiner cox', 'Boskoop'(Brizzolara *et al.*, 2017), 'Ariane' (Gasser and Von Arx, 2015) and 'Braeburn' (Zanella and Rossi, 2015). However, the beneficial capacity of DCA storage to reduce firmness loss was not visible for every cultivar (Gasser and Von Arx, 2015; Zanella and Rossi, 2015). The variation in response between apple varieties indicates that, within the same species, different hypoxia-related regulatory mechanisms may be present.

While the global effect DCA has on the main quality parameters is known, the precise mode of action of low oxygen concentrations on metabolic processes and compositional changes of apple fruit is not. There are some studies available on the effect of long-term CA storage at oxygen concentrations ranging from 1 to 3 kPa, which have provided important information on metabolic adaptations of apple fruit during CA storage (Bekele, 2015; Brizzolara *et al.*, 2017; Saquet and Streif, 2008), but the focus of most studies is on the processes and metabolites associated with the development of common physiological disorders in pome fruit during CA storage (Hatoum *et al.*, 2014; Mellidou *et al.*, 2014; Pedreschi *et al.*, 2009, 2008, 2007; Vandendriessche *et al.*, 2013). However, as of now little is known about the molecular and metabolic responses occurring under low-oxygen stress typically induced during DCA storage, nor on the regulatory mechanisms involved in the responses of apple fruit to hypoxic conditions. Cukrov *et al*. (2016) showed that 'Granny Smith' apples stored at 0.4 kPa or 0.8 kPa oxygen have a clearly different metabolic and transcriptomic profile. Both *et al*. (2014) found that the volatile profile of 'Royal Gala' fruit stored under low oxygen partial pressure was differentially

affected with some esters showing a reduced production at 0.5 kPa oxygen. Brizzolara e*t al*. (2017) clearly demonstrated that 'Granny Smith' and 'Red Delicious' apples respond differently to low oxygen storage. They suggested that the genetic background played a key role in determining and modulating the observed metabolic changes. Furthermore, they found that slight changes in low oxygen concentrations induced different physiological and metabolic responses depending on the genotype. Hence, to further optimize DCA storage it is important to get a better understanding on the fruit's central carbon metabolism and its regulation during low-oxygen stress.

## 2.2 Central carbon metabolism of apple fruit

Fruit is a biological system that needs energy to survive. Therefore, they metabolize complex substrates such as sugars, lipids and organic acids to less complex molecules, including $CO_2$ and water, with the purpose of producing energy in the form of adenosine triphosphate (ATP) (Taiz and Zeiger, 2010). The produced energy is necessary to maintain and regulate the cellular organization and membrane integrity. Depending on the oxygen status in the fruit, energy is produced through different metabolic pathways. In this section a distinction will be made between the metabolic pathways used under no oxygen stress and low-oxygen stress conditions (for definitions see Fig 2.2). During no oxygen stress conditions, no specific metabolic adaptations are required to provide enough energy for the plant to survive. When the plants are exposed to low-oxygen stress, they undergo physiological changes to remain able to provide enough energy to survive. As can be seen from Fig 2.2, apple fruit is normally stored under low-oxygen stress conditions, but at oxygen concentrations above the LOL.

In this section, an overview will be given of the pathways involved in the central carbon metabolism of apple fruit under no oxygen stress and low-oxygen stress conditions. Furthermore, the regulation of these pathways under both conditions will be elaborated. Finally, the mechanisms which sense and signal low-oxygen stress in plants and how they influence the metabolic responses will be discussed. For model species such as *Arabidopsis* and rice, extensive information is available on metabolic responses, oxygen signalling mechanisms and the transcriptional regulation occurring under low-oxygen stress (Van Dongen and Licausi, 2014). As limited information is yet available on these processes in apple fruit, the following sections present the combined information from various studies including information for pome fruit if available. However, it should be mentioned that apple fruit does not necessarily react in the same way as the model species to low-oxygen stress.

### 2.2.1 Central carbon metabolism under no oxygen stress conditions

When oxygen is not limiting, apples produce their energy by completely oxidizing sugars through the biochemical process of respiration. The respiratory metabolism consist of the following pathways: glycolysis, pentose phosphate pathways (PPP), tricarboxylic acid (TCA) cycle and the mitochondrial electron transport chain (mETC) (Fig. 2.4). Glycolysis is an $O_2$-independent pathway involving a series of enzymatic reactions that breaks down sugars into pyruvate. The main sugars metabolized through the respiratory metabolism are glucose, fructose and sucrose. To be able to degrade sucrose via the glycolytic pathway, it first needs to be cleaved into fructose and glucose by invertase (Copeland, 1990). The glycolysis can be divided into two phases: an energy consuming phase and an energy conserving phase. In the initial energy consuming phase a hexose (glucose or fructose) is phosphorylated twice, which requires 2 molecules of ATP, and is subsequently split into two triose phosphates, i.e., glyceraldehyde 3-phosphate and dihydroxyacetone-phosphate. In

the second energy conserving phase, each triose phosphate is oxidized to pyruvate, resulting in the production of 2 molecules of ATP and 1 molecule of reduced NADH. Hence, this sequence of enzymatic reactions resulted in a net production of two molecules of ATP and two molecules of NADH. NADH is the major biochemical electron transporter and co-enzyme in plants. Glycolysis can occur both in the cytosol and plastids of plant cells and exchange of glycolytic intermediates is possible between these two compartment (António *et al.*, 2016; Garrett and Grisham, 2005; Mauseth, 2008; Plaxton, 1996; Taiz and Zeiger, 2010).

An alternative route for the cell to oxidize sugars is provided by the PPP, which takes place in the cytosol and in the plastids (Fig. 2.4). The PPP is divided in two main parts, namely the oxidative and the non-oxidative branch. The initial oxidative branch of the PPP, oxidizes glucose 6-phosphate to ribulose 5-phosphate. In non-photosynthetic cells, like apple cells, the oxidative branch of the PPP is a major source of reduced NADPH, which is used in biosynthetic processes such as fatty-acid synthesis and the assimilation of inorganic nitrogen (Kruger and Von Schaewen, 2003; Neuhaus and Emes, 2000). Furthermore, NADPH plays an important role in maintaining the redox potential necessary to protect plants against oxidative stress (Juhnke *et al.*, 1996). Nowadays, the basic functions of the oxidative branch of the PPP are well-established (Garrett and Grisham, 2005; Mauseth, 2008; Taiz and Zeiger, 2010), but details of how the pathway operates in plants and how it influences other processes remain largely unknown. The reversible non-oxidative branch converts ribulose 5-phosphate to intermediates of the glycolysis, i.e., fructose 6-phosphate and glyceraldehyde 3-phosphate. This part of the PPP is a source of carbon skeletons for the synthesis of nucleotides, aromatic amino acids, phenylpropanoids and their derivatives. Although both glycolysis and the PPP are involved in sugar oxidation in *Arabidopsis*, the PPP may only account for 15 to 30 % of the hexose phosphate oxidized to glyceraldehyde 3-phosphate and $CO_2$ (Kruger and Von Schaewen, 2003). As of today, little information is available on the importance of the PPP in apple fruit.

The next step in the respiratory metabolism is the TCA cycle, which takes place in the matrix of the mitochondria. Pyruvate produced in the glycolytic pathway is used as a substrate to fuel the TCA cycle and can be transported across the inner membrane of the mitochondria by a mitochondrial pyruvate carrier (MPC) (Li *et al.*, 2014). Alternatively, pyruvate can be generated in the matrix from malate by the action of malic enzyme (Jacoby *et al.*, 2012). Inside the mitochondria, pyruvate will be oxidatively decarboxylated by the pyruvate dehydrogenase complex (PDH) to produce acetyl-CoA, $CO_2$ and NADH (Fig. 2.4). Acetyl-CoA is then incorporated in the TCA cycle by combining the acetate moiety with oxaloacetate to form citrate. In the next steps, the two remaining carbon atoms of pyruvate are released as $CO_2$. Besides the production of ATP by the conversion of succinyl-CoA to succinate by the action of succinyl-CoA synthetase, the TCA cycle also stores energy in the form of NADH and $FADH_2$. Apart from producing energy, the intermediates of the TCA cycle serve as substrates in the biosynthesis of amino acids, nucleic acids and cell wall components needed for plant growth and development (Harvey Millar *et al.*, 2011; Jacoby *et al.*, 2012; Taiz and Zeiger, 2010).

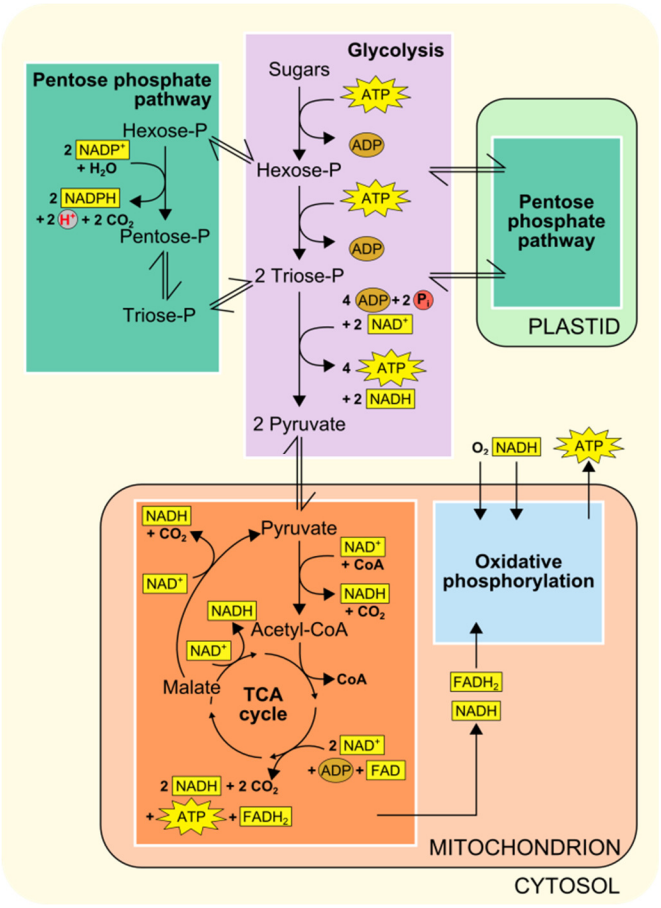


Figure 2.4: Overview of respiration including glycolysis in the cytosol; pentose phosphate pathway in the cytosol and plastids; TCA cycle and oxidative phosphorylation in the mitochondria (Based on Taiz and Zeiger, 2010 ).

The mitochondrial electron transport chain (mETC) is where the final and only oxygen consuming process of the respiratory metabolism, the oxidative phosphorylation, takes place (Fig. 2.4). The mETC is located in the inner mitochondrial membrane (IMM) and consists of several dehydrogenases, cytochrome oxidases and an alternative oxidase (AOX). The reducing equivalents (NADH and $FADH_2$) and succinate, produced inside the mitochondrion in the TCA cycle, transfer their electrons to NADH dehydrogenase (complex I) and succinate dehydrogenase (complex II), respectively. The mitochondria of plants contain several additional non-phosphorylating NAD(P)H dehydrogenases (ND2) on the outside, as

well as on the inside of the IMM (Fig. 2.5). These enzymes enable plant mitochondria to oxidize NADH and NADPH, formed in the glycolysis and PPP, directly from the cytosol. The reduced compounds need to be oxidized to enable the respiratory metabolism to function. All the dehydrogenases (complex I, complex II and ND2) are linked to the ubiquinone (UQ) pool. Ubiquinone is reduced by the input of electrons via the several dehydrogenases and again oxidized by the cytochrome oxidase pathway and/or AOX. The cytochrome pathway contains the enzymes cytochrome c reductase (complex III), cytochrome c (Cyt C) and cytochrome c oxidase (complex IV, COX). Cytochrome c reductase oxidizes ubiquinone and transfers the electrons to Cyt C, which passes on the electrons to COX. This complex reduces $O_2$ to two molecules of $H_2O$. Due to the activity of the complexes I, III and IV, an electrochemical proton gradient is formed across the IMM (Fig. 2.5). The ATP synthase (complex V) uses this potential energy to generate ATP from ADP and Pi by allowing protons to flow back across the IMM down the gradient. Furthermore, plants also contain an ubiquinol-oxidizing AOX. This oxidase transfers the electrons directly to oxygen, thereby bypassing the proton pumping of the cytochrome pathway (complex II and COX). Therefore, energy is not conserved via this pathway and lost as heat (Millenaar and Lambers, 2003; Päpke *et al.*, 2014; Van Dongen *et al.*, 2011). Several studies show that AOX activity plays an important role in preventing and reducing reactive oxygen species (ROS) by avoiding an “over-reduction” of UQ and by maintaining the oxygen homeostasis (Maxwell *et al.*, 1999; Mcdonald and Vanlerberghe, 2006). Under normoxia, neither AOX nor COX is active at full capacity and both have been shown to compete for the distribution of electrons (Päpke *et al.*, 2014; Van Dongen *et al.*, 2011).

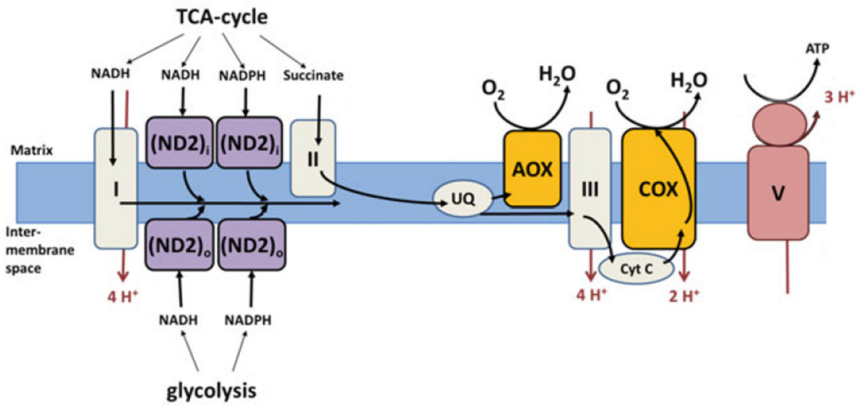


Figure 2.5: Representation of the mitochondrial electron transport chain with the conventional and alternative reactions located in the inner mitochondrial membrane. Complexes I-III, that is NADH dehydrogenase, succinate dehydrogenase, cytochrome c reductase, respectively; COX, cytochrome c oxidase; V, ATP synthase; AOX, alternative oxidase; cyt c, cytochrome c; ND2i and ND2o, type II NAD(P)H dehydrogenase located at the inside (i) and outside (o) of the mitochondrial inner membrane; UQ, ubiquinone pool. The electron flow is indicated with black arrows and the proton flow with red arrows (adapted from Päpke *et al.*, 2014; used with permission).

Taking together the ATP produced by the glycolysis, TCA cycle and mitochondrial electron transport chain, a total amount of 36 molecules of ATP is formed for each molecule of glucose used as substrate.

## 2.2.2 Regulation of central carbon metabolism under no oxygen stress conditions

In non-plant systems, it is well established that the glycolytic flux is regulated by the enzyme phosphofructokinase (PFK), with a secondary control by the enzyme pyruvate kinase (PK). That said, multiple studies demonstrated that the activity of the glycolysis in plants is controlled in a different way, namely, via a bottom up feedback inhibition of PFK by phosphoenolpyruvate (PEP) (Fig 2.6; Adams and Rowan, 1970; Beaudry *et al.*, 1989; Geigenberger and Stitt, 1991; Givan, 2007; Hatzfeld and Stitt, 1991; Huppe and Turpin, 1994; Kobr and Beevers, 1971; Paul *et al.*, 1995; Plaxton and Podesta, 2006; Plaxton, 1996; Van Dongen *et al.*, 2011; Vanlerberghe *et al.*, 1992). When the cytosolic PEP levels are reduced by the

increased activity of PK and PEP carboxylase (PEPC), the inhibition of PFK will be diminished, thereby elevating the glycolytic flux (Plaxton and Podesta, 2006). Pyruvate kinase catalyses the terminal reaction of the glycolysis by converting ADP and PEP to ATP and pyruvate. Therefore, the activity of PK has a critical role in the regulation of glycolysis. However, transgenic plants generated for a large proportion of glycolytic enzymes, only showed a minor, even negligible change in the rate of respiration. These data suggest that the control of the respiratory rate is unlikely to be mediated by individual enzymes of glycolysis only. Similarly, plants transgenic for enzymes of the TCA cycle also showed relatively small alterations in respiration in photosynthetic plants (Van Dongen *et al.*, 2011). However, chemical inhibition of the TCA cycle enzyme 2-oxoglutarate dehydrogenase in non-photosynthetic plant tissue had a clear negative impact on respiration as well as amino acid metabolism (Araújo *et al.*, 2008; Van Der Merwe *et al.*, 2010, 2009). Nevertheless, the fact that altering the levels of enzyme activities of the glycolytic and TCA cycle has no major impact on the rate of cellular respiration, does not mean that these pathways are not regulated. Both the glycolysis and TCA cycle are influenced by the availability of sucrose (Fernie *et al.*, 2002; Urbanczyk-Wochniak *et al.*, 2006) and the fluctuations in redox status (Araujo *et al.*, 2012; Kolbe *et al.*, 2006). Furthermore, while both ATP and UTP are used as energy source for certain steps of the glycolysis (see fig 2.7), the glycolysis appears to respond only to fluctuations in adenylate (Regierer *et al.*, 2002), but not uridylate (Geigenberger *et al.*, 2005) metabolism. This confirms the importance of ATP as main energy source in the cell. Altogether, these observations suggest that the respiration rate is mostly controlled by the mitochondrial electron transport chain itself (Van Dongen *et al.*, 2011).

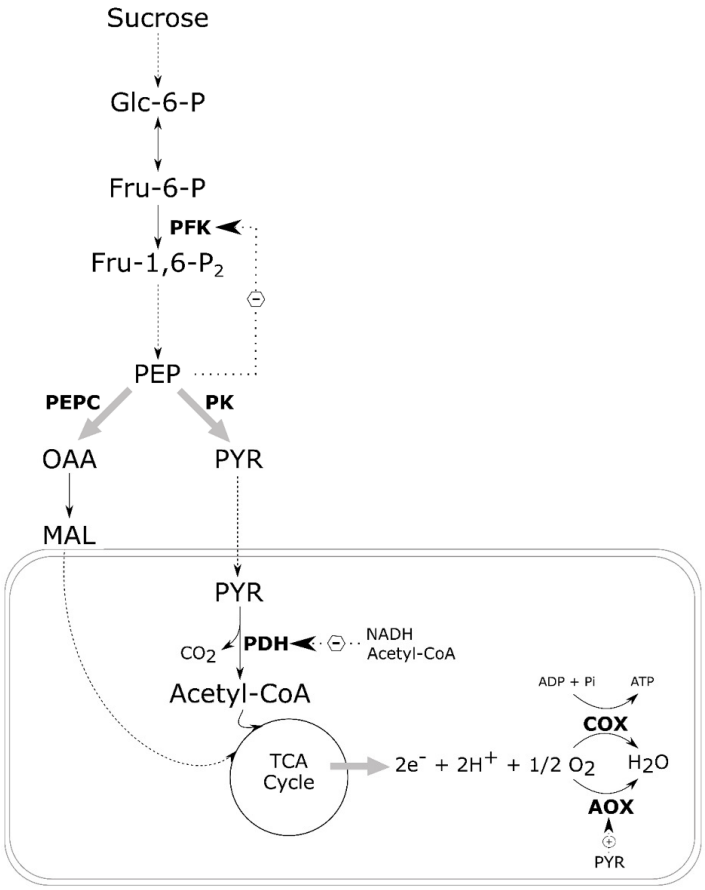


Figure 2.6: Schematic overview of the most important regulatory control sites of the carbon metabolism. The central role of PEP in the regulation of the glycolysis via a negative feedback mechanism is indicated, as well as the most important control sites of the mitochondrial respiration. Dotted arrows with a circled plus and minus sign indicate enzyme activation and inhibition, respectively, by allosteric effectors. Abbreviation are: Glc-6-P, glucose-6-phosphate; Fru-6-P, fructose-6-phosphate; Fru-1,6-$P_2$, fructose-1,6-biphosphate; PEP, phosphoenolpyruvate; PYR, pyruvate; OAA, oxaloacetate; MAL, malate; PFK, phosphofructokinase; PEPC, phosphoenolpyruvate carboxylase; PK, pyruvate kinase; PDH, pyruvate dehydrogenase complex; COX, cytochrome c oxidase; AOX, alternative oxidase (adapted from Plaxton and Podesta, 2006; used with permission).

During no oxygen stress conditions, the demand of ATP plays an important role in the regulation of the mETC. The activity of the complexes I-IV of the mETC is regulated by the strength of the proton motive force. When the demand of the cell for ATP is high, the flux of protons into the matrix is increased, thereby stimulating

the ATP synthase complex. To compensate for this increase in proton flux, the activity of complex I, III and IV will be elevated. However, if the redox status of ubiquinone would only be determined by the energy status of the cell, it would be very difficult to control the production of ROS, that is a byproduct of the mETC. Furthermore, like already mentioned in section 2.2.1, the mETC also has several different alternative electron donor and acceptor proteins as well, which all need to be regulated in a coordinated way (Van Dongen *et al.*, 2011). In both mammals and yeast, it has been shown that the activity of COX can be regulated by exchanging subunits of COX (Burke and Poyton, 1998; Semenza, 2007). Whether the same regulation exists in plants still needs to be elucidated. Another additional regulatory mechanism might be the different reversible phosphorylation sites on all the complexes of the mETC, although for most of them, it remains unknown whether phosphorylation of these sites indeed plays a role in the regulation of the mETC (Bykova *et al.*, 2003; Ito *et al.*, 2009; Kadenbach *et al.*, 2010). In addition to the classical linear operation of the mETC, the mitochondrial complexes can be ordered in protein superstructures with specific configuration and stoichiometry to form so-called supercomplexes or respirasomes (Boekema and Braun, 2007; Eubel *et al.*, 2004; Schäfer *et al.*, 2007). In plants, only complexes I, III and IV have been shown to be organized in supercomplexes (Schäfer *et al.*, 2007). The functional role of supercomplexes for the mETC is not yet clear. It was postulated that supercomplexes increase the stability of individual complexes (Diaz *et al.*, 2006) and they could affect the membrane structure, allowing an increase in protein density of the membrane (Boekema and Braun, 2007). However, most probably supercomplexes are helping to efficiently channel electrons between the reactive sites of the complexes, thereby affecting the respiratory rate and ATP production, but this still needs to be demonstrated (Päpke *et al.*, 2014; Van Dongen *et al.*, 2017, 2011).

## 2.2.3 Regulation of central carbon metabolism under low-oxygen stress conditions

### 2.2.3.1 Energy-saving metabolic adaptations upon low-oxygen stress

When fruit are exposed to very low oxygen partial pressures, their internal oxygen concentration will drop and low-oxygen stress will be induced. This will strongly affect the fruit's metabolism. One of the most direct effects of low-oxygen stress is the reduction of the energy status of the cells (Geigenberger, 2003). In an attempt to prevent, or at least postpone, the occurrence of internal anoxia and its concomitant negative consequences, plants try to save energy by adapting their metabolism (Bailey-Serres *et al.*, 2012; Geigenberger, 2003; Van Dongen *et al.*, 2011). One of these adaptations is the reduction of non-essential, energy-consuming processes such as the synthesis of storage products like starch, proteins and lipids (Geigenberger, 2003; Van Dongen and Licausi, 2015; Vigeolas *et al.*, 2003). A second metabolic adaptation is to favor pyrophosphate (PPi) dependent reactions above those which use ATP as substrate (Fig 2.7; Bailey-Serres *et al*., 2012; Kosmacz and Weits, 2014). There are at least three reactions known in the plant primary metabolism that have PPi-dependent alternative enzymes. The first known reaction involves the cleavage of sucrose. Instead of using invertases and hexokinases to provide hexose-phosphates from sucrose, which is an ATP consuming process, plants can use sucrose synthase (SUS) and UDP-glucose pyrophosphorylase (UGPase) to cleave sucrose. This alternative pathway is truly energy saving by using only one molecule PPi instead of two molecules ATP (Mustroph *et al.*, 2014). *SUS* has been reported to be one of the core-responsive genes to hypoxia in apple fruit. The gene expression of SUS in apple fruit is highly sensitive to changes in oxygen concentration in the environment (Cukrov *et al.*, 2016). Secondly, the ATP-dependent glycolytic enzyme phosphofructokinase (PFK), which catalyses the phosphorylation of fructose

6-phosphate, has a reversible PPi-using variant, i.e., pyrophosphate:fructose-6-phosphate phosphotransferase (PFP). However, the induction of *PFP* expression during hypoxia was not observed in all species (Mustroph *et al.*, 2014). Interestingly, *PFK* genes were observed to be expressed during hypoxia in all plant organisms studied so far (Mustroph *et al.*, 2010), suggesting that PFK and not PFP catalyses the main glycolytic pathway under hypoxic conditions in most organisms (Mustroph *et al.*, 2014). A rapid up-regulation of PFK expression during low-oxygen stress was observed in apple fruit (Cukrov *et al.*, 2016). However, how the *PFK/PFP* gene expression and activity is regulated in apple fruit still remains to be investigated. Also the last step of the glycolysis, where phoshoenolpyruvate is converted to pyruvate, might be catalysed by a PPi dependent enzyme; i.e., pyruvate-orthophosphate dikinase (PPDK), instead of pyruvate kinase (PK). Although these alternative pathways could compensate for the severe ATP deficiency during low-oxygen stress, their exact impact is not yet clear. PPi is a side product produced during biosynthetic reactions, which are known to be down-regulated during hypoxia. However, the content of PPi under hypoxia is reported to stay mostly stable, unlike ATP, suggesting PPi production from alternative sources. Furthermore, the alternative enzymes mostly catalyse reversible reactions, making it difficult to estimate which direction is the favourable one under low-oxygen stress (Mustroph *et al.*, 2014).

When plants try to save energy as the oxygen concentration drops, the demand of respiratory oxygen consumption decreases and the respiratory activity of the mETC slows down (Fig 2.7; Gupta *et al*., 2009; Zabalza *et al*., 2009). Nowadays, it is not clear whether the oxygen-consumption rate goes down because oxygen is becoming limited as a substrate or a proactive regulatory system is present to regulate the oxygen-consumption rate in response to low-oxygen stress. The first hypothesis is based on the gas-diffusion models (see section 2.1.3), which predict that the oxygen gradient is declining towards the centre of the plant organ, and thereby limiting the substrate for respiration (Ho *et al.*, 2011, 2010, 2008; Lammertyn *et al.*, 2003). The lower the oxygen concentration, the larger the area in the tissue where oxygen is a

limiting substrate. The other hypothesis states that an oxygen sensing mechanism is present which proactively regulates the rate of the respiratory metabolism to optimize the rate of oxygen consumption to oxygen availability (see section 2.2.4; Päpke *et al.*, 2014; Van Dongen and Licausi, 2015). These hypotheses are not mutually exclusive and a combination of both could be likely as well (Päpke *et al.*, 2014). Ho *et al.* (2018) recently showed that at low temperature a combination of both is necessary to regulate the respiratory metabolism in pear fruit, whereas at high temperature the regulation is mainly affected by diffusion limitations.

When oxygen levels are limited, plants try to make the ATP production per oxygen that is consumed in the mETC as efficient as possible. Gupta *et al*. (2009) observed that the ratio between the capacities of COX to AOX increases when the oxygen availability goes down. This suggest that the amount of ATP produced by the reduction of one molecule of oxygen will increase. Nowadays, the role of respiratory supercomplexes in the regulation of the electron flux to either AOX or COX is being investigated (Van Dongen *et al.*, 2011). Pyruvate can bind to AOX to activate the enzyme (Fig 2.6; Oliver *et al*., 2008; Zabalza *et al*., 2009). Therefore, it seems important to control the cellular concentrations of pyruvate during low-oxygen stress. However, in most plant species the affinity of AOX to oxygen is one or two orders of magnitude lower compared to the affinity of COX to oxygen. Hence, it is unlikely that AOX competes with COX for oxygen as a substrate during low-oxygen stress (Päpke *et al.*, 2014; Van Dongen *et al.*, 2011).

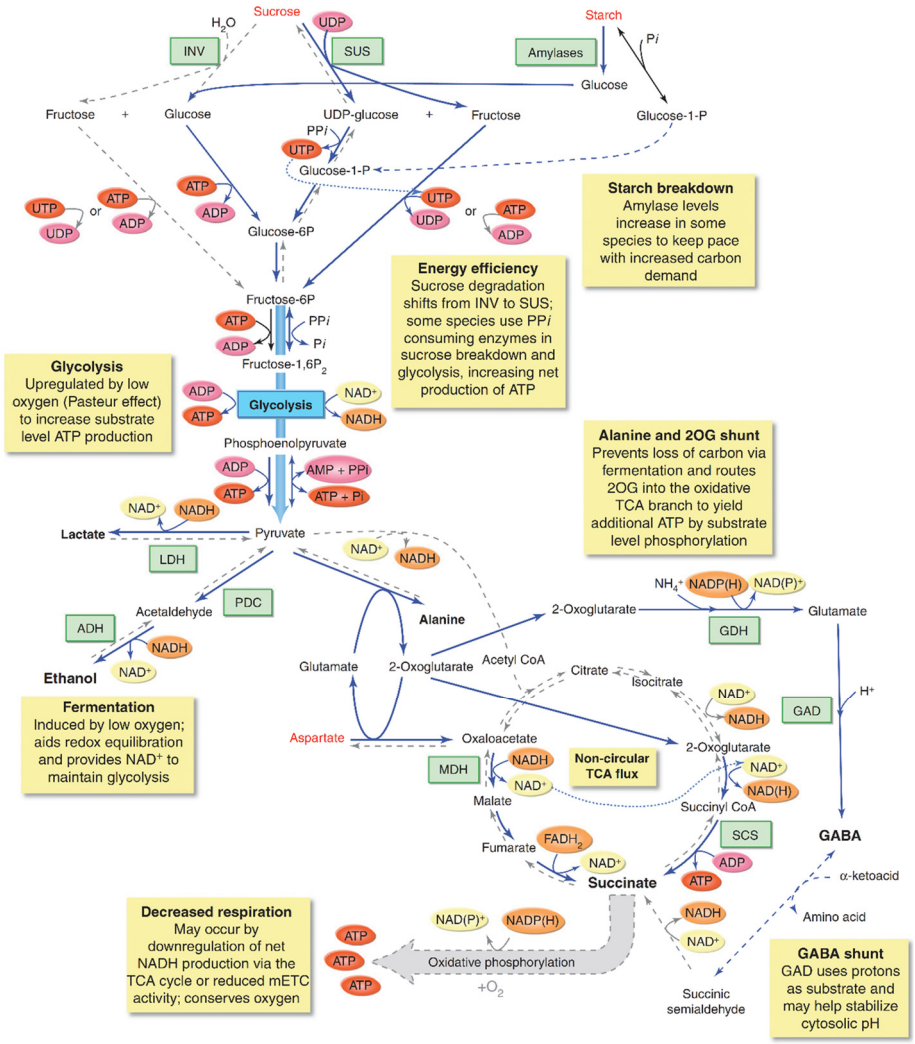


Figure 2.7: Metabolic responses of plants to low-oxygen stress. The yellow boxes highlight a number of metabolic changes that are known to happen when oxygen availability is limited, such as enhanced sucrose-starch metabolism, glycolysis, fermentation, a modified TCA flow, an alanine and 2-oxoglutarate (2-OG) shunt and a GABA shunt. Blue lines indicate pathways enhanced during low-oxygen stress, blue dashed lines indicate pathways proposed to be active during low-oxygen stress and grey dashed lines indicate reaction that are inhibited during low-oxygen stress. Metabolites that increase during low-oxygen stress are shown in enlarged black font; metabolites that decrease are shown in red font. Abbreviations are as follows: 2OG, 2-oxoglutarate; ADH, alcohol dehydrogenase; GAD, glutamic acid decarboxylase; GDH, glutamate dehydrogenase; INV, invertase; LDH, lactate dehydrogenase; MDH, malate dehydrogenase; PDC, pyruvate decarboxylase; SCS, succinyl CoA ligase; SUS, sucrose synthase. (Bailey-Serres *et al.*, 2012; used with permission).

### 2.2.3.2 Fermentative metabolism

The goal of postharvest storage of fruit is to lower the oxygen concentration to such a degree that the respiratory metabolism is reduced as much as possible, but without inducing too many negative effects on fruit quality. One of these negative effects is the induction of fermentation. When the low-oxygen stress induced in the tissue is too severe, the mitochondrial respiration is compromised too much, leading to insufficient supply of ATP for energy demanding processes. In an attempt to compensate for this decrease in respiratory energy production, plants increase their glycolytic flux to produce more energy with the conversion of glucose to pyruvate, a process known as the Pasteur effect (Fig. 2.7). Since apple fruit is a non-photosynthetic organ, it needs to hydrolyse starch to provide enough glucose to support the high glycolytic flux. The gene expression of the starch degrading enzyme, β-amylase, appears to be upregulated in 'Granny Smith' apples stored under hypoxia (Cukrov *et al.*, 2016). When the glycolytic flux increases, pyruvate starts to accumulate since it is no longer shuttled into the TCA cycle due to the decreased pyruvate dehydrogenase activity. Pyruvate dehydrogenase is inhibited by the high reduction levels of NADH/$NAD^+$ pool and the accumulation of acetyl-CoA (Fig 2.6; Päpke et al., 2014). However, to be able to maintain the high glycolytic flux, $NADP^+$ and $NAD^+$ have to be regenerated and the accumulation of pyruvate should remain limited (António *et al.*, 2016; Bailey-Serres *et al.*, 2012; Geigenberger, 2003). Therefore, the increase in glycolytic flux is typically coupled to fermentation. In this pathway pyruvate can be converted to either lactate or ethanol and $CO_2$, meanwhile maintaining the redox balance in the cell by the formation of $NAD^+$ (Fig 2.7; Perata and Alpi, 1993). Pyruvate is converted to lactate by the enzyme lactate dehydrogenase. The accumulation of lactic acid will cause cytoplasmic acidosis, which can result in cell damage (Perata and Alpi, 1993). The decreasing cytosolic pH results in a decreasing activity of lactate dehydrogenase and activation of pyruvate decarboxylase. This enzyme converts pyruvate to acetaldehyde, which is further converted to ethanol by alcohol dehydrogenase and finally to ethyl acetate by the

enzyme alcohol acyl transferase. These volatile fermentation metabolites (ethanol, acetaldehyde and ethyl acetate) readily diffuse out of the cells into the external environment, leading to a depletion of carbon reserves and causing off-flavors in the fruit (António *et al.*, 2016; Fukao and Bailey-Serres, 2004; Pesis, 2005; Tadege *et al.*, 1999). The accumulation of ethanol under extreme low oxygen concentrations and/or during prolonged CA storage has been reported in multiple apple cultivars (Bekele, 2015; Brizzolara *et al.*, 2017; Cukrov *et al.*, 2016; Mattheis *et al.*, 1991; Saquet and Streif, 2008), also in relation to the development of low oxygen-induced physiological disorders (Hatoum *et al.*, 2014; Lumpkin *et al.*, 2014; Vandendriessche *et al.*, 2013). Furthermore, it has been shown that the rate of ethanol accumulation increases with decreasing oxygen concentration (Brizzolara *et al.*, 2017; Cukrov *et al.*, 2016; Lumpkin *et al.*, 2014).

### 2.2.3.3 Alternative pathways induced by low-oxygen stress

Although the induction of fermentation helps apple fruit to tolerate low-oxygen stress by mitigating the damaging effects of energy crisis, it causes acidosis of the cytoplasmic pH and reduction of the carbon reserves (Limami, 2014). Changes in amino acids metabolism may help to reduce these negative effects of fermentation. More specifically, alanine metabolism plays an important role in maintaining the glycolytic flux by converting pyruvate with the help of alanine aminotransferase (AlaAT) to alanine, providing an alternative, non-detrimental end product (Fig 2.7). Alanine is observed in a number of species, including apple (Bailey-Serres *et al.*, 2012; Cukrov *et al.*, 2016; Hatoum *et al.*, 2014; Vandendriessche *et al.*, 2013). Alanine concentrations are found to be increased in 'Braeburn' apples after long term storage (up to 8 months) under 2.5 kPa $O_2$ and 3.7 kPa $CO_2$ conditions (Hatoum *et al.*, 2014). Furthermore, it was shown that alanine accumulated to different levels depending on the composition of the atmosphere (Brizzolara *et al.*, 2017; Cukrov *et al.*, 2016; Vandendriessche *et al.*, 2013). This is probably due to hypoxic stress inducing the expression of the genes coding for *AlaAT*. Cukrov *et al*. (2016) showed that the accumulation of *AlaAT* transcripts was extremely abundant in apples stored

under 0.4 kPa $O_2$, but in fruit stored under 0.8 kPa $O_2$, *AlaAT* gene expression appeared to remain at basal levels throughout the experiment. These findings suggest a low-oxygen threshold for this gene in apple. Since the concentration of alanine was clearly higher in apples stored under 0.8 kPa $O_2$ as compared to normoxia, another mode of regulation has to be present (Cukrov *et al.*, 2016). By feeding *Medicago truncatula* seedlings with $^{15}$N-glutamate or $^{15}$N-alanine, Ricoult *et al*. (2006) provided some evidence that under hypoxia the activity of the reversible enzyme AlaAT was directed towards alanine synthesis using glutamate as amino donor while the reaction of glutamate synthesis using alanine as amino donor was inhibited. These results show that AlaAT has a dual mode of regulation by hypoxia, both at transcriptional and posttranslational level (Limami, 2014). As can be seen from Figure 2.7, the synthesis of alanine is accompanied by the generation of 2-oxoglutarate, which can be further metabolized in the TCA cycle via 2-oxoglutarate dehydrogenase and succinate CoA ligase (SCS) to form succinate and produce ATP. The amount of ATP gained via this pathway doubles the amount of energy produced by the glycolysis alone. Succinate will accumulate as the TCA cycle will be further blocked due to the oxygen limitation at the reaction catalysed by complex II of the mETC. The $NAD^+$ that is required for this reaction is guaranteed by the oxidation of NADH via malate dehydrogenase (MDH) catalysing the reaction from oxaloacetate to malate in the reversed TCA cycle. During hypoxia, oxaloacetate is produced by aspartate aminotransferase (AspAT), simultaneously producing glutamate, which is used by AlaAT as a co-substrate for alanine synthesis (Fig. 2.7). Hence, the accumulation of alanine during low-oxygen stress as a C/N storage compound produces extra ATP, thereby diminishing an energy crisis and saving carbon atoms, which otherwise would be lost via ethanol (Bailey-Serres *et al.*, 2012; Limami, 2014; Limami *et al.*, 2008; Ricoult *et al.*, 2006; Rocha *et al.*, 2010). Furthermore, synthesis of alanine also limits cytoplasmic acidification by competing with lactate fermentation for the use of pyruvate (Ricoult *et al.*, 2006, 2005). In addition, alanine may accumulate as a byproduct of the GABA shunt, which is known to help stabilizing cytosolic pH (Fig 2.7). In the GABA shunt glutamate is decarboxylated into γ-

aminobutric acid (GABA) by glutamate decarboxylase (GAD). The formation of GABA is a proton consuming reaction, which increases the pH (Greenway and Gibbs, 2003). GABA can react further to succinic semialdehyde via GABA-T that uses pyruvate as amino acceptor under hypoxic conditions leading to the production of alanine (Limami, 2014). GABA content has been found to increase under low-oxygen stress in 'Granny Smith' and 'Red Delicious' apples (Brizzolara *et al.*, 2017; Cukrov *et al.*, 2016). Cukrov *et al*. (2016) found a similar trend in the accumulation patterns of alanine and GABA under hypoxia, suggesting that both pathways are co-regulated in apple fruit. Furthermore, the same authors saw a reduction of asparagine and aspartate by 0.4 kPa oxygen but not by 0.8 kPa oxygen. This could be the result from a different modulation of the carbon flux into the TCA cycle under these two stress levels (Cukrov *et al.*, 2016). Based on a metabolomics approach, Brizzolara *et al*. (2017) found that 'Granny Smith' and 'Red Delicious' apples have a different approach to balance the levels of pyruvate and to keep on producing energy under hypoxia. 'Red Delicious' apples are producing more ethanol and GABA, while 'Granny Smith' apples accumulate more alanine.

During low-oxygen stress, another alternative pathway is induced to recycle $NAD^+$ from NADH, to be able to maintain the high glycolytic flux (Igamberdiev and Hill, 2004). This alternative pathway is the nitric oxide (NO) cycle, in which NO is either produced by the reduction of nitrite by nitrate reductase (NR) or NO is produced in the mitochondrial matrix (Fig 2.8). In the latter case, nitrite is transported to the mitochondrial matrix through an yet unknown transport system, where it serves as an alternative electron acceptor at the sites of complex III and COX. The electrons necessary for this reaction are generated by the oxidation of NAD(P)H by the $Ca^{2+}$-sensitive NAD(P)H dehydrogenase on the inner mitochondrial membrane surface. In both cases, NO is scavenged by class-1 nonsymbiotic haemoglobins (Hb), which are found to be highly expressed during low-oxygen stress (Igamberdiev and Hill, 2004). Due to its high affinity for oxygen, Hb spontaneously oxygenates to oxyhaemoglobin, which catalyses the turnover of NO to nitrate. To complete the cycle, MetHb has to

be regenerated by a MetHb reductase (Igamberdiev and Hill, 2004; Limami, 2014; Limami *et al.*, 2014; Van Dongen and Licausi, 2015). Plants can protect the cells against deleterious nitrosative stress by regulating the NO levels via the NO cycle. Thereby, they can control the multiple functions exerted by NO, such as the involvement of NO in the hormone signal transduction cascade and its inhibitory effect on haeme- and Fe-S cluster-containing enzymes such as aconitase, COX and catalases (Fig 2.9). Through its inhibitory effect on these enzymes, NO can directly affect the energy status of the cell and their defence against ROS (Blokhina *et al.*, 2014).

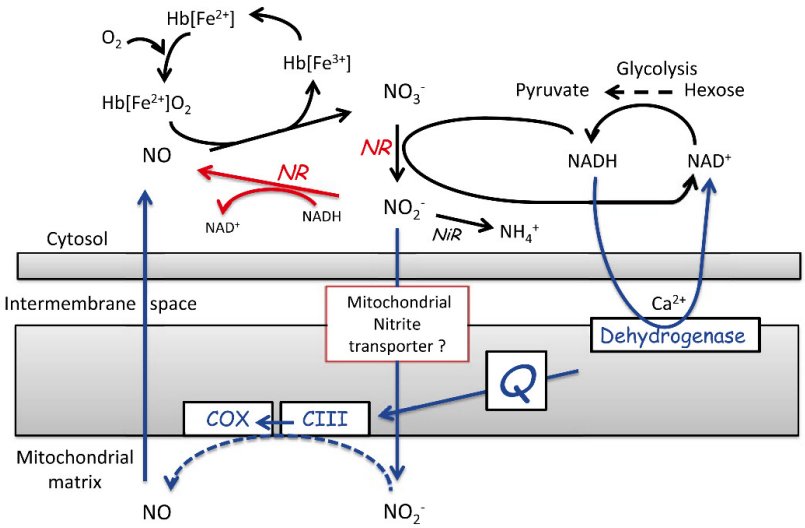


Figure 2.8: Representation of the nitric oxide (NO) cycle. NO is either produced by the reduction of nitrite by nitrate reductase (NR), shown in red or NO is produced in the mitochondrial matrix at levels of oxygen below the saturation of COX, shown in blue. When NO is produced, it is assumed to be scavenged by oxyhaemoglobin [Hb($Fe_2^+$)$O_2$] to regenerate $NO_3^-$ and metHb [Hb($Fe_3^+$)] in the NO cycle (Limami *et al.*, 2014; used with permission).

In *Arabidopsis* shoots, a metabolic association between the TCA cycle and the NO cycle under low-oxygen stress was suggested, as can be seen in Fig 2.9 (Blokhina *et al.*, 2014). Under low-oxygen stress, monodehydroascorbate reductase (MDHAR) can act as a MetHb reductase (Igamberdiev *et al.*, 2006), thereby simultaneously producing ascorbate. Based on metabolomics and microarray studies under oxygen

deprivation, a novel route, besides the ascorbate-glutathione cycle, is suggested to oxidize ascorbate. In the novel route, Fe-dependent 2-ketoglutarate oxygenase (Fe2KGO) utilizes 2 ketoglutarate (2KG) and ascorbate to form succinate. Under low-oxygen stress conditions, 2KG needed for the reaction is supplied through the metabolism of alanine. The novel route via Fe2KGO makes it possible to bypass the NO-inactivated TCA cycle components (Blokhina *et al.*, 2014). Also in apple fruit, Fe2KGO genes were found to be strongly upregulated under low-oxygen stress (Cukrov *et al.*, 2016).

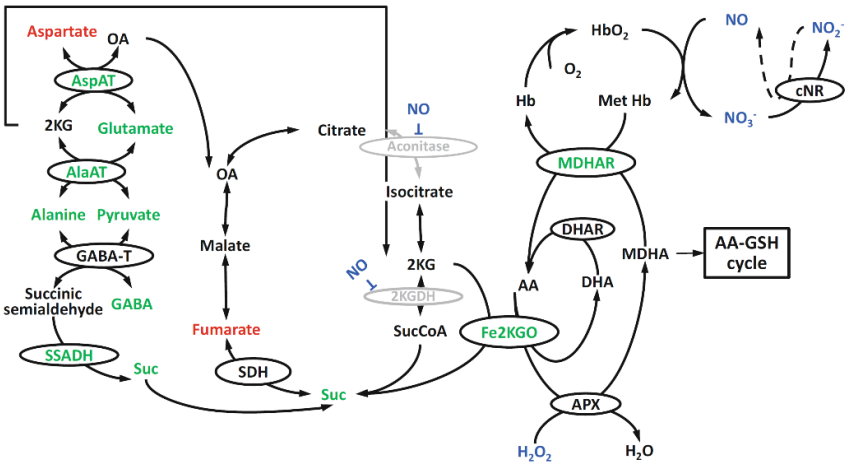


Figure 2.9: Hypoxia induced TCA cycle modification in *Arabidopsis* shoots: the involvement of Fe2+ dependent ketoglutarate oxidase, non-symbiotic haemoglobin's, NO, alanine metabolism and GABA shunt (Blokhina *et al.*, 2014; used with permission).

In conclusion, how well plants can tolerate low-oxygen stress highly depends on their ability to mitigate damaging effects of energy crisis and acidosis of cytoplasmic pH (Greenway and Gibbs, 2003).

## 2.2.4 Low-oxygen sensing and signalling

The regulation of the metabolic changes of the energy metabolism in plants upon low-oxygen stress demands an efficient and tuneable sensing mechanism for the oxygen availability in the tissue (Kosmacz and Weits, 2014; Van Dongen *et al.*, 2017; Van Dongen and Licausi, 2015). In this section the different mechanism of plants to sense the cellular oxygen concentration in the tissue will be discussed.

### 2.2.4.1 Direct oxygen sensing

The adaptive metabolic response to low oxygen in all higher plants tested so far includes the accumulation of transcripts coding for enzymes involved in metabolic reprogramming. Examples of these hypoxia responsive enzymes are pyruvate decarboxylase, alcohol dehydrogenase, lactate dehydrogenase, PFK, and alanine aminotransferase, as well as ACS and ACO (Mustroph *et al.*, 2010). Furthermore, some ROS-responsive transcripts are upregulated under hypoxic conditions. When the oxygen concentration is decreased even further and the mETC stops working, an additional set of ROS-responsive transcripts are induced, leading to an initial accumulation of ROS. However, in this case, ROS scavenging enzymes, protein chaperones and inhibitors of lipid peroxidation are also induced to prevent oxidative damage in the cell (Pucciariello *et al.*, 2012). Recently, some additional negative regulators of the adaptive metabolic response to low-oxygen stress were identified, which play a role when the plant returns to normoxic conditions (Weits *et al.*, 2014). This highlights the importance of the reversibility and timely control of the adaptive metabolic response to low-oxygen stress (van Dongen and Licausi, 2015).

A lot of research has been done to identify a primary 'oxygen sensor' which regulates the gene expression in response to the oxygen concentration in the cell (Gibbs *et al.*, 2011; Licausi *et al.*, 2011b). In *Arabidopsis*, it was found that low oxygen levels have a direct effect on the stability, and thus activity of the transcription factors from group-VII ethylene response factors (ERFs); e.g. RAP2.2, RAP2.12, RAP2.3, HRE1 and

HRE2 (Bailey-Serres *et al.*, 2012; Kosmacz and Weits, 2014; Licausi *et al.*, 2011b; Van Dongen *et al.*, 2017; van Dongen and Licausi, 2015). The protein levels of ERF-VII transcription factors are regulated through the N-end rule pathway (Fig 2.10), which acts as a safe-guard mechanism that continuously targets proteolysis under aerobic conditions (Gibbs *et al.*, 2016). The N-end rule pathway depends on the N-terminal amino acids, which for ERF-VII transcription factors is characterized by a cysteine residue in the penultimate positions (with the consensus sequence: MCGGAI; van Dongen and Licausi, 2015). The initial methionine is removed from the N-terminus via methionine aminopeptidase (MAP), which exposes cysteine to the activity of plant cysteine oxidases (PCOs). In the presence of oxygen and NO, PCO oxidizes cysteine to sulfinic or sulfonic acid (Weits *et al.*, 2014), which acts as an acceptor for the condensation of an arginine residue by arginyltransferase (ATE). The exposed arginine residue is subsequently ubiquitinated by the proteolysis (PRT) E3 ligases and targeted to the 26S proteasome for degradation (Kosmacz and Weits, 2014; Van Dongen *et al.*, 2017; van Dongen and Licausi, 2015). Therefore, this mechanism provides an efficient way to regulate the metabolic response under low-oxygen stress conditions; the presence of $O_2$ and NO causes ERF-VII destabilization, whereas their absence permits stabilization and accumulation of ERF-VII transcription factors in the nucleus (Gibbs *et al.*, 2011; Licausi *et al.*, 2011b; Van Dongen *et al.*, 2017; van Dongen and Licausi, 2015). However, it is still unclear how exactly $O_2$ and NO act together to oxidize ERF-VII (van Dongen and Licausi, 2015).

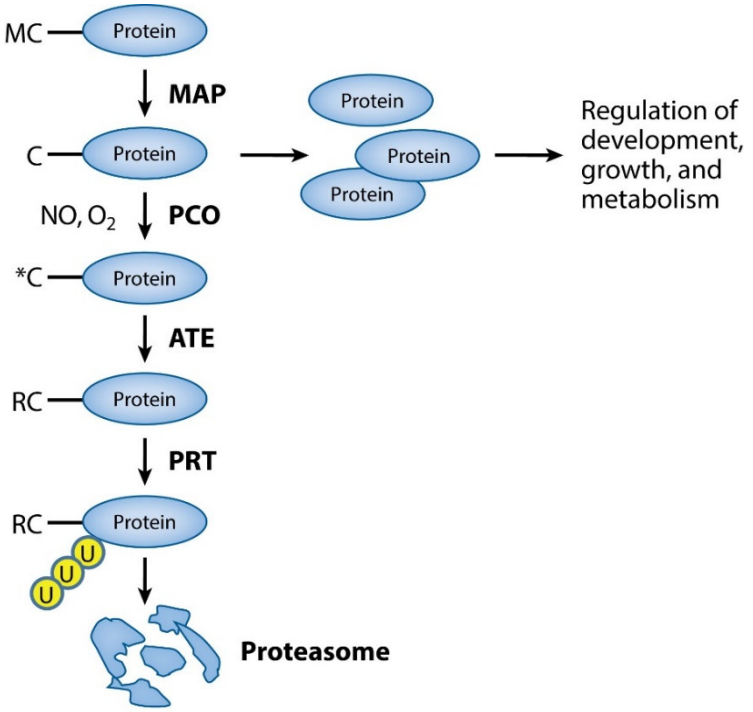


Figure 2.10: The cysteine branch of the N-end rule pathway in *Arabidopsis*. Abbreviations: MAP, methionine aminopeptidase; PCO, plant cysteine oxidase; ATE, arginyltransferase; PRT, proteolysis E3 ligases (van Dongen and Licausi, 2015, used with permission).

In *Arabidopsis*, the ERF-VII transcription factor RAP2.12 was found to be localized at the plasma membrane under aerobic conditions (Licausi *et al.*, 2011b). It was found that RAP2.12 can interact with peripheral membrane proteins acyl-coenzyme A-binding protein 1 (ACBP1) and ACBP2 (Fig 2.11). Additionally, this interaction protects RAP2.12 from degradation via the N-end rule pathway. RAP2.12 can detach from the membrane under hypoxic conditions and accumulate in the nucleus, where it induces the expression of hypoxia responsive genes. The accumulation of RAP2.12 at the plasma membrane even under normoxic conditions might be a reservoir of activators, which are able to quickly induce the low-oxygen response when oxygen levels decline (Kosmacz and Weits, 2014; van Dongen and Licausi, 2015).

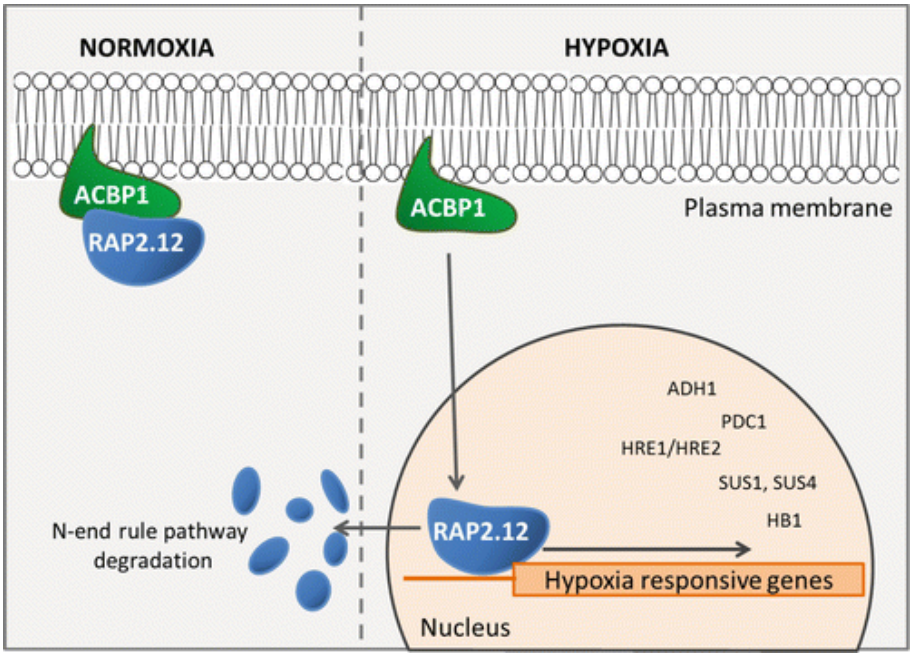


Figure 2.11: In *Arabidopsis*, RAP2.12 is located at the membrane by interacting with the membrane protein ACBP1 under normoxic conditions. However, when oxygen availability becomes limited, RAP2.12 disconnects from ACBP1 and moves to the nucleus to trigger the transcription of the hypoxia responsive genes (Kosmacz and Weits, 2014; used with permission).

Like previously mentioned, plants need to rapidly change their metabolism to ensure optimal adaptations to changing oxygen availability. When oxygen becomes available again, it is unlikely that the displacement of the ERF-VII proteins from the promotors of the hypoxia responsive genes and their degradation is sufficient to rapidly silence the expression of these genes (van Dongen and Licausi, 2015). In *Arabidopsis*, a transcriptional regulator, hypoxia response attenuator 1 (HRA1) has been found to repress the expression of hypoxia responsive genes by binding to RAP2.12 (Giuntoli *et al.*, 2014). Since RAP2.12 induces the expression of PCOs and HRA1, it acts as a positive regulator while PCOs and HRA1 restrict the function of RAP2.12 in a feedback loop depending on the availability of oxygen (Weits *et al.*, 2014). Furthermore, Gibbs *et al.* (2011) showed that not all hypoxia responsive genes are controlled by the N-end rule pathway, indicating that alternative regulatory pathways should exist.

The first evidence of an oxygen sensing mechanism based on the N-end rule pathway and on the post-translational regulation of ERF-VII protein stability in apple fruit has been given by Cukrov *et al*. (2016). However, further research is necessary to fully understand the behaviour of the oxygen sensing mechanism in apple fruit and its effect on the different metabolic responses upon low-oxygen stress between the different apple varieties.

#### 2.2.4.2 Low-oxygen-associated secondary signalling pathway

When respiration is affected by low-oxygen concentrations, it has an impact on many parameters and processes, including reactive oxygen and nitrogen species (ROS/RNS) homeostasis, redox status of NAD(P)H and antioxidant pools, ATP/ADP ratio, the proton-motive force, calcium and metabolites levels, which could all trigger the mitochondrial retrograde responses (Van Dongen *et al.*, 2017; Wagner *et al.*, 2018). Recently it has been shown that these signals could contribute to transcriptional reprogramming of the nuclei of hypoxic cells and is commonly referred to as the mitochondrial retrograde regulation. For a more detailed discussion on the role of these diverse signals in mitochondrial retrograde responses and its role in the low-oxygen response of plants, the reader is referred to the review of Wagner et al. (2018).

## 2.3 Unravelling the molecular and metabolic response induced by low-oxygen stress in a systems biology era

Like previously mentioned, when plants experience low-oxygen stress, a hypoxic response can be induced leading to molecular and metabolic changes. Due to the complexity of the hypoxic response, it is controlled by a number of factors at different levels, such as transcription, translation, enzyme deactivation/activation

and altering metabolite levels (Fig 2.12). In this section the different high-throughput techniques, which are available for the detection of the controlling factors at various organizational levels are briefly discussed. Furthermore, systems biology is introduced as a tool to understand how the different organizational levels are interacting to create the hypoxic response.

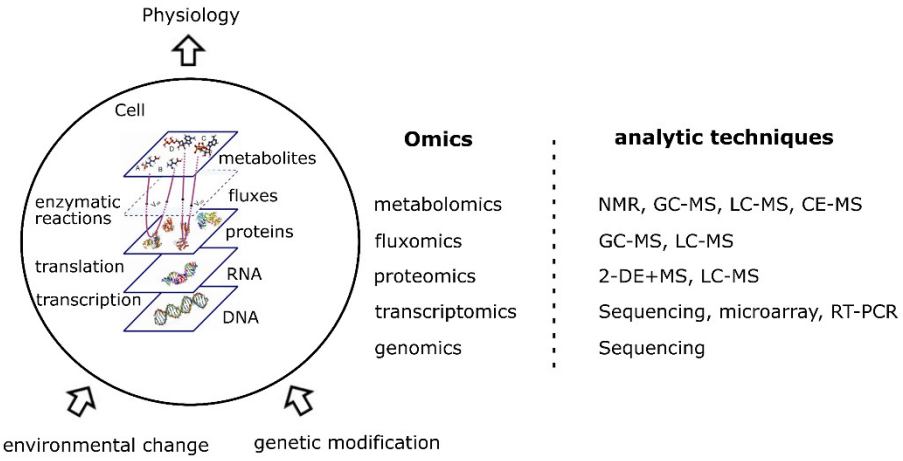


Figure 2.12: The different organizational levels of plants at which the hypoxic response could be studied (adapted from Matsuoka and Shimizu, 2012; used with permission).

## 2.3.1 High-throughput technologies to study the regulation of the hypoxic response

The first organizational level is the transcriptome, which is the sum of all RNA transcripts that are produced by the genome under specific circumstances or in a specific cell (Fig 2.12). The study of how gene expression changes in time upon different conditions is called transcriptomics. The first high throughput method used was the microarray, which is based on the hybridization of a defined set of transcripts to an array of complementary probes and measure their abundances (Tan *et al.*, 2003). However, the disadvantages of this technique are the need of knowing the sequence on beforehand, the cross-hybridization artefacts and poor quantification of lowly and highly expressed genes. Because of these technical issues, nowadays

sequencing-based methods are used to study the transcriptome (Lowe *et al.*, 2017). The sequencing-based methods evolved from Sanger sequencing of Expressed Sequence Tag libraries, to chemical tag-based methods, and finally to the current next-generation sequencing of cDNA or mRNA. Transcriptomics allows us to study how genes are regulated and how they could potentially control or change the physiology of the cell.

The second organizational level is the proteome, which is the complete set of proteins expressed by an organism (Fig 2.12). The best-known role of proteins is as enzymes, which are the key effectors of metabolic processes and hence very important to understand the hypoxic response, but many proteins are also involved in cell signalling, signal transduction or structural functions. Due to various factors, including both internal and external conditions, the proteome can actively change. Furthermore, it is important to note that the relative amounts of mRNA in the cell do not necessarily correlate to the expression levels of the proteins they code for (Hirano *et al.*, 2004). The study of the proteome is called proteomics. It enables us to understand how proteins change in terms of expression, structure and function, at a given time and under specific conditions. Furthermore, also posttranslational modification of the proteins can be elucidated using proteomics. The proteome can be studied by using a gel-based approach (2-dimensional gel electrophoresis), a gel-free approach (LC) or a combination of the two to separate the proteins (Baggerman *et al.*, 2005). Both gel-based and gel-free approaches are coupled with mass spectrometry (MS) to identify the proteins. However, to be able to identify the proteins in a correct way the genome of the organism needs to be sequenced and properly annotated (Baggerman *et al.*, 2005; Chandramouli and Qian, 2009; Pedreschi *et al.*, 2013, 2010).

The third organizational level is the metabolome, which reflects the interaction between an organism's genome and its environment (Fig 2.12). The metabolome is the complete set of low molecular weight compounds (primary and secondary

metabolites) present in an organism (Glish and Vachet, 2003). The study of the metabolome under a certain physiological and environmental condition is called metabolomics. Metabolic analyses can be carried out using three main procedures: (i) metabolic targeting, which focuses only on a few targeted metabolites (Andrews *et al.*, 1994), (ii) metabolic fingerprinting, which studies patterns of metabolites (Kopka *et al.*, 2004) and (iii) metabolic profiling, which involves detecting, identifying and quantifying the changes in metabolite groups associated with a metabolic network (Hall *et al.*, 2002; Kopka *et al.*, 2004). There are different metabolomics technologies available such as gas chromatography (GC), liquid chromatography (LC), or capillary electrophoresis (CE) all coupled to mass spectrometry (MS), nuclear magnetic resonance (NMR) spectroscopy and Fourier-transformation-infra-red spectroscopy. These measurement techniques differ in metabolite sensitivity, analysis speed, resolution, and potential throughput (Alonso *et al.*, 2015; Shulaev *et al.*, 2008; Weckwerth, 2003).

Among the different organizational levels, the metabolic flux distribution in the central metabolism may be the most important information in order to understand the complex molecular and metabolic response induced by low-oxygen stress (Fig 2.12). The metabolic fluxes resemble the enzyme activities involved in the metabolic network, which are influenced by the metabolite levels, as well as the kinetic properties, stability and cellular levels of the enzymes involved in the pathway. These enzymatic properties are controlled by gene expression, posttranscriptional, translational, and/or posttranslational modifications. Hence, the metabolic fluxes integrate information of the different organizational levels and therefore represents a unique picture of the phenotypic signature of the cells (Cortassa *et al.*, 2015; Winter and Krömer, 2013). To be able to measure metabolic fluxes, metabolic profiling experiments are coupled with isotope labelling experiments. In $^{13}C$ metabolic flux analysis, $^{13}C$-labelled substrates are fed to plant cells or tissue. The $^{13}C$-labelled substrate is metabolized and subsequently incorporated into all metabolites involved in the pathway. The distribution of $^{13}C$-label through the

pathway is a measure for the flux through each metabolite (Matsuoka and Shimizu, 2012). Metabolic fluxes can be determined under both steady-state or dynamic conditions (Cortassa *et al.*, 2015; Winter and Krömer, 2013).

### 2.3.2 Systems biology approach to interconnect all organizational levels

In order to fully understand the molecular and metabolic changes introduced under low-oxygen stress, it is important to study the response at all the different organizational levels and to take into account the connectivity between genes, enzyme activities and metabolites. It has already been shown that an n-fold increase in transcript levels does not always equates to a n-fold more enzyme and, hence, n-fold more activity in vivo (Plaxton and Podesta, 2006). The various high throughput 'omics'-techniques discussed in section 2.3.1 make it possible to study the response at the different organizational levels but comes with a huge amount of data. A systems biology approach can be used to cope with this amount of data and to understand how the different organizational levels are connected with each other. The aim of systems biology is to link the quantitative data across the different scales of biological organization into mathematical models and/or networks, ultimately reaching an unified understanding of the biological system. Not only does the systems biology approach make it able to understand certain mechanisms but it also allows us to formulate and test new hypotheses (Hertog *et al.*, 2011).

## 2.4 Conclusions

Although a lot is known about the regulation of the central carbon metabolism under no stress and low-oxygen stress conditions, several questions still remain unanswered, especially for apple fruit. For instance, how is COX of the mitochondrial electron transport chain regulated? What is the function of the supercomplexes? What is the role of PPP both under no stress and low-oxygen stress conditions in apple fruit? How is the fermentative metabolism regulated *in vivo*? How are the alternative pathways regulated in apple fruit and do they become more important during prolonged low-oxygen stress? How does the oxygen-sensing mechanism work in apple fruit? Does NO play an important role in oxygen sensing in apple fruit? How does the regulation of the carbon metabolism differs between cultivars? …

It becomes increasingly important to find answers to these questions and to fully understand the regulation of the central carbon metabolism during low-oxygen stress, especially given the recently developed DCA storage technology, in which apple fruit are stored under variable and often very low oxygen concentrations.

To improve our insights, the carbon metabolism needs to be studied at the different organizational levels. Therefore, a GC-MS based metabolite profiling study coupled to $^{13}C$ flux analysis would be the best approach, since the metabolic fluxes are an integration of the information from the different organizational levels. A GC-MS based metabolite profiling approach is most suitable to analyse the polar metabolites and it allows to simultaneously identify and quantify the levels of metabolites and perform $^{13}C$ label analysis from the extracted mass spectra of the various metabolites. Furthermore, transcriptomic analysis can give insights in the precise mode of action of low-oxygen sensing and the genetic response in apple fruit. Finally, a kinetic modelling approach based on *in vitro* experimental data, can help to gain insights in the *in vivo* regulation of the metabolism during low-oxygen stress.

# Chapter 3

# Kinetic modelling: an integrated approach to analyse enzyme activity assays

To study the *in vitro* enzyme activity of the two main enzymes of the ethanol pathway of the fermentative metabolism in apple fruit, the existing assays were optimized and a more elaborated method was developed, based on a kinetic modelling approach, to estimate the *in vitro* enzyme activity of PDC and ADH (used in chapter 4). The content of this chapter is based on: *Boeckx J., Hertog M., Geeraerd A., Nicolai B. (2017). Kinetic modelling: an integrated approach to analyse enzyme activity assays. Plant Methods, 13 (69), 1-12.*

# 3.1 Introduction

The most diverse and largest group of proteins are enzymes, biological catalysts that enhance the rates of metabolic reactions and thereby play an important role in the regulation of metabolic steps within a cell (Schomburg *et al.*, 2014). Michaelis and Menten discovered that the activity of an enzyme is highly dependent on conditions such as temperature, pH and the availability of substrate and cofactors inside the cell (Michaelis and Menten, 1913).

Many assays are described to measure enzyme activity *in vitro* (Bisswanger, 2011; Hans-Ulrich, 1983). Generally, data obtained with enzyme assays can only be reliably compared between different experiments and between different labs and publications if each time conditions that guarantee the highest possible enzyme activity have been used. Therefore, temperature, pH, nature and strength of ions, and the proper concentration of all assay components have to be strictly controlled (Bisswanger, 2014; Scopes, 2002). Most enzymatic assays are based on measuring the rate of the reaction catalysed by the enzyme. To this end, the consumption of the substrate or the generation of a product has to be monitored over a given time. The progress of the reaction can be monitored continuously (continuous assay) using spectroscopic (Eicher *et al.*, 2012; Kettling *et al.*, 1998; Shi *et al.*, 2008) or electrochemical techniques revealing the full progress curve. The advantage of a continuous assay is that the result is immediately available, and any erroneous influences and artefacts can be detected. However, if continuous monitoring is not feasible one has to obtain data at limited discrete time points using the same techniques or stop the reaction and measure the total amount of product formed or substrate consumed within the given reaction time by a subsequent chemical indicator reaction or a separation method (stopped assay) (Bisswanger, 2014, 2011; Scopes, 2002).

As long as the substrate concentrations are sufficiently high to saturate the enzyme and, thus ensure operation at its maximum rate, the velocity of the catalysed reaction is directly proportional to the enzyme concentration. Under these premises, this velocity can be taken as a measure of the amount of active enzyme present. However, to experimentally realize substrate saturation and engage 99 % of the enzymes binding sites, the substrate is required to be present in a 100-fold surplus of the $K_m$ value (Bisswanger, 2014). The enzyme database BRENDA contains a wide range of $K_m$ values for many enzymes and their substrates. As these $K_m$ values differ widely not only between species but also within one species, it becomes difficult to know when substrate saturation is achieved. Moreover, enzyme saturation cannot always be maintained throughout the course of the reaction due to substrate conversion; as the reaction progresses and substrate gets depleted, the reaction slows down and the progress curve becomes non-linear. While this final non-linear phase provides valuable information on the kinetics of the underlying reaction, it is the initial linear part of the progress curve that provides a proper measure of the maximum enzyme activity realized under the imposed assay conditions. Assuming linearity, linear regression can be applied to this initial part of the progress curve to calculate the rate of change as a measure of the enzyme activity and, therefore, of the amount of active enzyme present. However, the assumption of linearity is, too often, not explicitly checked in a stopped assay. Only when the reaction time of the stopped assay is restricted to the linear part of the progress curve, proper results will be obtained (Bisswanger, 2014, 2011; Scopes, 2002).

In this chapter an alternative, more elaborate procedure is developed to estimate the *in vitro* specific enzyme activity of pyruvate decarboxylase and alcohol dehydrogenase from the progress curve. The method is based on a kinetic modelling approach taking into account the complete progress curve, including the non-linear range.

# 3.2 Materials and Methods

## 3.2.1 Plant material

'Jonagold' apples (*Malus* x *domestica* Borkh., cv. 'Jonagold') were harvested from an orchard in Rotselaar, Belgium on September 24 2015, during the commercial harvest window for long term storage of 'Jonagold' apples.

## 3.2.2 Chemicals

MES hydrate, triton X-100 (laboratory grade), acetaldehyde (ACS reagent, ≥ 99.5%), β-nicotinamide adenine dinucleotide (reduced disodium salt hydrate ≥ 97% (HPLC)), thiamine pyrophosphate, alcohol dehydrogenase (*Deinococcus radiodurans* recombinant from *E. coli* ≥ 10000 units/mL), sodium pyruvate and polyvinylpyrrolidone were purchased from Sigma-Aldrich (Overijse, Belgium). Dithiothreitol was obtained from VWR International (Leuven, Belgium) and magnesium chloride from Chem-Lab Analytical (Zedelgem, Belgium).

## 3.2.3 Enzyme extraction

Enzymes were extracted according to Saquet and Streif (2008), with the following modifications. For each replicate, 0.5 g frozen fresh apple tissue was homogenized with 1 mL ice-cold extraction buffer. The extraction buffer contained 100 mM 2-(N-morpholino) ethane sulfonic acid (MES) buffer (pH 7.5), 5 mM dithiothreitol and 2.5 % (w/v) polyvinylpyrrolidone and 0.02 % (w/v) triton X-100 and mixed on a magnetic stirrer until all components were dissolved. The homogenate was kept below 4 °C for 20 min and stirred continuously in a thermomixer at 1400 rpm. The homogenate was centrifuged at 14,000 *g* for 20 min at 4 °C. In order to achieve 80 % efficiency for the extraction, the pellet was extracted once more using the same protocol. The supernatants of both extractions were well mixed and retained as enzyme extract

for measuring PDC and ADH activities. The protein concentration of the crude extracts was determined using the Bradford assay (Bradford, 1976). The measured enzyme activity in this study was expressed relative to the total protein content of the sample.

### 3.2.4 Enzyme activity measurement

The enzyme activity of PDC and ADH was assayed as described by Ke *et al*. (1994), Imahori *et al*. (2003) and Saquet and Streif (2008), with the following modifications. In order to study the *in vitro* enzyme activity of PDC and ADH, the oxidation of NADH by the extracts was monitored spectrophotometrically. ADH activity was measured by mixing 100 µL of crude extract with 115 µL 1M MES buffer (pH 6.5), 25 µL of 800 mM acetaldehyde and 10 µL of 10 mM NADH. As a crude extract was used, the total enzyme activity of ADH was measured in this assay without making a distinction between the different isozymes. PDC activity was assayed through coupling with the ADH catalysed reaction. To this end, 100 µL crude extract was mixed with 90 µL of 1M MES buffer (pH 6.5), 10 µL of 5 mM thiamine pyrophosphate, 10 µL of magnesium chloride, 5 µL of commercial ADH solution (containing 50 enzyme units), 25 µL of 500 mM sodium pyruvate and 10 µL of 10 mM NADH. In this PDC assay, a surplus of commercial ADH was added to make sure that acetaldehyde formed through the PDC reaction was directly converted to ethanol, meanwhile oxidizing NADH. For both assays the reactions were initiated by addition of the reaction buffer, which contained both substrates (NADH and pyruvate/acetaldehyde) and cofactors (thiamine pyrophosphate and magnesium chloride). The oxidation of NADH was measured by continuously recording the decrease in absorbance at 360 nm using a spectrophotometer (Multiskan spectrum microplate spectrum, ThermoLabsystems, Finland) until a steady base level was reached. To ensure the noise in the reaction was limited to a minimum, the absorbance spectra of all compounds involved in the reaction mixture were measured between 200 and 400 nm. The signal to noise ratio was determined by dividing the spectra of NADH by the sum of the spectra of the

other compounds involved in the reaction. In order to check the technical and biological variation between the different extracts, absorbance of different extracts was measured at 360 nm in duplicate. All assays and additional spectrophotometric measurements were executed in flat bottom 96 well microtiter plates (Thermo Fisher Scientific) with a final reaction volume of 250 µL per well. The pH and salt concentration used in this study was based on the existing protocols as described by Ke *et al*. (1994), Imahori *et al*. (2003) and Saquet and Streif (2008) and not subjected to further optimization.

## 3.2.5 Determination of the absorption coefficient of NADH

The absorbance coefficient of NADH was determined by making a calibration curve with varying amounts of NADH (0 mM – 0.2 mM – 0.4 mM – 0.6 mM – 0.8 mM – 1 mM) prepared under assay conditions. Based on this calibration curve, linearity of the absorbance data measured with the spectrophotometer was confirmed up to a value of 1.887 OD.

## 3.2.6 Data analysis

The differential equations of the developed model (as will be described below) were implemented and parameters were estimated in OptiPa (Hertog *et al.*, 2007), a dedicated optimization tool which was developed using Matlab (The MathWorks, Inc., Natick, MA, USA). The differential equations were solved using the MATLAB solver ode45 and the model parameters were estimated using non-linear least squares optimization applying the Levenberg-Marquardt method.

# 3.3 Results and Discussion

## 3.3.1 Optimization of the enzymatic assays

In most enzymatic assays, enzyme activity is calculated by measuring the rate of consumption of a substrate or the production of a product over a given time period. In the case of PDC and ADH, the rate of oxidation of NADH is monitored. Given NADH has a known maximum light absorbance at 340 nm, most enzymatic assays, which depend on the conversion of NADH to $NAD^+$, base themselves on the absorbance values measured at this wavelength. However, the spectrophotometric data obtained in the enzymatic assays of both PDC and ADH were not reaching zero (Fig 3.1) indicating NADH may not be the only compound in the reaction mixture absorbing UV light at 340 nm, introducing unwanted noise.

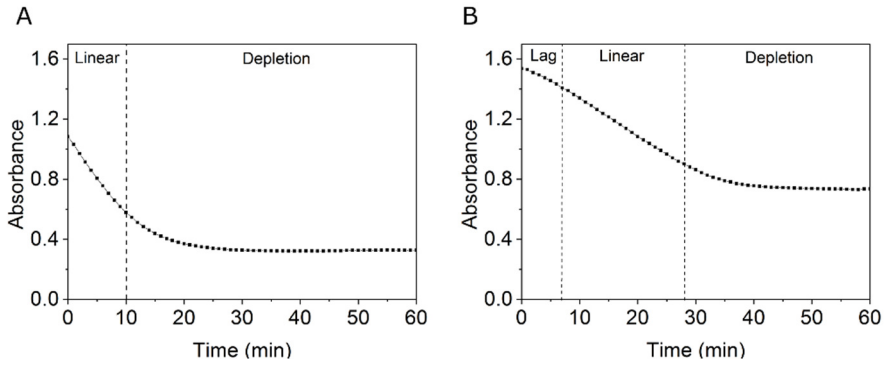


Figure 3.1: Representative example of spectrophotometric data obtained in the enzymatic assays. Spectrophotometric data obtained in the enzymatic assay to measure the activity of alcohol dehydrogenase (A) and pyruvate decarboxylase (B). Measured values (dots) are shown.

In general, the intensity of the signal produced by the reaction must exceed the noise produced by the other compounds by at least a factor two (Bisswanger, 2014). To understand which other compounds were absorbing UV light at 340 nm and if the noise could be limited to a minimum, the absorbance spectra of all compounds involved in the reaction mixture were measured between 200 and 400 nm (Fig 3.2).

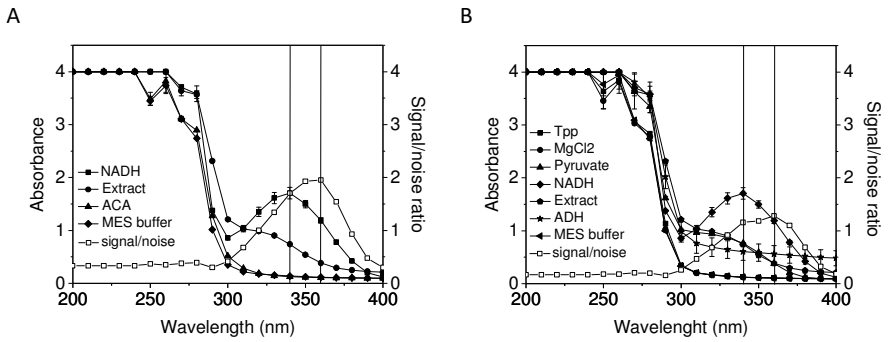


Figure 3.2: Spectra of all the compounds in the reaction mixture involved in the enzymatic assay. Spectra of all the compounds in the reaction mixture involved in the enzymatic assay to measure the activity of alcohol dehydrogenase (A) and pyruvate decarboxylase (B). (Tpp, thiamine pyrophosphate; MgCl2, magnesium chloride; ADH, alcohol dehydrogenase; ACA, acetaldehyde). Bars on top indicate standard error (n=3).

Acetaldehyde showed no absorbance in the range of 320 to 400 nm, making NADH the only substrate of the ADH assay absorbing light in this wavelength range. However, of the substrates involved in the PDC assay, pyruvate showed a clear absorbance in the UV range. Since pyruvate is present in excess, its concentration during the enzymatic assay will stay nearly constant, causing a nearly constant absorbance signal throughout the assay, explaining the much higher base level in the PDC assay (Fig 3.1B). Consequently, the decrease in absorbance in the PDC assay can still be assigned to the change in NADH. Interesting to notice is that in both example spectra the order of magnitude of the difference in absorbance between the enzymatic extracts was quite large (Fig 3.2). By comparing technical and biological replicates (Fig 3.3), it became clear that the variance in signal was not due to pipetting errors possibly induced by the foamy properties of the extract but rather came from compositional variation between the extracts.

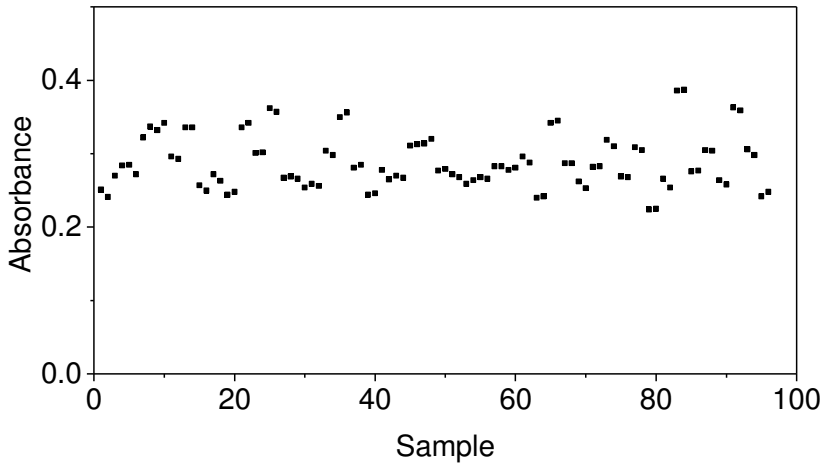


Figure 3.3: Absorbance data of 48 different extracts measured at 360 nm. Each two consecutive data points were technical repetitions of the same extract, each set of technical replicates was obtained from a different biological sample. Measured (dots) values are shown.

In order to increase the signal to noise ratio as much as possible, the measurement wavelength for the enzymatic assays was switched from 340 nm to 360 nm (Fig 3.2). In general, enzyme activity can be estimated from the spectrophotometric data, by taking the slope of the linear part of the progress curve resembling the rate of change in the substrate or product monitored. The concentration of the substrate, in this case NADH, can be calculated from the signal intensity applying an absorption coefficient (Bisswanger, 2014). The absorption coefficient of NADH (2.519 $mM^{-1}$) was determined by making a calibration curve with varying amounts of NADH prepared under assay conditions, at the same time confirming the linearity of the absorbance reading up to a value of 1.887 OD.

The overall change in absorbance during the enzyme assay, is due to the conversion of NADH to $NAD^+$. Assuming a complete conversion of NADH, this change in absorbance is directly related to the initial amount of NADH through its absorption coefficient. Interesting to notice is that the experimentally determined absorption coefficient of NADH (2.519 $mM^{-1}$) differed from the absorption coefficient calculated from the average difference in absorbance between the start and the end of the

enzyme assay. Additionally, this also differed between the two assays (2.410 $mM^{-1}$ for the ADH assay and 2.149 $mM^{-1}$ for the PDC assay, Fig 3.4). This discrepancy was more pronounced for the PDC assay, as compared to the ADH assay, suggesting some matrix effects occurred in this assay. Given the enzyme extracts used between the two assays were identical, this effect was not related to the sample matrix as such but to the other assay conditions.

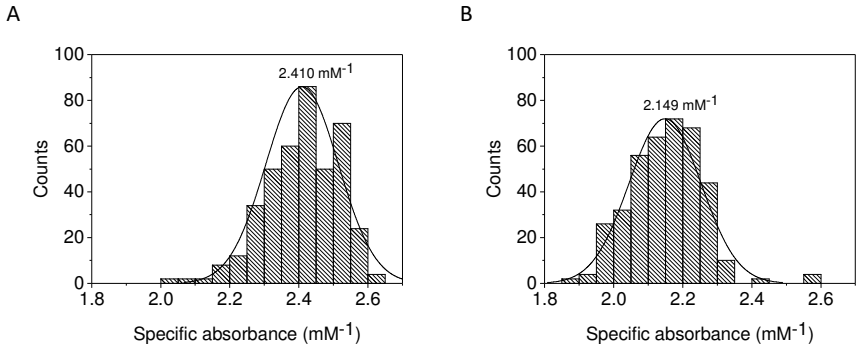


Figure 3.4: Distribution of the specific absorbance of NADH in the ADH assay (A) and the PDC assay (B). The specific absorbance of NADH is determined by the difference in absorption between the start and the end of the assay divided by the starting concentration of NADH. The average of the specific absorbance is indicated above the graph. The histograms are based on a total of 404 and 384 samples analysed for respectively the ADH and PDC assay.

Estimation of the enzyme activity through linear regression of the data should only be applied when linearity is true, which is often not the case or has not been checked. For example, the spectrophotometric data of coupled reactions like the PDC assay initially showed a lag phase before reaching a linear phase (Fig 3.1B). Since the enzyme activity of PDC can only be correctly estimated by taking the slope of the linear part of the progress curve, a large part of the progress curve cannot be taken into account. These data emphasize the importance of a continuous assay, as it is impossible to notice the initial non-linear part of the curve in a stopped assay. Furthermore, data like shown in Fig 3.1B are pointing out the need for a more elaborate model-based approach to determine the in *vitro* specific enzyme activity, which is also valid when the assumption of linearity is not fulfilled. To this end, dedicated kinetic models were developed.

## 3.3.2 Kinetic model development

Kinetic models were developed to estimate the *in vitro* specific enzyme activity of PDC and ADH from the spectrophotometric data. The kinetic models were based on the underlying reaction mechanism of the fermentative metabolism, summarized by equation 1 and 2.

$$\text{Pyruvate} + \text{PDC} \underset{k_{-1}}{\overset{k_1}{\rightleftharpoons}} \text{AC}_1 \xrightarrow{k_{PDC}} \text{Acetaldehyde} + \text{PDC} \quad (1)$$

$$\text{Acetaldehyde} + \text{NADH} + \text{ADH} \underset{k_{-2}}{\overset{k_2}{\rightleftharpoons}} \text{AC}_2 \xrightarrow{k_{ADH}} \text{Ethanol} + \text{NAD}^+ + \text{ADH} \quad (2)$$

where $AC_1$ and $AC_2$ are the intermediate enzyme-substrate complexes formed in the reaction.

During fermentation acetaldehyde is produced through pyruvate decarboxylation by PDC (Eq. 1). In the next step acetaldehyde is converted to ethanol by ADH using NADH (Eq. 2).

## 3.3.3 Kinetic model for alcohol dehydrogenase

The kinetic model to estimate the activity of ADH is based on Michaelis-Menten kinetics describing equation 2 of the fermentative metabolism. Michaelis-Menten kinetics was used with regard to NADH only as the acetaldehyde concentration in this reaction was kept at high levels assuming saturation. The Michaelis-Menten equation to describe the conversion of NADH to $NAD^+$ over time was defined as:

$$\frac{d[\text{NADH}]}{dt} = \frac{-V_{m,ADH} \cdot [\text{NADH}]}{K_{m,ADH} + [\text{NADH}]} \quad (3)$$

where $K_{m,ADH}$ is the Michaelis-Menten constant and $V_{m,ADH}$ is the maximum reaction rate which, on its turn, was defined as:

$$V_{m,ADH} = k_{ADH} \cdot [\text{ADH}]_0 \quad (4)$$

where $k_{ADH}$ is the maximum number of substrate molecules converted to product per enzyme molecule per second and $[ADH]_0$ is the initial concentration of ADH present in the reaction mixture. The concentration of enzyme present in the reaction mixture is related to the concentration of enzyme present in the extract ($[ADH_{extr}]$), the volume of extract taken ($V_{extr}$) and the total volume of the reaction mixture ($V$) leading to:

$$V_{m,ADH} = k_{ADH} \cdot \left( \frac{\left[ \mathrm{ADH_{extr}} \right] \cdot V_{extr}}{V} \right) \tag{5}$$

Given the theoretical rate constant $k_{ADH}$ and the extract depending enzyme concentration $[ADH_{extr}]$ are two unknowns appearing as a single product term, together being responsible for the overall perceived enzyme activity, a single composite replacement term, $k'_{ADH}$, was defined representing the ADH activity extracted from the sample. The Michaelis-Menten equation to describe the conversion of NADH to $NAD^+$ (Eq.3) was thus redefined as:

$$\frac{d[\mathrm{NADH}]}{dt} = \frac{-k'_{ADH} \cdot \left( V_{extr} / V \right) \cdot [\mathrm{NADH}]}{K_{m,ADH} + [\mathrm{NADH}]} \tag{6}$$

The numerical solution of this differential equation describes the concentration of NADH for every point in time ([NADH](t)), with $[NADH]_0$ as the initial condition. As the absorbance measured in the enzymatic assay is the sum of the absorbance by the changing levels of NADH and the constant, but sample specific, absorbance by the extract ($A_{extr}$), the modelled absorbance $A_{mod}$ is given by:

$$A_{\mathrm{mod}} = \left[ \mathrm{NADH} \right](\mathrm{t}) \cdot \alpha_{NADH} + A_{extr} \tag{7}$$

with $\alpha_{NADH}$ being the specific absorbance of NADH. To take into account the sample specific matrix effect (see Fig 3.4), the specific absorbance of NADH was determined for every sample following:

$$\alpha_{NADH} = \left( A_0 - A_{final} \right) / [\mathrm{NADH}]_0 \tag{8}$$

with $A_0$ the absorption measured at the start of the assay, $A_{final}$ the absorption measured at the end of the assay and $[NADH]_0$ the starting concentration of NADH.

The final model of the ADH assay as defined by Eqs. 6-8 was implemented in OptiPa (Hertog *et al.*, 2007) which was also used to estimate for every sample the unknown model parameters $k'_{ADH}$ and $K_{m,ADH}$ by fitting the model to the measured spectrophotometric data. The kinetic model to estimate the enzyme activity of ADH thus takes into account the entire progress curve, as shown in Fig 3.5.

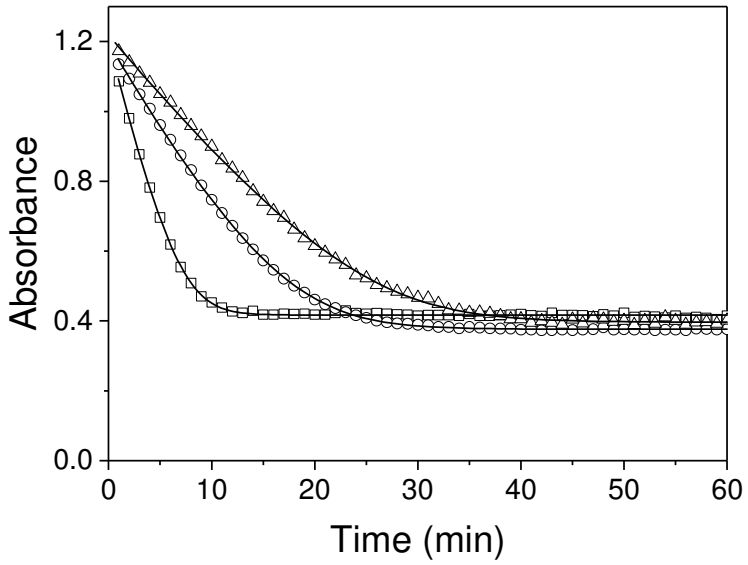


Figure 3.5: Results of the kinetic model describing the spectrophotometric data of the enzymatic assay to measure alcohol dehydrogenase activity. Results are shown for 3 representative biological apple fruit extracts. Fitted (line) and measured (symbols) values are shown. The estimated $k'_{ADH}$ values were respectively 419 ± 12.8 $mol.L^{-1}.s^{-1}.kg^{-1}$ (△), 650 ± 2.2 $mol.L^{-1}.s^{-1}.kg^{-1}$ (○) and 1682 ± 56.5 $mol.L^{-1}.s^{-1}.kg^{-1}$ (□), all expressed on a total protein weight base.

## 3.3.4 Kinetic model for pyruvate decarboxylase

Since the PDC assay is a coupled assay combining the decarboxylation reaction catalysed by PDC (Eq. 1) with the indicator reaction catalysed by ADH (Eq. 2), the kinetic model for the PDC assay has to cover both reactions. The indicator reaction is responsible for generating a measurable spectrophotometric response thanks to the conversion of NADH to $NAD^+$. To be able to unequivocally quantify the PDC

reaction, the indicator reaction catalysed by ADH should not become rate limiting. For this reason, commercial ADH was added to the reaction mixture to make sure that acetaldehyde formed in the PDC reaction was swiftly converted into ethanol. As acetaldehyde, as an intermediate substrate, was not assumed to reach saturating levels, first order kinetics was applied to describe the ADH reaction, at least with regard to acetaldehyde. As NADH can be expected to pass through the full concentration range from initial saturating levels to depletion, Michaelis-Menten kinetics was assumed for NADH. Pyruvate levels in the assay were several magnitudes higher than the levels of NADH. As a consequence, the ADH reaction lasts not long enough to act as an indicator for the complete depletion of pyruvate. The part monitored by the assay is therefore only mirroring the initial phase where the PDC reaction operates at its maximum velocity, which can therefore be described using zero order kinetics. The process can thus be defined by the following two equations:

$$\frac{d[\mathrm{ACA}]}{dt} = k_{PDC} \cdot [\mathrm{PDC}]_0 - \frac{k_{ADH} \cdot \mathrm{U_{ADH}} \cdot [\mathrm{ACA}] \cdot [\mathrm{NADH}]}{K_{m,NADH} + [\mathrm{NADH}]} \tag{9}$$

$$\frac{d[\mathrm{NADH}]}{dt} = -\frac{k_{ADH} \cdot \mathrm{U_{ADH}} \cdot [\mathrm{ACA}] \cdot [\mathrm{NADH}]}{K_{m,NADH} + [\mathrm{NADH}]} \tag{10}$$

where $k_{PDC}$ is the rate constant of PDC at saturating pyruvate levels, [PDC] is the concentration of PDC in the reaction mixture, $k_{ADH}$ is the rate constant of ADH, $K_{m,NADH}$ the Michaelis-Menten constant with regard to NADH, $U_{ADH}$ the amount of commercial ADH added to the reaction mixture and [ACA], [NADH] are the concentrations of acetaldehyde and NADH in the reaction mixture, respectively.

Like before, the amount of PDC present in the reaction mixture is related to the concentration of enzyme present in the extract ([$PDC_{extr}$]), the volume of the extract ($V_{extr}$), and the total volume of the reaction mixture (V). Hence, equation 9 can be written as:

$$\frac{d[\mathrm{ACA}]}{dt} = k_{PDC}\left(\frac{[\mathrm{PDC_{extr}}]\cdot V_{extr}}{V}\right) - \frac{k_{ADH}\cdot \mathrm{U_{ADH}}\cdot[\mathrm{ACA}]\cdot[\mathrm{NADH}]}{K_{m,NADH}+[\mathrm{NADH}]} \qquad (11)$$

Similar as for the kinetic model of ADH, a composite term $k'_{\mathrm{PDC}}$ was introduced which combines the rate constant $k_{PDC}$ and the concentration of PDC in the extract $[\mathrm{PDC_{extr}}]$ into a single measure of the enzyme activity of PDC as extracted from the sample. Therefore, equation 11 was rewritten as follows:

$$\frac{d[\mathrm{ACA}]}{dt} = k'_{PDC}\cdot\left(\frac{V_{extr}}{V}\right) - \frac{k_{ADH}\cdot \mathrm{U_{ADH}}\cdot[\mathrm{ACA}]\cdot[\mathrm{NADH}]}{K_{m,NADH}+[\mathrm{NADH}]} \qquad (12)$$

The concentration of NADH at every point in time ([NADH](t)) can be calculated by solving the two coupled differential equations, Eq.10 and Eq.12, using $[\mathrm{NADH}]_0$ and $[\mathrm{ACA}]_0$ as initial conditions.

According to Fig 3.2, not only NADH and the extract, but also pyruvate absorbed UV light at 360 nm. Because the absorbance measured in the enzymatic assay was thus a combination of the absorbance by the changing NADH levels and a constant absorbance ($A_{final}$) being, on its turn, a combination of a sample specific absorbance of the extract and the constant absorbance by pyruvate, the modelled absorbance $A_{\mathrm{mod}}$ is given by:

$$A_{\mathrm{mod}} = [\mathrm{NADH}](\mathrm{t})\cdot\alpha_{NADH} + A_{final} \qquad (13)$$

with $\alpha_{NADH}$ being the specific absorbance of NADH as determined by Equation 8, and [NADH](t) being the concentration of NADH estimated by the model for every time point.

The final model for the PDC assay as defined by Eqs. 8, 10, 12 and 13 was again implemented in OptiPa and used for estimating the unknown parameter values by fitting the model to the measured spectrophotometric data. The model parameters $k'_{\mathrm{PDC}}$ and $K_{\mathrm{m,NADH}}$ were estimated per sample, but the model parameter $k_{\mathrm{ADH}}$ was estimated in common over all samples, as the concentration of the enzyme ADH added to the reaction mixture was the same for all of them.

The kinetic model to estimate the enzyme activity of PDC takes into account the entire progress curve, as shown in Fig 3.6.

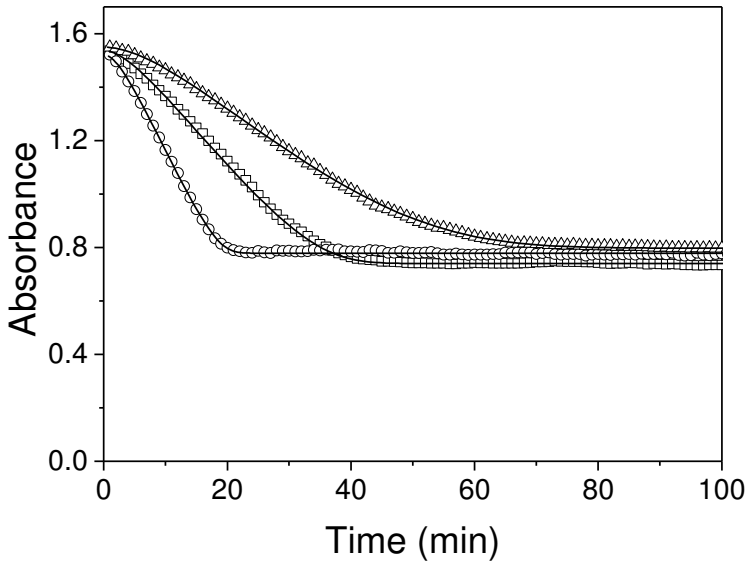


Figure 3.6: Results of the kinetic model describing the spectrophotometric data of the enzymatic assay to measure pyruvate decarboxylase activity. Results are shown for 3 representative biological apple fruit extracts. Fitted (line) and measured (symbols) values are shown. The estimated $k'_{PDC}$ values were respectively 276 ± 9.5 $mol.L^{-1}.s^{-1}.kg^{-1}$ (△), 386 ± 5.6 $mol.L^{-1}.s^{-1}.kg^{-1}$ (□) and 576 ± 16.9 $mol.L^{-1}.s^{-1}.kg^{-1}$ (○) all expressed on a total protein weight base.

## 3.3.5 Comparison between linear regression and kinetic modelling approach to estimate enzyme activity

The linear regression approach is generally used to estimate enzyme activity. In the next paragraph a comparison is made between the generally accepted linear regression approach and the kinetic modelling approach to estimate enzyme activity. Advantages of the latter method over the classic method are stressed in the text.

When optimum conditions are applied in the enzyme assay, i.e., substrate and cofactor saturation, standard pH, temperature and ionic strength, the slope of the linear part of the progress curve can be taken as a measure of the maximum enzyme

activity. To correctly compare the activity of different enzymes, it is important to always quantify their activity under the optimum working conditions. Like mentioned in the introduction, to experimentally realize substrate saturation, the substrate is required to be present in a 100-fold surplus of the $K_m$ value. However, in the case of NADH, to stay within the detection range, the NADH concentration should not exceed 0.2 mM (Bisswanger, 2014). As a result, it is practically impossible to estimate the theoretical maximum enzyme activity of PDC and ADH using a linear regression approach. Using the kinetic modelling approach the maximum activity of the enzyme can be estimated through extrapolation even if the saturating substrate conditions were not fully realized. The onset of the progress curve of single step reactions, like ADH, approximates linearity (Fig 3.1A). With the linear regression approach it is advisable to take a linear part long enough to get reliable results, especially in the presence of remarkable scattering of the data, without extending into the nonlinear part of the progress curve. Using the kinetic modelling approach the whole progress curve is taken into account making this method more robust to measurement noise. It becomes more complex in the case of a coupled reaction, like for PDC, where the progress curve often does not show an initial linear response as a function of time (Fig 3.1B). Depending on the size of the lag phase relative to the linear phase, and depending on whether both phases or only the linear part is considered, the final quantification of the slope will change (Fig 3.7). As an example, linear approximations were done for two extracts, one with a high (Fig 3.7A) and one with a low PDC activity (Fig 3.7B). Depending on the sample and the time interval used for the linear approach the obtained values are different. As more time points are used for the linear regression approach, the enzyme activity becomes higher and the 95 % confidence interval becomes smaller. If only the linear part of the curve is considered, the enzyme activity calculated is the most reliable. Furthermore, it is important to mention that, in case of the coupled PDC reaction, the enzyme activity estimated by the linear regression approach is a lumped value, encompassing the activity of both PDC and ADH. In contrast, when using the kinetic model the activity of PDC and ADH are estimated separately. This accounts for the completely different

values obtained by the model (Fig 3.7). The accuracy of the enzyme activity estimated by the model comes from an estimation error and is typically 1.77 % but is not affected by the user's choice of time interval and the fitness of the assumption of linearity.

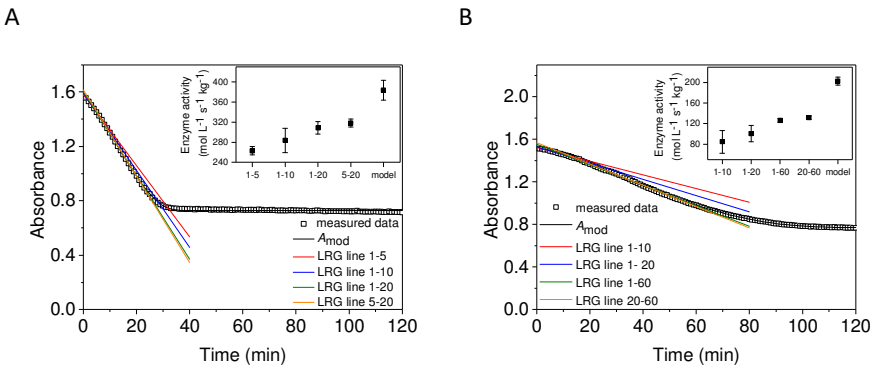


Figure 3.7: Changes in the final quantification of the slope when applying the linear regression approach. The linear regression approach is indicated by LRG. The results highly depend on whether the progress curve has a short lag phase (A) or a long lag phase (B) as compared to the linear phase and whether both phases or only the linear part is considered. The numbers in the legend indicate the respective start and stop times (in min) used for the linear approximations and the resulting activity calculated. The model outcome ($A_{mod}$) was based on the full progress curve. The activity calculated through the linear regression approach and the model as well as their 95 % confidence interval are indicated on the graph.

## 3.3.6 Insights given by the model

Fig 3.8A shows the data simulated by the model for the ADH assay. Once NADH is depleted, the reaction stops and ethanol is no longer produced. In the case of the coupled PDC reaction, the reaction mechanism is more complex.

Since two reactions are involved in the PDC assay, it takes a while before the formation and conversion of the intermediate becomes constant, causing an initial lag phase before reaching the linear phase. As can be seen from the simulated model data (Fig 3.8B), only once an initial amount of acetaldehyde is formed the conversion to ethanol by ADH becomes more or less constant, causing the initial lag phase of 5

to 10 min. While the progress curve seems to be quite linear from 10 min onwards, the slowly increasing level of acetaldehyde is indicating the contrary. With depleting levels of NADH the indicator reaction slows down further, resulting in an ongoing faster accumulation of the intermediate acetaldehyde. The moment NADH is completely finished, the indicator reaction stops and acetaldehyde is no longer converted to ethanol, causing an increase in the concentration of acetaldehyde as the PDC reaction will continue regardless (Fig 3.8B).

Of course, one should be aware of the limitations of the kinetic model related to the assumptions applied. As the model was focused towards the reaction period where NADH would still be present, the eventual depletion of pyruvate was not incorporated resulting in an everlasting increase of acetaldehyde. In reality, if the reaction would be allowed to continue, pyruvate would effectively be depleted after 100 h or more. From this it can be concluded that the assumption made was acceptable for the current application.

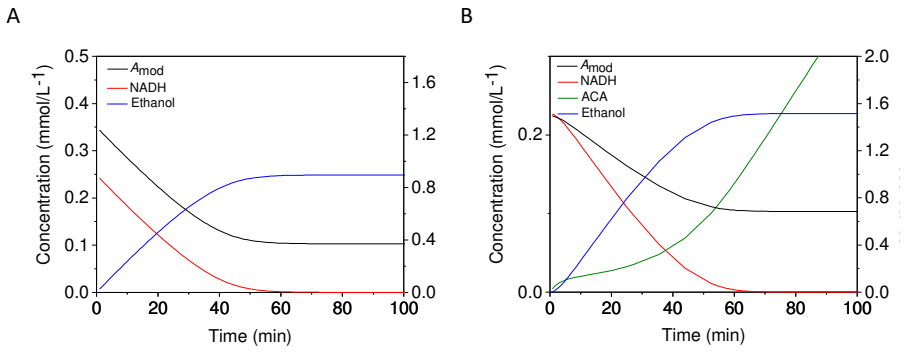


Figure 3.8: Changes in concentration of all the compounds involved in the reaction. This figure shows the changes in concentration of all the compounds involved in the reaction of alcohol dehydrogenase (A) and pyruvate decarboxylase (B), simulated by the kinetic models, in relation to the progress curve estimated by the model (ACA, acetaldehyde).

Furthermore, the models can help to optimize the assays by systematically studying the effect of the various design parameters like extract volume, substrate concentration and indicator enzyme amount. For instance, it was hypothesized that the initial lag phase in the PDC assay could be prevented by increasing the amount of ADH, in which case the initial amount of acetaldehyde that needs to accumulate before the conversion to ethanol starts would be less. As shown in Fig 3.9A, when the total enzyme activity of ADH is increased by adding more enzyme, the second reaction is no longer rate limiting resulting in a clear initial linear decrease with time as acetaldehyde is converted to ethanol much faster (Fig 3.9B). When the amount of ADH added to the reaction mixture is decreased, the opposite effect is observed and the nonlinearity of the curve becomes more pronounced (Fig 3.9A). In this case the ADH reaction becomes rate limiting, as indicated by the increasing time needed for acetaldehyde to accumulate before being converted to ethanol.

While the accuracy of the linear regression approach will benefit from an increased ADH level, the kinetic modelling approach can deal with nonlinear results, not necessarily requiring an increased ADH level. As an additional advantage, costs of the assay can be reduced.

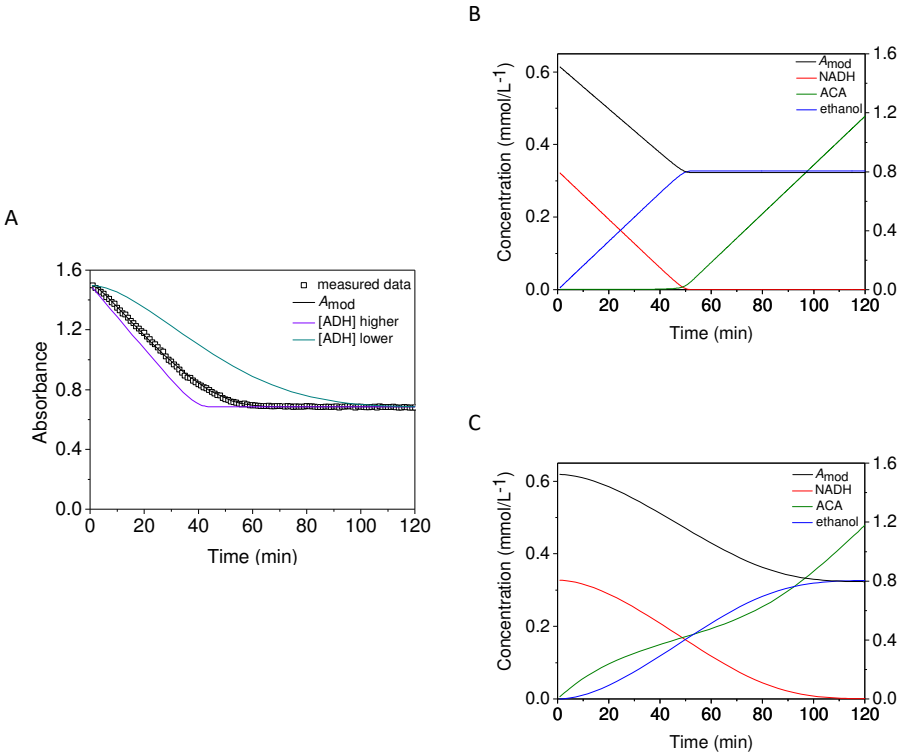


Figure 3.9: The models can help to optimize the assays by systematically studying the effect of the various design parameters. Changes in the progress curve if more or less alcohol dehydrogenase is added (A). Changes in concentration of all the compounds involved in the assay when high amounts (B) or low amounts (C) of alcohol dehydrogenase (ADH) are added. (ACA, acetaldehyde).

## 3.4 Conclusion

Existing enzyme assays to measure the *in vitro* specific enzyme activity of PDC and ADH were optimized in order to increase the signal to noise ratio. An elaborated kinetic model-based method was proposed to estimate the *in vitro* specific enzyme activity from the spectrophotometric assay data. The kinetic models developed in this chapter can accurately estimate the enzyme activity of PDC and ADH in the given

assays and will be used in the next chapters to study the behaviour of the fermentative metabolism.

In contrast to the linear regression approach, the models can be used to estimate the enzyme activity whether or not linearity is achieved since they take into account the complete progress curve. Using the kinetic modelling approach the maximum activity of the enzyme can be estimated through extrapolation even if the saturating substrate conditions were not fully realized in the enzyme assay, making it possible to compare the obtained results between different experiments and between different labs and publications. The developed models can be applied to routinely analyse continuous spectrophotometric enzyme activity data, but like shown in this chapter, they can also be used as a tool to optimize the enzyme assays by systematically studying the effect of the various design parameters. Finally, the use of kinetic models to estimate the *in vitro* specific enzyme activity can be extended to other enzymes as long as the underlying reaction mechanism is known and the reaction dynamics can be monitored in a continuous way. Furthermore, the differential equations of the developed models can be implemented in any software environment that supports estimation of kinetic parameters on ODE based models, e.g., Matlab (The MathWorks, Inc., Natick, MA, USA), Mathematica (Wolframe, Inc., Boston, MA, USA), Maple (Maplesoft, Inc., Japan) and R (R Foundation for statistical computing, Vienna, Austria), or in online web tools such as ENZO (enzyme kinetics; Bevc *et al.*, 2011).

# Chapter 4

# The fermentative metabolism in apple fruit exposed to low-oxygen stress reveals highly flexible regulation

In this chapter, the *in vivo* regulation of the fermentative metabolism is studied by using a combination of experimental techniques and a kinetic modelling approach to translate the *in vitro* measured enzyme activity (analysed by the models developed in chapter 3) into *in vivo* activities. New insights in the regulation of the fermentative metabolism are provided by the model.

# 4.1 Introduction

Almost half of the apple (*Malus* x *domestica* Borkh.) production is destined for long-term storage. Large volumes of apple fruit are routinely stored under controlled atmosphere (CA) conditions (low temperature, low oxygen and high carbon dioxide partial pressures) with recent developments moving towards dynamic CA (DCA) storage (Bessemans *et al.*, 2016; Mditshwa *et al.*, 2018; Prange *et al.*, 1989; Veltman *et al.*, 2003; Watkins, 2000; Wright *et al.*, 2012). During DCA storage, the oxygen concentration in the cool store is reduced towards the anaerobic compensation point until the physiological response of the fruit indicates that its metabolism has switched from aerobic respiration to fermentation. In this way, fruit ripening can be delayed more effectively than under regular CA storage (Bessemans *et al.*, 2016; Mditshwa *et al.*, 2018; Watkins, 2000). Crucial to any DCA approach is the close monitoring of the fruit's metabolic response, timely indicating increased low-oxygen stress (Bessemans *et al.*, 2016; Prange *et al.*, 1989; Veltman *et al.*, 2003; Watkins, 2000; Wright *et al.*, 2012). When the low-oxygen stress induced in the tissue is too severe, mitochondrial respiration is compromised too much, leading to insufficient supply of ATP for energy demanding processes. In an attempt to compensate for this decrease in respiratory energy production, plants increase their glycolytic flux to produce more energy with the conversion of glucose to pyruvate, a process known as the Pasteur effect (Bailey-Serres *et al.*, 2012). To be able to maintain this high glycolytic flux, $NADP^+$ and $NAD^+$ have to be regenerated and the accumulation of pyruvate should remain limited (António *et al.*, 2016; Bailey-Serres *et al.*, 2012; Geigenberger, 2003). Therefore, the increase in glycolytic flux is typically coupled to fermentation. In these pathways pyruvate can be converted to either lactate or ethanol and $CO_2$, meanwhile maintaining the redox balance in the cell by the formation of $NAD^+$ (Perata and Alpi, 1993). The conversion of pyruvate to lactate is catalysed by the enzyme lactate dehydrogenase (LDH). In the ethanol pathway of the fermentative metabolism, pyruvate is converted with the help of PDC into

acetaldehyde, which is further converted to ethanol by ADH and finally to ethyl acetate by the enzyme alcohol acyl transferase (AAT). Fermentative metabolites such as ethanol, acetaldehyde and ethyl acetate can diffuse out of the cells into the apoplast and out of the tissue, leading to a reduction of carbon reserves and causing off-flavours (António *et al.*, 2016; Fukao and Bailey-Serres, 2004; Pesis, 2005; Tadege *et al.*, 1999). Hence, fermentation should be avoided during postharvest storage of fruit.

As of today, little information is available on the *in vivo* regulatory mechanism of the fermentative metabolism under low-oxygen stress. Based on *in vitro* experiments, two mechanisms were suggested: (1) the molecular control of the transcript and protein levels of PDC, ADH and LDH and (2) the metabolic control of these enzymes by changing cytosolic pH set-points, cofactors and substrate levels (Chang *et al.*, 1983; Imahori *et al.*, 2003, 2002; John and Greenway, 1976; Ke *et al.*, 1995). However, experimental conditions *in vitro* are not necessarily a correct representation of the situation *in vivo*. Therefore, the focus of this study is to get a better insight into the regulation of the fermentative metabolism of apple *in vivo* under different oxygen concentrations and temperature levels, and immediately after harvest as well as after storage. By combining experimental techniques with a kinetic modelling approach, the measured *in vitro* enzyme activity are translated into *in vivo* activities based on which possible *in vivo* regulatory mechanisms are evaluated.

# 4.2 Materials and methods

## 4.2.1 Plant material

'Jonagold' apples (*Malus* x *domestica* Borkh., cv. 'Jonagold') were harvested from the same orchard in Rotselaar, Belgium on September 26, 2014 and September 24, 2015, during the commercial harvest window for long term storage of 'Jonagold' apples. Apples were cooled immediately upon arrival to a temperature of 1 °C and stored for either 7 d (2014) or 4 d (2015) in regular air before the start of the experiment at harvest. In 2015, half of the apples were used for the experiment at harvest and the other half were stored for 6 months under commercial CA conditions (1 kPa $O_2$, 2.5 kPa $CO_2$, 1 °C). In this case, the second experiment started after this 6 months of storage. Three days before the start of this experiment, apples were taken out of CA and stored under regular air for 2.5 days at 1 °C to allow for the metabolism to adjust to regular air conditions. The duration of the adaptation period was determined in a previous experiment by measuring the respiration and ethylene production rate of the fruit. For both experiments of 2015, at harvest and the second experiment after storage, the experiment took place at 18 °C, and 12 h before the start of the experiment apples were transferred to 18 °C, to allow for proper temperature equilibration.

## 4.2.2 Experimental design

To be able to control oxygen concentrations at the tissue level and to prevent the formation of oxygen gradients as usually occurring in bulky fruit tissue (Ho *et al.*, 2011, 2010), experiments were carried out on thin apple slices. Per apple, five apple slices of 2 mm thickness were cut from the region perpendicular to the axis excluding peel and core. These five slices of five replicate fruit were placed on a rack of perforated plastic (polypropylene) and placed in airtight PVC containers, which were designed for the purpose of these experiments. Each container contained the 5

tissue slices per biological replicate for a single sampling time point. The experimental setup is shown in Fig. 4.1. The containers (3.5 L) were flushed with humidified air (21 kPa $O_2$) at a continuous flow rate of 40 L/h for 24 h prior to applying the experimental oxygen concentrations.

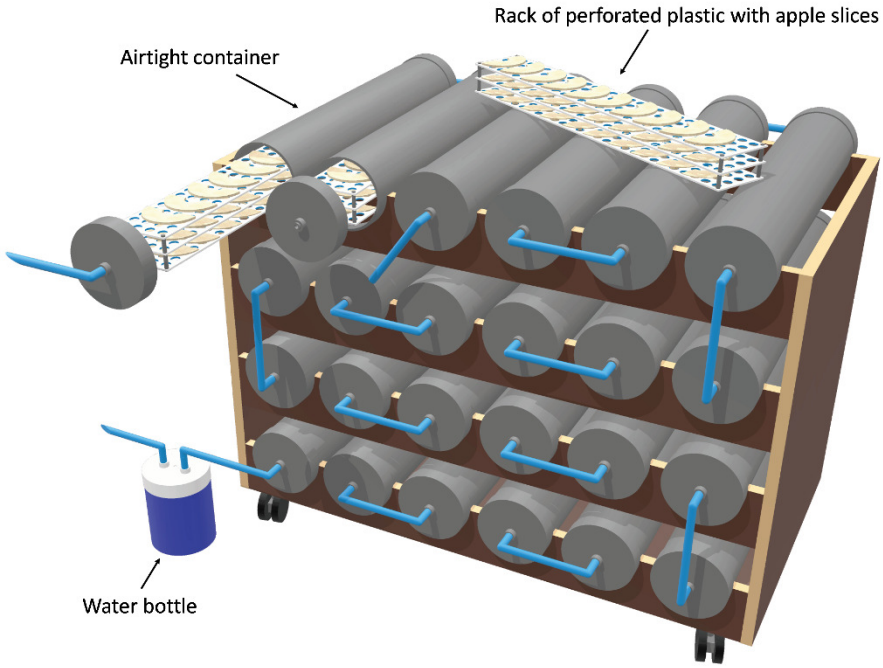


Figure 4.1: Representation of the experimental setup designed for this research. Apple slices of five biological replicates were put on a rack of perforated plastic, so the gas conditions could reach both sides of the apple slices, preventing the formation of oxygen gradients in the slice. The racks were placed in airtight PVC containers (3.5 L), which were connected in series in a temperature controlled room. The containers were flushed with the experimental gas conditions (flow rate of 40 L/h), which first passed through a water bottle to humidify the flow in order not to dry out the apple slices. The last container of the series was disconnected at regular time points for sampling, leaving the remaining containers undisturbed.

For the 2014 experiment at harvest, samples were exposed to 0.3 kPa $O_2$ balanced by $N_2$ for 72 h at 1 °C to induce fermentation. Based on the results of the 2014 experiment, it was decided to switch temperature from 1°C to 18°C to induce fermentation more strongly. Therefore, for the 2015 experiment at harvest, samples were exposed to either 0 kPa $O_2$ or 5 kPa $O_2$ both balanced by $N_2$ for 72 h at 18 °C.

Finally, for the 2015 experiment after 6 months of storage, samples were exposed to either 0 kPa $O_2$, 0.5 kPa $O_2$, 1 kPa $O_2$ or 5 kPa $O_2$, all balanced by $N_2$ for 72 h at 18 °C. In all three experiments, control samples were flushed with 21 kPa $O_2$. At regular time points during 72 h (detailed time scale indicated in the graphs), samples were taken by disconnecting a single container leaving the remaining containers undisturbed. The tissue was frozen using liquid nitrogen, ground into fine powder using an analytical mill (A11 Analytical mill, Ika, Belgium) and stored at -80 °C. These samples were used to measure the concentrations of fermentation metabolites (i.e., acetaldehyde, ethyl acetate and ethanol) and the enzyme activity of pyruvate decarboxylase and alcohol dehydrogenase.

## 4.2.3 Chemicals

MES hydrate, triton X-100 (laboratory grade), acetaldehyde (ACS reagent, ≥ 99.5 %), β-nicotinamide adenine dinucleotide (reduced disodium salt hydrate ≥ 97 %; HPLC grade), thiamine pyrophosphate, alcohol dehydrogenase (*Deinococcus radiodurans* recombinant from *E. coli* ≥ 10000 units/mL), sodium pyruvate, polyvinylpyrrolidone and sodium acetate (≥ 99 %) were purchased from Sigma-Aldrich (Overijse, Belgium). Dithiothreitol was obtained from VWR International (Leuven, Belgium), magnesium chloride from Chem-Lab Analytical (Zedelgem, Belgium), and ethyl acetate (99.5 %), sodium chloride and ethanol absolute from Fisher Scientific (Merelbeke, Belgium).

## 4.2.4 Enzyme extraction

Enzymes were extracted as described in Chapter 3 section 3.2.3.

## 4.2.5 Enzyme activity measurement

The enzyme activity of pyruvate decarboxylase (PDC) and alcohol dehydrogenase (ADH) was measured as described in chapter 3 in section 3.2.4.

## 4.2.6 Fermentation metabolites

To determine the concentrations of fermentation metabolites in the apple slices, 1 g of frozen powder sample was weighted in a 20 mL glass vial and 2 mL of 36 % sodium chloride solution was added and mixed with the sample to stop the enzymatic reactions during thawing. The vial was sealed and heated to 65 °C for 30 min to force the fermentation volatiles into the headspace. The content of the fermentation volatiles in the headspace of the vial was measured using a compact gas chromatograph (Interscience, Louvain-la-Neuve, Belgium). The compact GC was equipped with a 15 m MXT-wax column with a 0.53 mm internal diameter and 0.5 µm stationary phase thickness. The fermentation volatiles were detected with a flame ionization detector (using flowrates of 300 µL $min^{-1}$ of air and 30 µL $min^{-1}$ of $H_2$) using He as a carrier gas (flow rate 30 µL $min^{-1}$). To calculate the absolute concentration of the fermentation metabolites, a calibration line was established for acetaldehyde, ethanol and ethyl acetate using pure standards. The calibration line was obtained by treating 1 mL of a known concentration in the same way as a sample.

## 4.2.7 Model development

To interpret the *in vitro* determined enzyme activities in terms of their *in vivo* impact, a kinetic model was developed for the ethanol pathway of the fermentative metabolism. The model is based on the reaction mechanism of the ethanol pathway (shown in red), which can be described as:

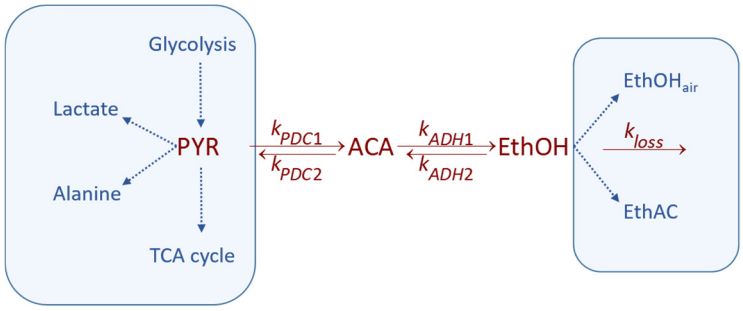


(1)

where PYR stands for pyruvate, ACA for acetaldehyde, EthOH for ethanol, EthAC for ethyl acetate and $EthOH_{air}$ for ethanol lost through diffusion in the air. The forward and backward reaction rate constants are represented by $k_{PDC1}$, $k_{PDC2}$, $k_{ADH1}$, $k_{ADH2}$ and $k_{loss}$.

The kinetic model to describe the ethanol pathway (Eq. 1) is assuming first order kinetics and is defined by the following ordinary differential equations (2 – 3):

$$\frac{d[\text{ACA}]}{dt} = \begin{aligned} & k_{PDC1}\cdot[\text{PDC}]\cdot[\text{PYR}] - k_{PDC2}\cdot[\text{PDC}]\cdot[\text{ACA}] \\ & -k_{ADH1}\cdot[\text{ADH}]\cdot[\text{ACA}] + k_{ADH2}\cdot[\text{ADH}]\cdot[\text{EthOH}] \end{aligned} \quad (2)$$

$$\frac{d[\text{EthOH}]}{dt} = \begin{aligned} & k_{ADH1}\cdot[\text{ADH}]\cdot[\text{ACA}] - k_{ADH2}\cdot[\text{ADH}]\cdot[\text{EthOH}] \\ & -k_{loss}\cdot[\text{EthOH}] \end{aligned} \quad (3)$$

with PDC the concentration of PDC and ADH the concentration of ADH measured experimentally.

As the kinetic models developed in chapter 3 estimate the maximal *in vitro* enzyme activity of PDC and ADH, the velocity of the catalysed reaction is directly proportional to the concentration of PDC and ADH present in the cell, and, therefore, used as a direct input of the concentration of PDC and ADH in the model (Eq. 2-3). The diffusion constant of ethanol in 'Jonagold' apple was not known and the change in ethyl acetate could not be modelled, since it is not entirely clear what other reactions it might be involved in. A lumped parameter $k_{loss}$ was therefore introduced to model the loss of ethanol due to conversion to ethyl acetate and/or diffusion to the environment (see Eq. 1).

The concentration of pyruvate was not measured experimentally, as only volatile components were measured with the compact GC. Therefore, the relative amount of pyruvate changing with time (*t* in h) was estimated by the model by using a fourth

order polynomial starting from an initial value of $PYR_0$ (set to unity) and truncated to positive values (Eq. 4).

$$[PYR]=\max\left(0,PYR_0 + p_1 \cdot t + p_2 \cdot t^2 + p_3 \cdot t^3 + p_4 \cdot t^4\right) \quad (4)$$

The concentration of pyruvate in the cell is a combination of the production of pyruvate through the glycolysis and a conversion of pyruvate to alanine, citrate (TCA cycle), lactate or acetaldehyde (see Eq. 1).

A smooth switch function was implemented for both $k_{PDC1}$ and $k_{ADH1}$ to model an increase in specific activity of the enzymes from a minimum $k_{i,min}$ to a maximum $k_{i,max}$ value assuming a logistic change over time with a rate of $k_{switch,i}$ while switching around the time point of $t_{switch,i}$. The switch function applied to both $k_{PDC1}$ and $k_{ADH1}$ follows the generic form of Eq. 5:

$$k_i = k_{i,\min} + \left(1 - \frac{1}{1+\exp\left(k_{switch,i} \cdot \left(t - t_{switch,i}\right)\right)}\right) \cdot \left(k_{i,\max} - k_{i,\min}\right) \quad (5)$$

So, by introducing this switch function, the specific activities of PDC1 and ADH1 became time dependent variables and we will refer to these time variable activities as rate functions. Everything in the model was expressed on a fresh weight basis. The differential equations of the developed model were implemented and parameters were estimated in OptiPa (Hertog *et al.*, 2007), a dedicated optimization tool which was developed using Matlab (The MathWorks, Inc., Natick, MA, USA). The differential equations were solved using the MATLAB solver ode15s and the model parameters $k_{PDC1_min}$ and $k_{PDC1_max}$ (mL), $k_{PDC2}$ (mL), $k_{ADH1_min}$ and $k_{ADH1_max}$ (L kg mmol$^{-1}$), $k_{ADH2}$ (L kg mmol$^{-1}$), $k_{loss}$ (s$^{-1}$), $k_{switch_i}$ (s$^{-1}$), and $t_{switch_i}$ (h) were estimated using non-linear least squares optimization applying the Levenberg-Marquardt method. Both equations (Eq. 2) and (Eq. 3) are initiated at their respective initial levels ($ACA_0$ and $EthOH_0$).

### 4.2.8 Data analysis

To determine the influence of $O_2$ on the concentration of the fermentation metabolites and enzyme activities of PDC and ADH in time, a one-way ANOVA was conducted to detect any treatment effect. Subsequently, a least square means comparison was performed for the different treatments at every time point with a planned comparison method ($p$<0.05). The statistical analysis was carried out with the statistical software package, JMP Pro. version 13.0 (SAS, USA).

## 4.3 Results

### 4.3.1 General model findings

Overall, the kinetic model was able to successfully describe the experimental data on acetaldehyde and ethanol of all three experiments (Fig. 4.2-4.4) with explained parts over 89.1 % (Table 4.1). Concerning the reactions catalysed by PDC and ADH, the rate constants of the backward reactions ($k_{PDC2}$, $k_{ADH2}$) were estimated not to be significantly different from zero, and could be neglected. In other words, only the forward reactions as defined by the rate functions for $k_{PDC1}$ and $k_{ADH1}$ played an essential role under the conditions studied. For two experimental conditions, the additional model complexity of the switch function was required to model an increase in the specific activity of PDC or ADH by modulating the rates of either $k_{PDC1}$ or $k_{ADH1}$. This model complexity is reflected by the number of model parameters included in the parameter optimization process, an overview of which is provided in Table 4.1.

Table 4.1: Overview of the parameters ± standard deviation estimated by the model (Equations (Eq. 1)-(Eq. 5)) for the three different experiments.

| | 1 °C | | 18 °C | | | | | | |
|---|---|---|---|---|---|---|---|---|---|
| | Harvest | | Harvest | | Storage | | | | |
| | 0.3 kPa $O_2$ | 21 kPa $O_2$ | 0 kPa $O_2$ | 5 kPa $O_2$ | 0 kPa $O_2$ | 0.5 kPa $O_2$ | 1 kPa $O_2$ | 5 kPa $O_2$ | 21 kPa $O_2$ |
| $k_{PDC1_min}$ (mL) | $4.10 \pm 1.89 \times 10^{-6}$ | | $4.29 \pm 1.49 \times 10^{-4}$ | | $1.76 \times 10^{1} \pm 8.79 \times 10^{-1}$ | | | | |
| $k_{PDC1_max}$ (mL) | / | / | $4.31 \times 10^{1} \pm 1.49 \times 10^{-3}$ | / | / | / | / | / | / |
| $k_{switch,PDC}$ ($s^{-1}$) | / | / | $6.92 \times 10^{-4} \pm 2.49 \times 10^{-5}$ | / | / | / | / | / | / |
| $t_{switch,PDC}$ (h) | / | / | $4.03 \pm 2.89 \times 10^{-2}$ | / | / | / | / | / | / |
| $k_{ADH1_min}$ (L kg $mol^{-1}$) | $5.53 \pm 1.27 \times 10^{-6}$ | | $5.74 \pm 2.31\ 10^{-4}$ | | $1.33 \pm 6.00 \times 10^{-2}$ | | | | |
| $k_{ADH1_max}$ (L kg $mol^{-1}$) | / | / | / | / | $8.68 \pm 1.27$ | / | / | / | / |
| $k_{switch,ADH}$ ($s^{-1}$) | / | / | / | / | $3.58 \times 10^{-5} \pm 9.08 \times 10^{-4}$ | / | / | / | / |
| $t_{switch,ADH}$ (h) | / | / | / | / | $2.04 \times 10^{1} \pm 0.02$ | / | / | / | / |
| $k_{loss}$ ($s^{-1}$) | $1.19 \times 10^{-1} \pm 5.58 \times 10^{-8}$ | | $2.64 \times 10^{-2} \pm 9.78 \times 10^{-4}$ | | $5.75 \times 10^{-2} \pm 2.78 \times 10^{-3}$ | | | | |
| $p_1$ | $2.47 \times 10^{-2} \pm 1.40 \times 10^{-8}$ | $6.98 \times 10^{-5} \pm 2.20 \times 10^{-3}$ | $3.12 \times 10^{-4} \pm 2.72\ 10^{-3}$ | $1.28 \times 10^{-3} \pm 6.15 \times 10^{-2}$ | $2.29 \times 10^{-1} \pm 1.48 \times 10^{-2}$ | $1.13 \times 10^{-1} \pm 1.28 \times 10^{-2}$ | $3.42 \times 10^{-2} \pm 7.83 \times 10^{-3}$ | $5.79 \times 10^{-3} \pm 2.25 \times 10^{-1}$ | $5.84 \times 10^{-4} \pm 1.16 \times 10^{-1}$ |
| $p_2$ | $5.89 \times 10^{-3} \pm 2.0 \times 10^{-9}$ | $1.14 \times 10^{-3} \pm 2.92 \times 10^{-4}$ | $8.52 \times 10^{-4} \pm 2.67 \times 10^{-4}$ | $3.14 \times 10^{-4} \pm 6.85 \times 10^{-3}$ | $2.41 \times 10^{-6} \pm 1.75 \times 10^{-6}$ | $1.55 \times 10^{-5} \pm 1.11 \times 10^{-3}$ | $3.75 \times 10^{-4} \pm 4.84 \times 10^{-4}$ | $7.53 \times 10^{-5} \pm 3.07 \times 10^{-2}$ | $3.39 \times 10^{-6} \pm 7.43 \times 10^{-3}$ |
| $p_3$ | $-7.80 \times 10^{-5} \pm 3.39 \times 10^{11}$ | $-2.93 \times 10^{-5} \pm 1.59 \times 10^{-5}$ | $-3.72 \times 10^{-5} \pm 8.51 \times 10^{-6}$ | $-1.47 \times 10^{-5} \pm 2.41 \times 10^{-4}$ | $-1.35 \times 10^{-4} \pm 1.29 \times 10^{-5}$ | $-3.88 \times 10^{-5} \pm 2.65 \times 10^{-5}$ | $-1.20 \times 10^{-5} \pm 1.02 \times 10^{-5}$ | $-9.39 \times 10^{-5} \pm 1.16 \times 10^{-3}$ | $-1.26 \times 10^{-4} \pm 3.80 \times 10^{-4}$ |
| $p_4$ | $3.08 \times 10^{-9} \pm 1.09 \times 10^{-15}$ | $1.72 \times 10^{-7} \pm 1.65 \times 10^{-7}$ | $3.25 \times 10^{-7} \pm 7.49 \times 10^{-8}$ | $3.58 \times 10^{-8} \pm 2.64 \times 10^{-6}$ | $1.25 \times 10^{-6} \pm 1.50 \times 10^{-7}$ | $2.38 \times 10^{-7} \pm 1.94 \times 10^{-7}$ | $2.69 \times 10^{-8} \pm 7.67 \times 10^{-8}$ | $1.82 \times 10^{-10} \pm 4.84 \times 10^{-5}$ | $1.50 \times 10^{-8} \pm 2.14 \times 10^{-5}$ |
| explained part (%) | 89.1 | | 97.9 | | 93.09 | | | | |

### 4.3.2 The effect of low-oxygen stress on the induction of fermentation at low temperature

To study the effect of low-oxygen stress at the commercial storage temperature of apple fruit, the first experiment was carried out at 1 °C at harvest. The effect of low-oxygen stress on the induction of fermentation was studied by measuring the concentration of the metabolites of the ethanol pathway (i.e., acetaldehyde, ethanol and ethyl acetate), as well as the *in vitro* enzyme activity of PDC and ADH (Fig. 4.2). The kinetic model was used to analyse the experimental data resulting in the model simulations shown in Fig. 4.2.

The apple slices exposed to 0.3 kPa $O_2$ at 1 °C experienced low-oxygen stress resulting in fermentation: the concentration of acetaldehyde and ethanol was already significantly increased after 4 h of exposure, and showed an even stronger increase after 17 h until 48 h (Fig. 4.2D-E). Afterwards, the concentration of both fermentation metabolites decreased again towards 72 h. The model was able to simulate the changes in acetaldehyde and ethanol concentrations with an explained part of 89.1 % (Fig. 4.2 and Table 4.1). The simulated concentration of pyruvate (Fig. 4.2C) showed a trend similar to the experimental data obtained for acetaldehyde and ethanol for both oxygen conditions. The concentration of ethyl acetate did follow a somewhat more delayed trend (Fig. 4.2F). Only after 20 h a significant increase was observed in ethyl acetate content, which dropped down again after 28 h. Although fermentation was induced, as could be observed from the fermentation metabolites, the measured *in vitro* activity of both fermentation enzymes did not show any significant changes during the experiment (Fig. 4.2A-B). Throughout time, the rate functions for $k_{PDC1}$ and $k_{ADH1}$ were kept constant at their minimum values ($k_{PDC1_min}$ = 4.1 mL and $k_{ADH1_min}$ = 5.53 L kg$^{-1}$ mol$^{-1}$, respectively), effectively cancelling out the switch function. This is represented by the relative rate functions kept at a value of 1 (Fig. 4.2A-B).

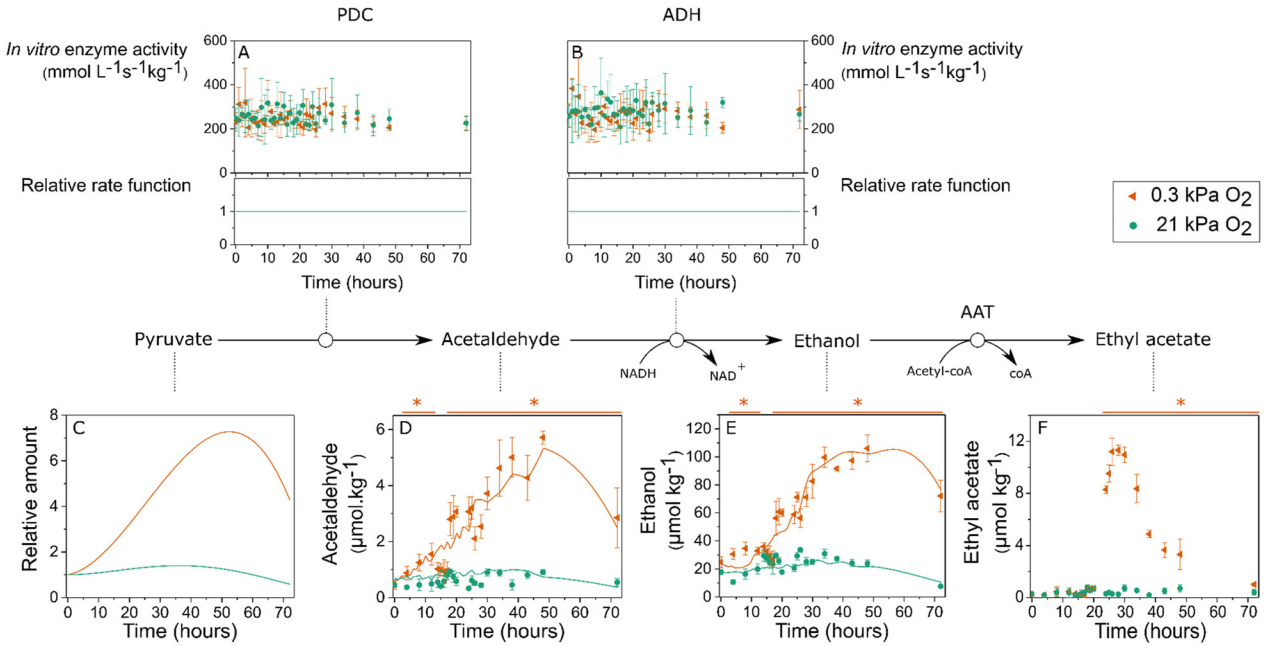


Figure 4.2: Schematic representation of the data obtained of the ethanol pathway of the fermentative metabolism at 1 °C at harvest. The experimental data are represented by symbols (0.3 kPa $O_2$: ◂ and 21 kPa $O_2$: ●) while the simulated data are represented by lines in the corresponding colours. The top graph A-B show the *in vitro* enzyme activity of PDC and ADH which was used as a measure for the amounts of enzymes used in the model. The lines in the bottom graph A-B represent the simulated rate functions coming from the switch function expressed as relative values. C-F show the compounds of the ethanol pathway. The experimental data are means of five biological replicates and the error bars represent their standard deviation. Significant differences between the two $O_2$ levels for the experimental data at a *p* level of 0.05 are indicated by the coloured lines at the top of each graph.

### 4.3.3 The effect of low-oxygen stress on the induction of fermentation at high temperature

To investigate whether the production of new fermentation enzymes is upregulated when fermentation is induced to a higher extent, a second experiment was performed at harvest in 2015, introducing anoxia at 18 °C storage (Fig. 4.3). As for this experiment the data of 21 kPa $O_2$ was lost due to a technical failure, the condition of 5 kPa $O_2$ was used as a control. Similar to the condition of 21 kPa $O_2$ at 1 °C, the concentration of the fermentation metabolites was slightly reduced in the apple slices exposed to 5 kPa $O_2$ at 18 °C. A clear induction of fermentation was observed in the apple slices exposed to anoxia (0 kPa $O_2$) at 18 °C. During the first 12 h, acetaldehyde accumulated to levels similar to the ones obtained after 48 h at 1 °C (Fig. 4.3D and Fig. 4.2D). Subsequently, the acetaldehyde levels decreased again. The concentration of ethanol measured after 48 h at 18 °C (0 kPa $O_2$) was ten times higher than the one measured at 1 °C (0.3 kPa $O_2$, Fig. 4.2E). Similar to the first experiment, the levels of ethanol dropped after 48 h. A small increase in ethyl acetate was observed at 0 kPa $O_2$ in the beginning of the experimental period but towards the end of the experiment the concentration of ethyl acetate declined for both oxygen conditions (Fig. 4.3F). The model was able to describe the experimental data with an explained part of 97.9 % (Fig. 4.3 and Table 4.1). The simulated relative amount of pyruvate was different from the experiment at 1 °C. The relative amount of pyruvate showed a slight increase at 0 kPa $O_2$ and stayed constant at 5 kPa $O_2$ in the first 30 h, after which a strong depletion was simulated for both conditions (Fig. 4.3C). A significant increase in *in vitro* enzyme activity was detected for both PDC and ADH, after 48 h and 30 h respectively. After 72 h, the *in vitro* activity of ADH was twice as high as that of PDC. The model demonstrated that in the case of 0 kPa $O_2$, the rate function of $k_{PDC1}$ had to be upregulated to a 10 times higher value (from $k_{PDC1_min}$ = 4.29 mL to $k_{PDC1_max}$ = 43 mL) to account for the observed changes in the metabolite data (Fig. 4.3A). The rate function for $k_{PDC1_min}$ at 5 kPa $O_2$ and the rate function for

$k_{ADH1}$ at 0 kPa $O_2$ and 5 kPa $O_2$ stayed constant during the experimental period (Fig. 4.3A-B) at their minimum values indicated in Table 1.

### 4.3.4 Does storage influence the induction of fermentation under low oxygen conditions?

To explore whether storage had an effect on the regulation of the fermentative metabolism, a third experiment was performed at 18 °C after 6 months of storage under commercial CA conditions (Fig. 4.4). In this experiment both anoxic and hypoxic conditions were tested. Three days before the start of the experiment, the fruit was taken out of CA storage to adapt to normal atmosphere conditions. However, as can be seen from Fig. 4.4, the starting values of the three fermentation metabolites and ADH are higher as compared to at harvest (Fig. 4.3)

Although the starting values for the third experiment are higher, the data obtained for the anoxic condition (0 kPa $O_2$) are similar to the data obtained for the same condition at harvest (Fig. 4.5). Only the *in vitro* enzyme activity of PDC did not increase as much as compared to at harvest. Interestingly, under hypoxic conditions (0.5 kPa and 1 kPa $O_2$), acetaldehyde and ethyl acetate accumulated to higher values as compared to anoxic conditions (Fig. 4.4D, F). Also the *in vitro* enzyme activity of ADH showed a similar behaviour (Fig. 4.4B). However, the ethanol concentration increased with decreasing oxygen concentration (Fig. 4.4E). No clear distinction could be made between the values measured for the *in vitro* enzyme activity of PDC at 0.5 kPa and 1 kPa $O_2$, but they increased less as compared to 0 kPa $O_2$ (Fig. 4.4A). No significant differences among samples flushed with 5 kPa and 21 kPa $O_2$ were detected throughout the experimental period. Similar to the previous experiments, the model was able to fit the experimental data of acetaldehyde and ethanol for all the different oxygen concentrations with an explained part of 93.09 % (Fig. 4.4 and Table 4.1). The relative amount of pyruvate, simulated by the model (Fig. 4.4C), showed a trend different from the one at harvest (Fig. 4.3C)..

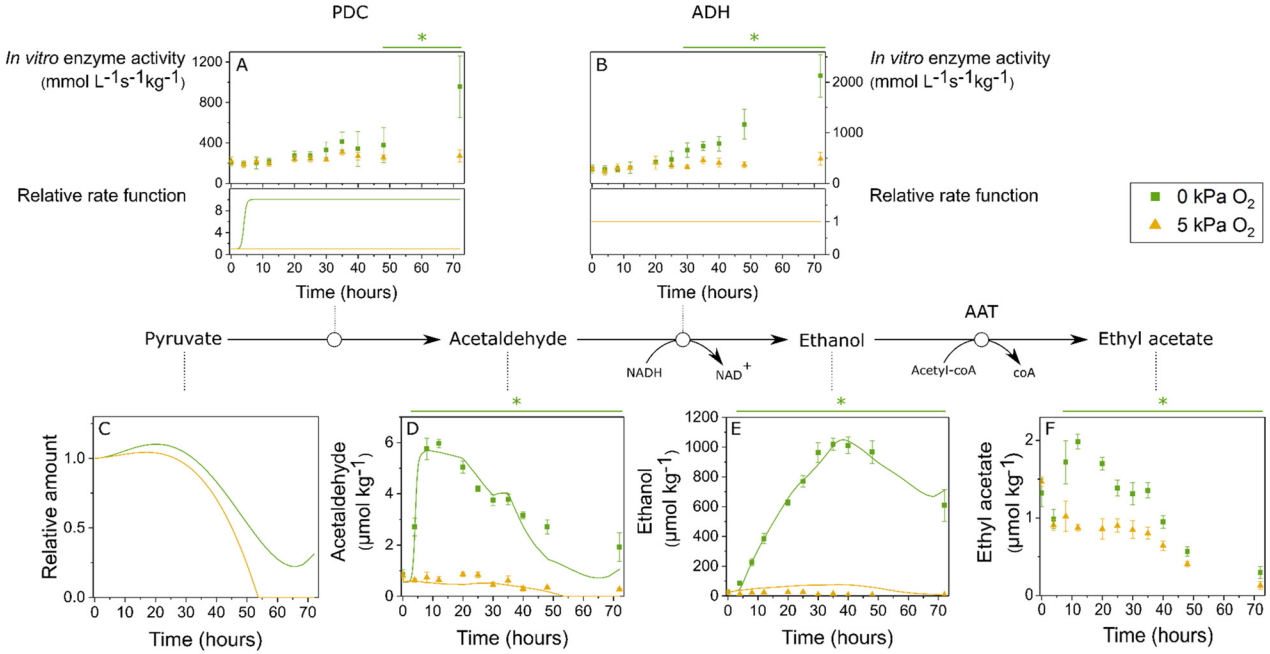


Figure 4.3: Schematic representation of the data obtained of the ethanol pathway of the fermentative metabolism at 18 °C at harvest. The experimental data are represented by symbols (0 kPa $O_2$: ■ and 5 kPa $O_2$: ▲) while simulated data are represented by lines in corresponding colours. The top graph A-B show the *in vitro* enzyme activity of PDC and ADH which was used as a measure for the amounts of enzymes used in the model. The lines in the bottom graph A-B represent the simulated rate functions coming from the switch function expressed as relative values. C-F show the compounds of the ethanol pathway. The experimental data are means of five biological replicates and the error bars represent their standard deviation. Significant differences between the two $O_2$ levels for the experimental data at a *p* level of 0.05 are indicated by the coloured lines at the top of each graph.

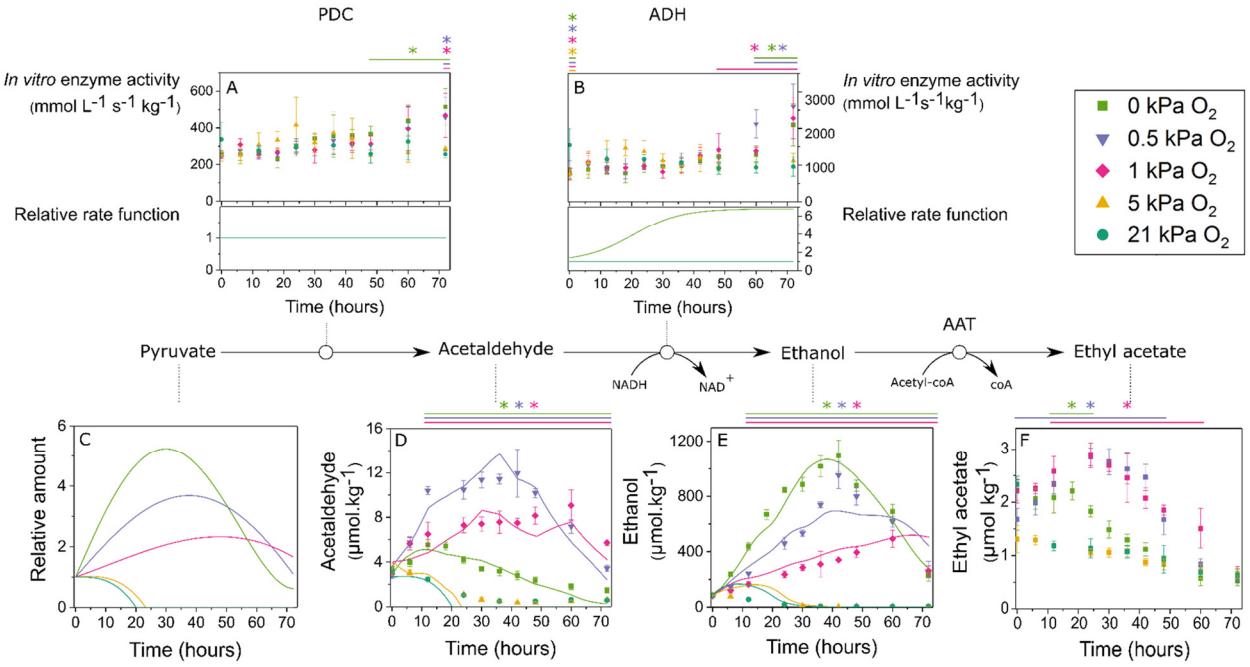


Figure 4.4: Schematic representation of the data obtained of the ethanol pathway of the fermentative metabolism at 18 °C after 6 months of normal CA storage. The experimental data are represented by symbols (0 kPa $O_2$: ■, 0.5 kPa $O_2$: ▼, 1 kPa $O_2$: ◆, 5 kPa $O_2$: ▲ and 21 kPa $O_2$: ●) while the simulated data are represented by lines in the corresponding colours. The top graph A-B show the *in vitro* enzyme activity of PDC and ADH which was used as a measure for the amounts of enzymes used in the model. The lines in the bottom graph A-B represent the simulated rate functions coming from the switch function expressed as relative values. C-F show the compounds of the ethanol pathway. The experimental data are means of five biological replicates and the error bars represent their standard deviation. Significant differences between the two $O_2$ levels for the experimental data at a *p* level of 0.05 are indicated by the coloured lines at the top of each graph.

Both for the anoxic and the hypoxic conditions, it increased in the first period of the experiment, but decreased again towards the end of the experimental period. In the case of 5 kPa $O_2$ and 21 kPa $O_2$ the relative amount of pyruvate decreased to zero. In this experiment after 6 months of storage, no increase in the rate function for PDC ($k_{PDC1_min}$ = 17.6 mL) was observed (Fig. 4.4A). However, the rate function for ADH was upregulated by a factor 6.5 (from $k_{ADH1_min}$ = 1.33 L kg $mol^{-1}$ to $k_{ADH1_max}$ = 8.68 L kg $mol^{-1}$) for the experimental condition of 0 kPa $O_2$ only (Fig. 4B). This switch happened slower than the one observed for PDC at harvest (Fig. 4.3B).

# 4.4 Discussion

## 4.4.1 General fermentation patterns confirmed

In accordance with previous studies on detached apple fruit (Brizzolara *et al.*, 2017; Cukrov *et al.*, 2016; Saquet and Streif, 2008; Volz *et al.*, 1998), our results confirmed the induction of the fermentative metabolism under extremely low oxygen conditions (Fig. 4.2-4.4). Interestingly, the fermentation metabolites were not zero at the start of the experiment and a small decrease in fermentation metabolites was observed in the control conditions at harvest both at 1 °C and 18 °C (Fig 4.2D-E and 4.3D-E), indicating that fermentation was already induced in the intact fruit, likely due to declining oxygen gradients towards the centre of the fruit (Ho *et al.*, 2011, 2010). As Saquet and Streif (2008) found that the production of lactate was negligible in the fermentative metabolism of 'Jonagold' apple fruit, only the ethanol pathway of the fermentative metabolism was studied here. The results in this study indicated that only the forward reactions of this pathway played an essential role and thus ethanol was not re-metabolized back to acetaldehyde under the conditions studied. This is in contrast to Veltman *et al.* (2003) who, based on observations that exogenous ethanol in a storage atmosphere filled with apples disappeared over time,

suggested that ethanol was re-metabolized by the apples. As Veltman *et al.* (2003) only measured the concentration of ethanol in the storage atmosphere and did not perform measurements on the fruit itself, it could be speculated that the apple fruit did take up the vaporized ethanol converting it to ethyl acetate rather than re-metabolizing it back to acetaldehyde. Besides acetaldehyde and ethanol, also ethyl acetate showed a clear response to the imposed conditions depending on the experiment (temperature, $O_2$, at harvest or after storage) but these results could not be unequivocally interpreted in terms of fluxes as its metabolic role is not covered by the current model. As the concentrations of ethyl acetate started to decline before the concentrations of ethanol declined, it could be speculated that acetyl-coA became the limiting factor in the formation of ethyl acetate. It is believed that the fermentative metabolism can be regulated by two mechanisms: via molecular control (transcription/translation) of LDH, PDC and ADH or via metabolic control by positive and/or negative feedback mechanisms of products and co-factors (Dixon and Hewett, 2000; Imahori *et al.*, 2003; Ke *et al.*, 1995). The results of this work indicate that the regulation of the fermentative metabolism is highly depending on the conditions applied.

### 4.4.2 The overall metabolic reaction rate influences the regulation of the fermentative metabolism

Temperature is one of the most important factors influencing the overall metabolic rate of the central carbon metabolism. The lower the temperature, the more the metabolic activity will slow down (Lammertyn *et al.*, 2001). Low temperature in combination with low oxygen stress reduces the metabolic rate even further (Biale, 1946; Teixeira and Durigan, 2010; Thompson, 2010; Yearsley *et al.*, 1996). Fermentation was only slightly induced at the low oxygen condition at 1 °C as compared to 18 °C, where a tenfold increase in ethanol levels was observed (Fig. 4.5E). Although acetaldehyde did not reach a higher absolute concentration at 18 °C as compared to 1 °C, the increase in concentration was much faster (Fig. 4.5D).

However, the similar values of $k_{PDC1_min}$ and $k_{ADH1_min}$ at the start of both experiments in which the fruit were already adapted to the different temperatures (see Table 4.1), indicated that temperature did not have a direct effect on the metabolic rate of the fermentative metabolism. Rather an indirect temperature effect occurred, due to the impact of temperature on the overall metabolic rate of the central carbon metabolism, resulting, for instance, in different pyruvate levels. In addition, the availability of co-factors and cytosolic pH could be different between the two conditions, leading to a difference in regulation of the fermentative metabolism.

#### 4.4.2.1 Fermentative metabolism is only metabolically controlled at a slow overall metabolic rate

At low temperature, no increase in *in vitro* enzyme activity of PDC nor ADH was observed during the experimental period of three days, indicating that the production of new fermentation enzymes was not required to induce fermentation to this extent. Furthermore, the model indicated that, given the experimental data, the rate functions for PDC and ADH could be considered constant (Fig 4.2A-B and 4.5A-B). These results imply that under these conditions the fermentative metabolism is only metabolically regulated. Ke *et al.* (1995) proposed that the concentration of pyruvate and NADH/$NAD^+$ may control the activity of PDC and ADH. The concentration of NADH was shown to increase and $NAD^+$ to decrease in 'Jonagold' apples stored under CA conditions (Saquet *et al.*, 2000). During low oxygen stress, the glycolytic flux increases and pyruvate starts to accumulate since it is no longer shuttled into the TCA cycle due to the decreased pyruvate dehydrogenase (PDH) activity, which is strongly inhibited by increasing NADH concentrations (Davies, 1980; Päpke *et al.*, 2014). On the other hand, in plants it is known that PDC is activated by a decreasing $NAD^+$/NADH ratio (Davies, 1980; John and Greenway, 1976). However, it can also be speculated that the increase in pyruvate is due to a change in the activity of the mitochondrial pyruvate carriers

(MPC). In yeast it has recently been shown that yeast cells express two different MPC complexes ($MPC_{OX}$ and $MPC_{FERM}$) depending on the conditions in the environment. Due to the low activity of $MPC_{FERM}$, the majority of pyruvate remains in the cytosol (Bender *et al.*, 2015). However, to our knowledge, very little is known about the actual biological functions and molecular mechanisms of MPCs in plants. So far, only three MPC proteins in yeast (Bender *et al.*, 2015), two MPC proteins in flies and mammals (Bricker *et al.*, 2012; Herzig *et al.*, 2012) and one MPC protein in plants (Li *et al.*, 2014) have been successfully identified.

Furthermore, the model showed a strong increase in the relative amount of pyruvate for the low oxygen condition at 1 °C (Fig 4.2E and 4.5E). Rivoal *et al.* (1989) observed that pyruvate could act both as an activator of PDC and as a substrate. Tadege *et al.* (1998) proposed that the difference in $K_m$ values of PDH and PDC for pyruvate could be an extra controlling factor which regulates whether pyruvate is shuttled into the TCA cycle or towards the fermentative metabolism. Since in plants the $K_m$ value of PDC for pyruvate is larger (mM range) than that of PDH (µM range; Tadege *et al.*, 1998), the increase in relative pyruvate levels simulated by the model indicates that more pyruvate became available for PDC. Together, this could explain why fermentation was induced during low oxygen stress at 1 °C without inducing the production of new enzymes.

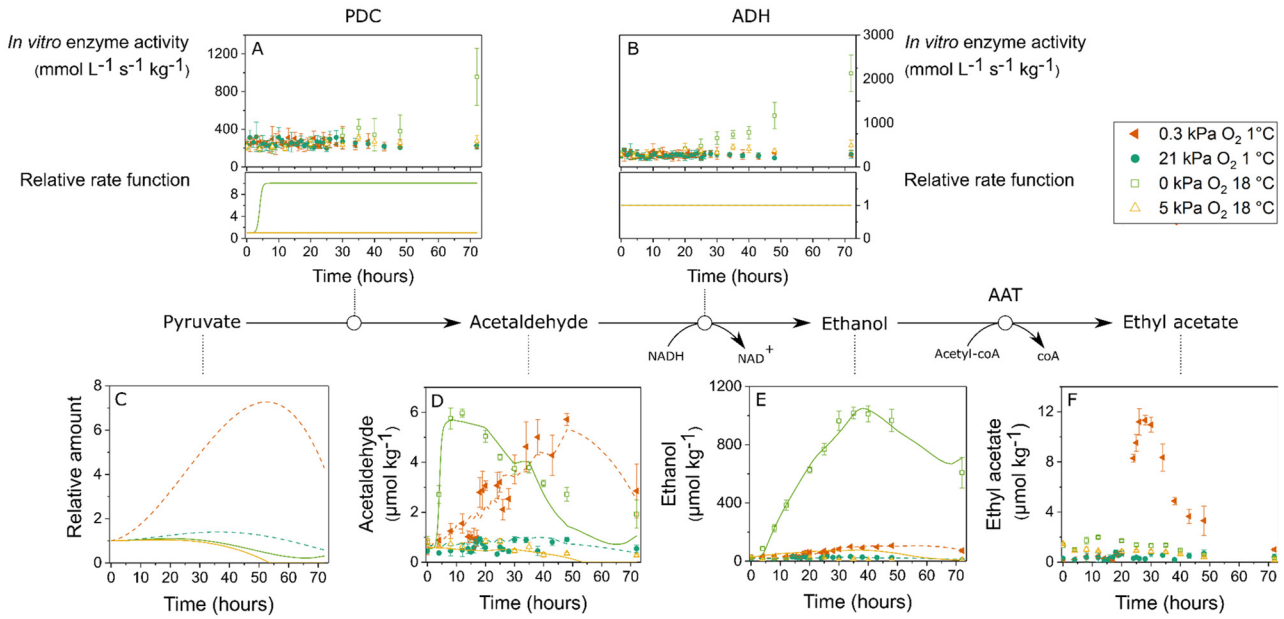


Figure 4.5: Schematic representation of the data obtained of the ethanol pathway of the fermentative metabolism at 1 °C and 18 °C at harvest. The experimental data are represented by symbols (0 kPa $O_2$: ■, 0.3 kPa $O_2$: ◀, 5 kPa $O_2$: ▲ and 21 kPa $O_2$: ●) while simulated data are represented by lines in corresponding colours. The top graph A-B show the *in vitro* enzyme activity of PDC and ADH which was used as a measure for the amounts of enzymes used in the model. The lines in the bottom graph A-B represent the simulated rate functions coming from the switch function expressed as relative values. C-F show the compounds of the ethanol pathway. The experimental data are means of five biological replicates and the error bars represent their standard deviation.

### 4.4.2.2 Combination of molecular and metabolic control regulates the fermentative metabolism at a high overall metabolic rate

A different regulation was observed when the metabolic rate was higher (18 °C). In this case, the fermentative metabolism was regulated by a combination of molecular and metabolic control mechanisms. As can be seen in Fig. 4.3A-B, a significant increase in *in vitro* enzyme activity and hence enzyme levels was detected for PDC after 48 h and for ADH after 30 h. However, this increase in *in vitro* enzyme activity was, by itself, not enough to explain the fast increase in acetaldehyde concentration. Model simulations indicated that a fast increase in constant function for PDC was required to explain the experimental data (Fig. 4.3A). Together with the regulation based on the changing pyruvate concentration and the $NAD^+$/NADH ratio, PDC could also be controlled by changes in cytosolic pH. Davies *et al.* (1974) introduced the pH stat hypothesis, which suggests that the reduction in cytosolic pH, caused by lactate production, selectively activates PDC. Although the importance of the decrease in cytosolic pH on the regulation of PDC was demonstrated in maize roots by Fox *et al.* (1995), it is questionable whether the drop in cytosolic pH is caused by the initial lactate production. Several studies have reported discrepancies between their findings and the pH stat hypothesis proposed by Davies *et al.* (1974). In some cases there was little to no lactate production (as is the case for 'Jonagold'; Saquet and Streif, 2008), decreases in cytosolic pH were not in accordance with the amount of lactate synthesized, or the timing of lactate synthesis and changes in cytosolic pH did not match. For a detailed overview of the different studies addressing this issue see the review by Gibbs and Greenway (2003). Greenway and Gibbs (2003) suggested that anoxia-tolerant plants lower their cytosolic pH set point from 7 to 6.5, to adapt to the energy crisis induced by low-oxygen stress. PDC is considered to be the rate-limiting step of the ethanol pathway of the fermentative metabolism in many plant tissues (Imahori *et al.*, 2003). By lowering the cytosolic pH set point, anoxia-tolerant plants stimulate the ethanol pathway by activating PDC. This initial drop in cytosolic pH is further strengthened by the enhanced $CO_2$ production during fermentation,

possibly increasing the activity of PDC even further (Lange and Kader, 1997). The drop in cytosolic pH would partially inhibit ADH activity, but since the *in vitro* ADH activity was higher than the PDC activity, this would not limit the conversion of acetaldehyde into ethanol (Ke *et al.*, 1995). We speculate that due to the high metabolic rate, the apple tissue exposed to the low oxygen condition at 18 °C experienced a more severe energy crisis as compared to the experiment at 1 °C, leading to a fast drop in cytosolic pH and consequently a fast activation of PDC. In future research cytosolic pH measurements should be performed to confirm this hypothesis.

### 4.4.3 Influence of storage on the regulation of the fermentative metabolism

Storing 'Jonagold' apple fruit for six months at normal CA conditions, clearly influenced the regulation of the ethanol pathway under anoxic conditions (Fig. 4.6). The higher starting values after storage indicated that the apple fruit already had experienced low-oxygen stress during storage and consequently their fermentative metabolism had already been activated before the start of the experiment. Several studies demonstrated that exposing plant tissue to a hypoxic pre-treatment prior to anoxia improved the tolerance to anoxic-stress as compared to plant tissue suddenly transferred to anoxia (Andrews *et al.*, 1994; Bertani *et al.*, 1980; Blackwell, 1983; Ellis and Setter, 1999; Germain *et al.*, 1997; Waters *et al.*, 1991; Webb and Armstrong, 1983; Zhang and Greenway, 1994). However, the exact mechanism of anoxia tolerance is not yet clear (Gibbs and Greenway, 2003). Although the starting values were different in the two experiments, the concentration of the fermentation metabolites had a very similar pattern, indicating that fermentation was induced to the same extent before and after storage (Fig. 4.6D-F). However, model simulations suggested that the ethanol pathway was subject to a different regulation (Fig. 4.6A-B).

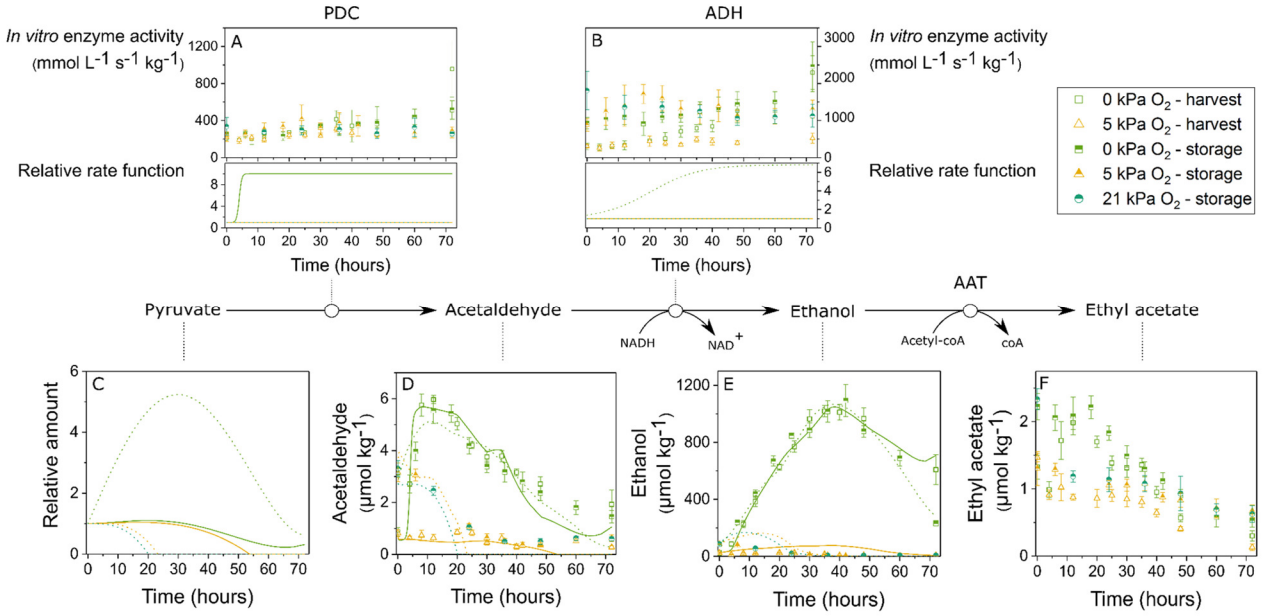


Figure 4.6: Schematic representation of the data obtained of the ethanol pathway of the fermentative metabolism at 18 °C at harvest and at 18 °C after 6 months of normal CA storage. The experimental data are represented by symbols (0 kPa $O_2$: ■ ; 0.3 kPa $O_2$: ◄; 1 kPa $O_2$: ◆ ; 5 kPa $O_2$: ▲ and 21 kPa $O_2$: ●) simulated data are represented by lines in corresponding colours. The top graph A-B show the *in vitro* enzyme activity of PDC and ADH which was used as a measure for the amounts of enzymes used in the model. The lines in the bottom graph A-B represent the simulated rate functions coming from the switch function expressed as relative values. C-F show the compounds of the ethanol pathway. The experimental data are means of five biological replicates and the error bars represent their standard deviation.

### 4.4.3.1 In vivo enzyme activity of PDC does not need additional activation after storage

Different from the experiment at harvest, the model indicated that after storage no activation of PDC, as reflected in its constant relative rate constant, was necessary. One could speculate that the adaptation period after CA storage at normal atmosphere conditions was not long enough to completely reverse the energy crisis in the apple tissue and, hence, restore the set point of the cytosolic pH. Therefore, PDC could already have been activated at the start of the experiment and, hence, no additional activation was needed. This hypothesis is confirmed by the model parameters as the rate function for $k_{PDC1}$ is higher after storage ($k_{PDC1_min}$ = 17.6 mL) as compared to at harvest ($k_{PDC1_min}$ = 4.29 mL). However, this is somewhat contradictory to the increase in relative amount of pyruvate simulated by the model. Further research is necessary to investigate whether the increase in pyruvate is due to an elevated glycolytic flux as compared to at harvest, or to a different regulation of PDC activity.

### 4.4.3.2 In vivo enzyme activity of ADH increases during anoxia after storage

The model also indicated that a slow increase in the relative rate constant of ADH was necessary to explain the experimental data after storage (Fig. 4.4B). However, it remains unknown which factors or control mechanism would cause this increase. One possible explanation could be the induction of a new ADH isozyme, as several studies in fruit and vegetables already reported that low oxygen stress could induce a new ADH isozyme with a higher specific activity (Ke *et al.*, 1995, 1994). In this case, the classic way to determine the overall *in vitro* enzyme activity of ADH is no longer correct as it ignores the possible difference in specific activity between the isozymes resulting in a lumped enzyme activity value. On the assumption that a new isozyme was induced, the slow increase in the relative rate constant would rather be an

indication that the estimated *in vitro* enzyme activity of ADH was not correct, instead of a real activation of ADH. This could also be a possible explanation why several studies reported a discrepancy between high levels of *in vitro* enzyme activity of ADH and the rate of ethanol production (Andrews *et al.*, 1994; Gibbs and Greenway, 2003; Imahori *et al.*, 2003, 2002; Ke *et al.*, 1995; Saquet and Streif, 2008). However, since the different isozymes of ADH were not determined in this study, this hypothesis could not be confirmed. Another explanation could be that the slow increase of $k_{ADH1}$ is caused by increasing levels of acetaldehyde and NADH and decreasing levels of $NAD^+$. The elevating pyruvate levels simulated by the model indicate that either the glycolytic flux is increasing after storage or the flux through TCA cycle is decreasing or a combination of both, all leading to higher NADH and lower $NAD^+$ levels as compared to at harvest. Finally, some studies reported elevated transcript levels of ADH upon hypoxia and anoxia (Cukrov *et al.*, 2016; Roberts *et al.*, 1989; van Dongen *et al.*, 2009). It has been reported that the ROP signal transduction pathway is required for the increase in *ADH* mRNA levels and enzyme activity in plant tissue (Baxter-Burrell *et al.*, 2002; Fukao and Bailey-Serres, 2004). However, due to the important role of $H_2O_2$ in the ROP pathway, this pathway will probably not be responsible for the increase in the relative rate constant under anoxia, indicated by the model. For a detailed explanation of the ROP pathway, the reader is referred to Baxter-Burrell *et al.* (2002). Overall, further research is necessary to get more insight in the regulatory mechanism of ADH during anoxia.

### 4.4.4 Fermentative metabolism is differently induced under anoxic and hypoxic conditions after storage

It has been shown in apple fruit that the concentration of the fermentation metabolites increase with decreasing oxygen levels (Cukrov *et al.*, 2016). A similar induction of fermentation was observed in the current experiments when apple tissue was exposed to hypoxic conditions. However, under anoxic conditions, the concentrations of acetaldehyde and ethyl acetate were lower again (Fig. 4.4D and

4.4F). The lower levels of acetaldehyde during anoxia were probably the result of a higher conversion to ethanol thanks to the activation of ADH. Interestingly, the *in vitro* ADH activity was higher under the hypoxic conditions as compared to the anoxic condition (Fig 4.4B). These observations are in line with those of Andrews *et al.* (1993) and Drew (1997), who observed that the increases in *ADH* mRNA and enzyme activity of ADH are significantly lower under anoxia. Also in apple fruit, Cukrov *et al.* (2016) observed a higher up-regulation of *ADH* genes for the lower hypoxic oxygen levels.

In an attempt to prevent, or at least postpone, the occurrence of internal anoxia and its concomitant negative consequences, plants try to save energy by adapting their metabolism (Bailey-Serres *et al.*, 2012; Geigenberger, 2003; Van Dongen *et al.*, 2011). In order to do so, they decrease the demand for respiratory oxygen consumption and slow down the respiratory activity of the mETC (Gupta *et al.*, 2009; Zabalza *et al.*, 2009). The less oxygen is available for the plant tissue, the less pyruvate will be shuttled into the TCA cycle for energy production via oxidative phosphorylation. Together with a different glycolytic flux, this could explain the decreasing amount of available pyruvate as simulated by the model for increasing oxygen levels.

### 4.4.5 Why are the concentrations of the fermentation metabolites decreasing towards the end of the experimental period?

In all three experiments the fermentation metabolites decreased towards the end of the experiment. The reason for this decrease is not yet clear. We hypothesize after a prolonged exposure to low oxygen stress the apple tissue will try to minimize its carbon losses through the inefficient fermentation pathway by switching to alternative pathways. In a number of species, including apple, one of this alternative

pathways can be the alanine metabolism. This pathway plays an important role in maintaining the glycolytic flux by converting, with the help of alanine aminotransferase, pyruvate to alanine, providing an alternative, non-detrimental end product (Bailey-Serres *et al.*, 2012; Cukrov *et al.*, 2016; Hatoum *et al.*, 2014; Vandendriessche *et al.*, 2013). Alanine concentrations are increased in 'Braeburn' apples after long term storage (up to 8 months) under 2.5 kPa $O_2$ and 3.7 kPa $CO_2$ conditions (Hatoum *et al.*, 2014). Brizzolara *et al.* (2017) observed in apple fruit an increase in alanine content when ethanol levels were going down, indicating that, after prolonged exposure to oxygen stress, pyruvate is possibly shuttled to alanine instead of into the ethanol pathway. However, further research using a labelled substrate would be required to examine the fluxes through these pathways.

Bucher and Kuhlemeier (1993) hypothesized that the anaerobic carbohydrate catabolism could have been downregulated during long-term anoxia. However, more convincing evidence is needed to confirm the downregulation of the glycolytic flux during anoxia (Gibbs and Greenway, 2003). Furthermore, it is somewhat contradictory that cells exposed to low-oxygen stress keep on producing more fermentation enzymes (Fig. 4.3A-B and 4.4A-B) even when the net synthesis of fermentation metabolites is going down (Fig 4.3C-E and 4.4C-E). It was proposed that the high levels of ADH could be important to use ethanol as a carbon source when oxygen levels start to increase again, but also here more research is needed (Gibbs and Greenway, 2003).

## 4.5 Conclusions

From the experimental data and the kinetic model simulations, it is evident that the regulation of the fermentative metabolism is highly depending on the conditions applied. The kinetic model helps to interpret the data and to provide new insights in

the regulation of the fermentative metabolism. Temperature changed the overall metabolic reaction rate, which appeared to have a large influence on the induction and regulation of the fermentative metabolism. At a low metabolic reaction rate, fermentation was only slightly induced and largely metabolically controlled. However, when apple tissue was exposed to a higher temperature to induce a faster overall metabolic rate, a ten-fold increase in ethanol levels was observed, although $k_{PDC1}$ and $k_{ADH1}$ themselves were not subjected to a direct temperature effect. In this case, the ethanol pathway was regulated by a combination of molecular and metabolic control systems. Also, storing the fruit for six months clearly influenced the fermentative metabolism under anoxic conditions. The model indicated that at harvest the regulation was located at the fast induction of PDC activity, whether after six months of storage an extra regulation on ADH activity seemed to be present. Furthermore, a different regulation of the ethanol pathway was observed between hypoxic and anoxic conditions. Overall, further research is necessary to test the regulatory mechanisms indicated by the model and to better understand why the levels of pyruvate, and consequently the fermentation metabolites, start to decrease again after prolonged low-oxygen stress.

# Chapter 5

# Unravelling the regulation of the central carbon metabolism during low-oxygen stress

The aim of this chapter is to study in detail the metabolic changes of the central carbon metabolism and its transcriptional regulation in order to get more insights in why the flux through the fermentative metabolism decreases after prolonged low-oxygen stress (see chapter 4).

# 5.1 Introduction

In model species such as *Arabidopsis* and rice, a considerable amount of information is available on metabolic responses, oxygen signalling mechanisms and the transcriptional regulation under low-oxygen stress (Van Dongen and Licausi, 2014). Much less is known about these processes in apple fruit exposed to low-oxygen stress during DCA storage. Based on metabolic and transcriptomic data, Cukrov *et al*. (2016) showed that 'Granny Smith' apple fruit changes its energy metabolism when exposed to low-oxygen stress. They no longer produce energy via the oxidative phosphorylation, instead they produce their energy by enhancing the glycolytic flux (Pasteur effect), thus enhancing the rate of pyruvate production. Increasing ethanol and alanine concentrations indicated that the amount of pyruvate could be reduced either via the fermentative metabolism or via the alanine pathway (Cukrov *et al.*, 2016). In the fermentative metabolism, pyruvate is converted either to lactate with the help of LDH or to ethanol in two subsequent reactions catalysed by PDC and ADH. Alternatively, pyruvate and glutamate can be converted to alanine and 2-oxoglutarate by the enzyme AlaAT. Several studies in model organisms showed that 2-oxoglutarate can re-enter the tricarboxylic acid cycle to produce another ATP molecule and eventually contribute to the accumulation of succinate in the cell (António *et al.*, 2016; Bailey-Serres *et al.*, 2012). Cukrov *et al*. (2016) observed that in 'Granny Smith' apples the gene expression levels of PDC, ADH, LDH and AlaAT and the concentration of pyruvate derived compounds are higher when oxygen levels are lower. GABA is reported to be another important metabolite during hypoxia in model species (António *et al.*, 2016; Bailey-Serres *et al.*, 2012). However, the behaviour of GABA during DCA storage of apple fruit is not yet clear. Cukrov *et al*. (2016) reported an increase in GABA levels in 'Granny Smith' apple fruit stored under low oxygen levels (0.4 kPa $O_2$ and 0.8 kPa $O_2$), whereas Brizzolara *et al*. (2017) reported more or less stable GABA levels throughout storage under low oxygen levels (0.45 kPa $O_2$) in 'Granny Smith' and 'Red Delicious' apple fruit. Furthermore, Brizzolara *et al*. (2017)

demonstrated that the metabolic changes introduced by low-oxygen stress during DCA storage can be different depending on the cultivar, with 'Red Delicious' producing more ethanol and GABA while 'Granny Smith' prefers to balance pyruvate levels via the alanine pathway.

However, these recent studies only provide information about the metabolite and transcript levels but the actual activity of the metabolic pathways remains unknown. To better understand the control and regulation of the metabolic changes in the energy metabolism under low-oxygen stress, metabolic flux analysis using isotope-labelled substrates together with transcriptomics is essential to understand the complete picture. In this study, uniformly labelled [U-$^{13}$C]pyruvate was used to investigate the metabolic changes introduced in 'Jonagold' apple fruit treated with different low oxygen concentrations. The choice of using [U-$^{13}$C]pyruvate instead of [U-$^{13}$C]glucose to study the metabolic response to low-oxygen stress was based on previous experiments conducted by our research group by Beshir et al. (2017), who demonstrated that mature apple fruit incorporated little to no $^{13}$C label coming from [U-$^{13}$C]glucose. Since the transport of pyruvate through the cell membrane happens through passive diffusion, our hypothesis is that pyruvate will be taken up more easily by the tissue in comparison to the actively transported glucose. Furthermore, Cukrov *et al*. (2016) reported that changes in the pyruvate metabolism in apple fruit are a key event occurring under low oxygen conditions, making [U-$^{13}$C]pyruvate the more suitable isotope-labelled substrate to study these changes. To our knowledge, it is the first time that dynamic isotope labelling experiments have been performed together with transcriptomics to study the metabolic response of apple fruit upon low-oxygen stress.

# 5.2 Materials and methods

## 5.2.1 Plant material

'Jonagold' apples (*Malus* x *domestica* Borkh., cv. 'Jonagold') were harvested from an orchard in Rotselaar, Belgium, in September 2016 during the commercial harvest window for long term storage of 'Jonagold' apples. The harvested apple fruit were split into two random groups. The first group was immediately used for the first experiment. The second group was stored for 7 d in regular air at 1 °C. One day before the start of the second experiment the apples were put at 18 °C to allow for proper temperature equilibration.

## 5.2.2 Experimental design

The aim of this study was to investigate the effect of low oxygen concentrations on the central carbon metabolism by a combination of metabolomic, fluxomic and transcriptomic analyses. Two different experiments were conducted. In the first experiment apple tissue discs were treated with 0.5 kPa $O_2$ and 21 kPa $O_2$ for 72 h at 18 °C, to investigate how the fluxes through the central carbon metabolism would change during prolonged low-oxygen stress. Besides metabolomics, fluxomic and transcriptomic analysis, the fermentation metabolites and enzyme activity of PDC and ADH were measured to see whether the same decreasing trend in fermentation metabolites could be observed as in chapter 4.

The goal of the second experiment was to investigate how the central carbon metabolism initially adapts to different low-oxygen stresses. Therefore, apple tissue discs were treated with 0 kPa $O_2$, 0.3 kPa $O_2$, 0.7 kPa $O_2$ and 1 kPa $O_2$ for 10 h at 18 °C. In these samples metabolomic, fluxomic and transcriptomic analysis were performed. A detailed overview of the experimental setup of both experiments is shown in Fig. 5.1.

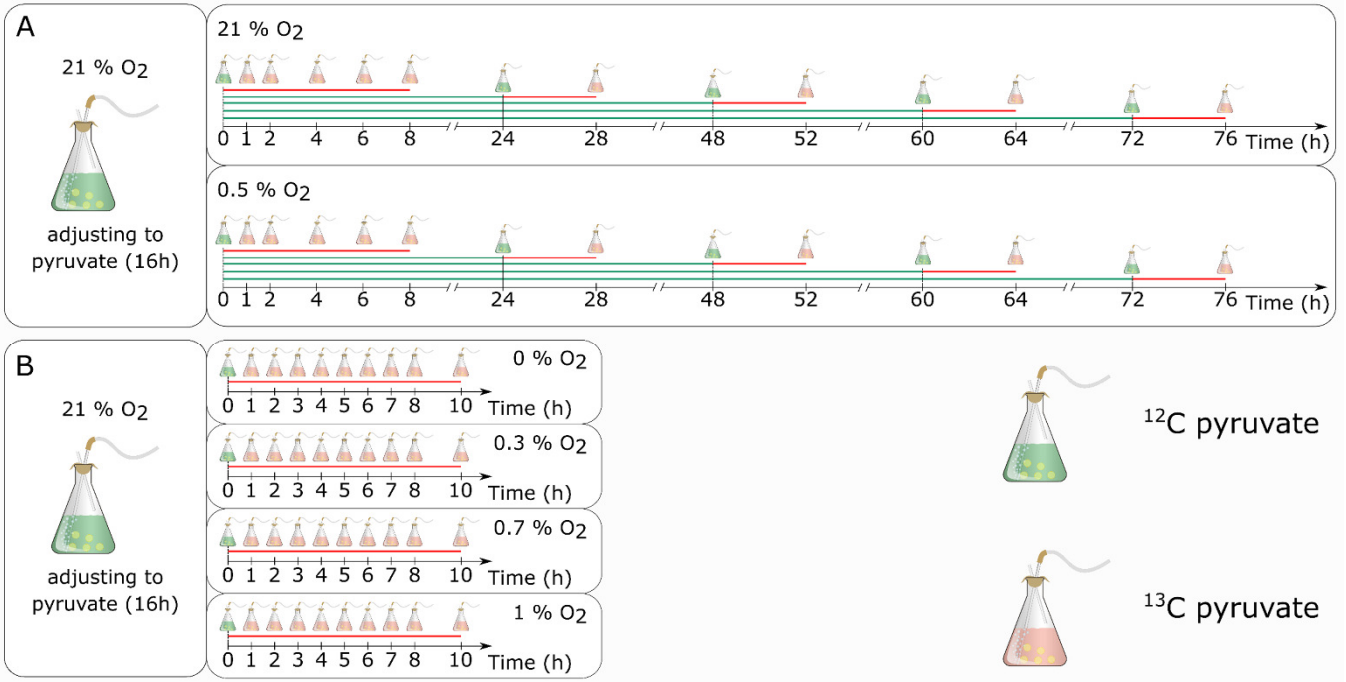


Figure 5.1: Schematic representation of the experimental setup of experiment 1 (A) and experiment 2 (B). The medium of all the Erlenmeyer's of experiment 1 was refreshed at 0, 24, 48, 60 and 72 h, indicated by the vertical lines. The green lines indicate the incubation period in medium with unlabelled pyruvate while the red lines mark the incubation period in medium containing $^{13}C$ labelled pyruvate. Each time point marked by a flask refers to an experimental sampling point.

*In vivo* $^{13}C$ labelling experiments were conducted in a similar way as described by Beshir *et al*. (2017). In brief, apple tissue discs (~10 mm diameter and ~1 mm thickness) were collected from the cortex using a cork borer. To remove damaged cells, the tissue discs were washed three times in an isotonic solution containing 50 mM HEPES/KOH buffer (pH 7.0), 2 mM $CaCl_2$, 2 mM $MgCl_2$, 2 mM DTT (1,4-dithiothreitol) using betaine as an osmoticum, while shaking at 90 rpm. The osmotic strength of the solution (730 mM) was adjusted based on the measured osmolality by Beshir *et al.* (2017). After washing thoroughly, depending on the experiment, a certain amount of tissue discs were placed in a 50 mL flask containing an identical buffer solution as the one used to prepare the tissue discs, but supplemented with 20 mM unlabelled pyruvate. The tissue discs were pre-incubated in the unlabelled solution for 16 h at 18 °C to allow the metabolism to adjust to the excess of pyruvate. After the pre-incubation period, the tissue discs were transferred to a solution containing 20 mM [U-$^{13}C$]pyruvate (see Fig. 5.1). The solution was continuously aerated with humidified air at 18 °C in a controlled environment. Due to the instability of DTT, the medium of all the Erlenmeyer's of experiment 1 was refreshed at 0, 24, 48, 60 and 72 h. Tissue discs were incubated for various time intervals (see Fig. 5.1) after label introduction. Subsequently, samples were washed three times using 100 mL of a hypotonic solution of 50 mM HEPES/KOH buffer (pH 7.0) to remove the incubation medium from the tissue. After washing, excess washing medium was removed from the discs using paper tissue. The tissue discs were divided in three groups and used as replicates in this study. Afterwards, the tissue samples were rapidly frozen and ground into fine powder in liquid nitrogen using a Mixer Mill (Retsch, MM 200, Haan, Germany) and stored at −80°C. These samples were used to measure primary metabolites and flux analysis with the GC-MS (exp. 1 and 2), to perform RNA sequencing analysis (exp. 1 and 2) and to measure the concentration of fermentation metabolites and the enzyme activity of PDC and ADH (exp. 1).

## 5.2.3 Primary metabolite analysis

The polar metabolites were extracted and derivatised based on the protocols described by Bekele *et al.* (2014). In brief, to extract the polar metabolites, the ground apple tissue (200 mg) was homogenized with 1 mL of ice cold methanol and incubated, while shaking (1400 rpm) in a thermomixer (Eppendorf AG, Hamburg, Germany) for 15 min at 70 °C. The mixture was centrifuged (22000 *g*) for 20 min at 4 °C. Subsequently, 100 µL of the supernatant was mixed with 30 µL of internal standard (3-(4-hydroxy-phenyl)propionic acid ( 0.1 g $L^{-1}$ methanol)) for the acids and 200 µL of the supernatant was mixed with 50 µL internal standard (phenyl-β-D-glucopyranoside (3 g $L^{-1}$ methanol)) for the sugars and dried under a stream of nitrogen gas. Afterwards, the dried residue was oxymated by adding 120 µL of methoxyamine hydrochloride (20 mg MEOX in 1 mL pyridine) to the dried sample and incubating while shaking (1400 rpm) in a thermomixer for 1 h at 30 °C. Derivatisation was carried out by adding 120 µL of BSTFA (N,O-bis(trimethylsilyl(TMS))trifluoroacetamide) to the sample and incubating it for 2 h at 45 °C.

GC-MS analysis for the sugar samples was performed on a GC 7890A coupled to a 5975C MS (Agilent Technologies, Palo Alto, CA) and for the acid samples on a TSQ 8000 GC/triple quadrupole MS (Thermo Scientific, Austin, USA). The chromatographic separation was on both machines performed on a HP-5ms column (30m x 250 µm ID, 0.25 µm film thickness, Supelco, Bellefonte, CA) with a programmed temperature ramp. The carrier gas used was helium, applied at a constant flow of 1 mL $min^{-1}$. The less abundant acid samples were injected with a split ratio of 5:1. For this injection, the oven temperature was set to 50 °C for 2 min, ramped at 10 °C $min^{-1}$ to 325 °C and held for 5 min at 325 °C (34.5 min total run time). The more abundant sugar samples were measured with a split ratio of 500:1. For this injection, the oven temperature was set to 90 °C for 2 min and ramped to 325 °C switching between 50 and 10 °C $min^{-1}$ and held at 325 °C for a further 5 min (17.3

min total run time). Both the device of Agilent and Thermo Scientific have a mass selective detector (MSD), and applied electron ionization (70 eV) operating a single quadrupole with the MS ion source temperatures maintained at 150 and 230 °C, respectively. The detector was programmed to scan the mass spectral range of 35-500 m/z.

## 5.2.4 Metabolite quantification and $^{13}$C-label enrichment

Metabolites were identified and quantified by using Agilent MSD Chemstation Software (Agilent Technologies, Santa Clara, USA) and AMDIS (automated mass spectral deconvolution and identification system) software (National Institute of Standards and Technology (NIST), USA). The acquired spectra were compared with an in-house built library, with the Agilent Fiehn Metabolomics Library, and with the NIST2011 Library. The percentage of $^{13}$C enrichment was calculated from a particular molecular ion fragment after being corrected for the natural occurring isotopes (Wahl *et al.*, 2004).

## 5.2.5 RNA extraction and precipitation

Total RNA was extracted from the three replicates separately and afterwards pooled to obtain the final concentration necessary for sequencing. The ground tissue samples (300 mg) were homogenized with 800 µL of pre-heated extraction buffer containing cetyl-trimethyl-ammonium bromide prepared according to Gasic *et al.* (2004). A glass bead and 80 µL of 20 % Sarkosyl detergent was added to the mixture and vortexed vigorously for 30 s to make the lysis of the cells more efficient. The mixture was incubated in a thermomixer (1400 rpm) at 70 °C for 10 min. Subsequently, an equal volume of chloroform/isoamyl alcohol (24:1) was added to the homogenate and mixed by vortexing. After an incubation period of 5 min at room temperature, the samples were centrifuged at top speed (21,500 *g*) for 10 min at 22 °C. The supernatant was transferred onto a gDNA eliminator column of the RNeasy

Plus mini kit (Qiagen) and centrifuged at 8000 *g* for 15-30 s at 22 °C. Afterwards, 400 µL of 100 % ethanol was added to the flow through, mixed immediately by pipetting and loaded on to the RNeasy mini column. The supernatant was removed by centrifuging the columns at 8000 *g* for 15-30 s at 22 °C and the RNA is bound to the filter of the column. The RNA was washed twice with 500 µL of RPE buffer. The RPE buffer is removed by centrifugation (8000 *g*) for 15-30 s at 22 °C. All traces of ethanol were removed by centrifuging the RNeasy mini columns for 2 min at 8000 g and 22 °C. The RNA was eluted from the column by adding 40 µL of DEPC water and centrifugation (8000 *g*) for 15 s at 22 °C. The final step was repeated twice to make sure all the RNA was eluted. The purity of total RNA extracted was determined in NanoDrop 2000 (Thermo Scientific) and integrity was checked by gel electrophoresis. Finally, the three replicates were pooled, RNA was precipitated with sodium acetate and ethanol according to the protocol described by Walker (2013) and dissolved again in 50 µL of DEPC water to obtain enough RNA for sequencing (between 3 – 5.5 µg).

## 5.2.6 Library construction, sequencing and data processing

Strand specific mRNA sequencing libraries were made by the sequencing company, Polar Genomics (Ithaca, USA), according to their protocol (Zhong *et al.*, 2011). Samples were sequenced on a Nextseq 500 (Illumina) with a 75 bp single-end read length. Libraries were all run in the same lane. The program Trimmomatic was first used to process the raw reads to remove the adapter and sequences with low-quality (Bolger *et al.*, 2014). Reads shorter than 40 bp after trimming were discarded. To remove ribosomal RNA reads, the resulting reads were aligned to the ribosomal RNA database (Quast *et al.*, 2012) using Bowtie (Langmead *et al.*, 2009) and aligned reads were discarded. No more than three mismatches per read were allowed. The remaining reads were aligned to the double-haploid 'Golden Delicious' apple genome (Daccord *et al.*, 2017b) using HISAT (Kim *et al.*, 2015). Again no more than three mismatches per read were allowed. For each gene the raw counts were

derived from the read alignments and normalized to TPM counts (transcripts per kilobase million). The TPM counts were calculated by dividing the raw counts by the length of each gene in kilobases, to get the reads per kilobase (RPK). Subsequently, all the RPK values in a sample were summed up and divided by 1 000 000, to get the per million scaling factor. And finally, the RPK values were divided by the per million scaling factor to get the TPM counts. All raw data processing was done by Polar Genomics (Ithaca, USA). The raw data and the TPM counts of both experiments can be accessed via the following link: https://kuleuven.box.com/s/pwwaukuc6ee5645w1n8mffkrrbb49zci

### 5.2.7 RNA-sequencing data analysis

To get a general overview of the most important up or down regulated processes under low-oxygen stress, gene expression data of the first experiment were clustered using Matlab (The MathWorks, Inc., Natick, MA, USA). Per gene, data were normalized over all samples by subtracting their mean expression value and dividing by their standard deviation. The difference in the normalized expression levels between 21 kPa $O_2$ and 0.5 kPa $O_2$ over time was calculated for the full 72 h experimental period. Based on linear regression analyses, those genes showing a significant effect of $O_2$ with time, as indicated by a $p < 0.05$, were kept for subsequent clustering analysis, thus excluding genes not showing any differential behaviour in response to $O_2$. For the selected genes, the normalized gene expression data at 21 kPa $O_2$ and 0.5 kPa $O_2$ combined with their differential gene expression data were subjected to a k-means clustering resulting in 9 characteristic clusters. The K-means clustering was done using the litekmeans function written by Mo Chen, publically available from the MathWorks FileExchange (File Exchange - MATLAB Central). Per cluster, the normalized expression data were averaged and used to visualize the overall behaviour as a heat map. For all the selected genes, the latest gene ontology (GO) annotation was obtained using the default parameters settings in Blast2Go v4.1.9 (Conesa and Götz, 2008). A GO enrichment analysis was performed, with a

reference set containing all the genes of the control condition, which had on average a TPM count greater than 1 over all the time points. The GOslim option was set to reduce the number of functional classes. Furthermore, pathway analysis was performed by using DESeq 2 to normalize the raw counts for library size, to perform shrinkage estimation for dispersion and to calculate the fold changes between the control and the treatment (Love *et al.*, 2014). For all the genes coding for the same enzyme, an average fold change (FC) was calculated on every time point, weighted for the difference in expression between control and treatment on that time point. For data visualization, the average fold change per time point for each enzyme was presented as a heat map (FC $-2 \leq \geq 2$) and plotted on the main metabolic pathways involved in low oxygen stress. Individual transcript expression profiles were checked in more detail to interpret the fold change pattern presented on the figures.

### 5.2.8 Enzyme extraction and activity measurement

Enzymes were extracted as described in Chapter 3 section 3.2.3. and the enzyme activity of pyruvate decarboxylase (PDC) and alcohol dehydrogenase (ADH) was measured as described in chapter 3 in section 3.2.4.

### 5.2.9 Fermentation metabolites

The fermentation metabolites were measured as described in Chapter 4 section 4.2.6.

### 5.2.10 Respiration measurement

To study the effect of feeding pyruvate on the respiration rate of the apple tissue discs, the oxygen consumption rate of tissue discs was monitored by using a biological oxygen monitor (BOM) equipped with a Clark's oxygen electrode (Qubit systems inc., Kingston, Canada) following the procedure by Lammertyn *et al.* (2001).

# 5.3. Results and Discussion

## 5.3.1 Preliminary experiments determining the optimal pyruvate concentration and confirming its cellular uptake

Zabalza *et al.* (2009) observed that the respiration rate of *Pisum sativum* roots increased after feeding with pyruvate. Therefore, a preliminary experiment was performed to find a concentration of pyruvate, which affects the respiration rate as little as possible but is still high enough to incorporate a sufficient amount of label in the apple tissue discs. A comparison between the respiration rate of apple tissue discs incubated with a buffer containing different pyruvate concentrations (between 0 and 100 mM) and control samples was performed 24 h after feeding. No consistent differences were observed between the respiration rate of the apple tissue discs fed with the different pyruvate concentrations (data not shown). Therefore, it was decided to use the same amount of pyruvate (20 mM) as used in another $^{13}$C-pyruvate labelling study on *Lotus japonicus* (António *et al.*, 2016). The influence of 20 mM pyruvate on the respiration rate of apple was studied more closely by incubating apple tissue discs of the same apple in a buffer with or without pyruvate. The respiration rate was measured at regular time points with the BOM in the first 24 h after feeding. As the respiration rate changed both in the control and the treated sample, the influence of pyruvate on the respiration rate was studied by calculating the differences (or delta) between the respiration rate of the control and the treated sample (Fig. 5.2). The respiration rate increased in the first 7.5 h with 72 % for the samples treated with pyruvate, whereas the respiration rate of the control only increased with 2 %. Afterwards the difference in respiration rate started to decrease again, almost disappearing by 24 h. This was not due to pyruvate depletion, as from the respiration rate it could be calculated that after 24 h only 0.00095 % of the 20 mM pyruvate in the medium was consumed by the tissue in the Erlenmeyer. Based on these results, it was hypothesized that the metabolism goes through an

adaptation period after being exposed to high concentrations of pyruvate for the first time. Therefore, in the real experiments, an adaptation period of 16 h before the start of the measurements was implemented, during which the apple tissue discs were incubated in a medium containing 20 mM of unlabelled pyruvate (Fig. 5.1).

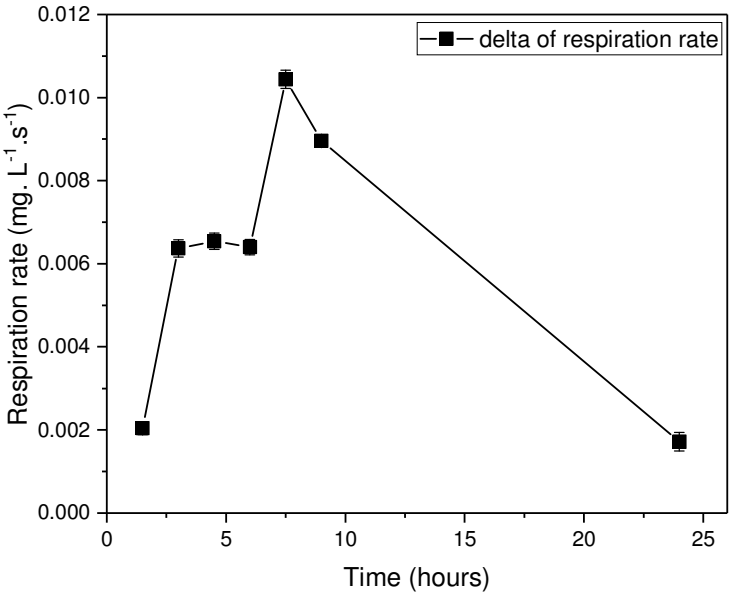


Figure 5.2: Influence of pyruvate (20 mM) on the respiration rate of 'Jonagold' apple tissue disks. The respiration rate is measured by monitoring the oxygen consumption rate. The symbols represent the delta between the respiration rate of the treated sample and the control. The error bars represent the standard error.

To check whether 20 mM of $^{13}$C-pyruvate allowed the incorporation of a sufficient amount of label in the apple tissue discs during normoxia and hypoxia, another preliminary experiment was performed in which apple tissue discs were incubated in a buffer containing 20 mM of $^{13}$C-pyruvate flushed with either 0.5 kPa $O_2$ or 21 kPa $O_2$ for 12 h at 18 °C. Samples were taken at regular time points. The percentage of $^{13}$C enrichment for every time point was obtained for four important metabolites derived from pyruvate, i.e., glutamate, succinate, malate and alanine. As the fermentation volatiles could not be detected with the GCMS, they were not included in the important metabolites derived from pyruvate. In all four metabolites, a clear

increase in $^{13}C$ percentage was observed both for the sample at 0.5 kPa $O_2$ and 21 kPa $O_2$ (Fig. 5.3) confirming our hypothesis on the effective take-up and metabolisation of pyruvate. The net $^{13}C$ incorporation was higher at 21 kPa $O_2$ as compared to 0.5 kPa $O_2$ for glutamate, succinate and alanine, indicating that the metabolism slows down when the oxygen levels drop. However, the net $^{13}C$ incorporation in malate was similar at 0.5 kPa $O_2$ and 21 kPa $0_2$ and showed an increase of only 5 %. This is probably due to the large pool of unlabelled malate present in apple fruit. As pyruvate is directly converted to alanine, the percentage $^{13}C$ enrichment already increased more than 20 % at 21 kPa $O_2$ after the first hour of feeding, while the $^{13}C$ incorporation in glutamate and succinate was slower.

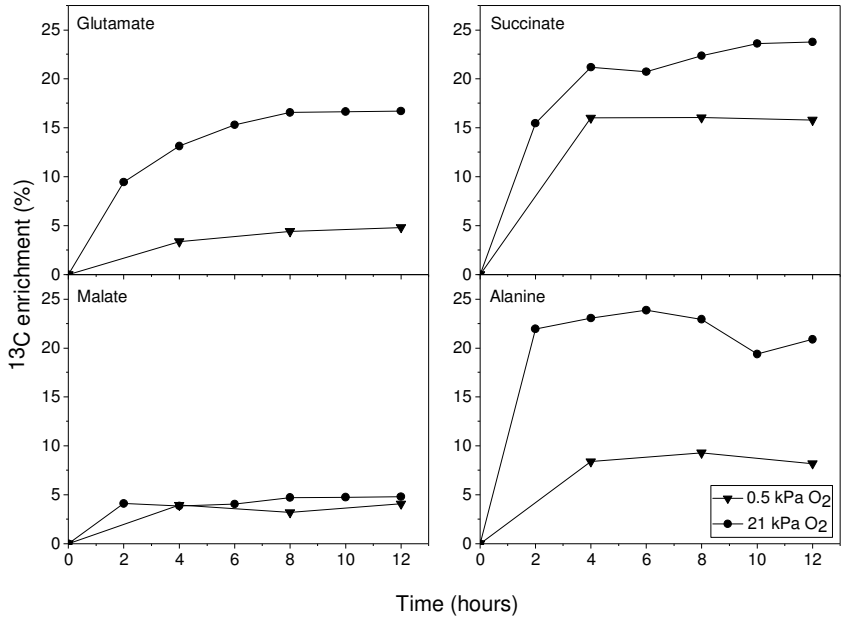


Figure 5.3: Time course of $^{13}C$-isotope enrichment of glutamate, succinate, malate and alanine. The experimental data are represented by symbols (0.5 kPa O2: ▼ and 21 kPa O2: ●).

## 5.3.2 Induction of fermentation

As one of the goals of this chapter was to get more insight in why the flux through the fermentative metabolism started to decrease after prolonged low-oxygen stress, it was first checked (as part of experiment 1) whether the current setup using tissue slices in liquid medium would provide trends similar to the trends observed in chapter 4 (Fig. 4.3) for tissue slices kept in a stream of air. Therefore, the concentrations of acetaldehyde, ethanol and ethyl acetate as well as the *in vitro* enzyme activity of PDC and ADH were measured (Fig. 5.4).

Although the gas conditions applied were comparable to the ones used in chapter 4, a different concentration profile of fermentation metabolites was observed. Instead of a smooth trend, fast drops in the concentration of the fermentation metabolites were observed every time the buffer solution was refreshed. At these occasions, the concentrations of the fermentation metabolites in the medium become zero, pulling down the concentrations of volatile metabolites in the tissue, explaining their fast drops. Due to the diffusion of the volatile fermentation metabolites into to buffer, the concentration of these metabolites inside the tissue could no longer be interpreted. Interestingly, ethanol was most subject to diffusion into the liquid medium as its concentration was ten times lower as compared to the tissue slices flushed with humidified air. In contrast, the concentration of acetaldehyde in the tissue reached similar values in both experimental setups (Fig 5.4 and 4.3).

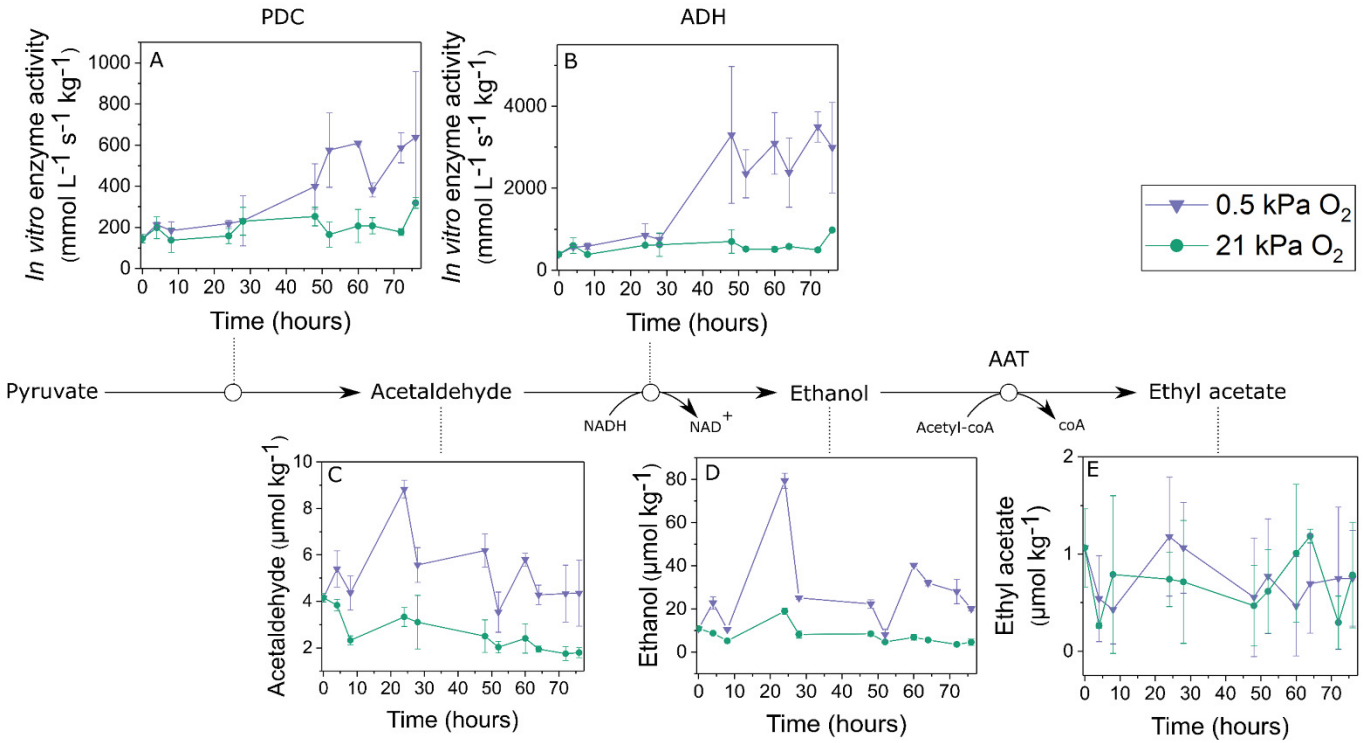


Figure 5.4: Schematic representation of the data obtained of the fermentative metabolism at 18 °C at harvest. The experimental data are represented by symbols (0.5 kPa O2: ▼ and 21 kPa O2: ●). A-B show the in vitro enzyme activity of PDC and ADH. C-F show the compounds of the ethanol pathway. The experimental data are means of three replicates and the error bars represent their standard deviation.

### 5.3.3 Metabolic profiling and flux analysis of the apple cortex under low oxygen-stress

Due to unresolved issues with the stability of the derivatisation process, in combination with a switch from an Agilent GC-MS to a ThermoFisher triple quadrupole GC-MS/MS, no reproducible results could be obtained. A lot of tests were performed and are still ongoing but no clear solution was found yet. Because of time constrains and sample exhaustion due to the many trials that eventually gave no stable results, no metabolic profiling nor flux analysis data was included in this manuscript. As a result, full attention is given to the transcriptome analysis of the collected samples.

### 5.3.4 Transcript profiling of the apple cortex under low-oxygen stress

An overview of the low-oxygen stress-related transcriptomic changes in the central carbon metabolism of 'Jonagold' apple was obtained via RNA sequencing. It provided detailed information on the influence of low-oxygen stress on the regulation of the central carbon metabolism. This section mainly discusses the transcriptomic changes observed during the first experiment, as the longer experimental period (in comparison with the second experiment) revealed more information. When transcriptomic data of the second experiment are discussed it will be explicitly mentioned in the text.

#### 5.3.4.1 General overview of transcriptomic changes induced by low-oxygen stress

To get a general overview of the most important processes which are up or down regulated during low-oxygen stress, a cluster analysis was performed on normalized gene expression data. Only genes showing a significant effect of oxygen with time

were used for the clustering analysis, resulting in nine characteristic clusters. The normalized expression data were averaged per cluster and visualized as a heat map (Fig 5.5).

The nine characteristic clusters could roughly be divided in two groups. One group contained clusters which showed an upregulation of the gene expression over time at 0.5 kPa as compared to 21 kPa $O_2$ (clusters 3, 4, 1, 9 and 8) and the other group contained the clusters which showed a downregulation of the gene expression over time at 0.5 kPa as compared to 21 kPa $O_2$ (clusters 2, 5, 7 and 6). Gene Ontology (GO) enrichment analysis was performed for both groups to characterize the nature of the overall transcriptomic changes over time (Fig 5.6).

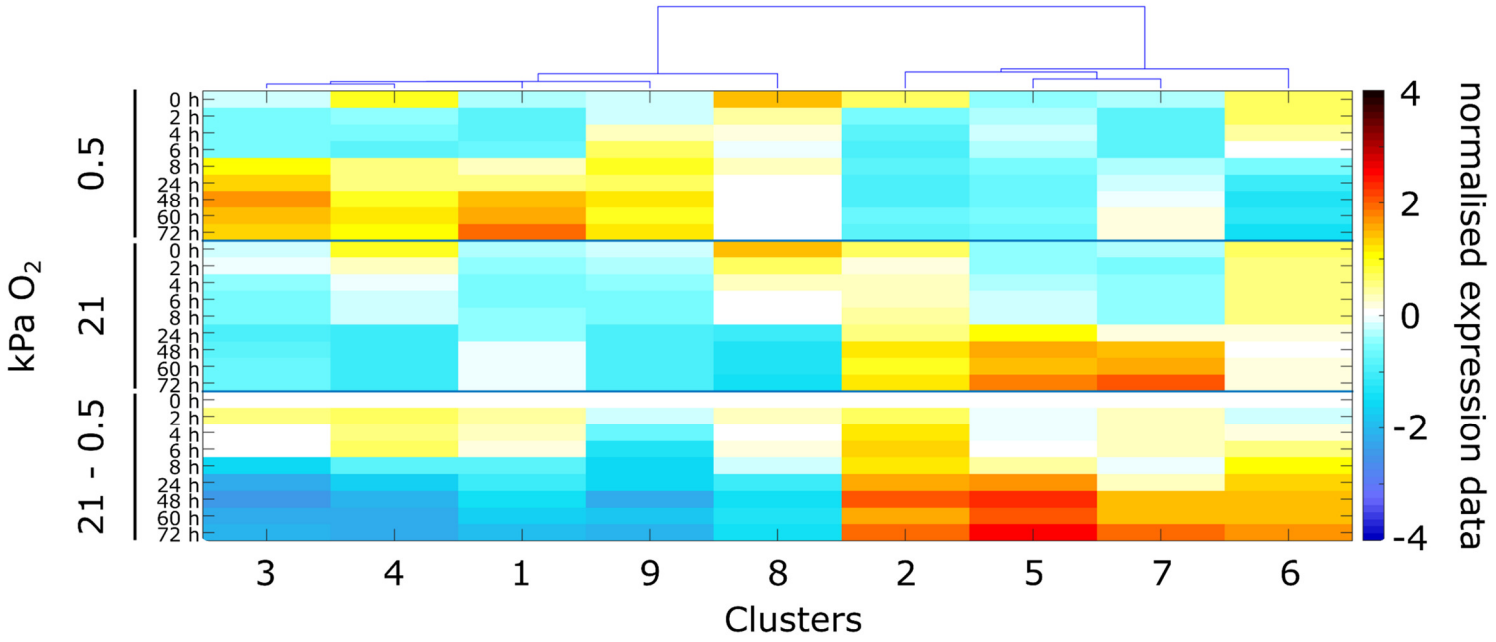


Figure 5.5: Visualization of the nine characteristic clusters. Per cluster, three heat maps are provided, the top one representing the expression pattern of 0.5 kPa $O_2$, the middle one of 21 kPa $O_2$ and the bottom one of the difference between 21 kPa $O_2$ and 0.5 kPa $O_2$. The row of each heat map represents a different sampling time, which is presented in the scheme next to the heat map. The expression data were normalized over all samples by subtracting their mean expression value and dividing by their standard deviation. The normalized gene expression data was subjected to a k means clustering.

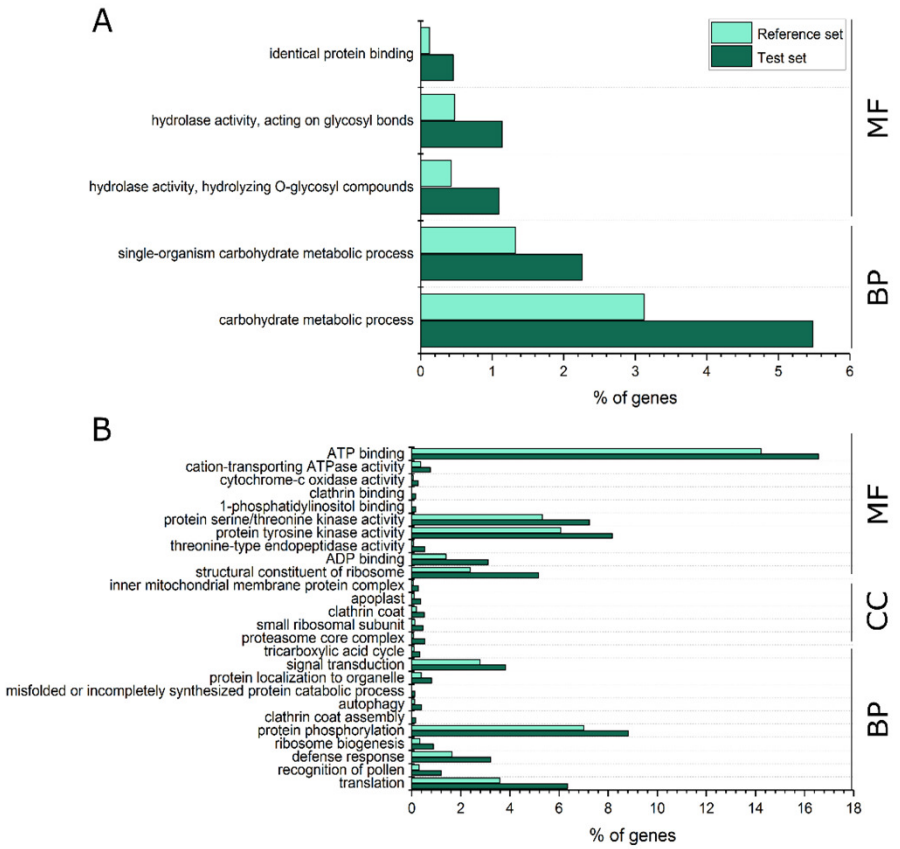


Figure 5.6: GO enrichment analysis of genes upregulated (A) and downregulated (B) under low-oxygen stress. The percentage of genes corresponding to a certain GO term in the test set and the reference set are represented. BP: biological process, MF: molecular function; CC: cellular component

The two biological processes significantly enriched in the group of genes that were upregulated during low-oxygen stress are both associated with the carbohydrate metabolic process (GO:0005975 and GO:0044723). This comes as no surprise as the upregulation of the glycolytic flux is a well-known phenomenon during low-oxygen stress. Furthermore, the molecular functions *hydrolase activity* (GO:0004553 and GO:0016798) and *identical protein binding* (GO:0042802) are upregulated during low-oxygen stress. Amongst the genes that were downregulated during low-oxygen stress a strong overrepresentation was found for a range of categories associated with biological processes such as *translation* (GO:0006412), *protein phosphorylation*

(GO: 0006468), *signal transduction* (GO:0007165) and *defence response* (GO:0006952). The biological process of the TCA cycle was also downregulated during low-oxygen stress. Only a very small percentage of genes was involved in the GO terms representing the category cellular components. For the molecular functions a strong over-representation was found for *ATP binding* (GO:0005524), *ADP binding* (GO:0043531) and *protein kinase activity* (GO:0004713 and GO:0004674). Furthermore, also the *cytochrome-c oxidase activity* (GO:0004129) was shown to be downregulated during low-oxygen stress. Together with the upregulation of the carbohydrate metabolic process and the downregulation of the TCA cycle this indicates that energy is lesser produced via oxidative phosphorylation but rather via an increase in glycolytic flux when 'Jonagold' tissue discs are exposed to 0.5 kPa $O_2$.

To further investigate how the central carbon metabolism is adapted and regulated during low-oxygen stress a more detailed analysis of the most important pathways known to be involved in low-oxygen stress was performed and discussed in the next sections.

### 5.3.4.2 Metabolic adaptations to save energy are induced

When plant tissue is exposed to low-oxygen stress, one of the most direct effects is the reduction of the energy status of the cells (Geigenberger, 2003). Therefore, plants try to adapt their metabolism in an attempt to save energy (Bailey-Serres et al., 2012; Geigenberger, 2003; Van Dongen et al., 2011). One of the metabolic adaptations that plants use to save energy is to favour pyrophosphate (PPi) dependent reactions above those which use ATP as substrate (Bailey-Serres et al., 2012; Kosmacz and Weits, 2014). The cleavage of sucrose is one of the reactions known to have a PPi-dependent alternative enzyme. Instead of using the ATP consuming invertases and hexokinases to provide hexose-phosphates from sucrose, plants can use sucrose synthase (SUS), UDP-glucose pyrophosphorylase (UGPase) and phosphoglucomutase to cleave sucrose into glucose 6-phosphate. This

alternative pathway uses only 1 molecule of PPi instead of 2 molecules of ATP (Mustroph *et al*., 2014). In this study, an upregulation of the genes of this alternative pathway was observed in the samples exposed to low-oxygen stress (Fig. 5.9A). Specially, four genes coding for SUS (MD02G1100500, MD02G1100600, MD11G1307000, MD15G1223500) showed a strong upregulation during low-oxygen stress (Fig. 5.7), leading to fold changes (FCs) above 2 in the first 8 h of the experiment, which started to decrease again after 24 h towards the end of the experiment. In contrast, the genes coding for invertase showed a strong downregulation with FCs < -2 after 48 h. Together, this indicates that the PPi dependent pathway is favoured in 'Jonagold' apples exposed to low-oxygen stress. Cukrov et al. (2016) observed a similar trend for SUS in 'Granny Smith' apples. Furthermore, the same authors reported that the expression of SUS in apple fruit is highly sensitive to changes in oxygen concentration in the environment. However, due to the short time series of the second experiment, we were not able to observe clear differences between the increasing expression levels of SUS induced by the different oxygen concentrations applied.

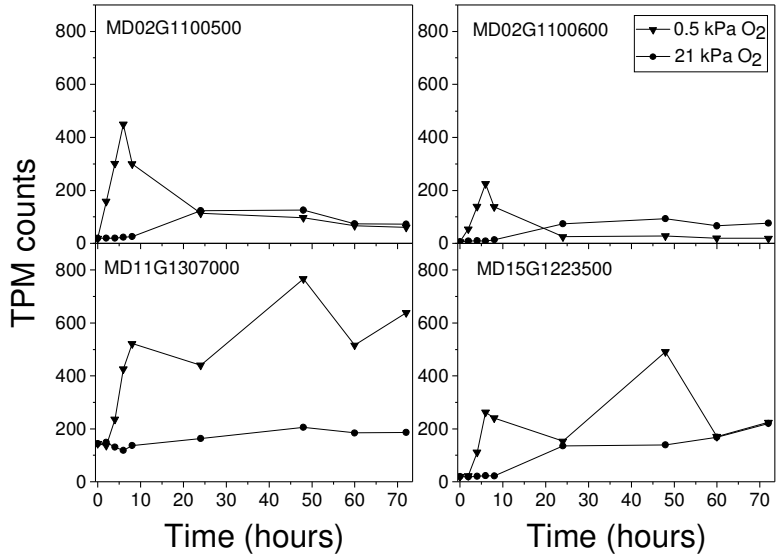


Figure 5.7: The expression profile of all the genes coding for SUS. ▼ = 0.5 kPa $O_2$; ● = 21 kPa $O_2$.

A second reaction which has a PPi using variant is the phosphorylation of fructose 6-phosphate into fructose-1,6-bisphosphate. Instead of using the ATP dependent enzyme phosphofructokinase (PFK), the reversible PPi using variant, i.e., pyrophosphate:fructose-6-phosphate phosphotransferase (PFP) could be favoured when energy levels are low. However, until now it is not completely clear how the *PFK*/*PFP* gene expression and activity is regulated in plants. Mustroph *et al.* (2010) reported that *PFK* genes were observed to be expressed during hypoxia in all plant organisms studied so far, in contrast to the induction of *PFP* expression, which was not observed in all species during hypoxia (Mustroph *et al.*, 2014). Therefore, Mustroph *et al.* (2014) suggested that PFK and not PFP catalyses the main glycolytic pathway under hypoxic conditions in most organisms. However, in our study, the expression levels of *PFK* and *PFP* suggested a different regulation in 'Jonagold' apple (Fig. 5.8B). In the first 6 h, a fast upregulation of *PFK* was observed (FC > 4) which started to decrease again towards 8 h (FC = 2.5) and declined even further towards the end of the experiment (FC ≤ -1.7). The initial increase in *PFK* was caused by a fast upregulation of the genes *MD15G1089400* and *MD08G1109700*, which decreased again after 6 h and reached similar levels as the control at 24 h. The decline in *PFK* expression levels at low oxygen stress was strengthened by a decrease in *MD02G1068900* after 8 h (Fig 5.9).

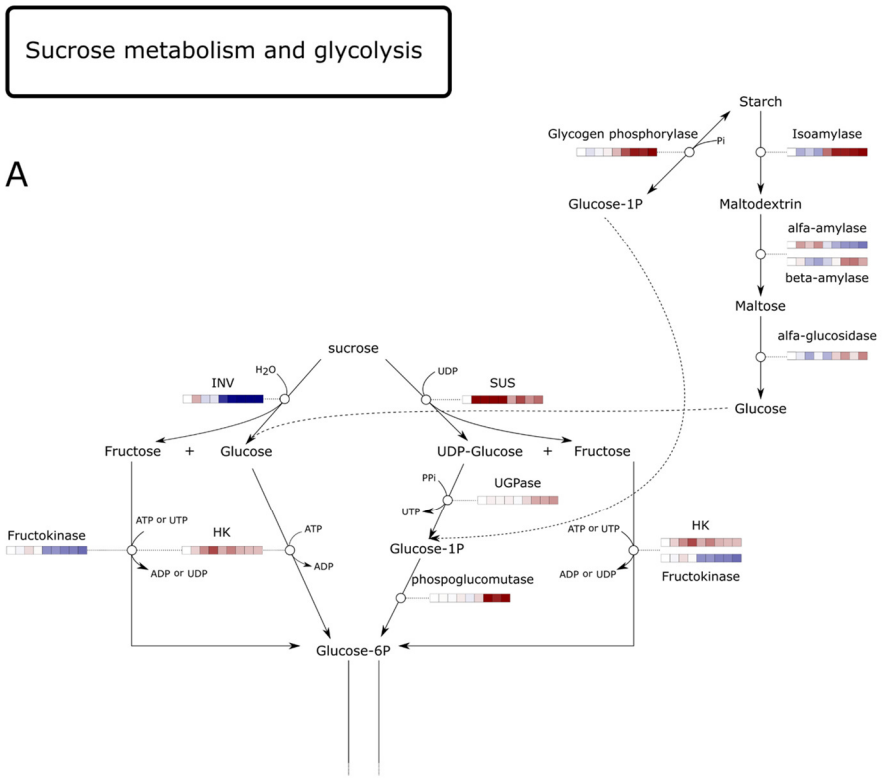
Sucrose metabolism and glycolysis
A
Starch
Glycogen phosphorylase
Pi
Isoamylase
Glucose-1P
Maltodextrin
alfa-amylase
beta-amylase
Maltose
alfa-glucosidase
Glucose
sucrose
INV
H2O
UDP
SUS
Fructose
+
Glucose
UDP-Glucose
+
Fructose
PPi
UGPase
UTP
Fructokinase
ATP or UTP
HK
ATP
ADP or UDP
ADP
Glucose-1P
phospoglucomutase
ATP or UTP
HK
ADP or UDP
Fructokinase
Glucose-6P

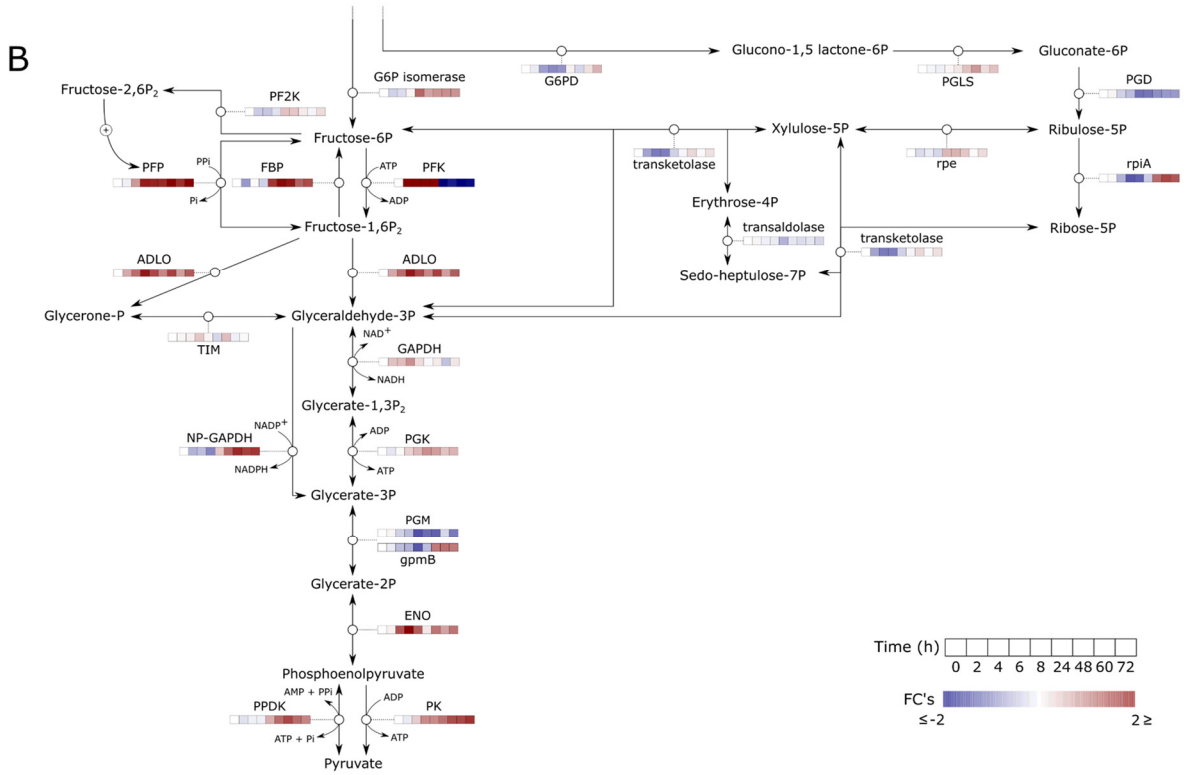


Figure 5.8: Pathway analysis of the sucrose metabolism (A) and the glycolysis (B). The heat maps represent the average fold change calculated on every time point, weighted for the difference in expression between control (21 kPa $O_2$) and treatment (0.5 kPa $O_2$) at that time point.

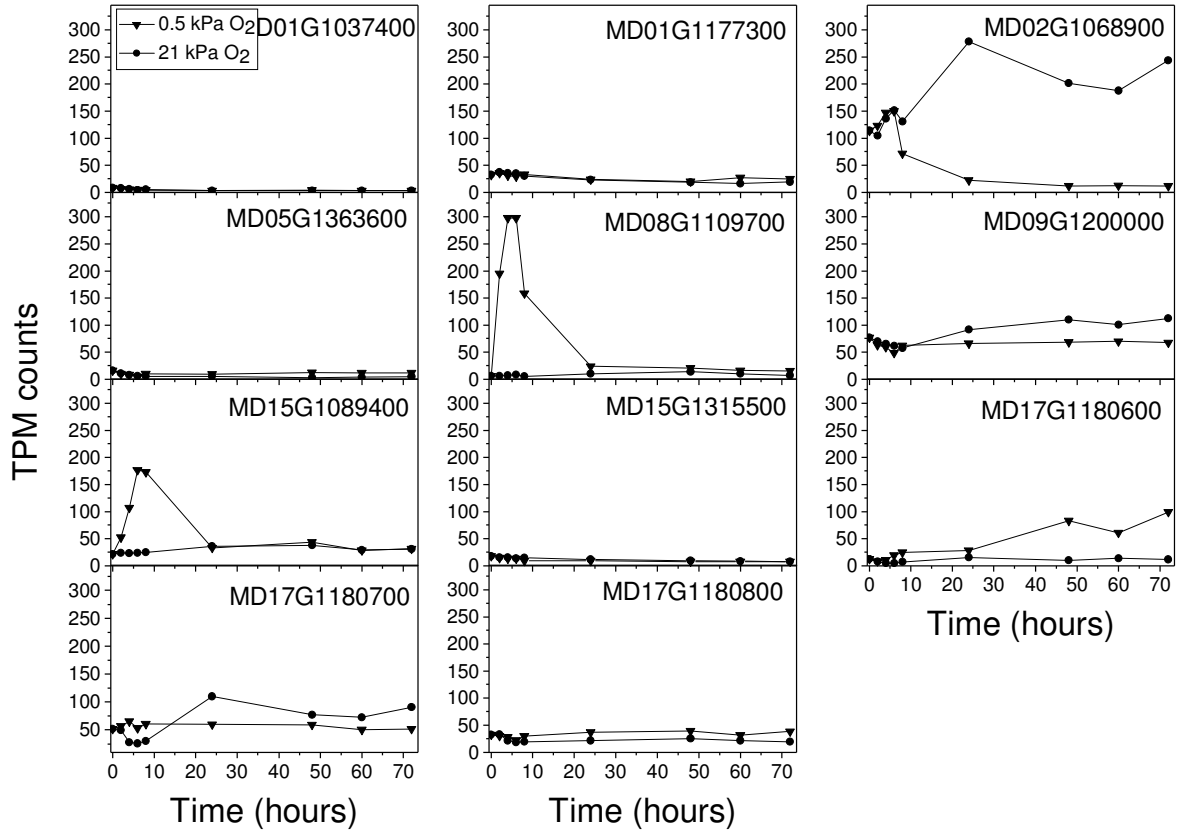


Figure 5.9: The expression profile of all the genes coding for PFK. ▼ = 0.5 kPa $O_2$; ● = 21 kPa $O_2$.

A similar trend of *PFK* expression during low-oxygen stress was observed in 'Granny Smith' apples (Cukrov *et al.*, 2016). However, also pyruvate kinase (PK) levels are increasing during low-oxygen stress, possibly leading to a reduction of PEP levels in the cell. If the PEP levels reduce in the cell, the inhibition of PFK by PEP will be diminished (Plaxton and Podesta, 2006). Hence, even if the expression levels of *PFK* decrease, the enzyme can be more active. Further research is necessary to study the enzyme activity of PFK *in vivo* under low oxygen stress in 'Jonagold'. In contrast to *PFK*, *PFP* showed a rapid upregulation at low oxygen stress (Fig. 5.9B), mainly caused by the gene *MD06G1002300* (Fig 5.10).

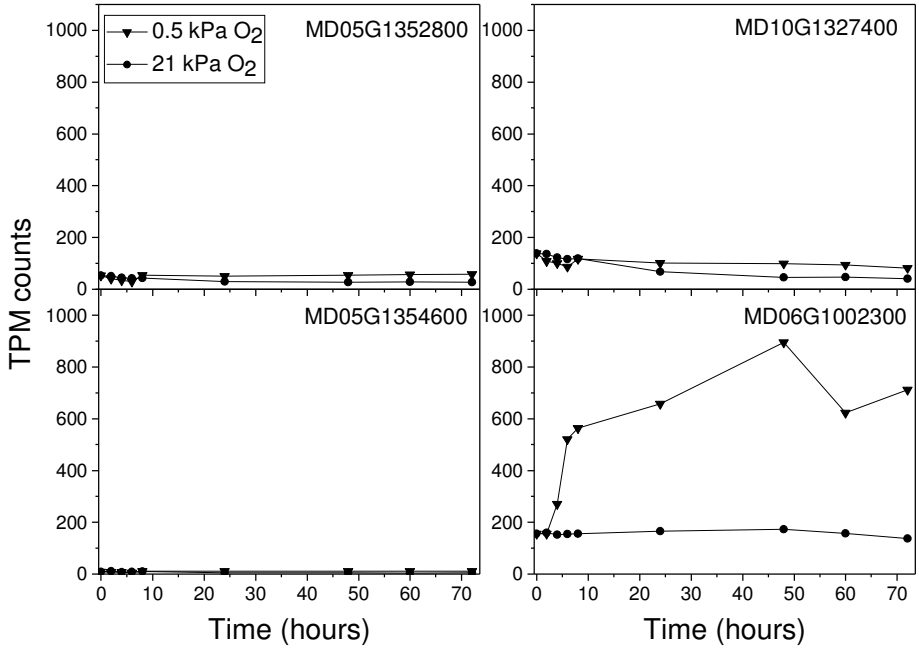


Figure 5.10: The expression profile of all the genes coding for PFP. ▼ = 0.5 kPa $O_2$; ● = 21 kPa $O_2$.

In contrast, no consistent difference in expression levels in time was observed for PF2K, which catalyses the conversion of fructose 6-phosphate into fructose-2,6-bisphosphate. The latter is known to be the activator of PFP in spinach (Theodorou and Kruger, 2001). Further research is necessary to investigate whether the increase in gene expression of PFP leads to an increase in enzyme activity of PFP. Based on the gene expression results, PFK and PFP seemed both to be important in the first hours when 'Jonagold' apple fruit was exposed to low-oxygen stress. However, after prolonged low-oxygen stress, the energy saving enzyme PFP became the most important enzyme.

Also the last step of the glycolysis, where phoshoenolpyruvate is converted into pyruvate, might be catalysed by a PPi dependent enzyme; i.e., pyruvate-orthophosphate dikinase (PPDK), instead of pyruvate kinase (PK). However, both *PPDK* and *PK* were expressed higher in 'Jonagold' apple exposed to low-oxygen stress (Fig.5.8B), suggesting they both play a role during low-oxygen stress. Furthermore, as mentioned in chapter 2, the alternative enzymes mostly catalyse reversible reactions, making it difficult to estimate which direction is actually favoured under low-oxygen stress (Mustroph *et al.*, 2014).

### 5.3.4.3 Glycolytic flux is increased

When the ATP production through mitochondrial respiration is compromised under severe low-oxygen stress, plants try to compensate for this decrease in energy by increasing their glycolytic flux to produce more energy, a process known as the Pasteur effect. The most profound changes in transcript levels were observed in the genes coding for the regulatory enzymes of the glycolysis, i.e., PFK, PFP, PK and PPDK. The other genes encoding glycolytic enzymes showed a more moderate increase in FCs or stayed more or less stable over the experimental period (Fig. 5.8B). Interestingly, the transcript levels of $NADP^+$-dependent glyceraldehyde-3-phosphate dehydrogenase (NP-GAPDH) also showed an increase towards the end of the experimental period after an initial decrease in the first 6 h during low oxygen stress (Fig. 5.8B and 5.11). The enzyme NP-GAPDH offers an alternative way to convert glyceraldehyde-3-phosphate into glycerate-3-phosphate, generating NADPH but no ATP. Nowadays, little information is available about the role of NP-GAPDH in plant tissue. Rius *et al.* (2006) reported that a deficiency in NP-GAPDH resulted in an inhibition of glycolysis, a decrease in $CO_2$ fixation and an increase of oxidative stress in *Arabidopsis*. We hypothesize that *NP-GAPDH* is upregulated in 'Jonagold' apples after prolonged low-oxygen stress to diminish the accumulation of ROS and to guarantee a high glycolytic flux. However, no explanation was found for the initial decrease in *NP-GAPD* expression levels in the first 6 h of low-oxygen stress (Fig. 5.11).

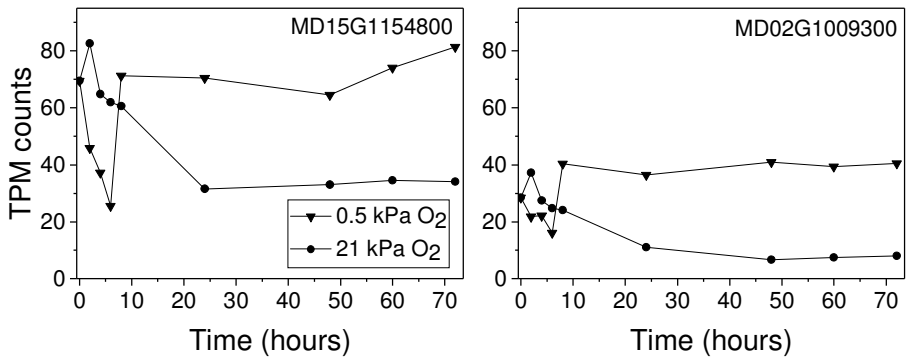


Figure 5.11: The expression profile of all the genes coding for NP-GAPD. ▼ = 0.5 kPa $O_2$; ● = 21 kPa $O_2$.

As a non-photosynthetic organ, apple fruit needs to hydrolyse starch to provide enough sucrose to support the high glycolytic flux. The starch degrading enzymes isoamylase and glycogen phosphorylase were strongly upregulated after 24 h of low-oxygen stress in 'Jonagold' apples (FCs ≤ 2), but β-amylase and α-glucosidase only showed a small increase and might be considered as being constitutively expressed (FCs ≤ 1; Fig. 5.8A). In contrast, Cukrov *et al.* (2016) reported an upregulation of β-amylase in 'Granny Smith' apples stored under hypoxia.

### 5.3.4.4 Pyruvate is no longer shuttled directly into the TCA cycle

During low oxygen stress, pyruvate is no longer shuttled into the TCA cycle due to a decrease in pyruvate dehydrogenase complex (PDH) activity (Tovar-Mendez *et al.*, 2003). The fold changes of the different genes coding for the enzymes of the PDH complex stayed more or less constant during the time series of the experiment, suggesting that the regulation of PDH is not happening at the transcription level (Fig. 5.12A). However, the expression levels of the genes coding for the enzymes of the PDH complex were affected by low-oxygen stress (Fig. S5.1, see appendices – chapter 5), but no conclusions could be drawn as some were upregulated and others were down regulated during low-oxygen stress resulting in an overall stable fold change.

More likely than a regulation at the transcriptional level, the decrease in PDH activity is caused by a strong inhibition of its products NADH and acetyl-CoA (Davies, 1980; Päpke *et al.*, 2014; Tovar-Mendez *et al.*, 2003). As cofactors are no longer reduced via oxidative phosphorylation in the electron transport chain during low oxygen stress, NADH starts to accumulate in the cell and negatively regulates the activity of PDH. Because PDH is the main entrance of pyruvate into the TCA cycle, it is an important regulatory point of the central carbon metabolism. Therefore, besides the regulation via product inhibition, PDH could also be regulated by reversible multisite seryl-phosphorylation of the E1a subunit of PDH by pyruvate dehydrogenase kinase (PDHK) and pyruvate dehydrogenase phosphatase (PDHP; Tovar-Mendez *et al.*, 2003). The expression of *PDHK* (*MD13G1140800*) increased towards the end of the experiment resulting in an increasing FC, whereas a decreasing FC was observed for *PDHK*. Together, these results suggested a stronger inhibition of PDH after prolonged low-oxygen stress (Fig. 5.12A).

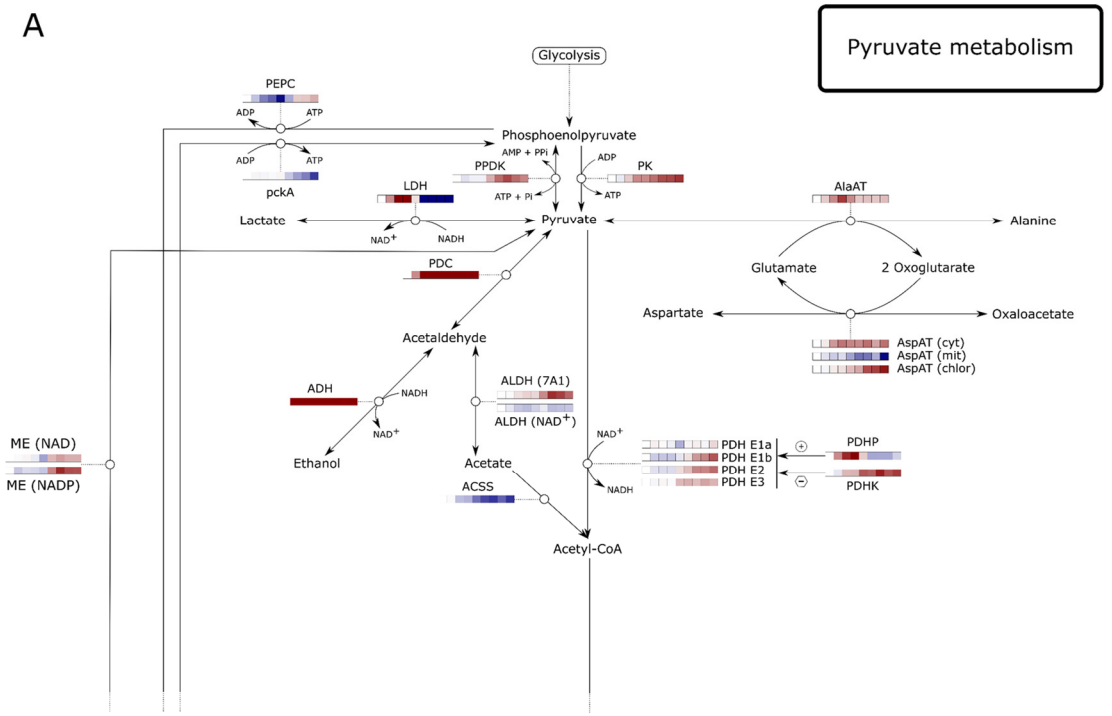
A
Pyruvate metabolism
Glycolysis
PEPC
ADP
ATP
Phosphoenolpyruvate
AMP + PPi
PPDK
ADP
PK
ATP
ATP + Pi
pckA
LDH
AlaAT
Lactate
NAD+
NADH
Pyruvate
Alanine
PDC
Glutamate
2 Oxoglutarate
Aspartate
Oxaloacetate
AspAT (cyt)
AspAT (mit)
AspAT (chlor)
Acetaldehyde
ADH
NADH
NAD+
ALDH (7A1)
ALDH (NAD+)
ME (NAD)
ME (NADP)
Ethanol
Acetate
NAD+
NADH
PDH E1a
PDH E1b
PDH E2
PDH E3
PDHP
PDHK
ACSS
Acetyl-CoA

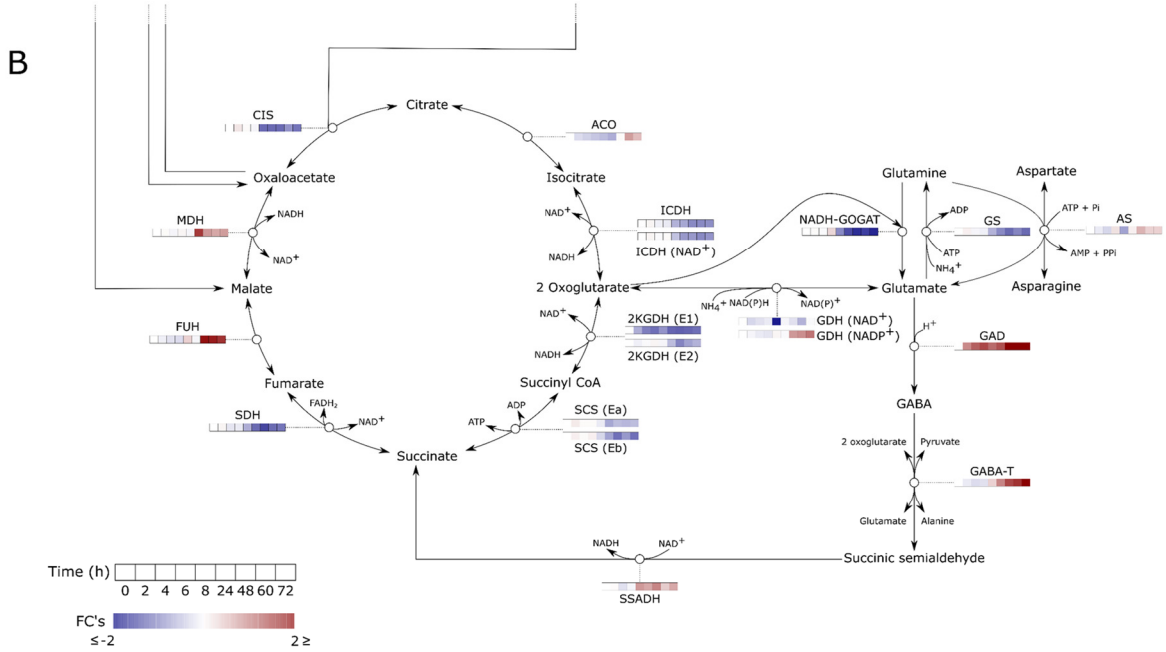


Figure 5.12: Pathway analysis of the pathways involved in pyruvate metabolism. The fermentative pathways, alanine pathway and the entry point of the TCA cycle are shown in A. The TCA cycle and GABA shunt are represented in B. The heat maps represent the average fold change calculated on every time point, weighted for the difference in expression between control (21 kPa $O_2$) and treatment (0.5 kPa $O_2$) at that time point.

### 5.3.4.5 Fermentative metabolism is induced

As the activity of PDH is inhibited during low-oxygen stress, pyruvate will be shuttled into the fermentative metabolism instead of into the TCA cycle; in this way accumulation of pyruvate is prevented and $NADP^+$ and $NAD^+$ is regenerated to maintain the high glycolytic flux (Geigenberger, 2003). In previous experiments an increase of the fermentation volatiles and enzyme activity of PDC and ADH was observed during low-oxygen stress in 'Jonagold' apple (see chapter 4). Also in this experiment an increase in the *in vitro* enzyme activity of PDC and ADH was detected. The induction of the ethanol pathway of the fermentative metabolism was further confirmed at the transcriptional level. A fast increase in the expression of *PDC* was observed in the first 6 h (FC = 3.4; Fig. 5.12A). Although the fold change of PDC between the control and the low-oxygen conditions was around 4 at the end of the experiment, the expression patterns of three out of the four genes coding for PDC showed a slightly decreasing trend towards the end of the experimental period (Fig. 5.13).

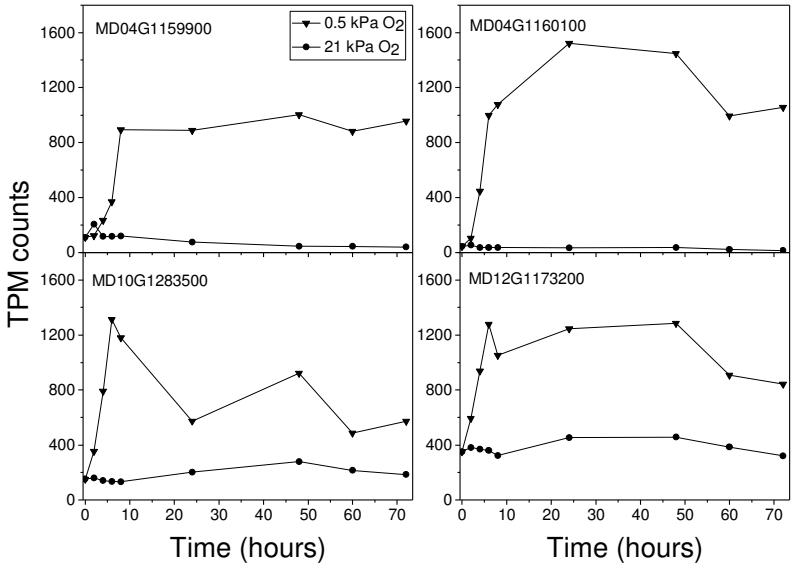


Figure 5.13: The expression profile of all the genes coding for PDC. ▼ = 0.5 kPa $O_2$; ● = 21 kPa $O_2$.

Similar to *PDC*, the expression levels of *ADH* also showed a fast increase in the first 6 h (FC = 5.3; Fig. 5.12A) and continued to increase towards the end of the experiment. Only six out of the thirteen genes coding for ADH showed a clear induction during low-oxygen stress and are represented in Fig. 5.14. Interestingly, *ADH* was also induced under normoxia after 24 h, but the reason for this increase is not yet clear since no induction was observed in the *in vitro* enzyme activity of ADH for the control condition (Fig. 5.4). Cukrov *et al.* (2016) reported that a subtle difference in terms of oxygen concentration induced a differential transcriptional upregulation of *PDC* and *ADH* genes in 'Granny Smith' apples. However, in the short period of our second experiment no clear differential expression was observed for *PDC* and *ADH* between the different oxygen concentrations.

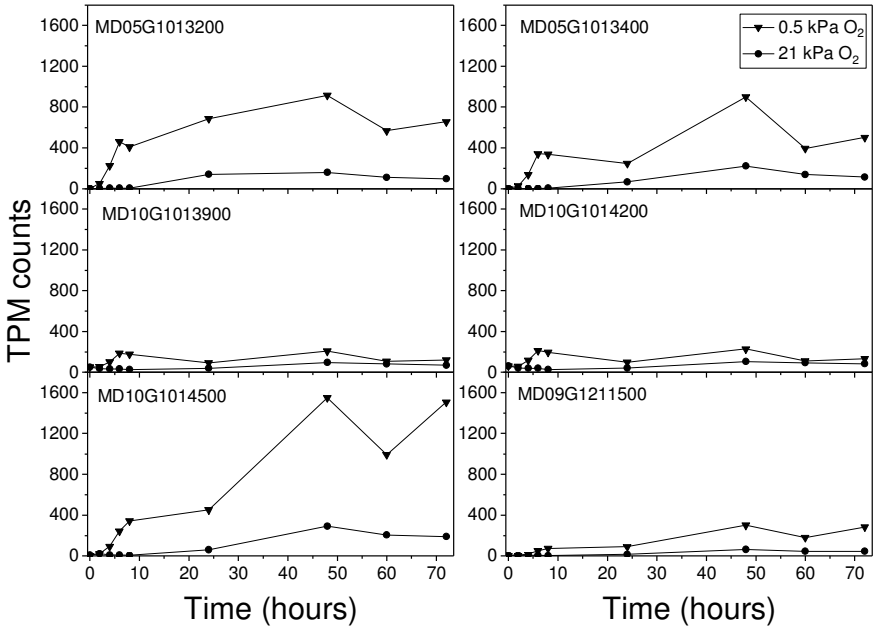


Figure 5.14: The expression profile of the six genes coding for ADH which were induced by low-oxygen stress. ▼ = 0.5 kPa $O_2$; ● = 21 kPa $O_2$.

Interestingly, a small upregulation of the expression levels of *lactate dehydrogenase (LDH)* was observed during low-oxygen stress in the first 6 h of the experiment (FC = 2.5; Fig. 5.12A) after which it started to decrease again (Fig. 5.15A). In contrast to

*PDC* and *ADH*, a clear differential transcriptional expression of *LDH* was observed between the anoxic and hypoxic conditions applied in the second experiment (Fig. 5.15B). The results of both experiments suggest that the conversion of pyruvate to lactate catalyzed by LDH only played a role in the onset of low-oxygen stress after which the ethanol pathway takes over. This is in accordance with the negligible role of lactate production in the fermentative metabolism observed by Saquet and Streif (2008) and the fast increase in *in vivo* enzyme activity of PDC after a few hours of low-oxygen stress observed in chapter 4 (Fig 4.3). Similar to *ADH*, an increase in *LDH* expression levels after 24 h was observed under normoxia (Fig 5.15A). Zabalza *et al.* (2009) reported that even under normoxic conditions, fermentation played an important role in the control of the levels of pyruvate in the tissue. Possibly, *ADH* and *LDH* are induced to cope with the extra pyruvate in the cell introduced by the feeding experiment, but further research is necessary.

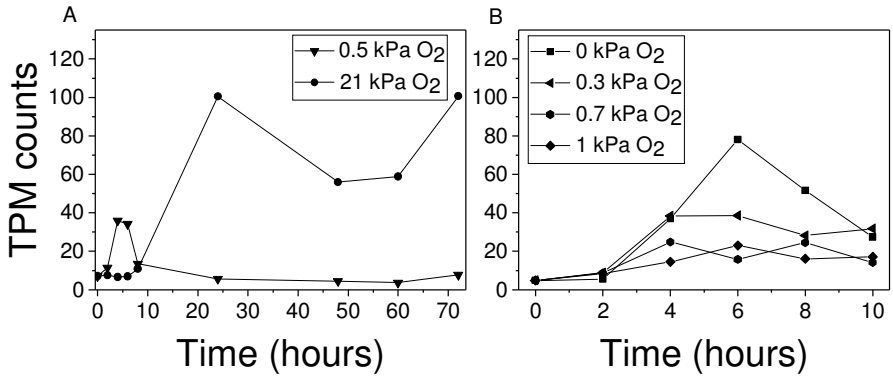


Figure 5.15: The expression profile LDH in the first experiment (A; ▼ = 0.5 kPa $O_2$; ● = 21 kPa $O_2$) and in the second experiment (B; ■ = 0 kPa $O_2$; ◄ = 0.3 kPa $O_2$; ⬢ = 0.7 kPa $0_2$; ◆ = 1 kPa $O_2$).

On one hand the induction of the fermentative metabolism facilitates apple fruit to cope with low-oxygen stress by helping the fruit to maintain a high glycolytic flux and thereby mitigating the damaging effects of an energy crisis; on the other hand it causes acidosis of the cytoplasmic pH and reduction of the carbon reserves as the volatile fermentation metabolites easily diffuse out of the cells (Limami, 2014).

### 5.3.4.6 Changes in amino acids metabolism

As discussed in chapter 2, plants may change their amino acids metabolism during low-oxygen stress, to diminish the negative effects of fermentation. It has been shown that alanine metabolism plays an important role during low-oxygen stress in maintaining the glycolytic flux by converting pyruvate with the help of alanine aminotransferase (AlaAT) to alanine (Fig. 5.12A), providing an alternative, non-detrimental end product (Bailey-Serres *et al.*, 2012; Cukrov *et al.*, 2016; Limami, 2014; Ricoult *et al.*, 2006). In several apple cultivars, alanine concentrations have been found to increase to different levels depending on the low-oxygen concentrations applied (Brizzolara *et al.*, 2017; Cukrov *et al.*, 2016; Hatoum *et al.*, 2014; Vandendriessche *et al.*, 2013). Cukrov *et al.* (2016) reported a low-oxygen threshold for the induction of the expression of the genes coding for *AlaAT* in 'Granny Smith' apples, as the transcript levels were extremely abundant in apples stored under 0.4 kPa $O_2$, whereas the transcript levels of *AlaAT* stayed at basal levels in fruit stored under 0.8 kPa $O_2$. However, in 'Jonagold' apple fruit we observed a clear upregulation of the transcript levels of *AlaAT* for all the low-oxygen conditions applied in both experiments (Fig. 5.16A and B), suggesting the low-oxygen threshold observed in 'Granny Smith' apple fruit is different or not existing in 'Jonagold' apple fruit. Similar to the other hypoxia responsive genes a peak in *AlaAT* transcript levels was observed in the first 6 h (FC = 1,5; Fig. 5.12A and 5.16A) in apple tissue discs exposed to 0.5 kPa $O_2$, which slowly started to decrease towards the end of the experiment. However, in the second experiment the *AlaAT* transcript levels kept on increasing until the end of the experiment (10 h). The reason for this discrepancy between both experiments is not clear. Furthermore, the results of the second experiment suggested a differential transcriptional upregulation of the expression of *AlaAT* for the different oxygen conditions applied (Fig. 5.16B).

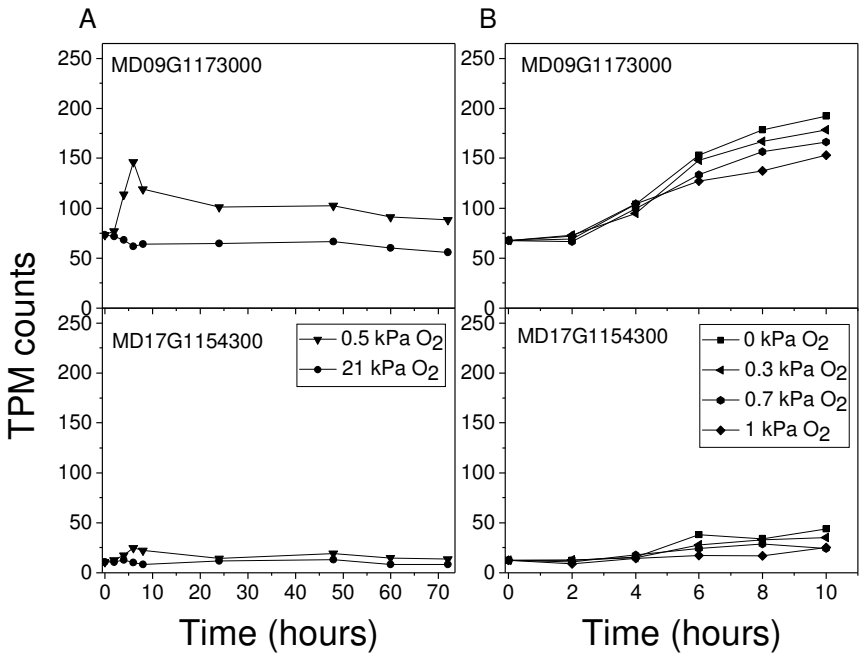


Figure 5.16: The expression profile of all the genes coding for AlaAT in the first experiment (A; ▼ = 0.5 kPa $O_2$; ● = 21 kPa $O_2$) and in the second experiment (B; ■ = 0 kPa $O_2$; ◄ = 0.3 kPa $O_2$; ⬢ = 0.7 kPa $0_2$; ◆ = 1 kPa $O_2$).

The conversion of pyruvate into alanine by AlaAT is accompanied by the generation of 2-oxoglutarate from glutamate (Fig. 5.12A). 2-oxoglutarate can be further metabolized in the TCA cycle via 2-Ketoglutarate dehydrogenase (2KGDH) and succinate CoA ligase (SCS) to form succinate and produce ATP (Bailey-Serres *et al.*, 2012; Limami, 2014; Rocha *et al.*, 2010). Although negative FCs are observed for *2KGDH* and *SCS* in 'Jonagold' apple fruit (Fig.5.12B), that does not necessarily mean that the pathway is not active during low oxygen stress, since the negative FCs were caused by more or less stable transcript levels of *2KGDH* and *SCS* during low oxygen stress, whereas the transcript levels of both enzymes increased during normoxia. Flux analyses are necessary to further investigate whether 2-oxoglutarate is metabolized in the TCA cycle to produce ATP in 'Jonagold' apples exposed to low-oxygen stress. Furthermore, the mitochondrial $NAD^+$ that is required to oxidize 2-oxoglutarate, could be recycled via the reversed TCA cycle (Rocha *et al.*, 2010), which

seemed to be activated in 'Jonagold' apple fruit during low-oxygen stress. The transcript levels of both *malate dehydrogenase* (*MDH*) and *fumarase* (*FUH*) were higher in the low-oxygen condition, leading to increasing FCs. Although for *SDH* was a negative FC observed (Fig. 5.12B). Flux analysis are necessary to confirm the activation of the reversed TCA cycle in 'Jonagold' apple fruit. MDH obtains its substrate, oxaloacetate, for the reversed TCA cycle either via the conversion of phosphoenolpyruvate catalysed by phosphoenolpyruvate carboxylase (PEPC) or via the conversion of aspartate catalysed via aspartate aminotransferase (AspAT), which simultaneously also converts 2-oxoglutarate back into glutamate (Fig. 5.12A and B; Rocha *et al.*, 2010). A slightly positive FC (FC = 0.6) for *PEPC* was observed towards the end of the experiment, which was mainly caused by the upregulation of *MD17G1230800* during low-oxygen stress. Also the transcript levels of the AspAT isozymes in the cytoplasm (*MD08G1117300, MD08G1117500, MD15G1096900*; Fig. 5.17A) and chloroplasts (*MD08G1060300*; Fig. 5.17B) were upregulated, whereas the transcript level of the AspAT isozyme localized in the mitochondria (*MD17G1264900*; Fig. 5.17C) was downregulated during low-oxygen stress (Fig. 5.12A). Similarly as observed in *Arabidopsis* (Mustroph *et al.*, 2014a), the cytoplasmic *AspAT* isozyme is highly expressed, suggesting it to be the most important isozyme of the AspAT isozyme family.

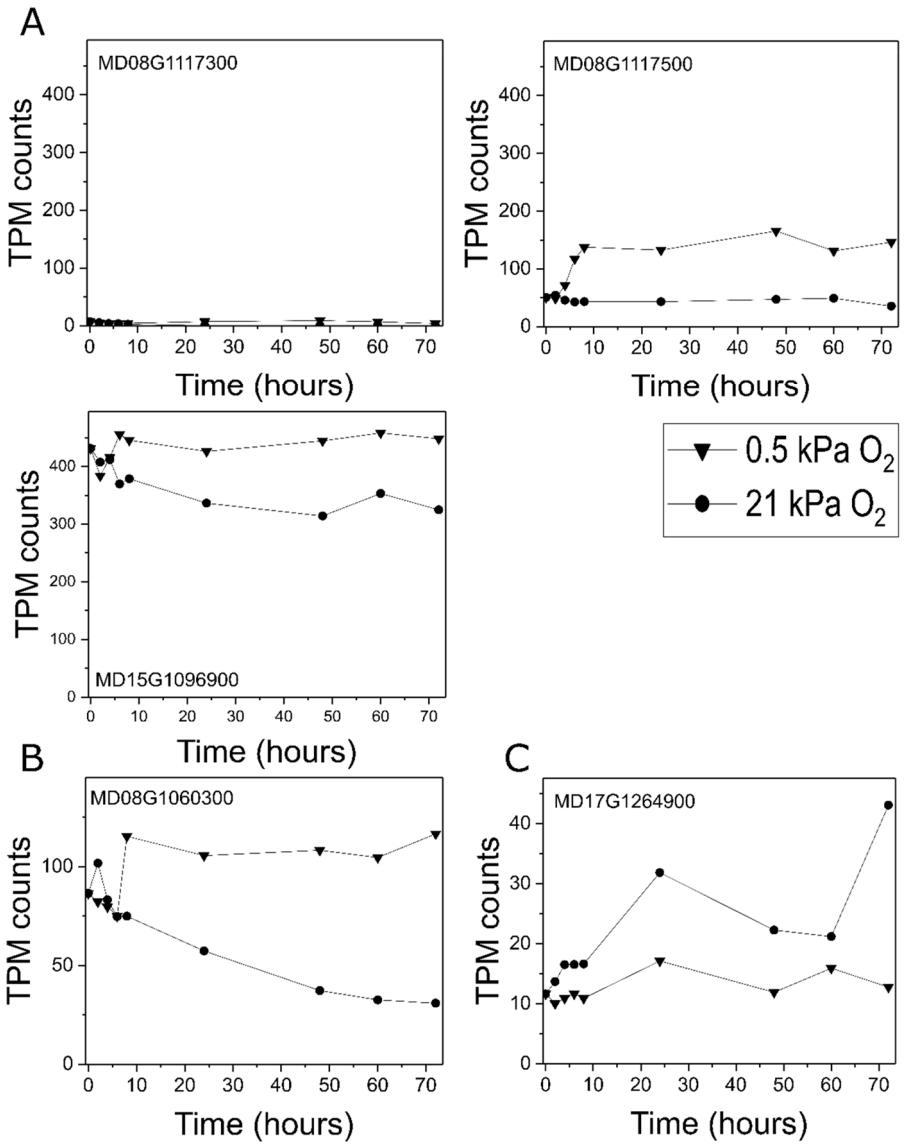


Figure 5.17: The expression profile of the genes coding for the AspAT isozyme in the cytoplasm(A), the AspAT isozyme in the chloroplast (B) and the AspAT isozyme in the mitochondria (C). ▼ = 0.5 kPa $O_2$; ● = 21 kPa $O_2$.

The alanine metabolism not only provides a link between the glycolysis and the TCA cycle via the AlaAT/AspAT cycle during low-oxygen stress. It can also be coupled to the GABA shunt via the AlaAT/NADH-GOGAT cycle (Fig. 5.12A and B; Diab and Limami, 2016; Limami, 2014). The activities of the ATP-consuming enzymes glutamine synthase (GS) and asparagine synthetase (AS) are reported to be inhibited during low-oxygen stress in plants (Limami, 2014). The expression levels of *GS* were downregulated during low oxygen stress in 'Jonagold' apple resulting in negative FC's, whereas more or less stable FC's were observed for *AS*, due to a downregulation of *AS* both at 0.5 kPa $O_2$ and 21 kPa $O_2$ (Fig. 5.12B). Therefore, the regeneration of glutamate as a substrate of AlaAT could occur through the reductive amination of 2-oxoglutarate by the NADH-dependent glutamine oxoglutarate amino transferase (NADH-GOGAT). Not only glutamate is synthesized in this reaction but also NADH is converted to $NAD^+$, enabling the glycolysis to proceed (Limami *et al.*, 2008). However, a strong decrease in *NADH-GOGAT* expression was observed during low oxygen stress in 'Jonagold' apple (FC = -1.6 at 72 h; Fig. 5.12B). Also in *Medicago truncatula* seedlings the expression of *NADH-GOGAT* was reported to be inhibited by hypoxia stress, but nevertheless the activity of NADH-GOGAT was increased (Limami *et al.*, 2008). Flux analyses are necessary to see whether this is also the case for 'Jonagold' apple fruit. Conversely, Limami *et al.* (2008) reported that the expression of *glutamate dehydrogenase* (*GDH*) was upregulated by hypoxic stress, while the *in vitro* enzyme activity of GDH was down-regulated in *Medicago truncatula* seedlings. Feeding experiments confirmed a very low *in vivo* activity of GDH in the seedlings and indicated that GDH was not contributing to glutamate synthesis. Therefore, the authors suggested that the upregulation of the expression of *GDH* was in anticipation of the return to aerobic conditions, where GDH can convert glutamate into 2-oxoglutarate to maintain the TCA cycle and produce NADH (Limami *et al.*, 2008). In 'Jonagold' apple fruit the expression levels of *GDH* ($NAD^+$; Fig. 5.18A) and *GDH* ($NADP^+$; Fig. 5.18B) were upregulated during low oxygen stress, except *MD01G1174400* was downregulated leading to more or less stable FCs for

GDH ($NAD^+$; Fig. 5.12B). To investigate the *in vivo* enzyme activity of GDH in 'Jonagold' apple flux analyses are necessary.

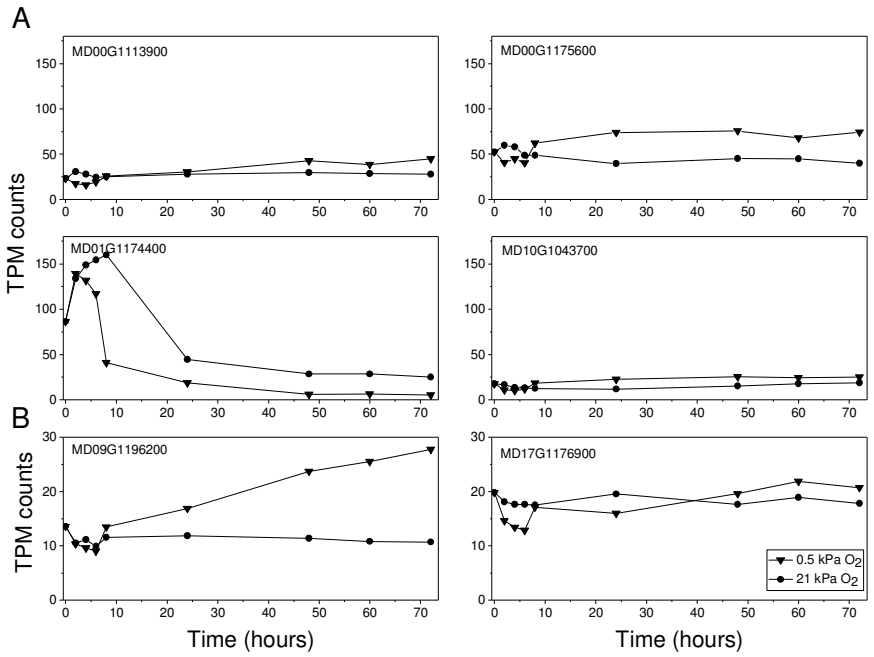


Figure 5.18: The expression profile of the genes coding for GDH ($NAD^+$) (A) and GDH ($NADP^+$) (B). ▼ = 0.5 kPa $O_2$; ● = 21 kPa $O_2$.

During low-oxygen stress, glutamate could be decarboxylated into GABA by glutamate decarboxylase (GAD), consuming a proton and thereby increasing the pH (Greenway and Gibbs, 2003). The GABA content was found to increase under low-oxygen stress in 'Granny Smith' and 'Red Delicious' apples (Brizzolara *et al.*, 2017; Cukrov *et al.*, 2016). Also a strong increase of the FC of *GAD* (FC=2.7 at 72 h; Fig. 5.12B) was observed in 'Jonagold' apple. Interestingly, when the expression profile of the different genes coding for GAD were studied in more detail, a fast upregulation of *MD09G1276300* and *MD09G127700* was observed in the first 6 h. The expression levels of both genes started to decrease again after 6 h, but the expression level of *MD06G1235500* started to increase simultaneously (Fig. 5.19). This suggested that *MD09G1276300* and *MD09G127700* mainly play a role at the onset of low-oxygen

stress, whereas *MD06G1235500* becomes more important during prolonged low-oxygen stress.

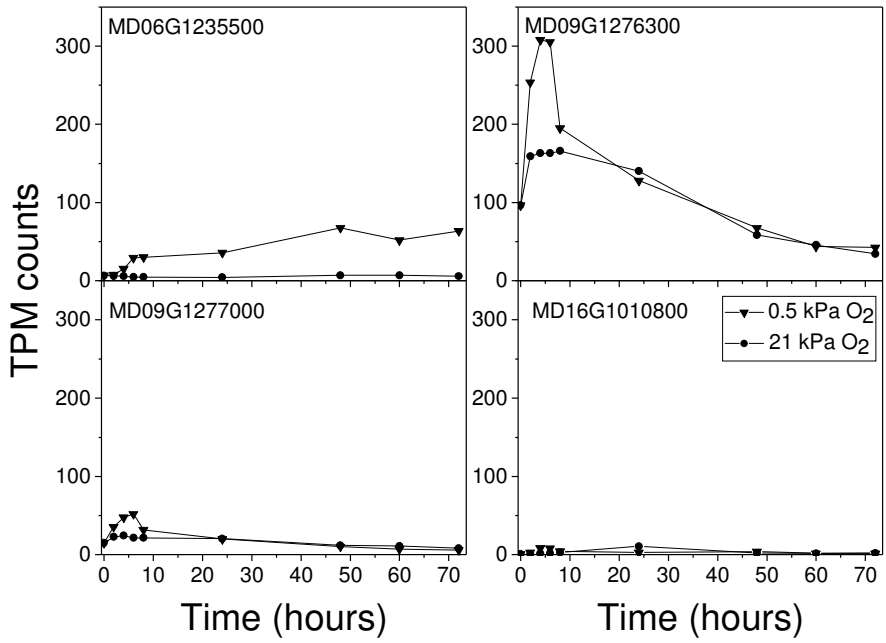


Figure 5.19: The expression profile of all the genes coding for GAD. ▼ = 0.5 kPa $O_2$; ● = 21 kPa $O_2$.

GABA could be further converted to succinic semialdehyde via GABA transaminase (GABA-T), using either pyruvate or 2-oxoglutarate as an amino acceptor. During low-oxygen stress, plant GABA-T seemed to preferentially use pyruvate, providing an alternative way to produce alanine (Fig. 5.12B; Diab and Limami, 2016; Limami *et al.*, 2008). The two genes (*MD09G1139200* and *MD17G1128700*) coding for GABA-T showed a similar increasing trend after 6 h of low-oxygen stress resulting in a FC=2 at 72 h (Fig. 5.12B and Fig. 5.20A). Finally, succinic semialdehyde could be converted to succinate via the enzyme succinate-semialdehyde dehydrogenase (SSADH). The two genes (*MD05G1238300* and *MD10G1216600*) coding for SSADH had a very similar trend as the genes coding for GABA-T in 'Jonagold' apple (Fig. 5.20B).

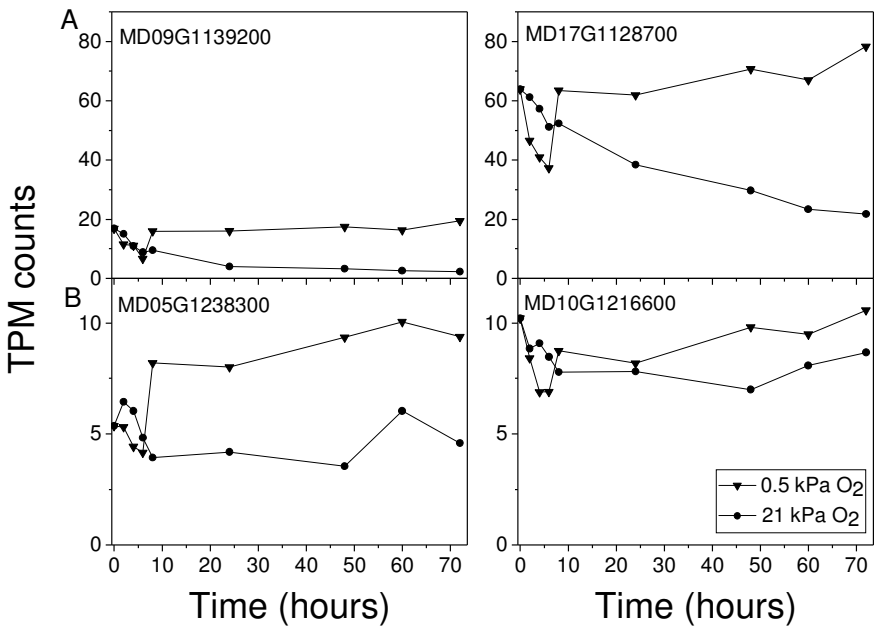


Figure 5.20: The expression profile of all the genes coding for GABA-T (A) and SSADH (B). ▼ = 0.5 kPa $O_2$; ● = 21 kPa $O_2$.

Hence, similarly as described in literature (Bailey-Serres *et al.*, 2012; Limami, 2014; Ricoult *et al.*, 2006; Rocha *et al.*, 2010), all these results suggest that the alanine metabolism and the GABA shunt are activated during low-oxygen stress in 'Jonagold' apple, thereby diminishing an energy crisis by producing an extra ATP molecule, saving carbon atoms which otherwise would be lost via ethanol and limiting cytoplasmic acidification by competing with lactate fermentation for the use of pyruvate and using protons in the GABA shunt.

### 5.3.4.7 Oxygen sensing mechanism

In plants the metabolic changes of the energy metabolism are regulated via an efficient and tunable sensing mechanism depending on the oxygen availability in the tissue (Kosmacz and Weits, 2014; Van Dongen *et al.*, 2017; Van Dongen and Licausi, 2015). It was found that the activity of the transcription factors from group-VII ethylene response factors (ERFs) in *Arabidospis*; e.g. *RAP2.2, RAP2.12, RAP2.3, HRE1*

and *HRE2* is directly affected by low oxygen levels in the cell. These transcription factors, also called 'oxygen sensors', are degraded under normoxic conditions and stabilized under low-oxygen stress via the N-end rule pathway (Bailey-Serres *et al.*, 2012; Kosmacz and Weits, 2014; Licausi *et al.*, 2011b; Van Dongen *et al.*, 2017; Van Dongen and Licausi, 2015). The group VII ERFs transcription factors specifically trigger the expression of certain hypoxia-responsive genes. Unlike in *Arabidopsis*, where the group VII ERFs consists of five TFs, Girardi *et al.* (2013) reported that the apple genome contains eight genes coding for ERF VII TFs. However, after blasting the eight ERF VII TFs to the newly sequenced genome (Daccord *et al.*, 2017) only six unique genes (*MD17G1152400, MD09G1174400, MD13G1163300, MD16G1162800, MD16G1162900, MD11G1306500*) could be retained. All six genes were found to be expressed in 'Jonagold' apple fruit (Fig. 5.21). No clear differences in expression pattern of the six genes was observed between the different low-oxygen concentrations in the second experiment. Only the transcription levels of *MD11G1306500* showed a clear induction for all the low-oxygen concentrations during the experimental period, whereas the expression levels of the other five genes stayed more or less stable (data not shown).This indicated that the regulation of the central carbon metabolism by the oxygen sensors was already activated from 1 kPa $O_2$.

In *Arabidopsis* it was found that *RAP2.12*, *RAP2.2* and *RAP2.3* were all constitutively expressed, whereas *HRE1* and *HRE2* are induced by hypoxia. This suggest that the individual ERF VII TFs differentially contribute to the response to low-oxygen stress (Gibbs *et al.*, 2015). The transcription of *HRE1* and *HRE2* is reported to be highly up-regulated under low oxygen conditions in *Arabidopsis*. Cukrov *et al.* (2016) described two orthologues of *Arabidopsis HRE* in apple fruit (*MDP0000288465* and *MDP0000848905*). However, after blasting the two apple orthologues against the newly sequenced genome of apple (Daccord *et al.*, 2017), they both showed a 100 % homology with only one gene (*MD11G1306500*). Similar to 'Granny Smith' apple (Cukrov *et al.*, 2016), a fast upregulation under low-oxygen stress was observed of

this one gene in 'Jonagold' apple (Fig. 5.21). Furthermore, the putative apple orthologues of *Arabidopsis* RAP2.12 and RAP2.2 (MD09G1174400 and MD17G1152400) are highly expressed both at 0.5 kPa $O_2$ and 21 kPa $O_2$ (Fig. 5.21), similarly as observed in *Arabidopsis* (Licausi *et al.*, 2011a). Cukrov *et al.* (2016) observed that the apple ERF-VII MdRAP2.12 protein accumulated to different levels depending on the oxygen concentration applied to the tissue. Whether this is also the case in 'Jonagold' apple fruit remains to be shown. The genes MD13G1163300, MD16G1162800 and MD16G1162900 have a very similar sequence and expression profile, suggesting they might be paralogues (Fig. 5.21). The different expression patterns of the group VII TFs suggest that the apple orthologue of *HRE* (*MD11G1306500*) regulates the initial fast response to hypoxia, after which the other members of the group VII TFs take over the regulation to maintain the expression of the hypoxia responsive genes to ameliorate tissue survival under low-oxygen stress.

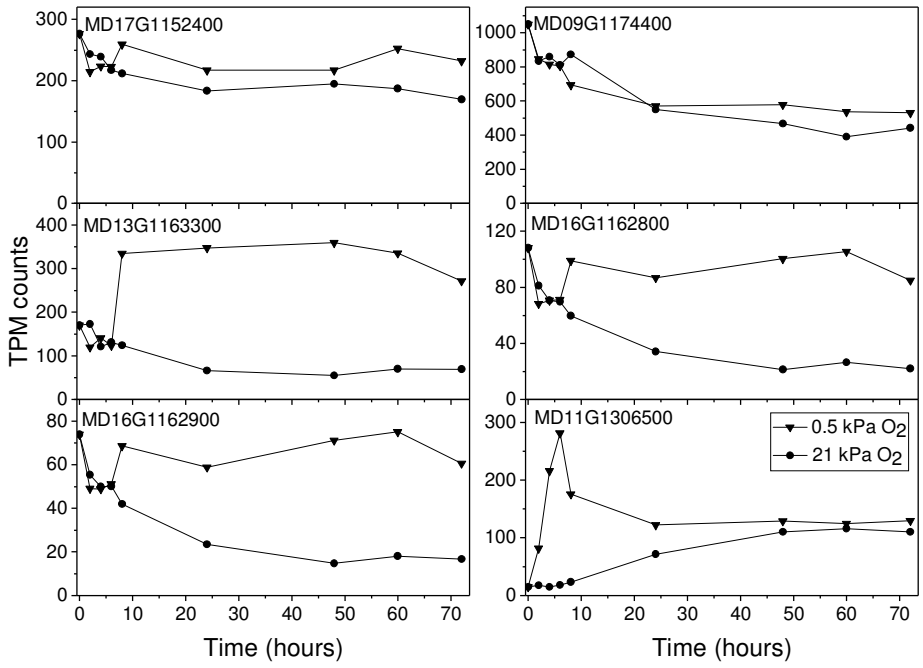


Figure 5.21: The expression profile of the six group VII ERF transcription factors found in apple. ▼ = 0.5 kPa $O_2$; ● = 21 kPa $O_2$.

The expression patterns of the group VII TFs (Fig. 5.21) showed high similarities to the expression patterns of most of the above discussed hypoxia responsive genes. To get an indication on which TF might be involved in the regulation of certain hypoxia responsive genes, the correlation between the expression difference between 0.5 kPa $O_2$ and 21 kPa $O_2$ for every group VII TFs and the expression difference between 0.5 kPa $O_2$ and 21 kPa $O_2$ for every hypoxia responsive gene was calculated. The difference in expression between the low-oxygen condition and the control was taken, as we were interested in the expression pattern specifically induced by the group VII TFs independently of possible expression effects induced by other TFs. The correlation matrix is represented in Table 5.1, where the correlations ≥ 0.7 are marked in grey and the correlations ≥ 0.9 marked in bold.

Table 5.1: Correlation matrix between the group VII TFs and the hypoxia responsive genes.

| Gene name | Gene ID | MD17G1152400 | MD09G1174400 | MD13G1163300 | MD16G1162800 | MD16G1162900 | MD11G1306500 |
|---|---|---|---|---|---|---|---|
| SUS | MD02G1100500 | -0.39 | -0.66 | -0.55 | -0.60 | -0.61 | **0.97** |
| | MD02G1100600 | -0.44 | -0.69 | -0.63 | -0.68 | -0.69 | **0.95** |
| | MD11G1307000 | 0.73 | 0.27 | 0.80 | 0.83 | 0.82 | -0.08 |
| PFK | MD17G1180600 | 0.67 | 0.61 | 0.66 | 0.80 | 0.81 | -0.42 |
| | MD08G1109700 | -0.59 | -0.55 | -0.66 | -0.70 | -0.70 | **0.92** |
| | MD15G1089400 | -0.17 | -0.74 | -0.34 | -0.41 | -0.43 | **0.91** |
| PFP | MD06G1002300 | 0.74 | 0.39 | 0.87 | 0.89 | 0.88 | -0.18 |
| NP-GAPD | MD15G1154800 | 0.86 | 0.47 | **0.90** | **0.92** | **0.91** | -0.68 |
| | MD02G1009300 | 0.87 | 0.48 | **0.96** | **0.98** | **0.97** | -0.57 |
| AlaAT | MD09G1173000 | 0.20 | -0.29 | 0.11 | 0.07 | 0.05 | 0.79 |
| AspAT | MD08G1117300 | 0.63 | 0.59 | **0.93** | **0.92** | **0.92** | -0.54 |
| | MD08G1117500 | 0.79 | 0.24 | 0.84 | 0.84 | 0.83 | -0.07 |
| | MD15G1096900 | 0.80 | 0.46 | 0.82 | 0.87 | 0.86 | -0.18 |
| | MD08G1060300 | **0.90** | 0.50 | **0.91** | **0.97** | **0.97** | -0.50 |
| GDH | MD00G1175600 | 0.84 | 0.43 | **0.94** | **0.93** | **0.91** | -0.56 |
| | MD09G1196200 | 0.79 | 0.72 | 0.75 | 0.89 | **0.90** | -0.62 |
| | MD10G1043700 | 0.79 | 0.32 | **0.97** | **0.91** | **0.90** | -0.46 |
| | MD17G1176900 | 0.71 | 0.51 | 0.61 | 0.75 | 0.76 | -0.71 |
| GAD | MD06G1235500 | 0.76 | 0.56 | 0.82 | **0.91** | **0.91** | -0.32 |
| | MD09G1276300 | -0.67 | -0.35 | -0.73 | -0.71 | -0.71 | 0.84 |
| | MD09G1277000 | -0.59 | -0.53 | -0.68 | -0.71 | -0.72 | **0.95** |
| GABA-T | MD09G1139200 | 0.85 | 0.52 | **0.92** | **0.96** | **0.96** | -0.57 |
| | MD17G1128700 | 0.85 | 0.60 | 0.85 | **0.94** | **0.94** | -0.66 |
| SSADH | MD10G1216600 | 0.69 | 0.46 | 0.79 | 0.85 | 0.86 | -0.73 |
| | MD05G1238300 | 0.84 | 0.32 | **0.95** | **0.94** | **0.94** | -0.52 |
| ADH | MD05G1013200 | 0.65 | 0.38 | 0.82 | 0.83 | 0.81 | -0.45 |
| | MD05G1013400 | 0.49 | 0.28 | 0.65 | 0.70 | 0.70 | -0.49 |
| | MD10G1014500 | 0.70 | 0.61 | 0.75 | 0.87 | 0.87 | -0.45 |
| | MD09G1211500 | 0.69 | 0.59 | 0.75 | 0.86 | 0.87 | -0.43 |
| | MD10G1013900 | 0.15 | -0.45 | 0.18 | 0.11 | 0.09 | 0.69 |
| | MD10G1014200 | 0.09 | -0.47 | 0.13 | 0.05 | 0.03 | 0.72 |
| PDC | MD04G1159900 | 0.88 | 0.32 | **0.96** | **0.96** | **0.95** | -0.33 |
| | MD04G1160100 | 0.68 | 0.22 | 0.85 | 0.79 | 0.77 | -0.02 |
| | MD10G1283500 | 0.08 | -0.49 | 0.04 | -0.02 | -0.04 | 0.82 |

The correlations in Table 5.1 suggested that some of the enzymes, i.e., SUS, PFK, AlaAT, GAD, ADH and PDC, have one or more genes which are regulated by *MD11G1306500* and are responsible for the fast initial metabolic changes during low-oxygen stress. Furthermore, most enzymes also have corresponding genes showing a high correlation with *MD13G1163300, MD16G1162800* and *MD16G1162900*, and some of them as well with *MD17G1152400,* which helped the tissue to survive longer periods of low-oxygen stress. Interestingly, the apple orthologue for RAP2.12 (*MD09G1174400*) was not highly correlated to any of the hypoxia induced genes, which makes sense as RAP2.12 is known to be constitutively expressed both under normoxic and hypoxic conditions (Van Dongen *et al.*, 2017). During normoxia, RAP2.12 is bound to the plasma membrane by interacting with peripheral membrane proteins acyl-coenzyme A-binding protein 1 (ACBP1) and ACBP2. When low-oxygen stress is introduced, RAP2.12 can detach from the membrane and translocate to the nucleus, where it induces the expression of hypoxia responsive genes (Kosmacz and Weits, 2014; Van Dongen and Licausi, 2015).

Similarly as in Granny Smith apple fruit (Cukrov *et al.*, 2016), the oxygen sensing group VII ERF TFs seemed to be present in 'Jonagold' apple fruit. However, further research is necessary to elucidate their precise mode of action. The correlations between the TFs and the hypoxia responsive genes gave us an indication about how the hypoxia responsive genes are regulated during low-oxygen stress, but further functional genomic and reverse genetic studies, as well as proteomic studies, are necessary to prove these hypotheses.

## 5.4. Conclusion

The detailed pathway analysis of the most important pathways of the central carbon metabolism during low-oxygen stress revealed that many of the findings in model organisms, such as *Arabidopsis* and rice, are also true for 'Jonagold' apple fruit. The PPi-dependent pathways seemed to be favoured during low-oxygen stress. Different from other plant organisms and from 'Granny Smith' apple fruit, both PFK and PFP seemed to be important in the first response to low-oxygen stress whereas after prolonged low-oxygen stress PFP became the most important enzyme. Furthermore, the gene expression data revealed that NP-GAPDH appeared to play a role in maintaining the high glycolytic flux in 'Jonagold' apple fruit during low oxygen stress, which was not reported before. Similarly as described for 'Granny Smith' apple fruit, low-oxygen stress activated the fermentation pathways as well as the alanine metabolism and the GABA shunt in 'Jonagold' apple fruit. In this study we were able to discriminate between genes that responded fast to the occurrence of low-oxygen stress, whereas others were slow responders suggesting their importance during prolonged low-oxygen stress. The observed changes were not always similar to the ones observed in 'Granny Smith' apples. This strengthens the suggestion of Brizzolara *et al.* (2017) that apple varieties do react differently to low-oxygen stress.

In this study, further evidence was provided supporting the presence of oxygen-sensing mechanisms in apple fruit. A comparison of the expression patterns of some of the known oxygen sensors with the expression patterns of the different hypoxia responsive genes suggested a strong regulation of the metabolic processes by the oxygen sensors. These results provide a first indication that besides the substrate inhibition of the electron transport chain by limiting oxygen levels, an active regulatory mechanism of the central carbon metabolism is present in 'Jonagold' apple fruit.

# Chapter 6

# General conclusions and future perspectives

## 6.1 General conclusions

The recent development of the DCA storage technology makes it possible to delay ripening of apple fruit more effectively, to improve its post storage quality and to better control certain storage disorders, as compared to CA or ULO storage. But storing fruit at lower oxygen concentrations is not without risks and can also have negative effects on fruit quality. As today little information is available on the precise effect of low-oxygen concentrations on the metabolic processes and compositional changes of apple fruit, solid science-based progress is slow. Therefore, this dissertation focuses on investigating low-oxygen stress in 'Jonagold' apple to unravel *the regulation of the respiratory metabolism of apple during (dynamic) controlled atmosphere storage*. Since it has been shown that oxygen gradients are present in apple fruit (Ho *et al.*, 2011), the experiments in these dissertation were all conducted

on thin apple slices of the cortex tissue of the fruit. In this way, oxygen gradients within the tissue were largely ruled out and the influence of a given oxygen concentration on the central carbon metabolism could be studied directly.

One of the known negative effects of storing fruit under low-oxygen concentrations is the induction of fermentation, which causes off-flavours in the fruit. Therefore, the first focus of this study was to characterize the conditions which activate the fermentative metabolism in 'Jonagold' apple fruit and to understand its regulation under the different experimental conditions applied (Chapter 4). In order to do so, enzyme assays to measure the activity of the two main enzymes of the ethanol pathway *in vitro*, i.e., pyruvate decarboxylase and alcohol dehydrogenase, were optimized to increase the signal to noise ratio. An elaborated kinetic model-based method was developed to accurately estimate the *in vitro* specific enzyme activity of PDC and ADH from the spectrophotometric assay data. In contrast to the classic linear regression approach, the models were able to estimate the enzyme activity whether or not the assay response achieved linearity since they take into account the complete progress curve. The advantage of using a kinetic modelling approach is that the maximum activity of the enzyme could be estimated through extrapolation, even if the saturating substrate conditions were not fully realized (Chapter 3).

In the next chapter (Chapter 4) the *in vitro* measured enzyme activity of PDC and ADH was translated into *in vivo* activities by using a combination of experimental techniques and a kinetic modelling approach. By doing so, new insights were provided in the *in vivo* regulation of the fermentative metabolism. The relative rate constants of PDC and ADH ($k_{PDC}$ and $k_{ADH}$) were not subjected to a direct temperature effect, but the change of the overall metabolic rate, induced by different temperatures, appeared to have a large influence on the induction and regulation of the fermentative metabolism. At a low overall metabolic reaction rate, fermentation was only slightly induced and largely metabolically controlled, while at a faster overall metabolic rate the induction of fermentation was more severe and the

ethanol pathway was regulated by a combination of molecular and metabolic control systems. Furthermore, at a high metabolic rate, the model indicated that under anoxic conditions at harvest the regulation was located at the fast induction of PDC activity, while after six months of storage an extra regulation on ADH activity seemed to be present. However, this extra regulation was not observed when hypoxic conditions were applied after six months of storage. Even though fermentation was clearly induced under all experimental conditions applied, the flux through the fermentative metabolism started to decrease again after prolonged low-oxygen stress, due to decreasing levels of pyruvate.

Although the induction of fermentation helps apple fruit to tolerate low-oxygen stress by mitigating the damaging effects of an energy crisis, it causes acidosis of the cytosolic pH and reduction of the carbon reserves (Limami, 2014). As it has been shown that plants can reduce these negative effects of fermentation by shuttling pyruvate into alternative pathways, a detailed pathway analysis of the central carbon metabolism was performed, to study its transcriptional regulation in more detail (Chapter 5). This revealed that many of the findings in model organisms, such as *Arabidopsis* and rice, are confirmed for 'Jonagold' apple fruit. Based on RNA sequencing data, the glycolytic flux seemed to be upregulated and the energy saving enzymes of the PPi-dependent pathways seemed to be favoured during low-oxygen stress. However, different from other plant organisms, including Granny Smith apple fruit, both PFK and PFP seemed to be important in the first response to low-oxygen stress whereas after prolonged low-oxygen stress PFP became the most important enzyme in 'Jonagold' apple fruit. As described for Granny Smith apple fruit, low-oxygen stress not only induced the expression of the genes of the fermentation pathways, but also of the genes involved in the alanine metabolism and the GABA shunt. The activation of the genes of these two pathways was speculated to explain the decreasing flux through the fermentative metabolism after prolonged low-oxygen stress. Furthermore, the activation of these two pathways will help the fruit to survive low oxygen stress as it saves on energy and carbon atoms and limits

cytosolic acidification. In addition, the observation of Brizzolara *et al.* (2017) that apple varieties reacted differently to low-oxygen stress was confirmed in this dissertation as the observed changes of the transcript levels of the hypoxia responsive genes were not always similar to the ones observed by Cukrov *et al.* (2016) in Granny Smith apple fruit.

In Chapter 5, the presence of an oxygen sensing-mechanism was confirmed in 'Jonagold' apple fruit. By comparing the expression patterns of the oxygen sensors with the expression patterns of the different hypoxia responsive genes, a strong regulation of the metabolic processes by the oxygen sensors was suggested. One of the oxygen sensors could be linked to genes activated as a fast response to low-oxygen stress, whereas the other oxygen sensors were kept responsible for activating slow responders, suggesting their role in prolonged low-oxygen stress. These findings support the hypothesis that besides direct substrate inhibition of the electron transport chain by limiting oxygen levels, an active regulatory mechanism of the central carbon metabolism is present in apple fruit as controlled by oxygen sensors.

## 6.2 Future perspectives

The results in this dissertation, obtained by dedicated experimental designs and state-of-the-art modelling and transcriptomic approaches, contribute to insights in the metabolic changes of the central carbon metabolism and its regulation introduced by low-oxygen stress in 'Jonagold' apple fruit. Nevertheless, several suggestions for future research can be made.

First of all, further research is necessary to test the regulatory mechanisms of the fermentative metabolism indicated by the model in chapter 4. Several variables

should be measured experimentally: the concentration of pyruvate to confirm the simulated concentration by the model, the concentrations of the cofactors involved, the cytosolic pH to confirm that the drop in cytosolic pH is responsible for the activation of PDC, the different isozymes of ADH, the enzyme activity of AAT, the diffusion rates of the volatiles, the involvement of a mitochondrial pyruvate carrier, etc. Furthermore, extra experiments could be conducted to understand the regulation of the ethanol pathway even better. The influence of hypoxic conditions at harvest at 18 °C, the influence of storage at 1 °C and the influence of anoxic conditions at 1 °C should be studied.

As the metabolic flux distribution in the central metabolism may be the most important information in order to fully understand the complex molecular and metabolic response induced by low-oxygen stress, the feeding experiments with [$^{13}$C]-pyruvate should be repeated. [$^{13}$C]-Pyruvate labelling can be used to study the flux through the TCA cycle, fermentation (lactate pathway), alanine metabolism and the GABA shunt. Moreover, other labelled substrates can be used to improve our insight in the metabolic changes imposed by low-oxygen stress. For example, the conversion of glutamate to succinate could be studied by using [$^{13}$C]-glutamate and [$^{15}$N]-ammonium. Optimal experimental design techniques could contribute to find optimal substrate mixtures (Bouvin *et al.*, 2015).

Furthermore, in order to improve DCA storage of apple fruit, it is important to characterize the influence of different low-oxygen conditions on the flux through the central metabolism as well as on the gene expression of the hypoxia responsive genes. In this way, it may be better predicted how severe the impact of the low-oxygen stress will be on fruit physiology and, later on, on the resulting fruit quality. Besides testing the different low-oxygen conditions, it will also be necessary to study the effects of dynamically changing oxygen concentrations in order to better understand how fast the central metabolism can adapt to the oxygen changes applied and if it is able to fully recover after being exposed to low-oxygen stress. As

it has been shown that different cultivars have a different response to low-oxygen stress, it would be of interest to characterize the response of low-oxygen stress in multiple cultivars.

Although first evidence was provided in this dissertation of the presence of an active regulation of the central carbon metabolism by oxygen sensors during low-oxygen stress in 'Jonagold' apple fruit, further research is necessary to resolve the following questions. Are only the group VII ERFs important to regulate the response to low-oxygen stress in apple, as is the case in *Arabidopsis*, or are there other transcription factors important as well? What is the precise role of the different oxygen sensors and how are they regulated? Does the N-end rule pathway play a role in the regulation of the oxygen sensors in apple fruit? What is the role of NO in the regulation of the oxygen sensors in apple fruit? Do the oxygen sensors play an important role in regulating the adaptation to the different dynamically changing oxygen concentrations? Do they react differently when the tissue is already exposed to low-oxygen stress? Do all the different cultivars have the same oxygen sensors and are they responsible for the different metabolic responses observed in the different cultivars?

The oxygen sensors have a direct effect on the metabolic changes of the central carbon metabolism depending on the oxygen concentrations applied. However, when respiration is affect by low-oxygen stress, it has an impact on many parameters and processes, including reactive oxygen and nitrogen species homeostasis, redox status of NAD(P)H and antioxidant pools, ATP/ADP ratio, the proton-motive force, calcium and metabolites levels, which could all trigger the mitochondrial retrograde responses (Van Dongen *et al.*, 2017; Wagner *et al.*, 2018). As all these signals could contribute to transcriptional reprogramming of the nuclei of hypoxic cells, it is important to study their specific role in apple fruit during low-oxygen stress.

As discussed in this dissertation, when apple fruit experience low-oxygen stress, a hypoxic response will be induced leading to molecular and metabolic changes. Due to the complexity of the hypoxic response, it is controlled by a number of factors at different organizational levels, such as transcription, translation, enzyme deactivation/activation, eventually altering metabolite levels. To fully explore the hypoxic *response* in apple fruit, the effect of low-oxygen stress has to be studied at all the different organizational levels and the connectivity between genes, enzyme activities and metabolites needs to be taken into account. Therefore, a systems biology model should be developed, implementing the huge amount of data of all the organizational levels. The model will help us to understand how the different organizational levels are connected with each other and to test new hypothesis. Furthermore, the system biology model could be implemented in the three-dimensional multiscale model for gas exchange in fruit developed by Ho *et al.* (2011). By taking into account the gas gradients in the fruit, the exact metabolism at every place in the fruit can be predicted. The combination of both models can be used to perform *in silico* analysis to study how far one can go in the implementation of DCA without leading to quality loss.

# Bibliography

Adams, P.B., Rowan, K.S., 1970. Glycolytic control of respiration during aging of carrot root tissue. Plant Physiol. 45, 490–494.

Alexander, L., Grierson, D., 2002. Ethylene biosynthesis and action in tomato: a model for climacteric fruit ripening. J. Exp. Bot. 53, 2039–55.

Alonso, A., Marsal, S., Julià, A., 2015. Analytical methods in untargeted metabolomics: state of the art in 2015. Front. Bioeng. Biotechnol. 3, 1-20.

Andrews, D. 1, Cobb, B.C., Johnson, J.R., Drew, M.C., 1993. Hypoxic and Anoxic lnduction of Alcohol Dehydrogenase in Roots and Shoots of Seedlings of Zea mayd Adh Transcripts and Enzyme Activity. Plant Physiol 101, 407–414.

Andrews, D.L., Drew, M.C., Johnson, J.R., Cobb, B.G., 1994. The Response of Maize Seedlings of Different Ages to Hypoxic and Anoxic Stress (Changes in Induction of Adh1 mRNA, ADH Activity, and Survival of Anoxia). Plant Physiol. 105, 53–60.

Andrews, D.L., MacAlpine, D.M., Johnson, J.R., Kelley, P.M., Cobb, B.G., Drew, M.C., 1994. Differential induction of mRNAs for the glycolytic and ethanolic fermentative pathways by hypoxia and anoxia in maize seedlings. Plant Physiol. 106, 1575–82.

António, C., Päpke, C., Rocha, M., Diab, H., Limami, A.M., Obata, T., Fernie, A.R., van Dongen, J.T., 2016. Regulation of Primary Metabolism in Response to Low Oxygen Availability as Revealed by Carbon and Nitrogen Isotope Redistribution. Plant Physiol. 170, 43–56.

Araujo, wagner L., Nunes-Nesi, A., Nikoloski, Z., Sweetlove, L.J., Ferni, A.R., 2012. Metabolic control and regulation of the tricarboxylic acid cycle in photosynthetic and heterotrophic plant tissues. Plant. Cell Environ. 35, 1–21.

Araújo, W.L., Nunes-Nesi, A., Trenkamp, S., Bunik, V.I., Fernie, A.R., 2008. Inhibition of 2-oxoglutarate dehydrogenase in potato tuber suggests the enzyme is

limiting for respiration and confirms its importance in nitrogen assimilation,. Plant Physiol. 148, 1782–1796.

Armstrong, W., Strange, M.E., Cringle, S., Beckett, P.M., 1994. Microelectrode and Modelling Study of Oxygen Distribution in Roots. Ann. Bot. 74, 287–299.

Atkin O.K., Bruhn D., Tjoelker M.G. (2005) Response of Plant Respiration to Changes in Temperature: Mechanisms and Consequences of Variations in Q10 Values and Acclimation. In: Lambers H., Ribas-Carbo M. (eds) Plant Respiration. Advances in Photosynthesis and Respiration, vol 18. Springer, Dordrecht

Baggerman, G., Vierstraete, E., De Loof, A., Schoofs, L., 2005. Gel-Based Versus Gel-Free Proteomics: A Review. Comb. Chem. High Throughput Screen. 8, 669–677.

Bailey-Serres, J., Fukao, T., Gibbs, D.J., Holdsworth, M.J., Lee, S.C., Licausi, F., Perata, P., Voesenek, L.A.C.J., van Dongen, J.T., 2012. Making sense of low oxygen sensing. Trends Plant Sci. 17, 129–138.

Baxter-Burrell, A., Yang, Z., Springer, P.S., Bailey-Serres, J., 2002. RopGAP4-Dependent Rop GTPase Rheostat Control of Arabidopsis Oxygen Deprivation Tolerance. Science. 296, 2026–2028.

Beaudry, R.M., Severson, R.F., Black, C.C., Kays, S.J., 1989. Banana ripening: implications of changes in glycolytic intermediate concentrations, glycolytic and gluconeogenic carbon flux, and fructose 2,6-bisphosphate concentration. Plant Physiol. 91, 1436–1444.

Bekele, E.A., 2015. Postharvest Metabolomics of Apples Stored Under Controlled Atmosphere (Unpublished doctoral dissertation). KU Leuven, Bio science engineering, MeBioS, Leuven, Belgium.

Bekele, E.A., Annaratone, C.E.P., Hertog, M.L.A.T.M., Nicolai, B.M., Geeraerd, A.H., 2014. Multi-response optimization of the extraction and derivatization protocol of selected polar metabolites from apple fruit tissue for GC–MS analysis. Anal. Chim. Acta 824, 42–56.

Bender, T., Pena, G., Martinou, J.-C., 2015. Regulation of mitochondrial pyruvate uptake by alternative pyruvate carrier complexes. EMBO J. 34, 911–24.

Bertani, A., Brambilla, I., Menegus, F., 1980. Effect of Anaerobiosis on Rice Seedlings: Growth, Metabolic Rate, and Fate of Fermentation Products. J. Exp. Bot. 31, 325–331.

Beshir, W.F., Mbong, V.B.M., Hertog, M.L.A.T.M., Geeraerd, A.H., Van den Ende, W., Nicolaï, B.M., 2017. Dynamic Labeling Reveals Temporal Changes in Carbon Re-Allocation within the Central Metabolism of Developing Apple Fruit. Front. Plant Sci. 8, 1-16.

Bessemans, N., Nicolai, B., Verboven, P., Verlinden, B., 2017. Automatical in situ control of the confined environment of metabolically active produce. European patent. Publication number: EP2017/062040.

Bessemans, N., Verboven, P., Verlinden, B.E., Nicolaï, B.M., 2016. A novel type of dynamic controlled atmosphere storage based on the respiratory quotient (RQ-DCA). Postharvest Biol. Technol. 115, 91–102.

Bevc, S., Konc, J., Stojan, J., Hodošček, M., Penca, M., Praprotnik, M., Janežič, D., 2011. ENZO: A Web Tool for Derivation and Evaluation of Kinetic Models of Enzyme Catalyzed Reactions. PLoS One 6, e22265.

Biale, J.B., 1946. Effect of Oxygen Concentration on Respiration of the Fuerte Avocado Fruit. Am. J. Bot. 33, 363-373.

Bisswanger, H., 2011. Practical Enzymology, Second Edition - Bisswanger - Wiley Online Library [WWW Document]. URL http://onlinelibrary.wiley.com/book/10.1002/9783527659227 (accessed 12.16.15).

Bisswanger, H., 2014. Enzyme assays. Perspect. Sci. 1, 41–55.

Blackman, F., Parija, P., 1928. Analytic Studies in Plant Respiration. I .— The Respiration of a Population of Senescent Ripening Apples. Proc. R. soc. London Ser. 103, 412–445.

Blackwell, P.S., 1983. Measurements of aeration in waterlogged soils: some improvements of techniques and their application to experiments using lysimeters. J. Soil Sci. 34, 271–285.

Blokhina, O.B., Törönen, P., Fagerstedt, K. V., 2014. Oxidative Stress Components Explored in Anoxic and Hypoxic Global Gene Expression Data. In: van Dongen, J.t. and Licausi, F. (Eds.), Low-oxygen stress in plants (pp. 19–39), Switzerland: Springer Nature.

Boekema, E.J., Braun, H.-P., 2007. Supramolecular structure of the mitochondrial oxidative phosphorylation system. J. Biol. Chem. 282, 1–4.

Boersig, M.R., Kader, A.A., Romani, R.J., 1988. Aerobic-anaerobic respiratory transition in pear fruit and cultured pear fruit cells. J. Amer. Soc. Hort. Sci. 113, 869–873.

Bolger, A.M., Lohse, M., Usadel, B., 2014. Trimmomatic: a flexible trimmer for Illumina sequence data. Bioinformatics 30, 2114–2120.

Borisjuk, L., Rolletschek, H., 2009. The oxygen status of the developing seed. New Phytol. 182, 17–30.

Both, V., Brackmann, A., Thewes, F.R., De, D., Ferreira, F., Wagner, R., 2014. Effect of storage under extremely low oxygen on the volatile composition of a “Royal Gala” apples. FOOD Chem. 156, 50–57.

Bouvin, J., Cajot, S., D’Huys, P.-J., Ampofo-Asiama, J., Anné, J., Van Impe, J., Geeraerd, A., Bernaerts, K., 2015. Multi-objective experimental design for 13C-based metabolic flux analysis. Math. Biosci. 268, 22–30.

Brackmann, A., 2015. Control apparatus for controlled atmosphere cells for storing perishable items. European patent. Publication number: EP2918179B1.

Bradford, M.M., 1976. A rapid and sensitive method for the quantitation of microgram quantities of protein utilizing the principle of protein-dye binding. Anal. Biochem. 72, 248–254.

Brady, C.J., 1987. Fruit ripening. Annu. Rev. Plan. Physiol. 38, 155–178.

Bricker, D.K., Taylor, E.B., Schell, J.C., Orsak, T., Boutron, A., Chen, Y.-C., Cox, J.E., Cardon, C.M., Van Vranken, J.G., Dephoure, N., Redin, C., Boudina, S., Gygi, S.P., Brivet, M., Thummel, C.S., Rutter, J., 2012. A Mitochondrial Pyruvate Carrier Required for Pyruvate Uptake in Yeast, Drosophila, and Humans. Science. 337, 96–100.

Brizzolara, S., Santucci, C., Tenori, L., Hertog, M., Nicolai, B., Stürz, S., Zanella, A., Tonutti, P., 2017a. A metabolomics approach to elucidate apple fruit responses to static and dynamic controlled atmosphere storage. Postharvest Biol. Technol. 127, 76–87.

Bron, I.U., Ribeiro, R.V., Cavalini, F.C., Jacomino, A.P., Trevisan, M.J., 2005. Temperature-related changes in respiration and Q10 coefficient of Guava. Sci. Agric. 62, 458–463.

Brückner, B., Wyllie, S.G., 2008. Fruit and vegetable flavour : recent advances and future prospects. Elsevier science, UK, p336.

Brummell, D.A., 2006. Cell wall disassembly in ripening fruit. Funct. Plant Biol. 33, 103–119.

Bucher, M., Kuhlemeier, C., 1993. Long-Term Anoxia Tolerance' Multi-Leve1 Regulation of Gene Expression in the Amphibious Plant Acorus calamus 1. Plant Physiol. 103, 441–448.

Burke, P. V, Poyton, R.O., 1998. structure/function of oxygen-regulated isoforms in cytochrom c oxidase. J. Exp. Biol. 201, 1163–1175.

Bykova, N. V., Egsgaard, H., Møller, I.M., 2003. Identification of 14 new phosphoproteins involved in important plant mitochondrial processes. FEBS Lett. 540, 141–146.

Cameron, A.C., Beaudry, R.M., Banks, N.H., Yelanich, M. V, 1994. Modified-atmosphere Packaging of Blueberry Fruit: Modeling Respiration and Package Oxygen Partial Pressures as a Function of Temperature. J. Amer. Soc. Hort. Sci. 119, 534–539.

Chandramouli, K., Qian, P.-Y., 2009. Proteomics: challenges, techniques and possibilities to overcome biological sample complexity. Hum. Genomics Proteomics 2009, 239204.

Chang, L.A., Hammett, L.K., Pharr, D.M., 1983. Carbon Dioxide Effects on Ethanol Production, Pyruvate Decarboxylase, and Alcohol Dehydrogenase Activities in Anaerobic Sweet Potato Roots. Plant Physiol. 71, 59–62.

Conesa, A., Götz, S., 2008. Blast2GO: A comprehensive suite for functional analysis in plant genomics. Int. J. Plant Genomics 2008, 619832.

Conesa, A., Verlinden, B.E., Artés-Hernández, F., Nicola, B., Artés, F., 2007. Respiration rates of fresh-cut bell peppers under supertamospheric and low oxygen with or without high carbon dioxide. Postharvest Biol. Technol. 45, 81–88.

Copeland, L., 1990. Enzymes of Sucrose Metabolism. Methods Plant Biochem. 3, 73–85.

Cortassa, S., Caceres, V., Bell, L.N., O'Rourke, B., Paolocci, N., Aon, M.A., 2015. From metabolomics to fluxomics: a computational procedure to translate metabolite profiles into metabolic fluxes. Biophys. J. 108, 163–172.

Cukrov, D., Zermiani, M., Brizzolara, S., Cestaro, A., Licausi, F., Luchinat, C., Santucci, C., Tenori, L., Van Veen, H., Zuccolo, A., Ruperti, B., Tonutti, P., 2016. Extreme Hypoxic Conditions Induce Selective Molecular Responses and Metabolic Reset in Detached Apple Fruit. Front. Plant Sci. 7, 1-18.

Daccord, N., Celton, J.-M., Linsmith, G., Becker, C., Choisne, N., Schijlen, E., van de Geest, H., Bianco, L., Micheletti, D., Velasco, R., Adele Di Pierro, E., Gouzy, J., Jasper Rees, D.G., Guérif, P., Muranty, H., Durel, C.-E., Laurens, F., Lespinasse, Y., Gaillard, S., Aubourg, S., Quesneville, H., Weigel, D., van de Weg, E., Troggio, M., Bucher, E., 2017. High-quality de novo assembly of the apple genome and methylome dynamics of early fruit development. Nat. Genet. 49, 1099-1106.

Davies, D.D., 1980. Anaerobic Metabolism and the Production of Organic Acids, In: Metabolism and Respiration. Elsevier, pp. 581–611.

Davies, D.D., Grego, S., Kenworthy, P., 1974. The control of the production of lactate and ethanol by higher plants. Planta 118, 297–310.

Delele, M.A., Nicolaï, B., Verboven, P., Verlinden, B., 2014. Storage of respiratory produce. European patent. Publication number: EP2547213 B1.

Diab, H., Limami, A.M., 2016. Reconfiguration of N Metabolism upon Hypoxia Stress and Recovery: Roles of Alanine Aminotransferase (AlaAT) and Glutamate Dehydrogenase (GDH). Plants 5, 1-9.

Diaz, F., Fukui, H., Garcia, S., Moraes, C.T., 2006. Cytochrome c oxidase is required for the assembly/stability of respiratory complex I in mouse fibroblasts. Mol. Cell. Biol. 26, 4872–4881.

Dilley, D.R., 2010. Controlled Atmosphere storage-chronology and technology. Act. Hort. 857, 493–502.

Dixon, J., Hewett, E.W., 1998. Temperature affects postharvest color change of apples. J. Amer. Soc. Hort. Sci. 123, 305–310.

Dixon, J., Hewett, E.W., 2000. Factors affecting apple aroma/flavour volatile concentration: a review. New Zeal. J. Crop Hortic. Sci. 28, 155–173.

Drew, M.C., 1997. Oxygen deficiency and root metabolism: Injury and Acclimation Under Hypoxia and Anoxia. Annu. Rev. Plant Physiol. Plant Mol. Biol. 48, 223–250.

Eicher, J.J., Snoep, J.L., Rohwer, J.M., 2012. Determining enzyme kinetics for systems biology with nuclear magnetic resonance spectroscopy. Metabolites 2, 818–843.

Ellis, M.H., Setter, T.L., 1999. Hypoxia Induces Anoxia Tolerance in completely Submerged Rice Seedlings. J. Plant Physiol. 154, 219–230.

El-ramady, H.R., Domokos-szabolcsy, É., Abdalla, N.A., Taha, H.S., Fári, M., 2015. Postharvest management of fruit and vegetables storage. In: Lichtfouse, E. (ed.), Sustainable Agriculture Reviews (pp65-115). Springer, switzerland.

Espino-Diaz, M., Sepulveda, D.R., Gonzalez-Aguilar, G., Olivas, G.I., 2016. Biochemistry of Apple Aroma: A review. Food Technol. Biotechnol 54, 375–394.

Eubel, H., Heinemeyer, J., Sunderhaus, S., Braun, H.-P., 2004. Respiratory chain supercomplexes in plant mitochondria. Plant Physiol. Biochem. 42, 937–942.

Falagán, N., Terry, L.A., 2018. Recent Advances in Controlled and Modified Atmosphere of Fresh Produce. Johnson Matthey Technol. Rev. 62, 107–117.

FAOstat, 2016, Food and agriculture organization of the united nations [WWW Document]. URL http://www.fao.org/faostat/en/#home

Fellman, J.K., Rudell, D.R., Mattinson, D.S., Mattheis, J., 2003. Relationship of harvest maturity to flavor regeneration after CA storage of 'Delicious' apples. Postharvest Biol. Technol. 27, 39–51.

Fernie, A.R., Tiessen, A., Stitt, M., Willmitzer, L., Geigenberger, P., 2002. Altered metabolic fluxes result from shifts in metabolite levels in sucrose phosphorylase-expressing potato tubers. Plant, Cell Environ. 25, 1219–1232.

File Exchange - MATLAB Central [WWW Document], n.d. URL https://nl.mathworks.com/matlabcentral/fileexchange/ (accessed 5.27.18).

Fruitboeren zien prijs appels en peren halveren [WWW Document], Belga,. URL http://deredactie.be/cm/vrtnieuws/economie/1.2101407 (accessed 7.3.18).

Fox, G.G., McCallan, N.R., Ratcliffe, R.G., 1995. Manipulating cytoplasmic pH under anoxia: A critical test of the role of pH in the switch from aerobic to anaerobic metabolism. Planta 195, 324–330.

Franck, C., Lammertyn, J., Ho, Q.T., Verboven, P., Verlinden, B., Nicolaï, B.M., 2007. Browning disorders in pear fruit. Postharvest Biol. Technol. 43, 1–13.

Fukao, T., Bailey-Serres, J., 2004. Plant responses to hypoxia--is survival a balancing act? Trends Plant Sci. 9, 449–56.

Ganai, S.A., Ahsan, H., Wani, I.A., Lone, A.A., Mir, S.A., Wani, S.M., 2015. Colour changes during storage of apple cv. Red delicious- influence of harvest date,

precooling, calcium chloride and waxing. Int. Food Res. J. 22, 196–201.

Garrett, R.H., Grisham, C.M., 2005. Biochemistry, 5th editio. ed. Thomson Brooks/Cole.

Gasic, K., Hernandez, A., Korban, S.S., 2004. RNA Extraction From Different Apple Tissues Rich in Polyphenols and Polysaccharides for cDNA Library Construction. Plant Mol. Biol. Report. 22, 437–438.

Gasser, F., Dätwyler, D., Schneider, K., Naunheim, W., Hoehn, E., 2005. Effects of decreasing oxygen levels in the storage atmosphere on the respiration and production of volatiles of “Idared” apples. Acta Hortic. 682, 1585–1592.

Gasser, F., Eppler, T., Naunheim, W., Gabioud, S., Hoehn, E., 2008. Control of the critical oxygene level during dinamic CA storage of applesby monitoring respirationas well as chlorophyll fluoresence. Acta Hortic. 796, 69–76.

Gasser, F., Von Arx, K., 2015. Dynamic CA storage of organic apple cultivars. Acta Hortic. 1071, 527–532.

Geigenberger, P., 2003. Response of plant metabolism to too little oxygen. Curr. Opin. Plant Biol. 6, 247–256.

Geigenberger, P., Fernie, A.R., Gibon, Y., Christ, M., Stitt, M., 2000. Metabolic Activity Decreases as an Adaptive Response to Low Internal Oxygen in Growing Potato Tubers. Biol. Chem. 381, 723–740.

Geigenberger, P., Regierer, B., Nunes-Nesi, A., Leisse, A., Urbanczyk-Wochniak, E., Springer, F., Van Dongen, J.T., Kossmann, J., Fernie, A.R., 2005. Inhibition of de Novo Pyrimidine Synthesis in Growing Potato Tubers Leads to a Compensatory Stimulation of the Pyrimidine Salvage Pathway and a Subsequent Increase in Biosynthetic Performance. Plant Cell 17, 2077–2088.

Geigenberger, P., Stitt, M., 1991. Regulation of carbon partitioning between sucrose and nitrogen assimilation in cotyledons of germinating Ricinus communis L. seedlings. Planta 185, 563–568.

Germain, V., Ricard, B., Raymond, P., Saglio, P.H., 1997. The Role of Sugars, Hexokinase, and Sucrose Synthase in the Determination of Hypoxically Induced Tolerance to Anoxia in Tomato Roots. Plant Physiol. 114, 167–175.

Gibbs, D.J., Bailey, M., Tedds, H.M., Holdsworth, M.J., 2016. From start to finish: amino-terminal protein modifications as degradation signals in plants. New Phytol. 211, 1188–1194.

Gibbs, D.J., Conde, J.V., Berckhan, S., Prasad, G., Mendiondo, G.M., Holdsworth, M.J., 2015. Group VII Ethylene Response Factors Coordinate Oxygen and Nitric Oxide Signal Transduction and Stress Responses in Plants. Plant Physiol. 169, 23–31.

Gibbs, D.J., Greenway, H., 2003. Review: Mechanisms of anoxia tolerance in plants. I. Growth, survival and anaerobic catabolism. Funct. Plant Biol. 30, 1-47.

Gibbs, D.J., Lee, S.C., Md Isa, N., Gramuglia, S., Fukao, T., Bassel, G.W., Correia, C.S., Corbineau, F., Theodoulou, F.L., Bailey-Serres, J., Holdsworth, M.J., 2011. Homeostatic response to hypoxia is regulated by the N-end rule pathway in plants. Nature 479, 415–418.

Giovannoni, J., 2001. Molecular biology of fruit maturation and ripening. Annu. Rev. Plant Physiol. Plant Mol. Biol. 52, 725–49.

Girardi, C.L., Rombaldi, C.V., Dal Cero, J., Nobile, P.M., Laurens, F.O., Bouzayen, M., Quecini, V., 2013. Genome-wide analysis of the AP2/ERF superfamily in apple and transcriptional evidence of ERF involvement in scab pathogenesis. Sci. Hortic. 151, 112–121.

Giuntoli, B., Lee, S.C., Licausi, F., Kosmacz, M., Oosumi, T., van Dongen, J.T., Bailey-Serres, J., Perata, P., 2014. A Trihelix DNA Binding Protein Counterbalances Hypoxia-Responsive Transcriptional Activation in Arabidopsis. PLoS Biol. 12, e1001950.

Givan, C. V., 2007. Evolving concepts in plant glycolysis: two centuries of progress. Biol. Rev. 74, 277–309.

Glish, G.L., Vachet, R.W., 2003. The basics of mass spectrometry in the twenty-first century. Nat. Rev. Drug Discov. 2, 140–150.

Graham, D., Patterson, B.D., 1982. responses of plants to low, nonfreezing temperatures: proteins, metabolism and acclimation. Ann. Rev. Plant Physiol. 33, 347–72.

Greenway, H., Gibbs, J., 2003. Review: Mechanisms of anoxia tolerance in plants. II. Energy requirements for maintenance and energy distribution to essential processes. Funct. Plant Biol. 30, 999-1036.

Gupta, K.J., Zabalza, A., van Dongen, J.T., 2009. Regulation of respiration when the oxygen availability changes. Plant Physiol. 137, 383–391.

Hall, R., Baele, M., Fiehn, O., Hardy, N., Sumner, L., Bino, R., 2002. Plant Metabolomics: The Missing Link in Functional Genomics Strategies. Plant Cell Online 14, 1437–1440.

Hans-Ulrich, B., 1983. Methods of Enzymatic Analysis. Elsevier Science p800.

Harvey Millar, A., Whelan, J., Soole, K.L., Day, D.A., 2011. Day Organization and Regulation of Mitochondrial Respiration in Plants. Annu. Rev. Plant Biol. 62, 79–104.

Hatoum, D., Annaratone, C., Hertog, M.L.A.T.M., Geeraerd, A.H., Nicolai, B.M., 2014. Targeted metabolomics study of “Braeburn” apples during long-term storage. Postharvest Biol. Technol. 96, 33–41.

Hatzfeld, W.-D., Stitt, M., 1991. Regulation of glycolysis in heterotrophic cell suspension cultures of Chenopodium rubrum in response to proton fluxes at the plasmalemma. Physiol. Plant. 81, 103–110.

Hertog, M.L.A.T.M., Peppelenbos, H.W., Evelo, R.G., Tijskens, L.M.M., 1998. A dynamic and generic model of gas exchange of respiring produce: the effects of oxygen, carbon dioxide and temperature. Postharvest Biol. Technol. 14, 335–349.

Hertog, M.L.A.T.M., Rudell, D.R., Pedreschi, R., Schaffer, R.J., Geeraerd, A.H., Nicolaï, B.M., Ferguson, I., 2011. Where systems biology meets postharvest. Postharvest Biol. Technol. 62, 223–237.

Hertog, M.L.A.T.M., Verlinden, B.E., Lammertyn, J., Nicolaï, B.M., 2007. OptiPa, an essential primer to develop models in the postharvest area. Computers and Electronics in Agriculture. 57, 99-106.

Herzig, S., Raemy, E., Montessuit, S., Veuthey, J.-L., Zamboni, N., Westermann, B., Kunji, E.R.S., Martinou, J.-C., 2012. Identification and Functional Expression of the Mitochondrial Pyruvate Carrier. Science. 337, 93–96.

Hirano, H., Islam, N., Kawasaki, H., 2004. Technical aspects of functional proteomics in plants. Phytochemistry 65, 1487–1498.

Ho, Q.T., Hertog, M.L.A.T.M., Verboven, P., Ambaw, A., Rogge, S., Verlinden, B.E., Nicolaï, B.M., 2018. Down-regulation of respiration in pear fruit depends on temperature. J. Exp. Bot. 69, 2049–2060.

Ho, Q.T., Verboven, P., Verlinden, B.E., Herremans, E., Wevers, M., Carmeliet, J., Nicolaï, B.M., 2011. A Three-Dimensional Multiscale Model for Gas Exchange in Fruit. Plant Physiol. 155, 1158–1168.

Ho, Q.T., Verboven, P., Verlinden, B.E., Lammertyn, J., Vandewalle, S., Nicolaï, B.M., 2008. A Continuum Model for Metabolic Gas Exchange in Pear Fruit. PLoS Comput. Biol. 4, e1000023.

Ho, Q.T., Verboven, P., Verlinden, B.E., Schenk, A., Delele, M.A., Rolletschek, H., Vercammen, J., Nicolaï, B.M., 2010. Genotype effects on internal gas gradients in apple fruit. J. Exp. Bot. 61, 2745–2755.

Ho, Q.T., Verboven, P., Verlinden, B.E., Schenk, A., Nicolaï, B.M., 2013. Controlled atmosphere storage may lead to local ATP deficiency in apple. Postharvest Biol. Technol. 78, 103–112.

Huppe, H.C., Turpin, D.H., 1994. Integration of Carbon and Nitrogen Metabolism in Plant and Algal Cells. Annu. Rev. Plant Physiol. Plant Mol. Biol. 45, 577–607.

Igamberdiev, A.U., Bykova, N. V., Hill, R.D., 2006. Nitric oxide scavenging by barley hemoglobin is facilitated by a monodehydroascorbate reductase-mediated ascorbate reduction of methemoglobin. Planta 223, 1033–1040.

Igamberdiev, A.U., Hill, R.D., 2004. Nitrate, NO and haemoglobin in plant adaptation to hypoxia: an alternative to classic fermentation pathways. J. Exp. Bot. 55, 2473–2482.

Imahori, B.Y., Matushita, K., Kota, M., Ueda, Y., Ishimaru, M., Chachin, K., 2003. Regulation of fermentative metabolism in tomato fruit under low oxygen stress. J. Hortic. Sci. Biotechnol. 78, 386–393.

Imahori, Y., Kota, M., Ueda, Y., Ishimaru, M., Cachin, K., 2002. Regulation of ethanolic fermentation in bell pepper fruit under low oxygen stress. Postharvest Biol. Technol. 25, 159–167.

Ito, J., Taylor, N.L., Castleden, I., Weckwerth, W., Millar, A.H., Heazlewood, J.L., 2009. A survey of the Arabidopsis thaliana mitochondrial phosphoproteome. Proteomics 9, 4229–4240.

Jackman, R., Yada, R., Marangoni, A., Parkin, K., Stanley, D., 1989. Chilling injury. A review of quality aspects. J. Food Qual. 11, 253–278.

Jacoby, R.P., Li, L., Huang, S., Pong Lee, C., Millar, A.H., Taylor, N.L., 2012. Mitochondrial Composition, Function and Stress Response in Plants. J. Integr. Plant Biol. 54, 887–906.

John, C.D., Greenway, H., 1976. Alcoholic Fermentation and Activity of some Enzymes in Rice Roots under Anaerobiosis. Aust. J. Plant Physiol. 3, 325–336.

Johnston, J.W., Hewett, E.W., Hertog, M.L.A.T.M., 2002. Postharvest softening of apple (Malus domestica) fruit: A review. New Zeal. J. Crop Hortic. Sci. 30, 145–160.

Juhnke, H., Krems, B., Kötter, P., Entian, K.-D., 1996. Mutants that show increased sensitivity to hydrogen peroxide reveal an important role for the pentose phosphate pathway in protection of yeast against oxidative stress. MGG Mol. Gen. Genet. 252, 456–464.

Kadenbach, B., Ramzan, R., Wen, L., Vogt, S., 2010. New extension of the Mitchell Theory for oxidative phosphorylation in mitochondria of living organisms. Biochim. Biophys. Acta - Gen. Subj. 1800, 205–212.

Kader, A.A., Zagory, D., Kerbel, E.L., Wang, C.Y., 1989. Modified atmosphere packaging of fruits and vegetables. Crit. Rev. Food Sci. Nutr. 28, 1–30.

Ke, D., Goldstein, L., O'Mahony, M., Kader, A., 1991a. Effects of Short-term Exposure to Low O 2 and High CO 2 Atmospheres on Quality Attributes of Strawberries. J. Food Sci. 56, 50–54.

Ke, D., Rodriguez-Sinobas, L., Kader, Adel, A., 1991b. Physiology and prediction of fruit tolerance to low-oxygen atmospheres. J. Am. Soc. Hortic. Sci. 116, 253–260.

Ke, D., Yahia, E., Hess, B., Zhou, L., Kader, A.A., 1995. Regulation of fermentative metabolism in avocado fruit under oxygen and carbon stresses. J. Am. Soc. Hortic. Sci. 120, 481–490.

Ke, D., Yahia, E., Mateos, M., Kader, A.A., 1994. Ethanolic Fermentation of ' Bartlett ' Pears as Influenced by Ripening Stage and Atmospheric Composition 119,

976–982.

Kerbel, E.L., Kader, A.A., Romani, R.J., 1988. Effects of Elevated CO(2) Concentrations on Glycolysis in Intact ;Bartlett' Pear Fruit. Plant Physiol. 86, 1205–1209.

Kettling, U., Koltermann, A., Schwille, P., Eigen, M., 1998. Real-time enzyme kinetics monitored by dual-color fluorescence cross-correlation spectroscopy. Biochemistry 95, 1416–1420.

Kim, D., Langmead, B., Salzberg, S.L., 2015. HISAT: a fast spliced aligner with low memory requirements. Nat. Methods 12, 357–360.

Knee, M., 1973. Effects of controlled atmosphere storage on respiratory metabolism of apple fruit tissue. J. Sci. Food Agric. 24, 1289–1298.

Kobr, M.J., Beevers, H., 1971. Gluconeogenesis in the castor bean endosperm: I. Changes in glycolytic intermediates. Plant Physiol. 47, 48–52.

Kolbe, A., Oliver, S.N., Fernie, A.R., Stitt, M., Van Dongen, J.T., Geigenberger, P., 2006. Combined Transcript and Metabolite Profiling of Arabidopsis Leaves Reveals Fundamental Effects of the Thiol-Disulfide Status on Plant Metabolism 1. Plant Physiol. 141, 412–422.

Kopka, J., Fernie, A., Weckwerth, W., Gibon, Y., Stitt, M., 2004. Metabolite profiling in plant biology: platforms and destinations. Genome Biol. 5, 109.

Kosmacz, M., Weits, D.A., 2014. Oxygen Perception in Plants. In van Dongen, J.t. and Licausi, F. (Eds.), Low-oxygen stress in plants (pp. 3–17), Switzerland: Springer Nature.

Krotkov, G., 1941. The respiratory metabolism of McIntosh apples during ontogeny, as determined at 22°C. Plant Physiol. 16, 799–812.

Kruger, N.J., Von Schaewen, A., 2003. The oxidative pentose phosphate pathway: structure and organisation. Curr. Opin. Plant Biol. 6, 236–246.

Kubo, Y., Inaba, A., 1989. Effects of High CO2 on Respiration in Various Horticultural Crops. J. Japan. Soc. Hort. Sci. 58, 731–736.

Lammertyn, J., Franck, C., Verlinden, B.E., Nicola, B.M., 2001. Comparative study of the O2 , CO2 and temperature effect on respiration between "Conference" pear cell protoplasts in suspension and intact pears. Journal of Experimental Botany 52, 1769–1777.

Lammertyn, J., Scheerlinck, N., Jancsók, P., Verlinden, B.., Nicolaï, B.., 2003. A respiration–diffusion model for 'Conference' pears I: model development and validation. Postharvest Biol. Technol. 30, 29–42.

Lange, D.L., Kader, A.A., 1997. Elevated carbon dioxide exposure alters intracellular pH and energy charge in avocado fruit tissue. J. Am. Soc. Hortic. Sci. 122, 253–257.

Langmead, B., Trapnell, C., Pop, M., Salzberg, S.L., 2009. Ultrafast and memory-efficient alignment of short DNA sequences to the human genome. Genome Biol. 10, R25.

Lau, O.L., 1990. Efficacy of Diphenylamine, Ultra-low oxygen, and ethylene scrubbing on scald control in “Delicious Apples.” J. Am. Soc. Hortic. Sci. 115, 959–961.

Lelievre, J.-M., Latche, A., Jones, B., Bouzayen, M., Pech, J.-C., 1997. Ethylene and fruit ripening. Physiol. Plant. 101, 727–739.

Lévesque, G.P., DeEll, J.R., Murr, D.P., 2006. Sequential controlled atmosphere storage of ‘McIntosh’ apples. HortScience. 41, 1322-1324.

Li, C.-L., Wang, M., Ma, X.-Y., Zhang, W., 2014. NRGA1, a Putative Mitochondrial Pyruvate Carrier, Mediates ABA Regulation of Guard Cell Ion Channels and Drought Stress Responses in Arabidopsis. Mol. Plant 7, 1508–1521.

Licausi, F., Giorgi, F.M., Schmälzlin, E., Usadel, B., Perata, P., van Dongen, J.T., Geigenberger, P., 2011a. HRE-Type Genes are Regulated by Growth-Related Changes in Internal Oxygen Concentrations During the Normal Development of Potato (Solanum tuberosum) Tubers. Plant Cell Physiol. 52, 1957–1972.

Licausi, F., Kosmacz, M., Weits, D.A., Giuntoli, B., Giorgi, F.M., Voesenek, L.A.C.J., Perata, P., van Dongen, J.T., 2011b. Oxygen sensing in plants is mediated by an N-end rule pathway for protein destabilization. Nature 479, 419–422.

Limami, A.M., 2014. Adaptations of Nitrogen Metabolism to Oxygen Deprivation in Plants. In van Dongen, J.t. and Licausi, F. (Eds.), Low-oxygen stress in plants (pp. 209–221), Switzerland: Springer Nature.

Limami, A.M., Diab, H., Lothier, J., 2014. Nitrogen metabolism in plants under low oxygen stress. Planta 239, 531–541.

Limami, A.M., Glévarec, G., Ricoult, C., Cliquet, J.-B., Planchet, E., 2008. Concerted modulation of alanine and glutamate metabolism in young Medicago truncatula seedlings under hypoxic stress. J. Exp. Bot. 59, 2325–2335.

Love, M.I., Huber, W., Anders, S., 2014. Moderated estimation of fold change and dispersion for RNA-seq data with DESeq2. Genome Biol. 15, 550.

Lowe, R., Shirley, N., Bleackley, M., Dolan, S., Shafee, T., 2017. Transcriptomics technologies. PLOS Comput. Biol. 13, e1005457.

Lumpkin, C., Fellman, J.K., Rudell, D.R., Mattheis, J., 2014. ‘Scarlett Spur Red Delicious’ Apple Volatile Production Accompanying Physiological Disorder Development during Low $pO_2$ Controlled Atmosphere Storage. J. Agric. Food Chem. 62, 1741–1754.

Lyons, J.M., 1973. Chilling injury in plants. Annu. rev. plant. physiol. 24, 445–466.

Mathooko, F.M., 1996. Regulation of respiratory metabolism in fruits and vegetables by carbon dioxide. Postharvest Biol. Technol. 9, 247–264.

Matsuoka, Y., Shimizu, K., 2012. 13C-Metabolic Flux Analysis and Metabolic Regulation, in: Ekinci, D. (ed.), Chemical Biology, ISBN: 978-953-51-0049-2, InTech.

Mattheis, J.P., Buchanan, D.A., Fellman, J.K., 1991. Change in apple fruit volatiles after storage in atmospheres inducing anaerobic metabolism. J. Agric. Food Chem. 39, 1602–1605.

Mauseth, J.D., 2008. Botany. An introduction to plant biology, 4th ed, Jones and Bartlett Titles in Biological Science. Jones & Bartlett Learning.

Maxwell, D.P., Wang, Y., McIntosh, L., 1999. The alternative oxidase lowers mitochondrial reactive oxygen production in plant cells. Proc. Natl. Acad. Sci. U. S. A. 96, 8271–8276.

Maxwell, K., Johnson, G.N., 2000. Chlorophyll fluorescence—a practical guide. J. Exp. Bot. 51, 659–668.

Mcdonald, A.E., Vanlerberghe, G.C., 2006. Origins, evolutionary history, and taxonomic distribution of alternative oxidase and plastoquinol terminal oxidase D1. Comparative Biochemistry and Physiology Part D: Genomics and proteomics. 1, 357–364.

Mditshwa, A., Fawole, O.A., Opara, U.L., 2018. Recent developments on dynamic controlled atmosphere storage of apples—A review. Food Packag. Shelf Life 16, 59–68.

Mellidou, I., Buts, K., Hatoum, D., Ho, Q.T., Johnston, J.W., Watkins, C.B., Schaffer, R.J., Gapper, N.E., Giovannoni, J.J., Rudell, D.R., Hertog, M.L., Nicolai, B.M., 2014. Transcriptomic events associated with internal browning of apple during postharvest storage. BMC Plant Biol. 14, 1-27.

Mendoza, F., Verboven, P., Mebatsion, H.K., Kerckhofs, G., Wevers, M., Nicolaï, B., 2007. Three-dimensional pore space quantification of apple tissue using X-ray computed microtomography. Planta 226, 559–570.

Michaelis, L., Menten, M.M.L., 1913. The kinetics of invertin action. FEBS Lett. 587, 2712–2720.

Millenaar, F.F., Lambers, H., 2003. The Alternative Oxidase: in vivo Regulation and Function. Plant Biol. 5, 2–15.

Monning, A., 1983. Studies on the reaction of krebs cycle enzymes from apple tissue (cv. cox orange) to increased levels of CO2. Acta Hortic. 138, 113-120.

Mustroph, A., Barding, G.A., Kaiser, K.A., Larive, C.K., Bailey-Serres, J., 2014a. Characterization of distinct root and shoot responses to low-oxygen stress in Arabidopsis with a focus on primary C- and N-metabolism. Plant, Cell Environ. 37, 2366–2380.

Mustroph, A., Hess, N., Sasidharan, R., 2014. Hypoxic Energy Metabolism and PPi as an Alternative Energy Currency. In: van Dongen, J.t. and Licausi, F. (Eds.), Low-oxygen stress in plants (pp. 165–184), Switzerland: Springer Nature.

Mustroph, A., Lee, S.C., Oosumi, T., Zanetti, M.E., Yang, H., Ma, K., Yaghoubi-Masihi, A., Fukao, T., Bailey-Serres, J., 2010. Cross-kingdom comparison of transcriptomic adjustments to low-oxygen stress highlights conserved and plant-specific responses. Plant Physiol. 152, 1484–500.

Nath, P., Bouzayen, M., Mattoo, A.K., Pech, J.C. (Eds.), 2014. Fruit ripening: physiology, signalling and genomics. CABI, Wallingford.

Neuhaus, H.E., Emes, M.J., 2000. Nonphotosynthetic metabolism in plastids. Annu. Rev. Plant Physiol. Plant Mol. Biol 51, 111–140.

Oliver, S.N., Lunn, J.E., Urbanczyk-Wochniak, E., Lytovchenko, A., Van Dongen, J.T., Faix, B., Schmälzlin, E., Fernie, A.R., Geigenberger, P., 2008. Decreased Expression of Cytosolic Pyruvate Kinase in Potato Tubers Leads to a Decline in Pyruvate Resulting in an in Vivo Repression of the Alternative Oxidase 1. Plant physiol 148, 1640–1654.

Päpke, C., Ramirez-Aguilar, S., Antonio, C. (Eds.), 2014. Oxygen Consumption Under Hypoxic Conditions, in: Low Oxygen Stress in Plants. Springer, Vienna, pp. 185–208.

Paul, M., Sonnewald, U., Hajirezaei, M., Dennis, D., Stitt, M., 1995. Transgenic tobacco plants with strongly decreased expression of pyrophosphate: Fructose-6-phosphate 1-phosphotransferase do not differ significantly from wild type in photosynthate partitioning, plant growth or their ability to cope with limiting phosphate, limiting nitrogen and suboptimal temperatures. Planta 196, 277–283.

Paul, V., Pandey, R., 2014. Role of internal atmosphere on fruit ripening and storability-a review. J. Food Sci. Technol. 51, 1223–1250.

Paul, V., Pandey, R., Srivastava, G.C., 2012. The fading distinctions between classical patterns of ripening in climacteric and non-climacteric fruit and the ubiquity of ethylene-An overview. J. Food Sci. Technol. 49, 1–21.

Pedreschi, R., Hertog, M., Lilley, K.S., Nicolaï, B., 2010. Proteomics for the Food Industry: Opportunities and Challenges. Crit. Rev. Food Sci. Nutr. 50, 680–692.

Pedreschi, R., Hertog, M., Robben, J., Lilley, K.S., Karp, N.A., Baggerman, G., Vanderleyden, J., Nicolaï, B., 2009. Gel-Based Proteomics Approach to the Study of Metabolic Changes in Pear Tissue during Storage. J. Agric. Food Chem. 57, 6997–7004.

Pedreschi, R., Hertog, M., Robben, J., Noben, J.-P., Nicolaï, B., 2008. Physiological implications of controlled atmosphere storage of “Conference” pears (Pyrus communis L.): A proteomic approach. Postharvest Biol. Technol. 50, 110–116.

Pedreschi, R., Lurie, S., Hertog, M., Nicolaï, B., Mes, J., Woltering, E., 2013. Post-harvest proteomics and food security. Proteomics 13, 1772–1783.

Pedreschi, R., Vanstreels, E., Carpentier, S., Hertog, M., Lammertyn, J., Robben, J., Noben, J.-P., Swennen, R., Vanderleyden, J., Nicolaï, B.M., 2007. Proteomic analysis of core breakdown disorder in Conference pears (Pyrus communis L.). Proteomics 7, 2083–2099.

Peppelenbos, H.W., Van 't Leven, J., 1996. Evaluation of four types of inhibition for modelling the influence of carbon dioxide on oxygen consumption of fruits and vegetables. Postharvest Biol. Technol. 7, 27–40.

Perata, P., Alpi, A., 1993. Plant responses to anaerobiosis. Plant Science. 93, 1–17.

Pesis, E., 2005. The role of the anaerobic metabolites, acetaldehyde and ethanol, in fruit ripening, enhancement of fruit quality and fruit deterioration. Postharvest Biol. Technol. 37, 1–19.

Plaxton, W., Podesta, F., 2006. The functional organization and control of plant respiration. CRC. Crit. Rev. Plant Sci. 159–198.

Plaxton, W.C., 1996. The organization and regulation of plant glycolysis. Annu. Rev. Plant Physiol. Plant Mol. Biol. 47, 185–214.

Prange, R.K., Delong, J.M., Harrison, P.A., 2005. Quality management through respiration control: Is there a relationship between lowest acceptable respiration, chlorophyll fluorescence and cytoplasmic acidosis? Acta Hortic. 682, 823–830.

Prange, R.K., Delong, J.M., Leyte, J.C., Harrison, P.A., 2003. Oxygen concentration affects chlorophyll fluorescence in chlorophyll-containing fruit. Postharvest Biol. Technol. 24, 201–205.

Prange, R.K., Delong, J.M., Wright, A.H., 1989. Storage of Pears Using Dynamic Controlled-Atmosphere ( DCA ), a Non-Chemical Method. Crit. Rev. Food Sci. Nutr. 28, 1–30.

Prange, R.K., Wright, A.H., DeLong, J.M., Zanella, A., 2013. History, Current Situation and Future Prospects for Dynamic Controlled Atmosphere (Dca) Storage of Fruits and Vegetables, Using Chlorophyll Fluorescence. Acta Hortic. 905–915.

Prange, Zanella, 2009. Dynamic controlled atmosphere (DCA) protocol (most apple cultivars) [WWW Document]. URL http://www.harvestwatch.net/send/10-dca-protocols/1-dca-protocol-most-apple-cultivars-english (accessed 3.20.18).

Pucciariello, C., Parlanti, S., Banti, V., Novi, G., Perata, P., 2012. Reactive Oxygen Species-Driven Transcription in Arabidopsis under Oxygen Deprivation. Plant Physiol. 159, 184–196.

Quast, C., Pruesse, E., Yilmaz, P., Gerken, J., Schweer, T., Yarza, P., Peplies, J., Glöckner, F.O., 2012. The SILVA ribosomal RNA gene database project: improved data processing and web-based tools. Nucleic Acids Res. 41, D590–D596.

Regierer, B., Fernie, A.R., Springer, F., Perez-Melis, A., Leisse, A., Koehl, K., Willmitzer, L., Geigenberger, P., Kossmann, J., 2002. Starch content and yield increase as a result of altering adenylate pools in transgenic plants. Nat. Biotechnol. 20, 1256–1260.

Ricoult, C., Cliquet, J.-B., Limami, A.M., 2005. Stimulation of alanine amino transferase (AlaAT) gene expression and alanine accumulation in embryo axis of the model legume Medicago truncatula contribute to anoxia stress tolerance. Physiol. Plant. 123, 30–39.

Ricoult, C., Echeverria, L.O., Cliquet, J.-B., Limami, A.M., 2006. Characterization of alanine aminotransferase (AlaAT) multigene family and hypoxic response in young seedlings of the model legume Medicago truncatula. J. Exp. Bot. 57, 3079–3089.

Rius, S.P., Casati, P., Iglesias, A.A., Gomez-Casati, D.F., 2006. Characterization of an Arabidopsis thaliana mutant lacking a cytosolic non-phosphorylating glyceraldehyde-3-phosphate dehydrogenase. Plant Mol. Biol. 61, 945–957.

Rivoal, J., Ricard, B., Pradet, A., 1989. Glycolytic and fermentative enzyme induction during anaerobiosis in rice seedings. Plant Physiol. Biochem. 27, 43–52.

Roberts, J.K., Chang, K., Webster, C., Callis, J., Walbot, V., 1989. Dependence of Ethanolic Fermentation, Cytoplasmic pH Regulation, and Viability on the Activity of Alcohol Dehydrogenase in Hypoxic Maize Root Tips. Plant Physiol. 89, 1275–1278.

Rocha, M., Licausi, F., Araújo, W.L., Nunes-Nesi, A., Sodek, L., Fernie, A.R., van Dongen, J.T., 2010. Glycolysis and the tricarboxylic acid cycle are linked by alanine aminotransferase during hypoxia induced by waterlogging of Lotus japonicus. Plant Physiol. 152, 1501–1513.

Saltveit, M.E., 1999. Effect of ethylene on quality of fresh fruits and vegetables. Postharvest Biol. Technol. 15, 279–292.

Saltveit, M.E., 2003. Is it possible to find an optimal controlled atmosphere? Postharvest Biol. Technol. 27, 3–13.

Sander, R., 2015. Compilation of Henry's law constants (version 4.0) for water as solvent. Atmos. Chem. Phys. 15, 4399–4981.

Saquet, A.A., Streif, J., 2008. Fermentative Metabolism in ' Jonagold ' Apples under Controlled Atmosphere Storage. Eur. J. Hortic. Sci. 73, 43–46.

Saquet, A.A., Streif, J., bangerth, F., 2000. changes in ATP, ADH and pyridine nucleotide levels related to the incidence of physiological disorders in "Conference" pears and "Jonagold" apples during controlled atmosphere storage. J. Hortic. Sci. Biotechnol. 75, 243–249.

Schaefer, D., Bishop, J.C., 2014. Dynamic control system and method for controlled atmosphere room. Europian patent. Publication number: CA2746152C.

Schäfer, E., Dencher, N.A., Vonck, J., Parcej, D.N., 2007. Three-Dimensional Structure of the Respiratory Chain Supercomplex I 1 III 2 IV 1 from Bovine Heart Mitochondria. Biochemistry 46, 12579–12585.

Shipway, M.R., Bramlage, W.J., 1973. Effects of Carbon Dioxide on Activity of Apple Mitochondria. Plant Physiol. 51, 1095–1098.

Schomburg, I., Chang, A., Schomburg, D., 2014. Standardization in enzymology—Data integration in the world's enzyme information system BRENDA. Perspect. Sci. 1, 15–23.

Schotsmans, W., Verlinden, B.E., Lammertyn, J., Nicolaï, B.M., 2004. The relationship between gas transport properties and the histology of apple. J. Sci. Food Agric. 84, 1131–1140.

Schouten, S.P., Prange, R.K., Verschoor, J., Lammers, T.R., Oosterhaven, J., 1998. Improvement of Quality of Elstar Apples by Dynamic Control of ULO Conditions. IFAC proceedings volumes. 31,25-29.

Scopes, R.K., 2002. Enzyme Activity and Assays, in: Encyclopedia of Life Sciences. John Wiley & Sons, Ltd, Chichester.

Semenza, G.L., 2007. Oxygen-dependent regulation of mitochondrial respiration by hypoxia-inducible factor 1. Biochem. J. 405, 1–9.

Shi, J., Dertouzos, J., Gafni, A., Steel, D., 2008. Chapter 7 Application of Single-Molecule Spectroscopy in Studying Enzyme Kinetics and Mechanism. Methods Enzymol. 450, 129–157.

Shulaev, V., Cortes, D., Miller, G., Mittler, R., 2008. Metabolomics for plant stress response. Physiol. Plant. 132, 199–208.

Song, J., Bangerth, F., 1996. The effect of harvest date on aroma compound production from 'Golden Delicious' apple fruit and relationship to respiration and ethylene production. Postharvest Biol. Technol. 8, 259–269.

Streif, J., 2010. Ripening management and postharvest fruit quality. Acta Hortic. 858, 121–130.

Tadege, M., Brandle, R., Kuhlemeier, C., 1998. Anoxia tolerance in tobacco roots: effect of overexpression of pyruvate decarboxylase. Plant J. 14, 327–335.

Tadege, M., Dupuis, I., Kuhlemeier, C., 1999. Ethanolic fermentation: new functions for an old pathway. Trends Plant Sci. 4, 320–325.

Taiz, L., Zeiger, E., 2010. Plant physiology, 5th editio. ed. Sinauer Associates.

Tan, P.K., Downey, T.J., Spitznagel, E.L., Xu, P., Fu, D., Dimitrov, D.S., Lempicki, R.A., Raaka, B.M., Cam, M.C., Cam, M.C., 2003. Evaluation of gene expression measurements from commercial microarray platforms. Nucleic Acids Res. 31, 5676–5684.

Teixeira, G.H.A., Durigan, J.F., 2010. Effect of Controlled Atmospheres with low oxygen levels on extended storage of guava fruit (Psidium guajava L. 'Pedro Sato'). HortScience 45, 918–924.

Theodorou, M.E., Kruger, N.J., 2001. Physiological relevance of fructose 2,6-bisphosphate in the regulation of spinach leaf pyrophosphate:fructose 6-phosphate 1-phosphotransferase. Planta 213, 147–157.

Thompson, A.K. (Ed.), 2010. Controlled atmosphere storage of fruits and vegetables. CABI, Wallingford.

Tovar-Mendez, A., Miernyk, J.A., Randall, D.D., 2003. Regulation of pyruvate dehydrogenase complex activity in plant cells. Eur. J. Biochem. 270, 1043–1049.

Urbanczyk-Wochniak, E., Usadel, B., Thimm, O., Nunes-Nesi, A., Carrari, F., Davy, M., Bläsing, O., Kowalczyk, M., Weicht, D., Polinceusz, A., Meyer, S., Stitt, M., Fernie, A.R., 2006. Conversion of MapMan to Allow the Analysis of Transcript Data from Solanaceous Species: Effects of Genetic and Environmental Alterations in Energy Metabolism in the Leaf. Plant Mol. Biol. 60, 773–792.

Van Der Merwe, M.J., Osorio, S., Araú, W.L., Balbo, I., Nunes-Nesi, A., Maximova, E., Carrari, F., Bunik, V.I., Persson, S., Fernie, A.R., 2010. Tricarboxylic Acid Cycle Activity Regulates Tomato Root Growth via Effects on Secondary Cell Wall Production 1. Plant Physiol. 153, 611–621.

Van Der Merwe, M.J., Osorio, S., Moritz, T., Nunes-Nesi, A., Fernie, A.R., 2009. Decreased Mitochondrial Activities of Malate Dehydrogenase and Fumarase in Tomato Lead to Altered Root Growth and Architecture via Diverse Mechanisms 1. Plant Physiol. 149, 653–669.

van Dongen, J.T., Fröhlich, A., Ramírez-Aguilar, S.J., Schauer, N., Fernie, A.R., Erban, A., Kopka, J., Clark, J., Langer, A., Geigenberger, P., 2009. Transcript and metabolite profiling of the adaptive response to mild decreases in oxygen concentration in the roots of arabidopsis plants. Ann. Bot. 103, 269–280.

Van Dongen, J.T., Gupta, K.J., Ramírez-Aguilar, S.J., Araújo, W.L., Nunes-Nesi, A., Fernie, A.R., 2011. Regulation of respiration in plants: A role for alternative metabolic pathways. J. Plant Physiol. 168, 1434–1443.

Van Dongen, J.T., Licausi, F. (Eds.), 2014. Low-Oxygen Stress in Plants, Plant Cell Monographs. Springer Vienna, Vienna.

van Dongen, J.T., Licausi, F., 2015. Oxygen Sensing and Signaling. Annu. Rev. Plant Biol. 66, 345–367.

Van Dongen, J.T., Schmidt, R.R., Weits, D.A., Feulner, C.F., 2017. Integrative oxygen sensing and signaling in plants. Plant Physiol. Preview. Publ. Novemb. 21.

Van Dongen, J.T., Schurr, U., Pfister, M., Geigenberger, P., 2003. Phloem Metabolism and Function Have to Cope with Low Internal Oxygen. Plant Physiol 131, 1529–

1543.

Vandendriessche, T., Schäfer, H., Verlinden, B.E., Humpfer, E., Hertog, M.L.A.T.M., Nicolaï, B.M., 2013. High-throughput NMR based metabolic profiling of Braeburn apple in relation to internal browning. Postharvest Biol. Technol. 80, 18–24.

Vanlerberghe, G.C., Huppe, H.C., Vlossak, K.D., Turpin, D.H., 1992. Activation of Respiration to Support Dark NO(3) and NH(4) Assimilation in the Green Alga Selenastrum minutum. Plant Physiol. 99, 495–500.

Veltman, R., 2013. Method and apparatus for controlling the atmosphere in a space filled with agricultural or horticultural products. Europian patent, publication number: EP2816890 A1.

Veltman, R.., Verschoor, J., van Dugteren, J.H.R., 2003. Dynamic control system (DCS) for apples (Malus domestica Borkh. cv 'Elstar'): optimal quality through storage based on product response. Postharvest Biol. Technol. 27, 79–86.

Verboven, P., Kerckhofs, G., Mebatsion, H.K., Ho, Q.T., Temst, K., Wevers, M., Cloetens, P., Nicola, B.M., 2008. Three-Dimensional Gas Exchange Pathways in Pome Fruit Characterized by Synchrotron X-Ray Computed Tomography. plant Physiol. 147, 518–527.

Vigeolas, H., van Dongen, J.T., Waldeck, P., Hühn, D., Geigenberger, P., 2003. Lipid Storage Metabolism Is Limited by the Prevailing Low Oxygen Concentrations within Developing Seeds of Oilseed Rape. Plant Physiol. 133, 2048–2060.

VILT, 2018. Vlaams infocentrum land- en tuinbouw. [WWW Document]. URL http://www.vilt.be/kwaliteitsstreven-wordt-de-weg-omhoog-voor-fruitsector

Volz, R.K., Biasi, W. V., Mitcham, E.J., 1998. Fermentative volatile production in relation to carbon dioxide-induced flesh browning in 'Fuji' apple. HortScience 33, 1231–1234.

Wagner, S., Van Aken, O., Elsässer, M., Schwarzländer, M., 2018. Mitochondrial energy signaling and its role in the low oxygen stress response of plants. Plant Physiol. 176, 1156-1170.

Wahl, S.A., Dauner, M., Wiechert, W., 2004. New tools for mass isotopomer data evaluation in13C flux analysis: Mass isotope correction, data consistency checking, and precursor relationships. Biotechnol. Bioeng. 85, 259–268.

Waldron, K.W., Parker, M.L., Smith, A.C., 2003. Plant Cell Walls and Food Quality. Compr. Rev. Food Sci. Food Saf. 2, 128–146.

Walker, S.E., 2013. RNA Purification – Precipitation Methods. Methods Enzymol. 530, 337–343.

Wang, C.Y., 2010. Approaches to Reduce Chilling Injury of Fruits and Vegetables, in: Horticultural Reviews. John Wiley & Sons, Inc., Oxford, UK, pp. 63–95.

WAPA, 2018. The world apple and pear association. [WWW Document]. URL http://www.wapaassociation.org

Waters, I., Morrel, S., Greenway, H., Colmer, T.D., 1991. Effects of Anoxia on Wheat Seedlings: II. Influence of O2 supply prior to anoxia on tolerance to anoxia, alcoholic fermentation, and sugar levels. J. Exp. Bot. 42, 1437-1447.

Watkins, C.B., 2000. Dynamic Controlled Atmosphere Storage – A New Technology for the New York storage industry? New york Fruit Q. 16, 23–26.

Watkins, C.B., Nock, J.F., 2012. Controlled-atmosphere Storage of ' Honeycrisp ' Apples. HortScience. 47, 886–892.

Webb, T., Armstrong, W., 1983. The Effects of Anoxia and Carbohydrates on the Growth and Viability of Rice, Pea and Pumpkin Roots. J. Exp. Bot. 34, 579–603.

Weber, A., Brackmann, A., De, R., Anese, O., Both, V., Pavanello, E.P., 2011. "Royal Gala" apple quality stored under ultralow oxygen concentration and low temperature conditions. Pesq. Qgropec.bras. 46, 1597–1602.

Weckwerth, W., 2003. Metabolomics in System Biology. Annu. Rev. Plant Biol. 54, 669–689.

Weits, D.A., Giuntoli, B., Kosmacz, M., Parlanti, S., Hubberten, H.-M., Riegler, H., Hoefgen, R., Perata, P., van Dongen, J.T., Licausi, F., 2014. Plant cysteine oxidases control the oxygen-dependent branch of the N-end-rule pathway. Nat. Commun. 5, 3425-3435.

Wills, R.B.H., Golding, J.B. (Eds.), 2016. Postharvest: an introduction to the physiology and handling of fruit and vegetables. CABI, Wallingford.

Winter, G., Krömer, J.O., 2013. Fluxomics - connecting 'omics analysis and phenotypes. Environ. Microbiol. 15, 1901–1916.

Wright, A.H., Delong, J.M., Gunawardena, A.H.L.A.N., Prange, R.K., 2011. Dynamic controlled atmosphere (DCA): Does fluorescence reflect physiology in storage? Postharvest Biol. Technol. 64, 19–30.

Wright, A.H., DeLong, J.M., Gunawardena, A.H.L.A.N., Prange, R.K., 2011. The interrelationship between the lower oxygen limit, chlorophyll fluorescence and the xanthophyll cycle in plants. Photosynth. Res. 107,

Yahia, E.M., 2006. modified and controlled atmospheres for tropical fruit. Stewart postharvest Rev. 5, 1–10.

Yahia, E.M. (Ed.), 2009. Modified and controlled atmospheres for the storage, transportation, and packaging of horticultural commodities. CRC Press/Taylor & Francis.

Yearsley, C.W., Banks, N.H., Ganesh, S., 1997. Temperature effects on the internal lower oxygen limits of apple fruit. Postharvest Biol. Technol. Biol. Technol. 1, 73–73.

Yearsley, C.W., Banks, N.H., Ganesh, S., Cleland, D.J., 1996. Determination of lower oxygen limits for apple fruit. Postharvest Biol. Technol. 8, 95–109.

Zabalza, A., van Dongen, J.T., Froehlich, A., Oliver, S.N., Faix, B., Gupta, K.J., Schmälzlin, E., Igal, M., Orcaray, L., Royuela, M., Geigenberger, P., 2009. Regulation of respiration and fermentation to control the plant internal oxygen concentration. Plant Physiol. 149, 1087–1098.

Zanella, A., 2003. Control of apple superficial scald and ripening a comparison between 1-methylcyclopropene and diphenylamine postharvest treatments, initial low oxygen stress and ultra low oxygen storage. Postharvest Biol. Technol. 27, 69–78.

Zanella, A., Cazzanelli, P., Rossi, O., 2008. Dynamic controlled atmosphere (DCA) storage by the means of chlorophyll fluorescence response for firmness retention in apple. Acta Hortic. 796, 77–82.

Zanella, A., Rossi, O., 2015. Post-harvest retention of apple fruit firmness by 1-methylcyclopropene (1-MCP) treatment or dynamic CA storage with chlorophyll fluorescence (DCA-CF). Eur. J. Hortic. Sci. 80, 11–17.

Zhang, Q., Greenway, H., 1994. Anoxia tolerance and anaerobic catabolism of aged beetroot storage tissues5. J. Exp. Bot. 45, 567–575.

Zhong, S., Joung, J.-G., Zheng, Y., Chen, Y.-R., Liu, B., Shao, Y., Xiang, J.Z., Fei, Z., Giovannoni, J.J., 2011. High-Throughput Illumina Strand-Specific RNA Sequencing Library Preparation. Cold Spring Harb. Lab. Press 8, 940–949.

# Appendices

## Appendix 1 – Chapter 3

### ADH_model

```
%------------------------------------------------------
% ParamDef: Initialising parameters.
%------------------------------------------------------
<ParamDef>
%-----------------------------------------------
% Defining constant global parameters.
% These parameters are not available for optimization.
%------------------------------------------------------
      cNADH = 2.519;    % Absorption coefficient of NADH
(OD/(mmol/L))
      V = 250;          % Total volume of the reaction
mixture (µl)
      Vextr = 100;      % Volume of the extract (µl)
      NADH0 = 0.4;      % Starting concentration of NADH
(mmol/L)
%------------------------------------------------------
% Declaration of model parameters including initial
values assigned.
% These parameters are available for optimization
%------------------------------------------------------
<Param> Km_ADH = 1.687;
<Param> K_ADH = 0.0031096;
```

```
<Param> A_0 = 1.2;
<Param> A_final = 0.4;
%-----------------------------------------------------
</ParamDef>

%-----------------------------------------------------
% StateDef: Assigning initial concentration of NADH and
ethanol
%-----------------------------------------------------
<StateDef>
      <State> NADH = (A_0-A_final)/cNADH;
      <State> ethanol = 0;
</StateDef>
%-----------------------------------------------------
% ModelDef: Defining michaelis menten equation for NADH
and ethanol
%-----------------------------------------------------
<ModelDef>
%-----------------------------------------------------
---------------
Deriv(NADH) = -Km_ADH *(Vextr/V)*NADH/(Km_ADH +NADH);
Deriv(ethanol) = Km_ADH *(Vextr/V)*NADH/(Km_ADH +NADH);
%-----------------------------------------------------
</ModelDef>

%-----------------------------------------------------
% TransOut: The output of the model is the modelled
absorbance
%-----------------------------------------------------
----------------------
<TransOut>
%-----------------------------------------------------
<Output> Amod = NADH*((A_0-_final)/NADH0)+A_final;
%-----------------------------------------------------
</TransOut>
```

## PDC_model

```
%--------------------------------------------------------
% ParamDef: Initialising parameters.
%--------------------------------------------------------
<ParamDef>
%-------------------------------------------------
% Defining constant global parameters.
% These parameters are not available for optimization.
%--------------------------------------------------------
cNADH = 2.519;    % Absorption coefficient of NADH
(OD/(mmol/L))
V = 250;          % Total volume of the reaction mixture
(µl)
Vextr = 100;      % Volume of the extract (µl)
U_ADH =50;        % the amount of commercial ADH added
to the reaction mixture (Units)
NADH0 = 0.4;      % Starting concentration of NADH
(mmol/L)
%--------------------------------------------------------
% Declaration of model parameters including initial
values assigned.
% These parameters are available for optimization
%--------------------------------------------------------
      <Param> k_PDC = 0.0064931;
      <Param> k_ADH = 0.041912;
      <Param> A_final = 0.6;
      <Param> Km_NADH = 0.04;
%--------------------------------------------------------
</ParamDef>

%--------------------------------------------------------
% StateDef: Assigning initial concentration of NADH,
Acetaldehyde and ethanol
%--------------------------------------------------------
<StateDef>
      <State> NADH = NADH0;
      <State> ACA = 0;
      <State> ethanol = 0;
</StateDef>

%--------------------------------------------------------
% ModelDef: Defining differential equations for NADH,
ACA and ethanol
%--------------------------------------------------------
Deriv(NADH) = -k_ADH*U_ADH*NADH*ACA/(Km_NADH+NADH);
```

```
Deriv(ACA) = k_PDC*(Vextr/V)-
k_ADH*U_ADH*ACA*NADH/(Km_NADH+NADH);
Deriv(ethanol) = k_ADH*U_ADH*NADH*ACA/(Km_NADH+NADH);
%-------------------------------------------------------
</ModelDef>

%-------------------------------------------------------
% TransOut: The output of the model is the modelled
absorbance
%-------------------------------------------------------
<TransOut>
<Output> Amod=NADH*((A_0(1)-A_final)/NADH0)+A_final;
</TransOut>
```

# Appendix 2 – Chapter 5

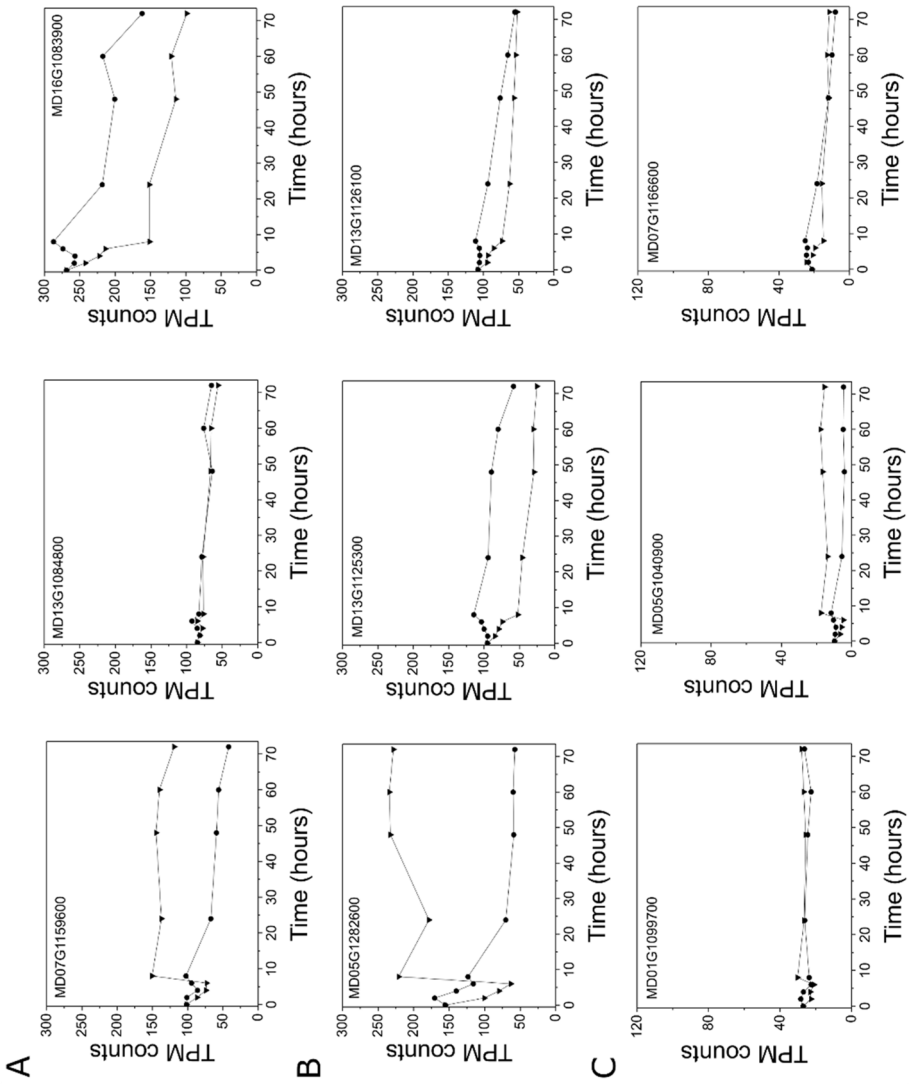

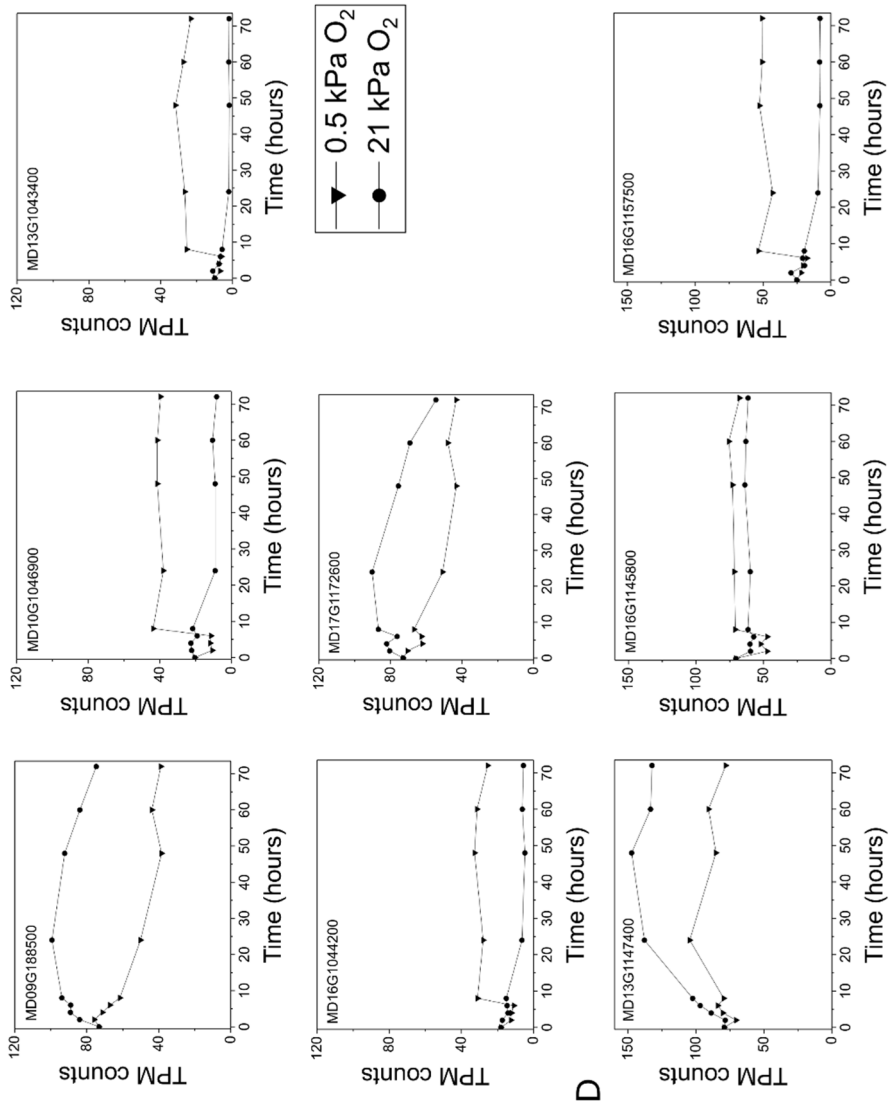


Figure S1: The expression profile of the genes coding for PDH E1a (A), PDH E1b (B), PDH E2 (C) and PDH E3 (D). ▼ = 0.5 kPa $O_2$; ● = 21 kPa $O_2$.

# Publications

## Articles in internationally reviewed academic journals

Boeckx, J., Hertog, M, Geeraerd, A., Nicolai, B. (2017). Kinetic modelling: an integrated approach to analyse enzyme activity assays. *Plant methods, 13, 69-81.*

Gwanpua S., Mellidou I., Boeckx J., Kyomugasho C., Bessemans N., Verlinden B., Hertog M., Hendrickx M., Nicolai B., Geeraerd A. (2016). Expression analysis of candidate cell wall-related genes associated with changes in pectin biochemistry during postharvest apple softening. *Postharvest Biology and Technology, 112*, 176-185.

## Papers at international scientific conferences and symposia published in full in proceedings

Boeckx, J., Hertog, M., Geeraerd, A., Nicolai, B. (2015). Kinetic modelling approach to analyse enzyme activity assays. *Model-IT.* Wageningen, The Netherlands. 11-14 October 2015.

Boeckx, J., Hertog, M., Geeraerd, A., Nicolai, B. (2016). Balancing between respiration and fermentation. *International Postharvest Symposium.* Cartagena, Spain. 21-24 June 2016.